Università degli Studi di Napoli Federico II

Scuola Politecnica e delle Scienze di Base

Dipartimento di Ingegneria Chimica dei Materiali e della Produzione Industriale

Sorption Thermodynamics and mass transport in glassy and rubbery polymers

Antonio Baldanza

A dissertation submitted for the degree of Doctor of Philosophy in
***Industrial Product and Process Engineering* (XXXIV Cycle)**

PhD Tutor: Prof. Giuseppe Mensitieri

PhD Co-tutor: PhD Pellegrino Musto

PhD Coordinator: Prof. Andrea D'Anna

Abstract

The study of mass transport of low molecular weight molecules in polymers assumes a great interest both for theoretical, technology and engineering field. For example, the technologic importance of glassy organic polymers is well known, in fact application fields are extremely diverse, and they range from structural (hyperbaric windows) to environmental (membranes for industrial gas separation), or moreover to electronic field (ionic conductors, surface coatings for printed circuit boards). To better describe this phenomenon a synergic experimental and theoretical approach is needed, in fact the aim of this research is to validate a model which allows to describe satisfactorily mass transport of gases (or vapors) in glassy and rubbery polymers. For this purpose, Non-Randomness Hydrogen-Bonding (NRHB) model is selected, since it has a great capability to predict thermodynamic sorption in rubbery polymer and it is also able to take into account for specific interactions (as hydrogen bonding), unlike other similar Lattice Fluid models present in literature as Sanchez-Lacombe model. In addition, this latter has been demonstrated to be thermodynamically inconsistent, as ideal gas state approaches, and the correction, proposed in literature onto the original Sanchez-Lacombe model, only partially circumvent the inconsistency. Conversely, during this study the thermodynamic consistency of the NRHB model has been demonstrated as ideal state approaches. Furthermore, to describe the behavior of thermodynamic sorption involving glassy polymers, NRHB is extended to Non-Equilibrium Thermodynamic Glassy Polymer (NETGP), and, for the first time, an explicit expression of the NETGP-NRHB multicomponent chemical potential is found. The achieved results have allowed to predict relevant thermal quantities, i.e., the isosteric heat of sorption and the polymer-penetrant interaction energy of PEI/CO_2 system. The predicted value of isosteric heat of sorption is compared to the one evaluated experimentally while the value of the intermolecular interaction energy is compared to the results of Density Functional Theory (DFT) calculations and applied to some ternary mixtures to predict satisfactorily thermodynamic solubility coefficients. Moreover, the equilibrium NRHB and the NETGP-NRHB are used in combination to study the glass transition temperature as function of the amount of penetrant gas in PMMA/CO_2 and Nylon 6,6/H_2O systems, this latter displaying specific interactions like hydrogen bonding. To complete the description of the mass transport, i.e., the diffusion or the permeation phenomena, an approach based on Free Volume theories is applied to NETGP-NRHB. The predictions of solubility and permeability of binary CO_2/CH_4 and CO_2/C_2H_4 mixtures in glassy polymeric membranes are compared with experimental data available in literature. The theoretical research cannot be completed without an appropriately experimental approach. At this aim, a new hyphenated technique based on concurrent pressure-decay and in situ FT-NIR vibrational spectroscopy measurements is implemented to study sorption of a low molecular weight compound in a polymeric membrane. The pressure-decay method is used to provide a quantitative information on the concentration of the penetrant within the polymer. This latter, once combined with the information gathered from vibrational spectroscopy about the IR absorbance of specific

peaks associated to the penetrant absorbed within the polymer, allows a quite accurate estimate of the molecular absorptivity of the analytic peaks. As a test case, thermodynamic and kinetic sorption at 35°C of CO_2 in Polydimethylsiloxane (PDMS) at pressure values up to 9 bar and up to up to 5.976 bar, respectively, are investigated. The results are compared with available literature data to validate the technique. Finally, the technique has been extended to the case of absorption of CO_2/CH_4 mixtures within PDMS at different temperature and the results of measurements are compared with the few data available in literature.

Contents

List of Figures

List of Tables

List of symbols

a_{β}^{i} the number of acceptor groups of type β in each molecule of type *i*

d_{α}^{i} the number of donor groups of type α in each molecule of type *i*

$E_{\alpha\beta}^{0}$ molar energy formation of a donor-α acceptor-β pair

$G_{\alpha\beta}^{0}$ molar Gibbs energy formation of a donor-α acceptor-β pair

k_{ij} mean field lattice fluid binary interactional parameter between the species i and j

k_{sw} the swelling factor associated to the polymer-penetrant couple

J_i mass flux of the component *i*

$\mathrm{l_i}$ defined as $\frac{\mathrm{z}}{2}(r_i - q_i) - (r_i - 1)$

L_{ii} mobility coefficient of the component *i*

L_{i0} pre-exponential factor of mobility coefficient of the component i

M_{wi} molecular weight of the component *i*

N_i moles of species *i*

N total moles

$\underline{N}$ vector of moles of the components

N_{ij}^0 moles of i-component and j-component pairs in random case

N_{ij} moles of i-component and j-component pairs

$\underline{N}_{ij}$ vector of moles of each i-component and j-component pairs

$\mathrm{N}_{\alpha\beta}^{\mathrm{HB}}$ moles of donor-α acceptor-β pairs

$\underline{\mathrm{N}}_{\alpha\beta}^{\mathrm{HB}}$ vector of moles of each donor-α acceptor-β pairs

N_d^α total moles of donor-α

N_a^β total moles of acceptor-β

p_i permeability coefficient of the component *i*

P_i partial pressure of the component *i*

P pressure

$\widetilde{\mathrm{P}}$ scaled pressure of the pure component or of the mixture

q average number of lattice contacts per molecule in the mixture

q_i number of external contacts made by one molecule of species *i*

R universal gas constant

r average number of sites occupied by one molecule in the mixture

r_i number of sites occupied by one molecule of species *i*

$S_{\alpha\beta}^0$ molar entropy formation of a donor-α acceptor-β pair

t time

T temperature

$\widetilde{\mathrm{T}}$ scaled temperature of the pure component or of the mixture

$\widetilde{\mathrm{T}}_i$ scaled temperature of the pure component *i* in the mixture

V volume

v molar volume

v^* characteristic molar volume, universal constant

$\tilde{v}$ scaled lattice fluid volume of the pure components or of the mixture

s number of lattice contacts per segment of molecule in the mixture

s_i number of lattice contacts per segment of molecule of component *i*

$v_{sp,0}$ is the temperature independent contribution to close packed specific volume

$v_{sp,1}$ characteristic parameter for a given homologous series

x spatial coordinate

x_i molar fraction of species *i*

z coordination number

Greek letters

$\alpha_{i,j}$ thermodynamic factor of the mass flux

β_{i} concentration factor of component *i*

Γ_{ij} non-random factor, defined as N_{ij}/N_{ij}^0

δ_i flexibility factor of species *i*

ε_h mean interaction energy per molar segment, enthalpic contribution

ε_s mean interaction energy per molar segment, entropic contribution

ε_{ii} lattice fluid interaction energy per mole of contact *i–i*

$\theta_i = \frac{x_i q I_i}{q}$

Θ_{i} surface fraction of component *i*

μ_i molar chemical potential of the species *i*

μ_i^{EQ} equilibrium molar chemical potential of the species *i*

μ_i^{NE} non-equilibrium molar chemical potential of the species *i*

ν_{H} average number of hydrogen bonds per molecular segment

$\nu_{\mathrm{d}}^{\alpha}$ average number of proton donor of type α per molecular segment

$\nu_{\alpha 0}$ average number of unbonded proton donor of type α per molecular segment

ν_{a}^{β} average number of proton acceptor of type β per molecular segment

$\nu_{0\beta}$ average number of unbonded proton acceptor of type β per molecular segment

$\nu_{\alpha\beta}$ average number per molecular segment of hydrogen bonding established between a proton donor of type α and a proton acceptor of type β

ξ membrane thickness

ρ mass density of the mixture

ρ_i mass density of the species *i*

$\rho_{p,0}$ out-of-equilibrium density of the polymer in glassy mixture

$\rho_{p,0}^{un}$ out-of-equilibrium density of the unpenetrated polymer

$\tilde{\rho}$ scaled lattice fluid density of the pure components or of the mixture

ϕ_i "close-packed" volumetric fraction of component *i*

ω_i mass fraction of the component *i*

Chapter 1
Thermodynamics of Rubbery and Glassy Polymers and their mixtures

1.1 Motivations

The study of sorption thermodynamics and mass transport of low molecular weight molecules in rubbery and glassy polymers is motivated both by a great theoretical interest and for their implications in technological and engineering applications, ranging from industrial membrane separations to pharmaceutical and biomedical applications, from polymer environmental durability to polymer foaming, to mention a few. However, a lack of understanding of the thermodynamics of pure glassy and rubbery polymers and their mixtures still exists, so that, to better understand and describe these phenomena a synergic development of experimental and theoretical approaches is needed. Aim of this thesis is, in fact, to develop and validate a consistent model which allows the adequate description of mass transport of multicomponent gases and/or vapors in glassy and rubbery polymers, accounting also for possible interactions occurring in the polymer/penetrants system. For this purpose, the equations of Non-Random Hydrogen-Bonding (NRHB) model and their extension to Non-Equilibrium Thermodynamic Glassy Polymer (NETGP-NRHB) have been developed to describe multicomponent mixture thermodynamics in presence of specific interactions (as hydrogen bonding) and to account for the non-equilibrium nature of glassy polymers, verifying their thermodynamic consistency. NRHB (and its extension to glassy polymers) has been applied to describe the retrograde vitrification of binary polymer/penetrant systems, one displaying hydrogen bonding, polymer/penetrant interaction energy, diffusion and permeation phenomena. However, an experimental activity specifically devoted to validate all the aspects of the modelling equations is necessary. In particular, a new hyphenated technique based on a combination of a pressure-decay technique and in situ FT-NIR vibrational spectroscopy measurements has been developed to study sorption of low molecular weight mixtures in a polymeric membrane.

1.2 Applications

Mass transport of light gases in polymers is a topic of interest for many fields of application. The importance of those is evident because these materials are largely used in different ways for their gas barrier and gas separation properties. Indeed, polymers with high barrier function are required for packaging of carbonated soft drinks and food in general, where the permeation of carbon dioxide, oxygen and water should be suppressed. Polymers present many attractive properties even in view of potential application in cold UHV (Ultra High Vacuum) system, since they are easily mouldable, light and resistant, moreover they are electrical insulators and transparent to subnuclear particles and radiation. Furthermore, thermoplastic polymers are useful in other applications like separation of gases, e.g., in petrochemical industry, transportation of flammable materials keeping inert the atmosphere, polymer matrix composites and electronic coatings [1].

The study of the melting and glass temperature (T_m and T_g respectively) is very important in processing of thermally labile polymers without degradation, while lowering of T_g and T_m is crucial in foaming with supercritical carbon dioxide as a physical blowing agent. Indeed, the sorption and the diffusion of penetrants in the polymer extend not only the foaming and the pore morphology, but also alter the polymer transition temperatures. In conclusion, the knowledge of T_g and T_m and the relative changes of mechanical and physical properties of polymers exposed to a soluble penetrant is fundamental in the processing of polymeric materials.

Since 1980s, the first industrial plants for the separation of Hydrogen from ammonia-plant [2, 3], let the application of polymer membranes for gas separation problems grow quickly; nowadays, the membrane market consists in nitrogen and hydrogen recovery, air drying industrial processes, carbon dioxide separation from natural gases. For example, nitrogen is produced from air as the residue of a membrane stage whereas oxygen is recovered from the permeate side, the flux of interest depends on the selectivity of the membrane, i.e., on which gas in the mixture is the most permeable.

Table 1.1: Nitrogen separation membranes [3]

Polymer	Oxygen permeabiliy (barrer)	Nitrogen permeabiliy (barrer)	Selectivity O_2/N_2
Poly(1-trimethylsilyl-1-propyne) (PTMSP)	7600	5400	1.4
Teflon AF 2400	1300	760	1.7
Silicone rubber	600	280	2.2
Poly(4-methyl-1-pentene) (TPX)	30	7.1	4.2
Poly(phenylene oxide) PPO	16.8	3.8	4.4
Ethyl cellulose	11.2	3.3	3.4
6FDA-DAF (polyimide)	7.9	1.3	6.2
Polyaramide	3.1	0.46	6.8
Tetrabromobisphenol A polycarbonate	1.4	0.18	7.5
Polysulfone	1.1	0.18	6.2

Some relevant examples are the separation of H_2 from the purge gas in ammonia plants, in order to recover the hydrogen from hydrotreating processes in the oil industry or from unreacted syngas in the petrochemical industry, with the objective to improve the productivity. For this purposes, Table 1.1 reports the polymer membrane properties in terms of selectivity. The former group can be used for gas blanketing, shipment of food and ultimately for creating inert atmosphere surrounding flammable materials. The latter finds its application in burners or compressors to improve the efficiency of combustion. Researchers are focusing their attention on these applications because the goal is to improve fluxes (i.e., recoveries) without depleting the selectivity (i.e., the separation capacity). Organic vapor is retrieved from air by using glassy or rubbery polymers as the residue or permeate stream respectively.

Table 1.2: Membrane materials and selectivities for separation of impurities from natural gas under [3]

Permeating compound	Polymer ysical state	Polymeric membrane	Selectivity over Methane
CO_2	glass	cellulose acetate, polyimide	10-20
H_2S	rubber	ether-amide block copolymer	20-30
N_2	glass	polyimide, perfluoro polymers	2-3
N_2	rubber	silicone rubber	0.35
H_2O	rubber or glass	Many	>200
Butane	rubber	silicone rubber	7-10

Typical glassy and rubbery polymers used to treat natural gases and their selectivities are given in Table 1.2. Future fields of expansion of gas separation membranes regard the sequestration of carbon dioxide, since nowadays Governments are starting to reduce CO_2 emissions in order to limit global warming: 35–40% of global carbon dioxide emissions can be ascribed to electrical power plants. Moreover, the production of oxygen enriched air and separation of organic vapors are further challenges for gas separation membranes. however, oxygen enriched air cannot be currently considered a real market for polymeric membranes if selectivities are not improved by a factor of 5-10, while organic vapors always plasticize the membrane, even at high temperatures when their solubility lowers, reducing dramatically the selectivity. Anyway, membranes are still attractive because it is still very expensive to separate organic vapors of similar boiling points with distillation processes.

1.3 Equilibrium Thermodynamic Statistical Lattice Fluid model

1.3.1 Sanchez and Lacombe Statistical lattice fluid model

Compressible lattice fluid models have been developed to describe the thermodynamics of pure components and their mixtures, including also compounds with a rather complex structures, as is the case of polymers. These models provide expressions for the basic thermodynamic quantities including equations of state (EoS) of pure components and mixtures as well as analytical equations for the chemical potentials. One of the first approaches of this kind is the Sanchez-Lacombe (SL) model [4-6] which can describe the thermodynamic behavior of pure fluids and mixtures, including polymer-solvent phase equilibrium. The Sanchez and Lacombe lattice fluid statistical theory follows the work of J. Paul Flory [7] however, it added the hypothesis of the presence of holes within the lattice. The main feature of the model is the random the mixing process of the r_i-mers with each other and with the vacant sites. The latter is also called random mean-field approximation which means that the probability of a site of being occupied or vacant is independent from the other occupied or empty sites. The primary statistical mechanical problem is to determine the number of configurations available to a system of N molecules of a single species or a mixture (each of which occupies r_i sites, i.e., an r_i-mer) and N_0 vacant sites (holes). Consequently, even in the case of a pure liquid compound, the model treats the fluid phase as a binary mixture, being the holes the second species. Moreover, the following features are used to describe the lattice framework:

a) The total number of lattice sites (N_r) of a binary mixture of N r-mers and N_0 empty sites is:

$$N_r = rN + N_0 \tag{1.1}$$

b) The coordination number of the lattice is z and each r-mer is surrounded by Q nearest non-bonded neighbors where:

$$Q = qz = r(z-2) + 2 \tag{1.2}$$

This time Flory's approximation is not followed. 'q' is then defined by the ratio between the total interacting number of sites for a r-mer and the interacting number of sites of a single mer, i.e., it is a parameter describing the amount of interacting surface of each r-mer.

c) A r-mer is characterized by a symmetry number σ (this parameter is of no quantitative importance to the SL theory)

d) A flexibility parameter δ characterizes the polymer chain and it is equal to the number of ways in which the r-mer can be arranged on the lattice after one of its mers has been fixed on a lattice site. It is a measure of the internal degree of freedom.

Contrary to Flory's theory, the polymer chain is not totally free to move. The close packed volume of a single chain is rv^* and it is independent of temperature and pressure. Three parameters describe a single compound:

a) r: the number of segments constituting the chain. Each segment can occupy a unique cell within the lattice.
b) v^*: the close packed volume of a single segment (or its lattice cell). Indeed, a hole occupies the same volume.
c) ε^*: the total interaction energy per segment or $\varepsilon^* = \frac{z}{2}\varepsilon$ where ε is the non-bonded mer-mer interaction energy.

The main result of the SL statistical theory is the derivation of the free energy (G) from the classical Boltzmann expression (1.3) and of an EOS as follows in equations (1.4).

$$\tilde{G} = \frac{G}{rN\varepsilon^*} = -\tilde{\rho} + \tilde{P}\tilde{v} + \tilde{T}\left[(\tilde{v}-1)\,log(1-\tilde{\rho}) + \frac{1}{r}log\left(\frac{\tilde{\rho}}{\omega}\right)\right] \tag{1.3}$$

$$\left(\frac{\partial\tilde{G}}{\partial\tilde{v}}\right)_{\tilde{T},\tilde{P}} = 0 \Leftrightarrow \tilde{P} = -\tilde{\rho}^2 - \tilde{T}\left[log(1-\tilde{\rho}) + \left(1-\frac{1}{r}\right)\tilde{\rho}\right] \tag{1.4}$$

where the upper signed variables are defined as follows:

$$\tilde{T} = \frac{T}{T^*} \tag{1.5a}$$

$$T^* = \frac{\varepsilon^*}{R} \tag{1.5b}$$

$$\tilde{P} = \frac{P}{P^*} \tag{1.5c}$$

$$P^* = \frac{\varepsilon^*}{v^*} \tag{1.5d}$$

$$\tilde{\rho} = \frac{1}{\tilde{v}} = \frac{V^*}{V} \tag{1.5e}$$

$$V^* = rNv^* \tag{1.5f}$$

Moreover, the combining rules aim to keep the additivity of:

a) the close packed pure volumes:

$$V^* = \sum_{i=1}^{n} r_i^0 v_i^* N_i = \sum_{i=1}^{n} r_i v^* N_i \tag{1.6}$$

b) the pair interactions of the components in their close packed pure states:

$$\frac{z}{2}rN = \frac{z}{2}\sum_{i=1}^{n} r_i^0 N_i = \frac{z}{2}\sum_{i=1}^{n} r_i N_i \tag{1.7}$$

c) the characteristic pressures are pairwise additive in the close packed mixtures:

$$P^* = \sum_{i=1}^{n}\sum_{j=1}^{n} \phi_i \phi_j P_{ij}^* \tag{1.8}$$

$$P_{ij}^* = \zeta_{ij}\left(P_i^* P_j^*\right)^{\frac{1}{2}} = (1 - k_{ij})\left(P_i^* P_j^*\right)^{\frac{1}{2}} \tag{1.9}$$

where the superscript 0 refers to the pure component parameter, v^* is the averaged close packed volume of the mixture and $N = N_1 + N_2$ is the total number of moles of the mixture. ζ describes the deviation of P_{ij}^* from the geometric mean and P_i^* is the characteristic pressure of the species i. The interaction energy of the mixture ε^* is given as follows:

$$\varepsilon^* = P^* v^* \tag{1.10}$$

and, consequently, it is not pairwise additive unless $v_1^* = v_2^*$. The other mixing rules are given in the following equations:

$$T^* = P^* \sum_{i=1}^{n} \phi_i^0 T_i^* / P_i^* \tag{1.11}$$

$$\frac{1}{r} = \sum_{i=1}^{n} \phi_i^0 / r_i^0 \tag{1.12}$$

$$\phi_i = \frac{\omega_i}{\rho_i^* \sum_{j=1}^{n} \omega_j / \rho_j^*} \tag{1.13}$$

$$\phi_i^0 = \frac{\phi_i P_i^* / T_i^*}{\sum_{j=1}^{n} \phi_j P_j^* / T_j^*} \tag{1.14}$$

where ω_i is the mass fraction of component *i* and ϕ_i is the volume fraction of component *i* and T_i^* is the characteristic pressure of the species *i*. The definition of the reduced variables as well as the EOS are the same for the mixture and the pure fluid respectively. In the following we show the free energy of a binary mixture, the chemical potential of component #1:

$$\tilde{G} = -\tilde{\rho} + \tilde{P}\tilde{v} + \tilde{T}\left[(\tilde{v} - 1)\, log(1 - \tilde{\rho}) + \frac{1}{r} log(\tilde{\rho})\right] + \tilde{T}\left[\frac{\phi_1}{r_1} log(\phi_1) + \frac{\phi_2}{r_2} log(\phi_2)\right] \tag{1.15}$$

$$\mu_1 = \left(\frac{\partial \tilde{G}}{\partial n_1}\right)_{\tilde{T},\tilde{P},n_2} = RT\left[log(\phi_1) + \left(1 - \frac{r_1}{r_2}\right)\phi_2 + \frac{r_1^0\tilde{\rho}\phi_2^2\Delta P^* v_1^*}{RT}\right] + r_1^0 RT\left\{-\frac{\tilde{\rho}}{\tilde{T}_1} + \frac{\tilde{P}_1\tilde{v}}{\tilde{T}_1} + \tilde{v}\left[(1-\tilde{\rho})\,log(1-\tilde{\rho}) + \frac{\tilde{\rho}}{r_1^0}log(\tilde{\rho})\right]\right\} \tag{1.16}$$

Where ΔP^*:

$$\Delta P^* = P_1^* + P_2^* - 2\zeta_{12}(P_1^* P_2^*)^{\frac{1}{2}} \tag{1.17}$$

Sanchez and Lacombe improve Flory’s theory and the new model is capable of predicting LCST’s and azeotropic behavior of solutions beyond retrograde condensation. However, the randomness hypothesis also implies that the energies associated with the bonds of like and unlike molecules are alike:

$$\varepsilon_{11} = \varepsilon_{22} = \varepsilon_{12} \tag{1.18}$$

1.3.2 The Thermodynamic inconsistency of Sanchez-Lacombe model

In 2002 E. Neau [8] showed that, if one considers a multicomponent fluid mixture in the limit of very low density, the expression of the chemical potential, equation (1.16), provided by the SL theory does not converge, as it should do, to a form consistent with the limit of ideal gas mixtures due to the mixing rule of the characteristic hard-core volume. This has obvious and detrimental effects on phase equilibrium calculations in multicomponent mixtures including, as shown by Neau [8], the reliability of prediction of sorption isotherms of fluids in a polymer matrix. Neau [8] has shown that the SL model recovers the required consistency when assuming the characteristic hard-core volume of the mixture to be concentration independent. This assumption represents quite a drastic simplification of the original mixing rules suggested by Sanchez et al. for the most common versions of their lattice fluid model. In the same contribution, Neau has developed a procedure, based upon an ad hoc use of fugacity coefficient in the SL framework, to properly calculate phase equilibrium, circumventing the SL inconsistency. This approach has been implemented in a following paper [9] aiming at modelling the solubility of a solid in supercritical fluids for several binary systems. However, this last procedure has been recently critically reconsidered by Thompson et al. [10-11]. Besides providing a further proof of the inconsistency of the SL theory in the ideal gas (IG) limit, arising from the proposed mixing rules, these authors have also demonstrated that the procedure developed by Neau for the calculation of phase equilibria based on an expression for fugacity, was itself incorrect. In fact, they argued that this procedure is affected by a physically inconsistent assumption since it does not account for the dependence of the total number of empty sites or holes on the system volume [12]. Thompson et al. re-obtained the expressions of the SL model starting from an off-lattice framework and established that the observed SL inconsistency is not intrinsically associated with the lattice fluid statistics, but it arises exclusively from the empirical mixing rules adopted for the empty-site volume, v_0, (which also represents the cell or site volume in the lattice). Based on this observation, these authors have then introduced a mixing rule which assumes a constant, composition-independent, hole volume of the mixture whose value depends on the type of components in the mixture, thus formulating the so-called 'ch-SL' ('constant hole' Sanchez-Lacombe) model. [12]. Although the ch-SL model overcomes the SL inconsistency in the IG limit, it is only 'nearly' consistent in ordinary phase equilibrium calculations, since a composition-independent v_0 obviously cannot converge to the pure-component limits, thus resulting in a discontinuity of the equilibrium chemical potential, which, in turn, induces a discontinuity in the solubility. This reflects an intrinsic inconsistency of the expression for the chemical potential of the given component over the full concentration range of the mixture at equilibrium. Nevertheless, as observed by Thompson et al. [12], the ch-SL theory can still provide reliable solubility predictions when v_0 of the mixture (retrieved by fitting solubility isotherm data) is quite close to the corresponding value of the pure component involved in the equilibrium calculation. In particular, the authors observed that this modified version of SL exhibits better performances in reproducing solubility data of gases in rubbery polymer when compared with the original SL model. It is worth noting that the issue of the inconsistency of the SL model also emerges in its extensions proposed in the literature to deal with fluid sorption thermodynamics in solid rigid silicates proposed by Brandani and named Rigid Adsorbent Lattice Fluid (RALF) model [13]. To address this drawback, this author corrected empirically the combinatorial term of the Helmholtz energy of the original SL model in the $(V, T, \underline{N})$ ensemble.

1.3.3 Non-Random Hydrogen Bonding Model

Besides the discussed problem related to the inconsistency when approaching the ideal gas state, the SL theory suffers also from inherent limitations arising from the adopted formulation of the partition function. In fact, the model accounts only for mean-field interactions and it assumes a random distribution of the lattice fluid contacts, including empty sites which are treated as an additional species endowed with zero interaction energy. Notably, such hypothesis is expected to hold true only if the mean field self-interaction energies are all equal which, in principle, never takes place in the presence of empty sites.

More recently, in order to deal with highly non-ideal multicomponent fluid mixtures exhibiting strong specific interactions (such as Lewis acid/base or hydrogen-bonding (HB) interactions) and with non-randomness in the distribution of intermolecular contacts, the Non-Random Hydrogen Bonding (NRHB) lattice-fluid model has been proposed by Panayiotou et al. [14-15]. The NRHB model has been extensively used to investigate liquid – liquid (LL) and vapor-liquid (VL) equilibrium data of systems displaying a variety of interactions, ranging from weak dispersion forces to strong specific interactions and proved to be highly versatile, with modelling performances which compare well with those of the widely used Statistical Associating Fluid Theory models, such as the sPC-SAFT. [16-17]. With specific reference to polymer systems, the NRHB model offers significant advantages over other models in many respects [18]. In fact, the NRHB theory has shown excellent modelling capability in dealing with sorption thermodynamics of water by polymers when both polymer-water (cross) and water-water (self) hydrogen-bonding interactions occur, as demonstrated by gravimetric and in situ FT-IR spectroscopy quantitative measurements [19-21]. Moreover, the NRHB model has been proved, by gravimetric and in situ volumetric measurements and Raman spectroscopy [19], to reproduce accurately both sorption thermodynamics and volumetric equilibrium behavior of supercritical CO_2 - amorphous rubbery polymer systems displaying cross acid-base (Lewis) interactions.

In the following, we will illustrate the NRHB model equations in a framework which accounts for the non-random distribution of empty sites and molecular segments and also for hydrogen bonding (and other specific interactions).

Let our molecular system consist of $\underline{N} = (N_1, N_2, \dots, N_t)$ (where N_i represents the number of molecules of component i, with i= 1, 2,…, t, respectively). The molecules are assumed to be arranged on a quasi-lattice of coordination number z and made of N_r sites, N_0 of which are empty.

N_r is given by the expression:

$$N_r = rN + N_0 \qquad (1.19)$$

Where $N = N_1 + N_2 + \cdots + N_t$ is the total number of molecules in the system and:

$$r = \sum_{i=1}^{t} x_i r_i \qquad (1.20)$$

In which x_i and r_i are the mole fraction and the number of segments of the component i, respectively.

The average intersegmental interaction energy per segment of
molecule i is given by:

$$\varepsilon_i^* = \frac{z}{2}\varepsilon_{ii} \tag{1.21}$$

where ε_{ii} is the interaction energy per i - i contact. Assuming the quantity $z \cdot q_i$, the number of external contacts per molecule i, one can define a geometric characteristic parameter s_i as $s_i = \frac{q_i}{r_i}$, which represents the "surface-to-volume" ratio of each molecule *i*.

This ratio is a very important parameter, which can be easily estimated for a large number of different species by using the UNIFAC group contribution model [22-23], conversely, it has to be estimated by fitting pure liquid-vapor equilibrium or dilatometric experimental data.

In a mixture, also q is calculated through the same mixing rules of r, eq. (1.20):

$$q = \sum_{i=1}^{t} x_i q_i \tag{1.22}$$

and so:

$$s = \frac{q}{r} \tag{1.23}$$

The LF contribution to the volume, V_{LF}, is given by the expression:

$$V_{LF} = N_r\, v^* \tag{1.24}$$

where the same average segmental volume v^* is assigned to an empty site as to an occupied site. Furthermore, it is assumed that two neighboring empty sites on the quasi-lattice remain discrete and do not coalesce. In what follows we will adopt the above mentioned "universal" value of 9.75 cm^3 mol^{-1} [15] for v^* for all fluids.

According to statistical mechanics, thermodynamic properties can be estimated from the canonical partition function [24], *Q*, that, in the framework of the NRHB approach, is hypothesized to be factorizable in three terms:

$$Q = (Q_R Q_{NR})Q_H = Q_{LF} Q_H \tag{1.25}$$

Here Q_R, Q_{NR} and Q_H account, respectively, for the random contribution, for the non-randomness correction and for the presence of hydrogen bonds. The generalized Staverman expression [25] is adopted for the Q_R, the Guggenheim's quasi-chemical theory [26] is used for the non-random correction term while the calculation of Q_H is based on Veytsman statistics [27]. Q_R and Q_{NR} are combined in the lattice fluid partition function Q_{LF}.

As a statistical mechanics standard procedure in searching for the expressions of thermodynamic functions at equilibrium for a given $(P, T, \underline{N})$, the sum of the partition function is approximated by its maximum term. For the Gibbs energy this is equivalent to equating its non-equilibrium value, *G*, to the logarithm of the generic term in the partition function, *Q*, and then minimizing it with respect to *internal* state variables $\left(\tilde{v}, \underline{N}_{ij}, \underline{N}_{\alpha\beta}^{HB}\right)$, whose definition will be explained in the following.

The non-equilibrium Gibbs energy of the mean-field lattice fluid, $\mathrm{G_{LF}}$, is given by:

$$\frac{G_{LF}}{kT} = -\ln Q_{LF} \tag{1.26a}$$

$$Q_{LF} = \Omega_R \Omega_{NR} \exp\left(-\frac{E_{LF}+PV_{LF}}{kT}\right) \tag{1.26b}$$

Here $\mathrm{E_{LF}}$ represents the total energy of the system associated to physical “mean-field” interactions and it will be specified in the following. Ω_R is the combinatorial term for a hypothetical system with a random distribution of the empty sites and molecular species and Ω_NR is a correction factor, which takes into account for the actual non-random distribution. As already said, in NRHB, the generalized Guggenheim-Staverman expression is adopted for Ω_R:

$$\Omega_R = \prod_i^t \delta_i^{N_i} \frac{N_r! \prod_i^t N_r^{l_i N_i}}{N_0! \prod_i^t N_i!} \left(\frac{N_q!}{N_r!}\right)^{z/2} \tag{1.27}$$

where δ_i is a characteristic quantity for fluid *i* called “flexibility parameter” which accounts for the flexibility and symmetry of the molecule. Prinos et al. [28] proposed a theoretical framework to calculate the δ_i as follows:

$$\delta_i^{N_i} = \frac{Z_i^{N_i}(Z_i-2)^{f_i N_i (r_i-2)}[(r_i-2)N_i]!}{[f_i N_i (r_i-2)]![(1-f_i)N_i(r_i-2)]!} \exp\left[-\frac{f_i N_i (r_i-2)\Delta u_i}{kT}\right] \tag{1.28a}$$

Z_i is the bond (lattice) coordination number (bond conformations) for bonds of type *i*. For simplicity we set $Z_1 = Z_2 = Z$. Δu_i is the flex energy for bonds of type *i*, which is the potential energy of the $Z-1$ bend conformations over the favored conformation. The equilibrium fraction f_i of bonds *i* in bent conformations is given by:

$$f_i = \frac{(Z_i-2)\exp\left(-\frac{\Delta u_i}{kT}\right)}{1+(Z_i-2)\exp\left(-\frac{\Delta u_i}{kT}\right)} \tag{1.28b}$$

In phase equilibrium calculations, this quantity cancels out. The Staverman parameter l_i is given by:

$$l_i = \frac{z}{2}(r_i - q_i) - (r_i - 1) \tag{1.29}$$

For Ω_{NR}, the quasi-chemical theory of Guggenheim is used:

$$\Omega_{NR} = \frac{\prod_{i=0}^{t} N_{ii}^{0}!\ \prod_{i=0}^{t}\prod_{j>i}^{t}\left[\left(\frac{N_{ij}^{0}}{2}\right)!\right]^2}{\prod_{i=0}^{t} N_{ii}!\ \prod_{i=0}^{t}\prod_{j>i}^{t}\left[\left(\frac{N_{ij}}{2}\right)!\right]^2} \tag{1.30}$$

where, N_{ij} is the number of external *i-j* contacts. In this equation, *i*=0, 1,…,t (where 0 represents empty site), while the superscript '0' refers to the case of random distribution. Notably, a constraint imposed by the balance equations for contacts holds:

$$2N_{ii} + \sum_{i\neq j}^{t} N_{ij} = N_i z q_i \qquad \text{for each } i = 0,1,\dots,t \tag{1.31}$$

the equations (1.31) state that only a sub-set of all N_{ij} is independent, so that, in the following, the sub-set of selected independent variables is indicated as $\underline{N}_{ij}$, intending the sub-set of all N_{ij} with i,j =0, 1, …, t and $j > i$.

The number of LF contacts in the random case can be calculated once one has defined the "surface contact" fraction, θ_i:

$$\theta_i = \frac{N_i q_i}{\sum_{i=1}^{t} N_i q_i} = \frac{N_i q_i}{qN} \tag{1.32}$$

$$\theta_r = \frac{qN}{qN + N_0} = \frac{qN}{N_q} = \frac{q/r}{q/r + \tilde{v} - 1} = 1 - \theta_0 \tag{1.33}$$

$$\Theta_i = \theta_r \theta_i \tag{1.34}$$

$$\Theta_0 = \theta_0 \tag{1.35}$$

And so:

$$N_{00}^{0} = \frac{z}{2} N_0 \frac{N_0}{N_q} = \frac{z}{2} N_0 \Theta_0 \tag{1.36}$$

$$N_{0j}^{0} = z N_0 \frac{N_j q_j}{N_q} = z N_0 \Theta_j \tag{1.37}$$

$$N_{ii}^{0} = \frac{z}{2} N_i q_i \frac{N_i q_i}{N_q} = \frac{z}{2} N_i q_i \Theta_i \tag{1.38}$$

$$N_{ij}^{0} = z N_i q_i \frac{N_j q_j}{N_q} = z N_i q_i \Theta_j \tag{1.39}$$

We may then express the number of intermolecular contacts in the non-random case by using a non-randomness factor Γ_{ij}, defined as:

$$N_{ij} = N_{ij}^{0}\, \Gamma_{ij} \tag{1.40}$$

Trivially, in the case of random distribution, all non-random factors, Γ_{ij}, are equal to one. By using the equations from (1.31) to (1.39), the (1.40) can be re-written as:

$$\sum_{i=0}^{t} \Theta_i \Gamma_{ij} = 1 \qquad \text{with } j=0, 1,\ldots, t \tag{1.41}$$

In the LF approach, only first-neighbor molecular segment – segment interactions give a contribute to the potential energy E_{LF} of the system, therefore, for a mixture, the potential energy E_{LF} is given by:

$$E_{LF} = -\sum_{i=0}^{t} N_{ii}\varepsilon_{ii} - \sum_{i=0}^{t}\sum_{j>i}^{t} N_{ij}\, \varepsilon_{ij} \tag{1.42a}$$

By using the (1.31), the (1.42a) can be simplified as follows:

$$\begin{aligned} E_{LF} &= -\sum_{i=0}^{t} \left(\frac{N_i z q_i}{2} - \sum_{j\neq i}^{t} \frac{N_{ij}}{2}\right) \varepsilon_{ii} - \sum_{i=0}^{t}\sum_{j>i}^{t} N_{ij}\, \varepsilon_{ij} = \\ &= -\sum_{i=0}^{t} \frac{N_i z q_i}{2} \varepsilon_{ii} - 2\sum_{i=0}^{t}\sum_{j>i}^{t} \frac{N_{ij}}{2} \varepsilon_{ij} + \sum_{i=0}^{t}\sum_{j\neq i}^{t} \frac{N_{ij}}{2} \varepsilon_{ii} = \\ &= -\sum_{i=0}^{t} \frac{N_i z q_i}{2} \varepsilon_{ii} - \sum_{i=0}^{t}\sum_{j>i}^{t} \frac{N_{ij}}{2} \left(2\varepsilon_{ij} - \varepsilon_{ii} - \varepsilon_{jj}\right) = \\ &= -\sum_{i=0}^{t} \frac{N_i z q_i}{2} \varepsilon_{ii} + \sum_{i=0}^{t}\sum_{j>i}^{t} \frac{N_{ij}}{2} \Delta\varepsilon_{ij} \end{aligned} \tag{1.42b}$$

Where:

$$\Delta\varepsilon_{ij} = \varepsilon_{ii} + \varepsilon_{jj} - 2\varepsilon_{ij} \tag{1.43a}$$

$$\varepsilon_{ij} = \sqrt{\varepsilon_{ii}\, \varepsilon_{jj}}\, (1 - k_{ij}) \tag{1.43b}$$

k_{ij} is a binary adjustable interaction parameter for the pair *i, j*. This parameter depends on the couple of components i and j and it can be retrieved by fitting experimental data of the corresponding binary system, for example solubility data (as it will be shown in the following chapters).

By substituting eq. (1.26b), (1.27) and (1.30) in eq. (1.26a), the expression for G_{LF} is obtained:

$$\frac{G_{LF}}{kT} = -rN\left\{\sum_{i=1}^{t}\frac{\phi_i}{r_i}ln\,\delta_i + \frac{l}{r} - \sum_{i=1}^{t}\frac{\phi_i}{r_i}ln\frac{\phi_i}{r_i} - \frac{ln\,\tilde{\rho}}{r} - (\tilde{v}-1)\,ln(1-\tilde{\rho}) + \frac{z}{2}\left(\tilde{v}-1+\frac{q}{r}\right)ln\left(1-\tilde{\rho}+\frac{q}{r}\tilde{\rho}\right)\right\} + rN\left\{\sum_{i=0}^{t}\frac{z}{2}\frac{N_i q_i}{rN}ln\left[\Gamma_{ii}\,exp\left(-\frac{\varepsilon_{ii}}{kT}\right)\right] + \sum_{i=0}^{t}\sum_{j>i}^{t}\frac{N_{ij}}{2rN}ln\left[\frac{{\Gamma_{ij}}^2}{\Gamma_{ii}\,\Gamma_{jj}}exp\left(\frac{\Delta\varepsilon_{ij}}{kT}\right)\right] + \frac{\tilde{P}\,\tilde{v}}{\tilde{T}}\right\} \tag{1.44}$$

In equation (1.44), ϕ_i represent the segmental fraction of the species *i,* which is equal to $\phi_i = \frac{r_i N_i}{rN}$, while $\tilde{P}, \tilde{T}$, $\tilde{v}$ and $\tilde{\rho}$ represent the reduced variables, defined as:

$$\tilde{T} = \frac{T}{T^*} = \frac{k\,T}{\varepsilon^*} \tag{1.45}$$

$$\tilde{P} = \frac{P}{P^*} = \frac{P\,v^*}{\varepsilon^*} \tag{1.46}$$

$$\tilde{v} = \frac{V_{LF}}{V^*} = \frac{N_r}{rN} \tag{1.47}$$

$$\tilde{\rho} = \frac{\rho}{\rho^*} = \frac{1}{\tilde{v}} \tag{1.48}$$

In the (1.46) and (1.47), the following mixing rules have been applied:

$$\varepsilon^* = \sum_{i=1}^{t}\sum_{j=1}^{t}\theta_i\theta_j\varepsilon_{ij}^* \tag{1.49}$$

$$\varepsilon_{ij}^* = \sqrt{\varepsilon_i^*\,\varepsilon_j^*}\,(1-k_{ij}) \tag{1.50}$$

The reported expressions of G_{LF} only represent the lattice-fluid contribution to the generic term of Gibbs energy of the system.

The contribution to the non-equilibrium Gibbs energy derived by the specific interaction, G_H, is obtained starting from the extension of the Veytsman statistics to the general case of multigroup molecules, whose combinatorial term is here reported:

$$Q_H = \Omega_H\,\exp\left(-\frac{\sum_{\alpha}^{m}\sum_{\beta}^{n}N_{\alpha\beta}^{HB}E_{\alpha\beta}^{0} + P\sum_{\alpha}^{m}\sum_{\beta}^{n}N_{\alpha\beta}^{HB}V_{\alpha\beta}^{0}}{kT}\right) \tag{1.51a}$$

$$\Omega_H = \prod_{\alpha}^{m}\frac{N_d^{\alpha}!}{N_{\alpha 0}^{HB}!}\prod_{\beta}^{n}\frac{N_a^{\beta}!}{N_{0\beta}^{HB}!}\prod_{\alpha}^{m}\prod_{\beta}^{n}\frac{{P_{\alpha\beta}}^{N_{\alpha\beta}^{HB}}}{N_{\alpha\beta}^{HB}!} \tag{1.52b}$$

m and *n* are the numbers of kind of proton donor groups and kind of proton acceptor groups, respectively. $N_{\alpha\beta}^{HB}$ is the number of donors α-acceptor β pair ($\underline{N}_{\alpha\beta}^{HB}$ stands for the set of all $N_{\alpha\beta}^{HB}$), N_d^{α} is the total number of donor groups of type α and, similarly, N_a^{β} is the total number of acceptor groups of type β. $N_{\alpha 0}^{HB}$ and $N_{0\beta}^{HB}$ are the number of unbonded donors of type α

and unbonded acceptors of type β, respectively. $P_{\alpha\beta}$ is the probability for a donor α-acceptor β pair. Formally:

$$N_d^{\alpha} = \sum_{i=1}^{t} d_{\alpha}^{i} N_i \tag{1.53}$$

$$N_a^{\beta} = \sum_{i=1}^{t} a_{\beta}^{i} N_i \tag{1.54}$$

$$N_{\alpha 0}^{HB} = N_d^{\alpha} - \sum_{\beta}^{n} N_{\alpha\beta}^{HB} \tag{1.55}$$

$$N_{0\beta}^{HB} = N_a^{\beta} - \sum_{\alpha}^{m} N_{\alpha\beta}^{HB} \tag{1.56}$$

$$P_{\alpha\beta} = e^{S_{\alpha\beta}^{0}/k}\ \tilde{\rho}/rN \tag{1.57}$$

In equations (1.53) and (1.54), d_{α}^{i} and a_{β}^{i} represent the number of donors of type α and the number of acceptors of type β per molecule of species i, respectively. $S_{\alpha\beta}^{0}$ is the molecular entropy loss (intrinsically negative) of formation of $\alpha - \beta$ hydrogen bonding formation. $\mathrm{E}_{\alpha\beta}^{0}$ is the molecular energy of formation of $\alpha - \beta$ hydrogen bonding formation, while $V_{\alpha\beta}^{0}$ is the molecular volume change associated to the formation of an $\alpha - \beta$ hydrogen bond. It is worth notice that $V_{\alpha\beta}^{0}$ can assume negative values, since it is a correction on the lattice fluid volume due the formation of the hydrogen bond. In fact, the total volume of the system, V, is equal to $V = V_{LF} + \sum_{\alpha}^{m}\sum_{\beta}^{n} \mathrm{N}_{\alpha\beta}^{\mathrm{HB}}\mathrm{V}_{\alpha\beta}^{0}$. However, $V_{\alpha\beta}^{0}$ in a lot of applications of interest is assumed null, since it does not give a significant contribution to the system volume. In particular in the application of this study, we will assume $V = V_{LF}$.
Finally, G_H can be obtained as:

$$\frac{G_H}{kT} = -\ln Q_H = rN\left\{\sum_{\alpha}^{m}\sum_{\beta}^{n} \nu_{\alpha\beta}\left[1 + \frac{G_{\alpha\beta}^{0}}{kT} + \ln\left(\frac{\tilde{v}\,\nu_{\alpha\beta}}{\nu_{\alpha 0}\nu_{0\beta}}\right)\right] + \sum_{\alpha}^{m} \nu_d^{\alpha} \ln\left(\frac{\nu_{\alpha 0}}{\nu_d^{\alpha}}\right) + \sum_{\beta}^{n} \nu_a^{\beta} \ln\left(\frac{\nu_{0\beta}}{\nu_a^{\beta}}\right)\right\} \tag{1.58}$$

In (1.40) we have defined:

$$\nu_{\alpha\beta} = \frac{N_{\alpha\beta}^{HB}}{rN} \tag{1.59}$$

$$\nu_{\alpha 0} = \frac{N_{\alpha 0}^{HB}}{rN} \tag{1.60}$$

$$\nu_{0\beta} = \frac{N_{0\beta}^{HB}}{rN} \tag{1.61}$$

$$\nu_d^{\alpha} = \frac{N_d^{\alpha}}{rN} \tag{1.62}$$

$$\nu_a^{\beta} = \frac{N_a^{\beta}}{rN} \tag{1.63}$$

$$A^0_{\alpha\beta} = E^0_{\alpha\beta} - TS^0_{\alpha\beta} \tag{1.64}$$

$$G^0_{\alpha\beta} = A^0_{\alpha\beta} + PV^0_{\alpha\beta} \tag{1.65}$$

The generic term of the non-equilibrium Gibbs energy of the NRHB model, under the hypothesis (1.25), is given by the sum of the equations (1.44) and (1.58):

$$\frac{G}{kT} = -\ln Q = -\ln(Q_{LF}Q_H) = -rN\left\{\sum_{i=1}^{t}\frac{\Phi_i}{r_i}\ln\delta_i + \frac{l}{r} - \sum_{i=1}^{t}\frac{\Phi_i}{r_i}\ln\frac{\Phi_i}{r_i} - \frac{\ln\tilde{\rho}}{r} - (\tilde{v}-1)\ln(1-\tilde{\rho}) + \frac{z}{2}\left(\tilde{v}-1+\frac{q}{r}\right)\ln\left(1-\tilde{\rho}+\frac{q}{r}\tilde{\rho}\right)\right\} + rN\left\{\sum_{i=0}^{t}\frac{z}{2}\frac{N_i q_i}{rN}\ln\left[\Gamma_{ii}\exp\left(-\frac{\varepsilon_{ii}}{kT}\right)\right] + \sum_{i=0}^{t}\sum_{j>i}^{t}\frac{N_{ij}}{2rN}\ln\left[\frac{{\Gamma_{ij}}^2}{\Gamma_{ii}\Gamma_{jj}}\exp\left(\frac{\Delta\varepsilon_{ij}}{kT}\right)\right] + \frac{\tilde{P}\,\tilde{v}}{\tilde{T}}\right\} + rN\left\{\sum_{\alpha}^{m}\sum_{\beta}^{n}\nu_{\alpha\beta}\left[1+\frac{G^0_{\alpha\beta}}{kT} + \ln\left(\frac{\tilde{v}\,\nu_{\alpha\beta}}{\nu_{\alpha0}\nu_{0\beta}}\right)\right] + \sum_{\alpha}^{m}\nu_d^{\alpha}\ln\left(\frac{\nu_{\alpha0}}{\nu_d^{\alpha}}\right) + \sum_{\beta}^{n}\nu_a^{\beta}\ln\left(\frac{\nu_{0\beta}}{\nu_a^{\beta}}\right)\right\} \tag{1.66a}$$

Moreover, by the equations (1.27), (1.30) and (1.52b), one can calculate the non-equilibrium entropy, *S*, starting from the combinatorial terms of the random, non-random and hydrogen bonding distributions:

$$\frac{S}{k} = S_R + S_{NR} + S_H = \ln(\Omega_R\Omega_{NR}\Omega_H) = -rN\left\{-\sum_{i=1}^{t}\frac{\Phi_i}{r_i}\ln\delta_i - \frac{l}{r} + \sum_{i=1}^{t}\frac{\Phi_i}{r_i}\ln\frac{\Phi_i}{r_i} + \frac{\ln\tilde{\rho}}{r} + (\tilde{v}-1)\ln(1-\tilde{\rho}) - \frac{z}{2}\left(\tilde{v}-1+\frac{q}{r}\right)\ln\left(1-\tilde{\rho}+\frac{q}{r}\tilde{\rho}\right)\right\} - rN\left\{\sum_{i=0}^{t}\left(\frac{N_i z q_i}{2rN}\right)\ln[\Gamma_{ii}\,] + \sum_{i=0}^{t}\sum_{j>i}^{t}\frac{N_{ij}}{2rN}\ln\left[\frac{{\Gamma_{ij}}^2}{\Gamma_{ii}\Gamma_{jj}}\right]\right\} - rN\left\{\sum_{\alpha}^{m}\sum_{\beta}^{n}\nu_{\alpha\beta}\left[1-\frac{S^0_{\alpha\beta}}{kT} + \ln\left(\frac{\tilde{v}\,\nu_{\alpha\beta}}{\nu_{\alpha0}\nu_{0\beta}}\right)\right] + \sum_{\alpha}^{m}\nu_d^{\alpha}\ln\left(\frac{\nu_{\alpha0}}{\nu_d^{\alpha}}\right) + \sum_{\beta}^{n}\nu_a^{\beta}\ln\left(\frac{\nu_{0\beta}}{\nu_a^{\beta}}\right)\right\} \tag{1.66b}$$

The equations (1.66a) and (1.66b) represent the generic terms of the NRHB Gibbs energy and of the NRHB entropy in the ensemble $(P, T, \underline{N})$, respectively, according to the maximum term approximation. Their expressions must be minimized with respect to the sets of internal state variables $(\tilde{v}, \underline{N}_{ij}, \underline{N}^{HB}_{\alpha\beta})$:

$$\left(\frac{\partial G}{\partial N_{ij}}\right)_{P,T,\underline{N},\tilde{v},N_{rs\neq ij},\underline{N}^{HB}_{\alpha\beta}} = 0 \qquad \text{for each } i,j = 0,1,\dots,t \text{ and } j > i \tag{1.67a}$$

$$\left(\frac{\partial G}{\partial N^{HB}_{\alpha\beta}}\right)_{P,T,\underline{N},\tilde{v},N^{HB}_{\gamma\delta\neq\alpha\beta},\underline{N}_{ij}} = 0 \qquad \text{for each } \alpha,\beta \tag{1.68a}$$

$$\left(\frac{\partial G}{\partial \tilde{v}}\right)_{P,T,\underline{N},\underline{N}_{ij},\underline{N}^{HB}_{\alpha\beta}} = 0 \tag{1.69a}$$

With some algebra, we obtain the minimization conditions of the NRHB model:

$$\frac{{\Gamma_{ij}}^2}{\Gamma_{ii}\,\Gamma_{jj}} = exp\left(-\frac{\Delta\varepsilon_{ij}}{kT}\right) \qquad \text{for each } i,j = 0,1,\dots,t \text{ and } j > i \qquad (1.67b)$$

$$\frac{\nu_{\alpha\beta}}{\nu_{\alpha 0}\nu_{0\beta}} = \tilde{\rho}\, exp\left(-\frac{G^0_{\alpha\beta}}{kT}\right) \qquad \text{for each } \alpha,\beta \qquad (1.68b)$$

$$\tilde{P} + \tilde{T}\left[ln(1-\tilde{\rho}) - \tilde{\rho}\left(\sum_{i=1}^{t}\Phi_i\frac{l_i}{r_i} - \nu_H\right) - \frac{z}{2}ln\left(1-\tilde{\rho}+\frac{q}{r}\tilde{\rho}\right) + \frac{z}{2}ln\Gamma_{00}\right] = 0 \qquad (1.69b)$$

With $\nu_H = \sum_{\alpha}^{m}\sum_{\beta}^{n}\nu_{\alpha\beta}$.
In order to obtain the equilibrium expression of Gibbs energy, G^{eq}, and of the equilibrium entropy, S^{eq}, from which all the main equilibrium thermodynamic quantities can be obtained, the equations (1.66a) and (1.66b) need to be coupled with the equations (1.67b), (1.68b) and (1.69b). This latter is a particular minimization condition, in fact, it represents the equation of state (EoS) of the NRHB model. However, no closed form of $G^{eq}(T,P,\underline{N})$ and of $S^{eq}(T,P,\underline{N})$ are available, since the whole set of equations (1.67b), (1.68b) and (1.69b) can only be solved numerically. Assuming that the expression of $G^{eq}(T,P,\underline{N})$ is available, the equilibrium molecular chemical potential of species *i* can be calculated as:

$$\mu_i^{eq}(T,P,\underline{N}) \equiv \left(\frac{\partial G^{eq}}{\partial N_i}\right)_{P,T,N_{j\neq i},} \qquad (1.70)$$

Actually, $\mu_i^{eq}(T,P,\underline{N})$ could be obtained numerically deriving the (1.62) coupling it with the minimization conditions. In order to avoid numerical errors associated to numerical scheme of derivative, it is possible to adopt the following procedure based upon the chain-rules of derivative:

$$\mu_i^{eq}(T,P,\underline{N}) \equiv \left(\frac{\partial G^{eq}}{\partial N_i}\right)_{P,T,N_{j\neq i},} = \left(\frac{\partial G}{\partial N_i}\right)_{P,T,N_{j\neq i},\tilde{v},\underline{N}_{ij},\underline{N}^{HB}_{\alpha\beta}} +$$
$$\sum_{i=0}^{t}\sum_{j>i}^{t}\left(\frac{\partial G}{\partial N_{ij}}\right)_{P,T,\underline{N},\tilde{v},\underline{N}^{HB}_{\alpha\beta},N_{rs\neq ij}}\left(\frac{\partial N_{ij}}{\partial N_i}\right)_{P,T,N_{j\neq i}} +$$
$$\sum_{\alpha}^{m}\sum_{\beta}^{n}\left(\frac{\partial G}{\partial N^{HB}_{\alpha\beta}}\right)_{P,T,\underline{N},\tilde{v},\underline{N}_{ij},N^{HB}_{\gamma\delta\neq\alpha\beta}}\left(\frac{\partial N^{HB}_{\alpha\beta}}{\partial N_i}\right)_{P,T,N_{j\neq i}} + \left(\frac{\partial G}{\partial \tilde{v}}\right)_{P,T,\underline{N},\underline{N}_{ij},\underline{N}^{HB}_{\alpha\beta}}\left(\frac{\partial \tilde{v}}{\partial N_i}\right)_{P,T,N_{j\neq i}} \qquad (1.71a)$$

Since the equation (1.71a) is coupled with the minimization conditions:

$$\mu_i^{eq}(T,P,\underline{N}) = \left(\frac{\partial G}{\partial N_i}\right)_{P,T,N_{j\neq i},\tilde{v}^{eq},\underline{N}^{eq}_{ij},\underline{N}^{HB,eq}_{\alpha\beta}} \qquad (1.71b)$$

where the superscript *eq* remarks that the corresponding quantities are evaluated at equilibrium, i.e., they are provided by solving the set of minimizations equations. The non-equilibrium expression of the chemical potential of the species i is here reported to help the readability of the thesis:

$$\mu_i\left(P,T,\underline{N},\tilde{v},\underline{N}_{ij},\underline{N}_{\alpha\beta}^{HB}\right)=\left(\frac{\partial G}{\partial N_i}\right)_{P,T,N_{j\neq i},\tilde{v},\underline{N}_{ij},\underline{N}_{\alpha\beta}^{HB}}=ln\frac{\phi_i}{\delta_i\, r_i}-r_i\sum_{j=1}^{t}\frac{\phi_j l_j}{r_j}+ln\,\tilde{\rho}+r_i(\tilde{v}-1)\,ln(1-\tilde{\rho})-\frac{z}{2}r_i\left(\tilde{v}+-1+\frac{q_i}{r_i}\right)ln\left(1-\tilde{\rho}+\frac{q}{r}\tilde{\rho}\right)+\frac{z\,q_i}{2}\left[ln\,\Gamma_{ii}+\frac{r_i}{q_i}(\tilde{v}-1)\,ln\,\Gamma_{00}\right]+r_i\frac{\tilde{P}\,\tilde{v}}{\tilde{T}}-\frac{q_i}{\tilde{T}_i}+r_i\nu_H+-\sum_{\alpha}^{m}d_{\alpha}^{i}\,ln\left(\frac{\nu_d^{\alpha}}{\nu_{\alpha 0}}\right)-\sum_{\beta}^{n}a_{\beta}^{i}\,ln\left(\frac{\nu_a^{\beta}}{\nu_{0\beta}}\right)\qquad(1.72)$$

The equation (1.71b) is obtained once the $\tilde{v}^{eq}\left(T,P,\underline{N}\right),\underline{N}_{ij}^{eq}\left(T,P,\underline{N}\right)$ and $\underline{N}_{\alpha\beta}^{HB,eq}\left(T,P,\underline{N}\right)$ are substituted in the equation (1.72).

It is worth noting that the whole set of the above equations holds for a generic multicomponent system and includes, as a particular case, mono-component systems. The equations for the pure component case, $t=1$, are consistently obtained by setting $\phi_1=1$.

In the following we will focus on the fitting parameters of the model. These parameters are involved in the scaling procedure which allows to re-cast the described set of equations into a dimensionless form. In fact, in the framework of NRHB theory, each component is characterized by four lattice fluid parameters, that are independent of composition, so that they can be estimated by fitting the equilibrium thermophysical properties of the pure components. To this aim, in general vapor-liquid equilibrium data are used in the case of low molecular weight compounds while equilibrium PVT data are used in the case of polymers.

In detail, two parameters are related to the mean interaction energy per molar segment, ε_i^* (the physical meaning of such parameter is related to the "mean field" interactions) that is expressed as a combination of an "enthalpic contribution" parameter, $\varepsilon_{i,h}^*$, and an "entropic contribution" parameter, $\varepsilon_{i,s}^*$, according to the following equation:

$$\varepsilon_i^*=\varepsilon_{i,h}^*+(T-298.15)\cdot\varepsilon_{i,s}^*\qquad(1.73)$$

The third parameter, $v_{i,sp,0}^*$, represents the temperature-independent contribution to the close packed specific volume of the pure component i, $v_{i,sp}^*$:

$$v_{i,sp}^*=v_{i,sp,0}^*+(T-298.15)\cdot v_{sp,1}^*-c\cdot P\qquad(1.74)$$

$v_{i,sp}^*$ is needed to calculate the close packed density, ρ_i^*, which is defined as:

$$\rho_i^* = 1/v_{i,sp}^* \tag{1.75}$$

$\varepsilon_{i,h}^*$, $\varepsilon_{i,s}^*$ and $v_{i,sp,0}^*$, represent the three parameters commonly retrieved for any component i by fitting its equilibrium thermophysical properties. In equations (1.73) and (1.74), T represents the temperature in Kelvin and P the pressure in MPa. Model parameters of polymers are fitted to PVT data of the melt over a wide temperature and pressure range. In order to correlate the experimental data over the full pressure range (usually from 0.1 MPa to 200 MPa), a small "compressibility" correction, c, has been introduced to the scaling constant $v_{i,sp}^*$. This correction is not needed in applications at low pressures to 10 MPa. The value of factor c is set equal to -0.135· 10^{-3} cm^3/(g·MPa) for polymers at high pressures (over 10 MPa) otherwise 0 cm^3/(g·MPa). The parameter $v_{sp,1}^*$ in equation (1.74) is treated as a constant for each compound belonging to the same homologous group. Its value is equal to - 0.412·10^{-3} cm^3 g^{-1} K^{-1} for non-aromatic hydrocarbons, - 0.310·10^{-3} cm^3 g^{-1} K^{-1} for alcohols, - 0.240·10^{-3} cm^3 g^{-1} K^{-1} for acetates, - 0.300·10^{-3} cm^3 g^{-1} K^{-1} for water and 0.150·10^{-3} cm^3 g^{-1} K^{-1} for all the other fluids [4]. The number of cells occupied by a mole of molecules of component i, is given by the relation $r_i = M_{wi}v_{i,sp}^*/v^*$, where M_{wi} is the molar weight of component i.

Finally, the fourth, composition independent, LF parameter associated to each component i is s_i. As anticipated before, the shape factor can be, in principle, determined along with the other described LF parameters by a non-linear regression of equilibrium data of the component considered. However, to reduce the number of fitting parameters involved in such procedure, it is commonly estimated through the UNIFAC group contribution method. Moreover, for systems displaying Hydrogen Bonding interactions as well as Lewis acid/Lewis base interactions, it is required the knowledge of two additional parameters for each kind of specific association that is established: $E_{\alpha\beta}^0$ and $S_{\alpha\beta}^0$. It is worth reminding that in general, a third parameter, i.e., $V_{\alpha\beta}^0$, is needed to complete the modelling, however, it is usually set equal to zero for a large number of applications of interest. In the application purposes of the Ph.D. program $V_{\alpha\beta}^0$ is set equal to zero. This assumption implies that the total volume of the system is given only by the LF contribution.

The values of the association parameters regarding the specific self-interactions of a given component can be retrieved by using these parameters, concurrently with the LF ones, to fit equilibrium thermophysical properties of the component itself. As for the specific cross-interaction parameters they can be, in principle, retrieved by fitting equilibrium properties of ad hoc systems displaying the couple of functional groups involved in such interaction. Alternatively, to reduce the number of unknown parameters, combining rules can be used for estimating the cross-interaction parameters in the multicomponent system. To this regard, the following combining rules have been proposed [29] for the cross interaction between two self-associating groups:

$$E^0_{\alpha\beta} = \frac{E^0_{\alpha\alpha}+E^0_{\beta\beta}}{2} \tag{1.76}$$

$$S^0_{\alpha\beta} = \left(\frac{{S^0_{\alpha\alpha}}^{1/3}+{S^0_{\beta\beta}}^{1/3}}{2}\right)^3 \tag{1.77}$$

while, for the cross interaction between one self-associating α and one non self-associating group β the combining rules proposed are [29]:

$$E^0_{\alpha\beta} = \frac{E^0_{\alpha\alpha}}{2} \tag{1.78}$$

$$S^0_{\alpha\beta} = \frac{S^0_{\alpha\alpha}}{2} \tag{1.79}$$

Indeed, this approach will be used in the present investigation in modelling the HB contribution.

1.4 Glassy Polymer: NETGP-NRHB framework

In order to deal with glassy polymer-penetrants systems exhibiting specific interactions, such as hydrogen-bonding, the NRHB model has been extended by Scherillo et al. [30] on the basis of the Non-Equilibrium Thermodynamics Glassy Polymer (NETGP) framework, proposed by Sarti and Doghieri [18, 31].

As shown before, the internal state variables to be accounted for the description of the glassy state, are the set of variables $\underline{N}^{HB}_{\alpha\beta}$, $\underline{N}_{ij}$, while the reduced volume $\tilde{v}$ is substituted by the polymer mass density in the mixture, ρ_P, i.e., the mass of polymer per unit volume of the mixture. Once again, the value of these variables at equilibrium is given by the minimization conditions of Gibbs energy. Conversely, in non-equilibrium conditions, the values of these variables are determined by the system of ordinary differential equations expressing their evolution kinetics. These kinetics expressions are complex functions of the non-equilibrium state of the system. If we assume that the polymer is insoluble in the external fluid phase in contact with it, the number of polymer molecules, N_p, is constant in the polymer phase.

External state variables are then required to define the state of the system: these are the temperature, *T*, the pressure, *P*, and the set of variables representing the number of molecules of each component present in the mixture, i.e., $\underline{N} = \left(N_1, N_2, \dots, N_{t-1}, N_p\right)$. The external fluid phase, assumed to be without polymer macromolecules, is considered as being in an equilibrium state, so it is represented only by the external variables P, T and number of molecules of each penetrant.

The expression for Gibbs energy, for the polymer-penetrant mixture in a non-equilibrium condition, is generically represented as:

$$G = g\left(T, P, N_1, N_2, \dots, N_{t-1}, N_p, \rho_p, \underline{N}_{ij}, \underline{N}_{\alpha\beta}^{HB}\right) \tag{1.80}$$

The expression of the function g has been obtained by the equation (1.66a). This latter must be coupled with the systems of constitutive equations describing the evolution kinetics of all the internal variables of the polymer-penetrants mixture, in non-equilibrium conditions:

$$\frac{\partial \rho_P}{\partial \mathrm{t}} = r_\rho\left(T, P, N_1, N_2, \dots, N_{t-1}, N_p, \rho_P, \underline{N}_{ij}, \underline{N}_{\alpha\beta}^{HB}\right) \tag{1.81}$$

$$\frac{\partial \underline{N}_{ij}}{\partial \mathrm{t}} = \underline{r}_{\underline{N}_{ij}}\left(T, P, N_1, N_2, \dots, N_{t-1}, N_p, \rho_P, \underline{N}_{ij}, \underline{N}_{\alpha\beta}^{HB}\right) \tag{1.82}$$

$$\frac{\partial \underline{N}_{\alpha\beta}^{H}}{\partial \mathrm{t}} = \underline{r}_{\underline{N}_{\alpha\beta}^{H}}\left(T, P, N_1, N_2, \dots, N_{t-1}, N_p, \rho_P, \underline{N}_{ij}, \underline{N}_{\alpha\beta}^{HB}\right) \tag{1.83}$$

Since it is difficult to identify a proper expression for these evolution kinetics, one can assume that these rates are infinitely fast, so that, the variables are always at their equilibrium values or assume that these rates are infinitely slow, therefore, the variables stay indefinitely at whatever value they may have. In particular, an instantaneous evolution kinetics has been assumed for the two sets of internal state variables $\underline{N}_{ij}$ and $\underline{N}_{\alpha\beta}^{H}$ while, the polymer density in the glassy mixture, ρ_P, is considered to be in a kinetically hindered state resulting in a time invariant non-equilibrium value, $\rho_{P,\infty}$.

The local rearrangement of the system, that involves the dynamic of evolution of the state variables $\underline{N}_{ij}$ and $\underline{N}_{\alpha\beta}^{HB}$, takes place on a time scale much smaller than the long-time scale of the relaxation processes associated with the volumetric ageing of the mixture toward a true equilibrium state. So, it is assumed that the values of these two variables are the ones that the system would exhibit if it was at equilibrium at the current values of polymer density, pressure, temperature and concentration. The values of these variables are provided by minimization conditions of G toward $\underline{N}_{ij}$ and $\underline{N}_{\alpha\beta}^{HB}$, but do not correspond to the equilibrium ones, in view of the fact that the value of ρ_P is not the one dictated by the equilibrium condition.

This assumption is called instantaneous equilibrium (IE) hypothesis for the state variables $\underline{N}_{ij}$ and $\underline{N}_{\alpha\beta}^{HB}$, so the non-equilibrium value of G has to be calculated as follows:

$$G^{IE} = g\left(T,P,N_1,\dots,N_{t-1},N_p,\rho_P,\underline{N}_{ij}^{IE}\left(T,P,N_1,\dots,N_{t-1},N_p,\rho_P\right),\underline{N}_{\alpha\beta}^{IE,HB}\left(T,P,N_1,\dots,N_{t-1},N_p,\rho_P\right)\right) = g^{IE}\left(T,P,N_1,\dots,N_{t-1},N_p,\rho_P\right) \tag{1.84}$$

The value of the internal state variable, ρ_P, is provided by its evolution equation:

$$\frac{\partial \rho_P}{\partial t} = r_p\left(T,P,N_1,\dots,N_{t-1},N_p,\rho_P,\underline{N}_{ij}^{IE}\left(T,P,N_1,\dots,N_{t-1},N_p,\rho_P\right),\underline{N}_{\alpha\beta}^{IE,HB}\left(T,P,N_1,\dots,N_{t-1},N_p,\rho_P\right)\right) = r_{\,p}^{\,IE}\left(T,P,N_1,\dots,N_{t-1},N_p,\rho_P\right) \tag{1.85}$$

And so, it follows that:

$$\left(\frac{\partial G}{\partial \rho_P}\right)_{P,T,\underline{N},N_{ij},N_{\alpha\beta}^{HB}} \neq 0 \tag{1.86}$$

It is worth noting that the constitutive class of the polymer-penetrant system, $\{T,P,N_1,\dots,N_{t-1},N_p,\rho_P\}$, is perfectly equivalent to the constitutive class of the original version of multicomponent NETGP formulation, whit ρ_P as the sole internal state variable. It is now possible to replicate the same procedure of NETGP approach, with the simplifying assumption that the value of ρ_P takes a time invariant value, $\rho_{P,\infty}$ for infinitely slow evolution kinetics,

$$\frac{\partial \rho_P}{\partial t} = r_P^{IE}\left(T,P,N_1\,\dots,N_{t-1},N_p,\rho_{P,\infty}\right) \cong 0 \tag{1.87}$$

Under there assumptions, phase equilibrium is still dictated by the equivalence of chemical potentials for each generic penetrant *i* in the two phases in contact:

$$\mu_{i,pol}^{IE}\left(T,N_1^{PE},\dots,N_{t-1}^{PE},N_P,\rho_{P,\infty}\right) = \mu_{i,ext}^{EQ}\left(T,P,N_{1,ext},\dots,N_{t-1,ext}\right) \quad \text{for } i=1,2,\dots,t\text{-}1 \tag{1.88}$$

Here $\mu_{i,pol}^{IE}$ represents the IE molecular chemical potential of the penetrant *i* within the polymer-penetrant mixture and it is calculated by performing the derivative, with respect to N_i, of the IE expression of the Gibbs energy, G^{IE}. Repeating the same discussion of the equilibrium chemical potential of the species *i* (Section 1.3.2), operatively, the $\mu_{i,pol}^{IE}$ is calculated by the chain rules:

$$\mu_{i,pol}^{IE} = \left(\frac{\partial G^{IE}}{\partial N_i}\right)_{P,T,N_{j\neq i},\rho_{p,\infty}} = \left(\frac{\partial G}{\partial N_i}\right)_{P,T,N_{j\neq i},\rho_{p,\infty},\underline{N}_{ij},\underline{N}_{\alpha\beta}^{HB}} + \sum_{i=0}^{t}\sum_{j>i}^{t}\left(\frac{\partial G}{\partial N_{ij}}\right)_{P,T,\underline{N},\rho_{p,\infty},\underline{N}_{\alpha\beta}^{HB},N_{rs\neq ij}}\left(\frac{\partial N_{ij}}{\partial N_i}\right)_{P,T,N_{j\neq i},\rho_{p,\infty}} + \sum_{\alpha}^{m}\sum_{\beta}^{n}\left(\frac{\partial G}{\partial N_{\alpha\beta}^{HB}}\right)_{P,T,\underline{N},\rho_{p,\infty},\underline{N}_{ij},N_{\gamma\delta\neq\alpha\beta}^{HB}}\left(\frac{\partial N_{\alpha\beta}^{HB}}{\partial N_i}\right)_{P,T,N_{j\neq i},\rho_{p,\infty}} \tag{1.89a}$$

It is worth noting that since:

$$\tilde{v} = \frac{\omega_p\,\rho^*}{\rho_{p,\infty}} \tag{1.90}$$

With:

$$\rho^* = \frac{\sum_{i=1}^{t} x_i M_{w_i}}{r v^*} \tag{1.91}$$

where ω_p and M_{w_i} are the polymer mass fraction and molecular weight of component i, respectively, the minimization conditions (1.67b) and (1.68b) are exactly the same in the constitutive class $\{T, P, N_1, \dots, N_{t-1}, N_p, \rho_{p,\infty}, \underline{N}_{ij}, \underline{N}_{\alpha\beta}^{HB}\}$. Moreover, in general in IE condition we cannot use (1.69b) since *G* is not minimized as function of $\rho_{p,\infty}$, so $\tilde{v}$ is calculated by the (1.90).
Since the (1.89a) is coupled with the (1.67b) and (1.68b), we obtain:

$$\mu_{i,pol}^{IE} = \left(\frac{\partial G}{\partial N_i}\right)_{P,T,N_{j\neq i},\rho_{p,\infty},\underline{N}_{ij}^{IE},\underline{N}_{\alpha\beta}^{HB,IE}} \tag{1.89b}$$

Finally, the (1.89b) for the penetrant *i* can be obtained once $\underline{N}_{ij}^{IE}(T, N_1, \dots, N_{t-1}, N_p, \rho_P)$ and $\underline{N}_{\alpha\beta}^{HB,IE}(T, N_1, \dots, N_{t-1}, N_p, \rho_P)$ are coupled with $\left(\frac{\partial G}{\partial N_i}\right)_{P,T,N_{j\neq i},\rho_{p,\infty},\underline{N}_{ij},\underline{N}_{\alpha\beta}^{HB}}$, where:

$$\frac{1}{kT}\left(\frac{\partial G}{\partial N_i}\right)_{P,T,N_{j\neq i},\rho_{p,\infty},\underline{N}_{ij},\underline{N}_{\alpha\beta}^{HB}} = ln\frac{\phi_i}{\delta_i \cdot r_i} + ln\,\tilde{\rho} - r_i\,ln(1-\tilde{\rho}) - \frac{z}{2}r_i\left(\frac{q}{r}-1\right)ln\left(1-\tilde{\rho}+\frac{q}{r}\cdot\tilde{\rho}\right) + \frac{z}{2}\cdot q_i\left(ln\,\Gamma_{ii} - \frac{r_i}{q_i}ln\,\Gamma_{00}\right) - \frac{q_i}{\tilde{T}_i} - \sum_{\alpha=1}^{m}\left[d_\alpha^i\cdot ln\left(\frac{\nu_d^\alpha}{\nu_{\alpha 0}}\right)\right] - \sum_{\beta=1}^{n}\left[a_\beta^i\cdot ln\left(\frac{\nu_a^\beta}{\nu_{0\beta}}\right)\right] \tag{1.92}$$

where $\tilde{\rho}$ is calculated using the (1.90) and the (1.48). It is worth noting that the expression (1.92) is valid only for calculating the chemical potential of the penetrant i in the polymer phase and it is independent on pressure.

1.5 Prediction of the glass transition of a polymer-penetrant mixture

It is possible to construct a theoretical framework for prediction of the glass transition temperature of polymer-penetrant mixtures by combining, as originally proposed by Condo et al [32], Equation of State lattice fluid theories for random mixtures with the Gibbs-Di Marzio criterion [33-35] for glass transition, that states the equilibrium configurational entropy is zero at the glass transition. Several types of behaviour have been identified (types I, II, III and IV [32]) for the dependence of the T_g of the polymer-penetrant mixture as a function of the pressure of the penetrant vapour to which the mixture is in contact. Of particular interest for the polymer/penetrant system is the occurrence of the so-called retrograde vitrification phenomenon, i.e., the transition from a rubbery to a glassy state induced by temperature increase at a fixed pressure of vapor. In brief, this effect is related to the interplay, at isobaric conditions, between the intrinsic increase of the macromolecular mobility associated to the increase of temperature and the decrease of the mobility induced by the decrease of penetrant concentration within the polymer promoted by a lowering of its solubility as the temperature increases. Retrograde vitrification is observed when the second effect prevails on the first one. The Gibbs-Di Marzio criterion refers, for pure compounds, to the rubber-to-glass transition as a true thermodynamic second order transition that occurs, at a fixed pressure, at a temperature T_2 at which the equilibrium configurational entropy of the system, as calculated by means of a proper lattice fluid theory, becomes equal to zero. This transition is the one would observe, in the case of non-crystallizable materials, when the temperature is decreased at an infinitely slow rate. This ‘ideal’ transition is not experimentally accessible and, as matter of fact, the glass transition temperature that is commonly measured, referred to as T_g, is higher than T_2 and represents a kinetically affected value of it. The transition temperature T_2 has been reported [36-38] to be roughly equal to $0.77 \cdot T_g$. Following Panayiotou et al. [28], for all practical purposes, one may assume the configurational entropy to be zero at the T_g. The same approach can be used to deal with the glass transition in the case of mixtures, assuming, also in this case, that at the experimentally accessible glass transition equilibrium configurational entropy is zeroed. In a series of papers [14, 28, 39] Panayiotou et al. have used the expression provided by the NRHB lattice fluid approach for the entropy of pure amorphous polymers and of polymer-penetrant mixtures in combination with the Gibbs–Di Marzio criterion to predict the dependence on penetrant pressure of the glass transition of polymer-penetrant-polymer mixtures. Since the NRHB model accounts only for configurational entropy, it is the whole expression for entropy supplied by the theory that is zeroed:

$$S^{eq} = 0 \tag{1.93}$$

where S^{eq} is the equilibrium entropy calculated by the NRHB model by coupling equations (1.66b) with (1.67b) to (1.69b).

A parameter needed for each component of the mixture to proceed with the calculation of the random term of entropy, and hence to determine the T_g value for the mixture, is δ_i [31-32]. The expression for δ_i is given by the (1.28a) and (1.28b).

In the present context, it is made the simplifying assumption that the flex energy is independent of temperature and composition, with consequences on the expression of chemical potentials. One may retrieve the value of flex energy by imposing that the entropy is zero at the experimentally accessible value of glass transition temperature, T_g, on the basis of the arguments invoked by Panayiotou et al. [28]. The value of polymer flex energy obtained using this approach, should be better referred to as an 'apparent' flex energy. Conversely, for the case of the low molecular weight compound, it has been assumed that the molecule is fully flexible, thus implying that $\Delta u_1 = 0$, as proposed by Condo et al. [32].

The theoretical prediction of the T_g of a polymer-penetrant mixture as a function of pressure of penetrant vapor in contact with it, can be obtained by solving, at each value of pressure, the set of equations counting the phase equilibrium condition between polymeric mixture phase and penetrant vapor, and the zeroing of equilibrium configurational entropy of the mixture. To solve the set of equations, one needs to know the values of model parameters, i.e., the NRHB binary interaction parameter (k_{ij}) and the 'apparent' molecular flex energy of the polymer. In detail, at each selected value of pressure, the solution provides, the densities of the two phases and the composition of the binary mixture at equilibrium, as well as the value of the temperature at which the transition occurs, i.e., T_g. It is worth noting that, at each selected pressure, more than one solution could be obtained and hence more than one glass transition temperature could be found. By proceeding in this way, the map of T_g vs. pressure of penetrant can be constructed.

1.6 Thermodynamic Mass Transport model

In this section it is illustrated the development of a model aimed at the determination of a constitutive equation for the isothermal and isobaric diffusion through a multicomponent mixture, “frozen” in an amorphous out-of-equilibrium glassy state, which is formed by a polymer and low-molecular weight compounds. For the sake of clarity, the model is here expressed directly for the cases of ternary and binary systems since these are the ones of interest in the present investigation. Moreover, the model equations will be properly simplified to deal with mixtures in which each penetrant concentration is significantly low (dilute mixture), which is the condition occurring for all the experimental permeability data analysed in this contribution.

In the framework of linear irreversible thermodynamics [40], Sarti and Minelli have assumed the following constitutive equations for the isothermal diffusion in a ternary system formed by two low molecular weight penetrants and a glassy amorphous polymer at uniform temperature, *T*, and pressure, *P*, and neglecting gravitational forces [40]:

$$\boldsymbol{J_1} = L_{11}\boldsymbol{d_1} + L_{12}\boldsymbol{d_2} + L_{1p}\boldsymbol{d_p} \tag{1.94a}$$

$$\boldsymbol{J_2} = L_{21}\boldsymbol{d_1} + L_{22}\boldsymbol{d_2} + L_{2p}\boldsymbol{d_p} \tag{1.94b}$$

$$\boldsymbol{J_p} = L_{p1}\boldsymbol{d_1} + L_{p2}\boldsymbol{d_2} + L_{pp}\boldsymbol{d_p} \tag{1.94c}$$

In all (1.94), subscripts ‘1’ and ‘2’ refer to the corresponding penetrant and ‘p’ to the polymer. $\boldsymbol{J_i}$ represents the diffusive mass flux of component i referred to the mass average velocity of the mixture, and $\boldsymbol{d_i}$**,** the driving force contribution for component *i*, related to the corresponding chemical potential gradient according to the following constitutive expression:

$$\boldsymbol{d_i} = -\rho\omega_i\nabla\left(\frac{\mu_i}{RT}\right)_{T,P} \tag{1.95}$$

where ρ is the mass density of the mixture, ω_i and μ_i are, respectively, the mass fraction and the molar chemical potential of the component *i*.

The Gibbs-Duhem equation imposes the following restriction on the three driving forces:

$$\boldsymbol{d_1} + \boldsymbol{d_2} + \boldsymbol{d_p} = \boldsymbol{0} \tag{1.96}$$

Substituting eq. (1.96) into equations (1.94), the following equations are obtained:

$$\boldsymbol{J_1} = (L_{11} - L_{12})\boldsymbol{d_1} + \left(L_{1p} - L_{12}\right)\boldsymbol{d_p} \tag{1.97a}$$

$$\boldsymbol{J_2} = (L_{22} - L_{21})\boldsymbol{d_2} + (L_{2p} - L_{21})\boldsymbol{d_p} \tag{1.97b}$$

In the case of dilute penetrant-polymer mixtures the chemical potential of the polymer is quite uniform so that the assumption $\boldsymbol{d_p} \cong \boldsymbol{0}$ is reasonable. In this respect, the (1.97a-b) can be simplified as:

$$\boldsymbol{J_1} = (L_{11} - L_{12})\boldsymbol{d_1} \tag{1.98a}$$
$$\boldsymbol{J_2} = (L_{22} - L_{21})\boldsymbol{d_2} \tag{1.98b}$$

Under the same dilute mixture condition, Toni~~,~~ et al. [41] have proposed that the cross-mobility coefficients L_{12} and L_{21} are negligible in comparison, respectively, with L_{11} and L_{22}. Considering this last assumption, equations (1.98a-b) become:

$$\boldsymbol{J_1} = L_{11}\boldsymbol{d_1} \tag{1.99a}$$
$$\boldsymbol{J_2} = L_{22}\boldsymbol{d_2} \tag{1.99b}$$

In the same framework, for a binary penetrant-polymer system, in place of equations (1.98a-b), the following equations can be assumed:

$$\boldsymbol{J_1} = L_{11}\boldsymbol{d_1} + L_{1p}\boldsymbol{d_p} \tag{1.100a}$$
$$\boldsymbol{J_p} = L_{p1}\boldsymbol{d_1} + L_{pp}\boldsymbol{d_p} \tag{1.100b}$$

Again, in view of the Gibbs-Duhem equation, one has:

$$\boldsymbol{d_1} + \boldsymbol{d_p} = \boldsymbol{0} \tag{1.101}$$

And so, from eqs. (1.100a-b) one obtains:

$$\boldsymbol{J_1} = \left(L_{11} - L_{1p}\right)\boldsymbol{d_1} \tag{1.102a}$$
$$\boldsymbol{J_p} = (L_{p1} - L_{pp})\boldsymbol{d_1} \tag{1.102b}$$

Toni et. al., similarly, to the simplification proposed for the ternary system, have assumed that in the case of a binary-system the mutual cross mobility coefficients are negligible as compared to the corresponding self-mobility coefficients, i.e. $L_{1p} \ll L_{11}$ and $L_{p1} \ll L_{pp}$. Consequently equations (1.102a-b) become:

$$\boldsymbol{J_1} = L_{11}\boldsymbol{d_1} \tag{1.103a}$$
$$\boldsymbol{J_p} = -L_{pp}\boldsymbol{d_1} = L_{pp}\boldsymbol{d_p} \tag{1.103b}$$

According to the definition of mass diffusive flux referred to the mass average velocity, one trivially has that $\boldsymbol{J_1} + \boldsymbol{J_p} = \boldsymbol{0}$ so that the two equations of the set of the constitutive equations for diffusive flux can be expressed in terms of the same mobility coefficient, i.e., $L_{11} = L_{pp}$. The mobility coefficients, L_{ij}, are, in principle, dependent on both concentration and temperature. Based on the analysis of penetrant permeation in several isothermal binary amorphous glassy polymer-penetrant mixtures, the group of Sarti et. al. [41-47]~~,~~ have found that an exponential dependence of the penetrant mobility coefficient on penetrant mass fraction was effective in describing experimental results:

$$L_{11} = L_{10}\, exp(\beta_1 \omega_1) \tag{1.104}$$

Starting from equation (1.104), Toni et. al. [41] have inferred that a suitable extension of such dependence in the case of an isothermal penetrant/penetrant/polymer glassy ternary system can be given by:

$$L_{11} = L_{10}\, exp(\beta_1 \omega_1 + \beta_2 \omega_2) \tag{1.105a}$$
$$L_{22} = L_{20}\, exp(\beta_1 \omega_1 + \beta_2 \omega_2) \tag{1.105b}$$

In both binary and ternary systems, L_{i0} represents the positive pre-exponential coefficient of the mobility factor of the species *i,* and it is assumed to be only function of temperature for a given system. β_i is a plasticization factor accounting for the effect of mass concentration of species *i* on the mobility factors and it is also assumed as a constant parameter for a given penetrant-polymer system. A further key feature of the model is that, by setting the mass fraction of a penetrant equal to zero, the equations (1.105a) and (1.105b) at a given *T*, consistently collapses into the corresponding binary sub-system (1.104). It means that L_{i0} (at a given *T*) and β_i (at any *T*) are two constant parameters depending only on the specific couple polymer-penetrant i that is being considered. Therefore L_{i0} and β_i can be retrieved by a non-linear regression of each of the binary polymer-penetrant data corresponding to the multicomponent model under consideration.

In the mass transport model described here, μ_i represents the molar chemical potential of species i at each point, for the considered multicomponent system. In the case of polymer-penetrant mixtures in an amorphous rubbery state, the local expressions of the equilibrium chemical potential and of the equilibrium mixture density as a function of the local concentration, at the fixed uniform values of T and P fields, are needed. To this aim any equilibrium EoS theory could be adopted. When dealing with polymer-penetrant mixtures in a glassy state, the proper expressions of the molar chemical potential fields should be provided by a model specifically suited to describe such kinetically hindered state. In such a case the two sides of a glassy polymer membrane are exposed to gas mixtures (penetrants) with different, time invariant, compositions and/or pressure. In formulating the constitutive expressions of mass flux of penetrant through the polymer membrane, the convective contribution has been neglected since this effect is not to be considered at steady state**.**

Notably, as dictated by the II law of thermodynamics [48-49], both NELF and NETGP-NRHB expressions of the penetrant chemical potential are only function of T and composition. This allows to adopt the isothermal and isobaric constitutive equations described in this section, independently from the knowledge of the current value of the pressure field established within the membrane in the steady state (SS) permeation process. Actually, this situation holds in all the investigated systems, in which the polymeric membrane is exposed on one side to a gas mixture with a fixed higher-pressure P^{up} and a given upstream concentration (upstream side) and on the other side is in contact with a gas mixture with a fixed lower pressure P^{d} and a given downstream concentration (downstream side).

In summary, equations (1.95), (1.99a) and (1.99b) and equations (1.95), (1.103a) and (1.103b) represent the operative expressions adopted here to model the permeation of binary gas mixtures and pure gases, respectively, and the expressions of the molar chemical potential adopted for the penetrants involved are provided by the NETGP-NRHB theory.

In view of the geometry of the systems investigated, i.e., fixed uniform B.C. and a value of membrane thickness, ξ, much smaller than that of the other two membrane dimensions, we can focus on the simpler case of 1-D mass transport so that equations (1.95), (1.99a) and (1.99b), expressed in a rectangular Cartesian coordinate system, become:

$$\boldsymbol{J_1} = -\rho L_{11}\left(\omega_1 \frac{\partial}{\partial \omega_1}\left(\frac{\mu_1}{RT}\right)\frac{\partial \omega_1}{\partial x} + \omega_1 \frac{\partial}{\partial \omega_2}\left(\frac{\mu_1}{RT}\right)\frac{\partial \omega_2}{\partial x}\right)\hat{\boldsymbol{x}} \tag{1.106a}$$

$$\boldsymbol{J_2} = -\rho L_{22}\left(\omega_2 \frac{\partial}{\partial \omega_1}\left(\frac{\mu_2}{RT}\right)\frac{\partial \omega_1}{\partial x} + \omega_2 \frac{\partial}{\partial \omega_2}\left(\frac{\mu_2}{RT}\right)\frac{\partial \omega_2}{\partial x}\right)\hat{\boldsymbol{x}} \tag{1.106b}$$

Where x represents the Cartesian coordinate taken along the membrane thickness, and $\hat{\boldsymbol{x}}$ represents the corresponding unit-vector. Consequently, four different thermodynamics factors are involved, which are related to the molar chemical potential dependence from the mass fraction of the two penetrants at fixed T:

$$\alpha_{i,j}(\omega_1, \omega_2) \equiv \omega_i \frac{\partial}{\partial \omega_j}\left(\frac{\mu_i}{RT}\right) \quad i = 1,2; j = 1,2 \tag{1.107}$$

In a similar fashion, under the same 1-D mass transport case, equations (1.95), (1.103a) and (1.103b), provide, for the expression of the penetrant diffusive mass flux:

$$\boldsymbol{J_1} = -\rho L_{11}\omega_1 \frac{\partial}{\partial \omega_1}\left(\frac{\mu_1}{RT}\right)\hat{x} \tag{1.108}$$

where $\alpha_{1,1}(\omega_1) \equiv \omega_1 \frac{\partial}{\partial \omega_1}\left(\frac{\mu_1}{RT}\right)$ represents the binary thermodynamic factor of interest.
As discussed above, in a dilute polymer-penetrants mixture in isothermal conditions, the corresponding penetrant mass transport mechanism can be effectively described as a pure diffusive phenomenon. For a polymer membrane exposed to a binary penetrant mixture (ternary system), under time-invariant B.C.s, uniform on each of the two surfaces, at steady state the penetrant mass balance equations become:

$$\begin{cases} 0 = \frac{\partial \rho_1}{\partial t} = -\frac{\partial\left(\rho L_{11}\left(\omega_1 \frac{\partial}{\partial \omega_1}\left(\frac{\mu_1}{RT}\right)\frac{\partial \omega_1}{\partial x} + \omega_1 \frac{\partial}{\partial \omega_2}\left(\frac{\mu_1}{RT}\right)\frac{\partial \omega_2}{\partial x}\right)\right)}{\partial x} \\ 0 = \frac{\partial \rho_2}{\partial t} = -\frac{\partial\left(\rho L_{22}\left(\omega_1 \frac{\partial}{\partial \omega_1}\left(\frac{\mu_2}{RT}\right)\frac{\partial \omega_1}{\partial x} + \omega_1 \frac{\partial}{\partial \omega_2}\left(\frac{\mu_2}{RT}\right)\frac{\partial \omega_2}{\partial x}\right)\right)}{\partial x} \\ \qquad x = 0 : \rho_1 = \rho_1^{up} \;\; \rho_2 = \rho_2^{up} \\ \qquad x = \xi : \rho_1 = \rho_1^{d} \;\; \rho_2 = \rho_2^{d} \end{cases} \tag{1.109}$$

where superscripts ‘up’ and ‘d’ indicate, respectively, the upstream side and the downstream side of the polymeric membrane. ρ_i indicates the density of penetrant *i* within the polymer-penetrant mixture and finally ξ represents the SS membrane thickness.
Equations (1.109) represent a II order boundary value problem where the unknowns are the SS concentration profiles of the two penetrants which comply to the imposed B.C.s. These profiles allow the calculation of spatially uniform values of $\boldsymbol{J_1^{ss}}$ and $\boldsymbol{J_2^{ss}}$. This problem can be solved numerically by using a finite difference scheme so that it results in a system of non-linear algebraic equations, which can be trivially solved using the Newton-Raphson method. The B.C.s to be imposed to the penetrants mass concentrations within the polymer at the upstream and downstream interfaces must be consistently provided by the PE predictions provided by the NETGP-NRHB model, for the assigned values of *P*, *T* and composition of the external gas phase, at the upstream and downstream sides.
Similarly, in the case of a binary polymer-penetrant systems we have the following SS boundary value problem:

$$\begin{cases} 0 = \frac{\partial \rho_1}{\partial t} = -\frac{\partial\left(\rho L_{11}\omega_1 \frac{\partial}{\partial \omega_1}\left(\frac{\mu_1}{RT}\right)\frac{\partial \omega_1}{\partial x}\right)}{\partial x} \\ \qquad x = 0 : \rho_1 = \rho_1^{up} \\ \qquad x = \xi : \rho_1 = \rho_1^{d} \end{cases} \tag{1.110}$$

where subscript '1' refers to the penetrant.

Once equations (1.109) or (1.110) have been solved, the SS mass concentration profiles are determined so that, according to equations (1.106a), (1.106b) and (1.108) for the ternary and binary cases, respectively, the SS expressions for the penetrants diffusive mass fluxes can be obtained. Finally, the SS permeability of penetrant i, p_i, can be calculated, in the case of a polymer membrane exposed to gas mixtures at different partial pressure, as:

$$p_i = \frac{J_{i,x}^{SS}\xi/M_{wi}}{P_i^{up}-P_i^{d}} \tag{1.111}$$

where $J_{i,x}^{SS}$ represents the SS component of the mass flux $\boldsymbol{J_i^{SS}}$ in the x directions, P_i^{up} and P_i^{d} the partial pressure of penetrant *i* in the external gas mixture at upstream and at downstream sides, respectively.

In both binary and ternary systems, L_{i0} represents the positive pre-exponential coefficient of the mobility factor of the species *i,* and it is assumed to be only function of temperature for a given couple of i-th species and polymer. β_i is a "concentration" factor accounting for the effect of mass concentration of species i on the mobility factors and it is also assumed to be a constant parameter for a given penetrant within a given polymeric system. Therefore, L_{i0} and β_i to be used in the case of permeation of multicomponent gaseous mixtures can be retrieved by a non-linear regression of the corresponding binary polymer-penetrant mass transport data.

References

[1] J. J. Licari, Coating Materials for Electronic Applications, Noyes Publications: Totnes, Devon UK, (2004).

[2] E. Kirian, J. C. Hassler, High-Pressure Torsional Braid Analysis (HP-TBA): A new technique for assessment of thermal transitions and changes in moduli ofpolymers exposed to supercritical or compressed fluids, J. Supercrit. Fluids, 143 (2019).

[3] R. D. Noble, S. A. Stern, Membrane Separations Technology Principles and Applications, Membrane Science and Technology Series, 2 (1995).

[4] I. C. Sanchez, R. H. Lacombe, An Elementary Molecular Theory of Classical Fluids. Pure Fluids, The Journal of Physical Chemistry, (1976) 80 (21), 2352-2362.

[5] R. H. Lacombe, I. C. Sanchez, Statistical Thermodynamics of Fluid Mixtures, The Journal of Physical Chemistry, (1976) 80 (23), 2568-2580.

[6] I. C. Sanchez, R. H. Lacombe, Statistical Thermodynamics of Polymer Solutions, (1978) 11 (6), 1145-1156.

[7] P. J. Flory, Principles of Polymer Chemistry, Cornell University Press, New York, USA (1953) 495—539.

[8] E. Neau, A consistent method for phase equilibrium calculation using the Sanchez–Lacombe lattice–fluid equation-of-state, Fluid Phase Equilibria (2002) 203, 133–140.

[9] C. Nicolas, E. Neau, S. Meradjiac, I. Raspoac, The Sanchez-Lacombe lattice fluid model for the modelling of solids in supercritical fluids, Fluid Phase Equilibria (2005) 232, 219–229.

[10] K. von Konigslow, C.B. Park, R.B. Thompson, Phys. Rev. Appl. (2017) 8, 044009.

[11] K. von Konigslow, An Off-lattice Derivation and Thermodynamic Consistency Consideration for the Sanchez-Lacombe Equation of State, Ph.D. Thesis University of Waterloo, Waterloo, Ontario, Canada, 2017.
[12] K. von Konigslow, C.B. Park, R.B. Thompson, Soft Matter (2018) 14, 4603-4614.
[13] S. Brandani, The Rigid Adsorbent Lattice Fluid Model for Pure and Mixed Gas Adsorption, AIChE J, (2019) 65, 1304-1314.
[14] C. Panayiotou, M. Pantoula, E. Stefanis, I. Tsivintzelis, I. G. Economou, Nonrandom Hydrogen-Bonding Model of Fluids and Their Mixtures. 1. Pure Fluids, Ind. Eng. Chem. Res. (2004) 43, 6592-6606.
[15] C. Panayiotou, I. Tsivintzelis, I. G. Economou, Nonrandom Hydrogen-Bonding Model of Fluids and Their Mixtures. 2. Multicomponent Mixtures, Ind. Eng. Chem. Res. (2007) 46, 2628-2636.
[16] A. Grenner, I. Tsivintzelis, I. G. Economou, C. Panayiotou, G. M. Kontogeorgis, Evaluation of the Nonrandom Hydrogen Bonding (NRHB) Theory and the Simplified Perturbed-Chain-Statistical Associating Fluid Theory (sPC-SAFT). 1.Vapor-Liquid Equilibria, Ind. Eng. Chem. Res. (2008) 47, 5636–5650.
[17] I. Tsivintzelis, A. Grenner, I. G. Economou, G. M. Kontogeorgis, Evaluation of the Nonrandom Hydrogen Bonding (NRHB) Theory and the Simplified-Perturbed-Chain-Statistical Associating Fluid Theory (sPC-SAFT). 2. Liquid-Liquid Equilibria and Prediction of Monomer Fraction in Hydrogen Bonding Systems, Ind. Eng. Chem. Res. (2008) 47, 5651–5659.
[18] G. Mensitieri, G. Scherillo, C. Panayiotou, P. Musto, Towards a predictive thermodynamic description of sorption processes in polymers: The synergy between theoretical EoS models and vibrational spectroscopy, Materials Science & Engineering R (2020) 140, 100525.
[19] G. Scherillo, L. Sanguigno, L. Sansone, E. Di Maio, M. Galizia, G. Mensitieri, Thermodynamics of water sorption in poly(ε-caprolactone): A comparative analysis of lattice fluid models including hydrogen bond contributions, Fluid Phase Equilibria 313 (2012) 127– 139.
[20] G. Scherillo, M. G. Pastore Carbone, M. Petretta, P. La Manna, C. Panayiotou, D. N. Bikiarise, P. Musto, G. Mensitieri, Water sorption thermodynamics in poly(propylene sebacate), Polymer (2016) 97, 346-371.
[21] M. G. Pastore Carbone, P. Musto, M. Pannico, A. Braeuer, G. Scherillo, G. Mensitieri, E. Di Maio, Raman Line Imaging of Poly(ε-caprolactone)/Carbon Dioxide Solutions at High Pressures: A Combined Experimental and Computational Study for Interpreting Intermolecular Interactions and Free-Volume Effects, Phys. Chem. B (2016) 120, 9115−9131.
[22] A. Fredenslund, R.L. Jones, J.M. Prausnitz, AIChE J. (1975) 21, 1086.
[23] A. Fredenslund, M.J. Sorensen, In: Models for Thermodynamic and Phase Equilibria Calculations; Sandler S., Ed.; Marcel Dekker: New York (1994).
[24] M.M. Coleman, J.F. Graf, P.C. Painter, P.C., Specific Interactions and the Miscibility of Polymer Blends. Technomic: Lancaster, PA, (1991).
[25] A. J. Staverman, The Entropy of High Polymer Solutions. Generalization of Formulae. Recl. Trav. Chim. Pays-Bas (1950) 69, 163-174.
[26] E. A. Guggenheim, Mixtures, Oxford University Press: Oxford, U.K., (1952).
[27] B. A. Veytsman, Are Lattice Models Valid for Fluids with Hydrogen Bonds?, J. Phys. Chem. (1990) 94, 8499-8500.
[28] J. Prinos, C. Panayiotou, Glass transition temperature in hydrogen-bonded polymer mixtures, Polymer 36 (1995) 1223.
[29] I. Tsivintzelis, I. G. Economou, G. M. Kontogeorgis, Modeling the Phase Behavior in Mixtures of Pharmaceuticals with Liquid or Supercritical Solvents, J. Phys. Chem. B 113 (2009) 6446–6458.
[30] G. Scherillo, M. Galizia, P. Musto and G. Mensitieri, Water Sorption Thermodynamics in Glassy and Rubbery Polymers: Modeling the Interactional Issues Emerging from FTIR Spectroscopy, Ind. Eng. Chem. Res. 52 (2013) 8674−8691.
[31] G.C. Sarti, F. Doghieri, Predictions of the solubility of gases in glassy polymers based on the NELF model, Chem. Eng. Sci. 53, 19 (1998) 3435-3447.
[32] P. D. Condo, I. C. Sanchez, C. G. Panayiotou, K. P. Johnston, Glass Transition Behavior Including Retrograde Vitrification of Polymers with Compressed Fluid Diluents. Macromolecules, 25 (1992) 6119-6127.
[33] J. H. Gibbs, E. [33] A. Di Marzio, Nature of the Glass Transition and the Glassy State. J. Chem. Phys., 28 (1958) 373-383.
[34] E. A. Di Marzio, J. H. Gibbs, Chain Stiffness and the Lattice Theory of Polymer Phases. J. Chem. Phys., 28 (1958) 807-813.

[35] E. A. Di Marzio, J. H. Gibbs, Molecular Interpretation of Glass Temperature Depression by Plasticizers. J. Pol. Sci.: Part A, 1 (1963) 1417-1428.

[36] D. Pierleoni, M. Minelli, G. Scherillo, G. Mensitieri, V. Loianno, F. Bonavolontà, F. Doghieri, Analysis of Polystyrene-Toluene System through 'Dynamic' Sorption Tests: Glass Transitions and Retrograde Vitrification', J. Phys. Chem. B, 121 (2017) 9969-9981.

[37] A. B. Bestul, S. S. J. Chang, Chem. Phys., ,40 (1964) 731.

[38] G. Adam, J. H. J. Gibbs, Chem. Phys., 43 (1965), 139.

[39] I. Tsivintzelis, A. G. Angelopoulou, C. Panayiotou, Foaming of polymers with supercritical CO2: An experimental and theoretical study. Polymer, 48 (2007) 5928-5939.

[40] R.B. Bird, D.J. Klingenberg, Multicomponent diffusion brief review, Adv. Water Res. 62 (2013) 238-242.

[41] E. Toni, M. Minelli, G. C. Sarti, A predictive model for the permeability of gas mixtures in glassy polymers, Fluid Phase Equilibria 455 (2018) 54-62.

[42] M. Minelli, G.C. Sarti, Permeability and diffusivity of CO_2 in glassy polymers with and without plasticization, J. Membrane Sci. 435 (2013) 176-185.

[43] M. Minelli, G.C. Sarti, Thermodynamic model for the permeability of light gases in glassy polymers, AIChE J. 61 (2015) 2776-2788.

[44] M. Minelli, G.C. Sarti, Thermodynamic basis for vapor permeability in Ethyl Cellulose, J. Membrane Sci. 473 (2015) 137-145.

[45] M. Minelli, G.C. Sarti, Thermodynamic modeling of gas transport in glassy polymeric membranes, Membranes 7 (2017) 46.

[46] M. Minelli, G.C. Sarti, Permeability and solubility of carbon dioxide in different glassy polymer systems with and without plasticization, J. Membrane Sci. 444 (2013) 429-439.

[47] M. Minelli, Modeling CO_2 solubility and transport in poly(ethylene terephthalate) above and below the glass transition, J. Membrane Sci. 451 (2014) 305-311.

[48] F. Doghieri, M. Canova, G.C. Sarti, B.D. Freeman, I. Pinnau, Polymer Membranes for Gas and Vapor Separation, Am. Chem. Soc. Symp. Series 733, ACS, Washington D.C., 1999.

[49] G. Scherillo, L. Sanguigno, M. Galizia, M. Lavorgna, P. Musto, G. Mensitieri, Non-equilibrium compressible lattice theories accounting for hydrogenbonding interactions: Modelling water sorption thermodynamics influorinated polyimides, Fluid Phase Equilibr. 334 (2012) 166-188.

Chapter 2
Thermodynamic consistency of NRHB model for multicomponent mixtures

A fundamental aim of the Ph.D. program has been to assess the thermodynamic consistency of the NRHB model for multicomponent systems in the limit of ideal gas mixtures. This is not a trivial task, since the development of the NRHB model involves a larger set of *internal* state variables as compared to the SL model, thus making this assessment more complex to perform. The first part of this chapter is dedicated to a mathematical revision of the NRHB model in the ($\underline{\mathrm{N}}$, V, T) ensemble, which is a key point in order to simplify mathematical procedure required for the assessment of consistency of the NRHB model. Next, the analysis has been carried out by checking that the expressions provided by the NRHB theory for both the EoS and the chemical potentials in multicomponent mixtures converge, in the limit for $P \to 0$ or for $V \to +\infty$ (i.e., IG limit), to those of a mixture of ideal gases. Finally, the results obtained in the ($\underline{\mathrm{N}}$, V, T) ensemble have been correlated to the original and operative ($\underline{\mathrm{N}}$,P,T) ensemble of the NRHB model. The obtained results and the procedure have been already published in literature by the author of the thesis, the interested reader can also refer to the original article [1] to study in deep the mathematical procedure and the outcomes. However, an exhaustive summary is reported in this chapter.

2.1 Revisiting the NRHB constitutive class in $\left(V, T, \underline{N}\right)$ ensemble

As mentioned above, before assessing the consistency of the NRHB theory, we first perform a re-elaboration of the model adopting as a general, non-equilibrium, constitutive class the set of *external* and *internal* state variables $\left(V, T, \underline{N}, \underline{N}_{ij}, \underline{N}_{\alpha\beta}^{HB}\right)$ in place of the one adopted in the original $\left(P, T, \underline{N}, V, \underline{N}_{ij}, \underline{N}_{\alpha\beta}^{HB}\right)$. Correspondingly, at equilibrium, the state variables that are used in the present context are the set $\left(V, T, \underline{N}\right)$ in place of $\left(P, T, \underline{N}\right)$. Based on thermodynamics with *internal* [2-6] state variables, developed to describe non-equilibrium systems [2], and applying the constraints dictated by the II law of thermodynamics inequality on the system with the constitutive class $\left(V, T, \underline{N}, \underline{N}_{ij}, \underline{N}_{\alpha\beta}^{HB}\right)$, one can obtain the minimization conditions for Helmholtz energy, A, as a function of the *internal* state variables, i.e., $\underline{N}_{ij}, \underline{N}_{\alpha\beta}^{HB}$, and can also recover the classical equilibrium relationships between thermodynamic properties.

The symbols used in this chapter have the same meaning and definition of the ones already shown in the Chapter 1.

We recall that in the $(V, T, \underline{N})$ ensemble, the NRHB model refers to a spatially uniform closed system displaying a set of t component molecules $\underline{N} = (N_1, N_2, \dots, N_t)$, a temperature T and a volume V.

In particular, $(V, T, \underline{N})$ represents the set of *external* state variables while $(\underline{N}_{ij}, \underline{N}^{HB}_{\alpha\beta})$ represents the set of *internal* state variables [3, 4, 7, 8], where the vector variables $\underline{N}_{ij}$ and $\underline{N}^{HB}_{\alpha\beta}$ represent the set of N_{ij} and $N^{HB}_{\alpha\beta}$ contacts, respectively, already defined in the Section 1.3.3. All the thermodynamic state functions depend on the *external* and *internal* variables through constitutive expressions. We also remark that according to the (1.31) only a sub-set of $\underline{N}_{ij}$ is made of independent variables, in particular the sub-set selected is intended containing all N_{ij} with $j > i$.

By applying the II law inequality for the constitutive class of interest (see calculation details in Section A.1 in the Appendices) one obtains the following equilibrium minimization conditions:

$$\left[\left(\frac{\partial A}{\partial N_{ij}}\right)_{V,T,\underline{N},N_{rs\neq ij},\underline{N}^{HB}_{\alpha\beta}}\right]^{eq} = 0 \quad \text{for each } i = 0, 1, \dots, t \text{ and } j > i \tag{2.1}$$

$$\left[\left(\frac{\partial A}{\partial N^{HB}_{\alpha\beta}}\right)_{V,T,\underline{N},\underline{N}_{ij},N^{HB}_{\gamma\delta\neq\alpha\beta}}\right]^{eq} = 0 \quad \text{for each } \alpha = 1, 2, \dots, n \text{ and } \beta = 1,2, \dots, m \tag{2.2}$$

and recovers the fundamental relationship [9, 10]:

$$\left(\frac{\partial A}{\partial V}\right)^{eq} = -P^{eq} \tag{2.3}$$

The superscript '*eq*' indicates the equilibrium conditions. By following an analogous procedure showed in Section 1.3.3, the equation (2.3), coupled with equations (2.1) and (2.2), can be used to obtain the Equation of State (EoS) starting from the expression of the Helmholtz energy, A, provided by the NRHB model. The expression of the EoS obtained in this way is, consistently, identical to the expression originally obtained by Panayiotou et al. [7, 8] in the $(P, T, \underline{N})$ equilibrium ensemble.

As already explained, a statistical mechanics standard procedure consists in searching for the expressions of thermodynamic functions at equilibrium for a given $(V, T, \underline{N})$, the sum of the partition function is approximated by its maximum term. For the Helmholtz energy this is equivalent to equating its non-equilibrium value, A, to the logarithm of the generic term in the partition function and then minimizing it with respect to *internal* state variables (obtaining equations (2.1) and (2.2)).

Alternatively, the expression of non-equilibrium A in the $(V, T, \underline{N})$ ensemble can be obtained from the equation (1.66a), provided by the NRHB model [1]:

$$\frac{A}{kT} = \frac{A}{kT} + \frac{P\left(V_{LF} + \sum_{\alpha}^{m} \sum_{\beta}^{n} N_{\alpha\beta}^{HB} V_{\alpha\beta}^{0}\right)}{kT} = -rN\left\{-\sum_{i=1}^{t} \frac{\phi_i}{r_i} ln\, \delta_i - \frac{l}{r} + \sum_{i=1}^{t} \frac{\phi_i}{r_i} ln \frac{\phi_i}{r_i} + \frac{ln\, \tilde{\rho}}{r} + (\tilde{v} - 1)\, ln(1 - \tilde{\rho}) - \frac{z}{2}\left(\tilde{v} - 1 + \frac{q}{r}\right) ln\left(1 - \tilde{\rho} + \frac{q}{r}\tilde{\rho}\right)\right\} + rN\left\{\sum_{i=0}^{t}\left(\frac{N_i z q_i}{2rN}\right) ln\left[\Gamma_{ii}\, exp\left(-\frac{\varepsilon_{ii}}{kT}\right)\right] + \sum_{i=0}^{t}\sum_{j>i}^{t} \frac{N_{ij}}{2rN}\, ln\left[\frac{{\Gamma_{ij}}^{2}}{\Gamma_{ii}\Gamma_{jj}}\, exp\left(-\frac{\Delta\varepsilon_{ij}}{kT}\right)\right]\right\} + rN\left\{\sum_{\alpha}^{m}\sum_{\beta}^{n} \nu_{\alpha\beta}\, \left[1 + \frac{A_{\alpha\beta}^{0}}{kT} + ln\left(\frac{\tilde{v}\, \nu_{\alpha\beta}}{\nu_{\alpha 0}\, \nu_{0\beta}}\right)\right] + \sum_{\alpha}^{m} \nu_{d}^{\alpha}\, ln \frac{\nu_{\alpha 0}}{\nu_{d}^{\alpha}} + \sum_{\beta}^{n} \nu_{a}^{\beta}\, ln \frac{\nu_{0\beta}}{\nu_{a}^{\beta}}\right\} \tag{2.4}$$

The meaning of the symbols used in equation (2.4) and in the following expressions related to the NRHB theory is reported in ref. [11] and have the same meaning of the Chapter 1. It is worth reminding that the molecular volume of the mixture, depends on the lattice fluid volume contribution corrected by the hydrogen bonds contribution. Formally:

$$v = \frac{V}{N} = \frac{1}{N}(N_0 + rN)\, v^* + \frac{1}{N}\sum_{\alpha}^{m}\sum_{\beta}^{n} N_{\alpha\beta}^{HB}\, V_{\alpha\beta}^{0} = r\tilde{v}v^* + \frac{1}{N}\sum_{\alpha}^{m}\sum_{\beta}^{n} N_{\alpha\beta}^{HB}\, V_{\alpha\beta}^{0} \tag{2.5a}$$

and then:

$$\tilde{v} = \frac{v}{rv^*} - \frac{1}{rNv^*}\sum_{\alpha}^{m}\sum_{\beta}^{n} N_{\alpha\beta}^{HB}\, V_{\alpha\beta}^{0} \tag{2.5b}$$

Notably, in the NRHB theory the characteristic cell volume of the lattice (or, equivalently the segmental volume), v^*, is assumed to be a universal constant (equal to 9.75/N_A cm^3/molecular segment, where N_A is the Avogadro number) differently from the SL model in which v^* depends instead on the composition.

Inserting equations (2.4), (2.5a-b) into equations (2.1) and (2.2) respectively, one obtains:

$$\frac{{\Gamma_{ij}}^{2}}{\Gamma_{ii}\,\Gamma_{jj}} = exp\left(-\frac{\Delta\varepsilon_{ij}}{kT}\right) \quad \text{for each } i, j = 0,1, \ldots, t \text{ and } j > i \tag{2.6}$$

and

$$ln\left(\frac{\tilde{v}\,\nu_{\alpha\beta}}{\nu_{\alpha 0}\,\nu_{0\beta}}\right)+\frac{A^0_{\alpha\beta}}{kT}-\frac{V^0_{\alpha\beta}}{v^*}\left[ln(1-\tilde{\rho})-\tilde{\rho}\left(\frac{l}{r}-\nu_H\right)-\frac{z}{2}ln\left(1-\tilde{\rho}+\frac{q}{r}\tilde{\rho}\right)+\frac{z}{2}ln\Gamma_{00}\right]=0$$

for each α,β (2.7)

Once again, the solution of the sets of minimization conditions provides the equilibrium functions $\underline{N}^{eq}_{ij}(V,T,\underline{N})$ and $\underline{N}^{HB,eq}_{\alpha\beta}(V,T,\underline{N})$ that can be then substituted in eq. (2.4) to provide the equilibrium expression of A, i.e., $A^{eq}(V,T,\underline{N})$. However, analogously to the expressions for the *internal* variables of the Section 1.3, no analytical closed form is available for $A^{eq}(V,T,\underline{N})$.

In the ensemble $(V,T,\underline{N})$ the Helmholtz energy A is a potential for pressure, both at equilibrium and non-equilibrium conditions, as detailed in section 1 of the Appendices, so one can write:

$$P=-\left(\frac{\partial A}{\partial V}\right)_{T,\underline{N},\underline{N}_{ij},\underline{N}^{HB}_{\alpha\beta}} \qquad (2.8)$$

After some algebra, eq. (2.8) can be expressed as:

$$P=-\frac{kT}{v^*}\left[ln(1-\tilde{\rho})-\tilde{\rho}\left(\frac{l}{r}-\nu_H\right)-\frac{z}{2}ln\left(1-\tilde{\rho}+\frac{q}{r}\tilde{\rho}\right)+\frac{z}{2}ln\Gamma_{00}\right] \qquad (2.9)$$

Equation (2.11) holds in general and provides the out of equilibrium value of pressure. At a given $(V,T,\underline{N})$, the equilibrium pressure is still provided by $P^{eq}=-\left(\frac{\partial A^{eq}}{\partial V}\right)_{T,\underline{N}}$ and it can be calculated using the general out-of-equilibrium expression of the pressure, (2.9), in combination with the minimization conditions equations (2.6-2.7).

The expression of the equilibrium chemical potential of species i is obtained by calculating the partial derivative of $A^{eq}(V,T,\underline{N})$ with respect to N_i, at fixed V, T and $N_{j\neq i}$. However, since, as discussed above, a closed analytical form for $A^{eq}(V,T,\underline{N})$ is unavailable, the chemical potential has to be calculated using the chain rule for the evaluation of derivatives by reminding that $A^{eq}(V,T,\underline{N})=A\left(V,T,\underline{N},\underline{N}^{eq}_{ij}(V,T,\underline{N}),\underline{N}^{HB,eq}_{\alpha\beta}(V,T,\underline{N})\right)$, thus:

$$\frac{\mu_i^{eq}}{kT} \overset{\text{def}}{=} \frac{1}{kT}\left(\frac{\partial A^{eq}}{\partial N_i}\right)_{V,T,N_{j\neq i}} = \frac{1}{kT}\left(\frac{\partial A}{\partial N_i}\right)_{V,T,N_{j\neq i},\underline{N}_{ij}^{eq},\underline{N}_{\alpha\beta}^{HB,eq}} +$$
$$\sum_{i=0}^{t}\sum_{j>i}^{t}\left(\frac{\partial A}{\partial N_{ij}}\right)_{V,T,\underline{N},N_{rs\neq ij}^{eq},\underline{N}_{\alpha\beta}^{HB,eq}}\left(\frac{\partial N_{ij}^{eq}}{\partial N_i}\right)_{V,T,N_{j\neq i}} +$$
$$\sum_{\alpha}^{m}\sum_{\beta}^{n}\left(\frac{\partial A}{\partial N_{\alpha\beta}^{HB}}\right)_{V,T,\underline{N},\underline{N}_{ij}^{eq},N_{\gamma\delta\neq\alpha\beta}^{HB,eq}}\left(\frac{\partial N_{\alpha\beta}^{HB,eq}}{\partial N_i}\right)_{V,T,N_{j\neq i}} \tag{2.10}$$

Recalling the minimization conditions, equations (2.1-2.2), one obtains:

$$\frac{\mu_i^{eq}(V,T,\underline{N})}{kT} = \frac{1}{kT}\left(\frac{\partial A}{\partial N_i}\right)_{V,T,N_{j\neq i},\underline{N}_{ij}^{eq},\underline{N}_{\alpha\beta}^{HB,eq}} \tag{2.11}$$

In conclusion, operatively, the expression of the chemical potential at equilibrium is obtained by coupling its non-equilibrium expression, i.e. $\frac{1}{kT}\left(\frac{\partial A}{\partial N_i}\right)_{V,T,N_{j\neq i},\underline{N}_{ij},\underline{N}_{\alpha\beta}^{HB}}$, with the sets of minimization conditions.

The expression of the non-equilibrium chemical potential of a generic species *i*, in the framework of the NRHB model, is given by:

$$\frac{\mu_i}{kT} = ln\frac{\Phi_i}{\delta_i\, r_i} - r_i\frac{l}{r} + ln\,\tilde{\rho} + r_i(\tilde{v}-1)\,ln(1-\tilde{\rho}) - \frac{z}{2}r_i\left(\tilde{v}-1+\frac{q_i}{r_i}\right)ln\left(1-\tilde{\rho}+\frac{q}{r}\tilde{\rho}\right) + \frac{z\,q_i}{2}\left[ln\,\Gamma_{ii} + \frac{r_i}{q_i}(\tilde{v}-1)\,ln\,\Gamma_{00}\right] - \frac{q_i}{\tilde{T}_i} + r_i\nu_H - \sum_{\alpha}^{m} d_{\alpha}^{i}\,ln\left(\frac{\nu_d^{\alpha}}{\nu_{\alpha 0}}\right) - \sum_{\beta}^{n} a_{\beta}^{i}\,ln\left(\frac{\nu_a^{\beta}}{\nu_{0\beta}}\right) - \left[ln(1-\tilde{\rho}) - \tilde{\rho}\left(\frac{l}{r}-\nu_H\right) - \frac{z}{2}ln\left(1-\tilde{\rho}+\frac{q}{r}\tilde{\rho}\right) + \frac{z}{2}ln\Gamma_{00}\right]r_i\tilde{v} \tag{2.12}$$

In view of the previous discussion, the equilibrium chemical potential of a generic species *i* is then operatively obtained by coupling eq. (2.6) eq. (2.7) and eq. (2.12).

Starting from equation (2.9), it can be demonstrated that eq. (2.7) becomes:

$$ln\left(\frac{\tilde{v}\,\nu_{\alpha\beta}}{\nu_{\alpha 0}\,\nu_{0\beta}}\right) + \frac{A_{\alpha\beta}^{0}}{kT} - \frac{V_{\alpha\beta}^{0}}{v^{*}}\left[ln(1-\tilde{\rho}) - \tilde{\rho}\left(\frac{l}{r}-\nu_H\right) - \frac{z}{2}ln\left(1-\tilde{\rho}+\frac{q}{r}\tilde{\rho}\right) + \frac{z}{2}ln\Gamma_{00}\right]$$
$$= ln\left(\frac{\tilde{v}\,\nu_{\alpha\beta}}{\nu_{\alpha 0}\,\nu_{0\beta}}\right) + \frac{A_{\alpha\beta}^{0}}{kT} + \frac{PV_{\alpha\beta}^{0}}{kT} = 0 \iff$$
$$\frac{\tilde{v}\,\nu_{\alpha\beta}}{\nu_{\alpha 0}\,\nu_{0\beta}} = \exp\left(-\frac{A_{\alpha\beta}^{0}+PV_{\alpha\beta}^{0}}{\mathrm{kT}}\right) = \exp\left(-\frac{G_{\alpha\beta}^{0}}{\mathrm{kT}}\right) \quad \text{for each } \alpha,\beta \tag{2.13}$$

while eq. (2.12) becomes:

$$\frac{\mu_i}{kT} = ln\frac{\Phi_i}{\delta_i\, r_i} - r_i\frac{l}{r} + ln\,\tilde{\rho} + r_i(\tilde{v}-1)\,ln(1-\tilde{\rho}) - \frac{z}{2}r_i\left(\tilde{v}-1+\frac{q_i}{r_i}\right)ln\left(1-\tilde{\rho}+\frac{q}{r}\tilde{\rho}\right) + \frac{z\,q_i}{2}\left[ln\,\Gamma_{ii}+\frac{r_i}{q_i}(\tilde{v}-1)\,ln\,\Gamma_{00}\right] - \frac{q_i}{\tilde{T}_i} + r_i\nu_H - \sum_{\alpha}^{m} d_{\alpha}^{i}\,ln\left(\frac{\nu_d^{\alpha}}{\nu_{\alpha 0}}\right) - \sum_{\beta}^{n} a_{\beta}^{i}\,ln\left(\frac{\nu_a^{\beta}}{\nu_{0\beta}}\right) + \mathrm{r_i}\frac{\tilde{\mathrm{P}}\,\tilde{\mathrm{v}}}{\tilde{\mathrm{T}}} \tag{2.14}$$

We can now prove that the expressions for the equilibrium chemical potentials of the components of a mixture obtained in the $(V,T,\underline{N})$ ensemble are identical to those obtained in the $(P,T,\underline{N})$. As first point, we observe that eq. (2.9) takes the same form of the general non-equilibrium expression for P provided by Panayiotou et al. through minimization of Gibbs energy (see Section 1.3) as a function of V in the $(P,T,\underline{N})$ ensemble [7, 8, 11]. Similarly, also eqs. (2.6) take the same form of expressions obtained by Panayiotou in the $(P,T,\underline{N})$ ensemble starting from the G [7, 8, 11]. Finally, provided that P is given by eq. (2.9), eq. (2.13) and eq. (2.14) take the same form of the corresponding expressions obtained in the $(P,T,\underline{N})$ ensemble. Since, Panayiotou et al. have shown in $(P,T,\underline{N})$ ensemble that the equilibrium chemical potential is obtained by coupling its non-equilibrium expression with the minimization conditions [7, 8, 11], therefore, we can conclude that the equilibrium expressions of the chemical potential of a species i at a given $(V,T,\underline{N})$ corresponds to its equilibrium chemical potential at a given $(P,T,\underline{N})$ when $P = P^{eq}(V,T,\underline{N})$.

Details of the calculations involved to obtain the results reported above are described in Section A.2 of the Appendices. All the details of the calculation have been developed by the author of this thesis and can be found in literature [1]

2.2 Thermodynamic consistency of NRHB Equation-of-State for multicomponent mixtures at equilibrium in the ideal gas limit

The first step in the assessment of the thermodynamic consistency of the NRHB theory in the limit of IG behavior, consists in analyzing if the compressibility factor, $\bar{Z}^{eq} = \frac{P^{eq}\,V}{N\,k\,T}$, approaches the value of 1 when the mixture volume diverges at given T and $\underline{N}$.

At fixed T and $\underline{N}$, r is fixed and $\underline{N}_{\alpha\beta}^{HB}$ and $V_{\alpha\beta}^{H}$ are bounded terms. Therefore, based on eqs. (2.5), the limit of IG state can be expressed equivalently in terms of all the following limiting procedures:

$$V \to +\infty \Leftrightarrow v \to +\infty \;\Leftrightarrow\; \rho \to 0 \;\Leftrightarrow \tilde{\rho} \to 0 \;\Leftrightarrow \tilde{v} \to +\infty \tag{2.15}$$

The fourth and fifth limit conditions above hold both for the general non-equilibrium expressions of $\tilde{\rho}$ and $\tilde{v}$ (according to eq. (2.5)) as well as for $\tilde{\rho}^{eq}$ and $\tilde{v}^{eq}$. The latter are obtained from eq. (2.5) where equilibrium values of $\underline{N}_{\alpha\beta}^{HB}$, i.e., $\underline{N}_{\alpha\beta}^{HB,eq}$, are used. Moreover, indicating with N_0 the total number of empty sites in the lattice:

$$\tilde{\rho} = \frac{1}{\tilde{v}} = \frac{rN}{N_0 + rN} \tag{2.16}$$

In other words, any function of N_0, generically indicated as $f(N_0)$, at a fixed composition, according to eq. (2.16) can be transformed in a function of $\tilde{\rho}$, as $f(N_0(\tilde{\rho})) = g(\tilde{\rho})$, and, in view of the theorem of the limit of composite functions, when performing the limit procedure we have $\lim_{\tilde{\rho}\to 0} g(\tilde{\rho}) = \lim_{N_0 \to +\infty} f(N_0)$. Note that eq. (2.16) also relates $\tilde{\rho}^{eq}$ and N_0^{eq} and will be exploited in some limit calculations to perform a change of variables.
As a first step to assess that $\bar{Z}^{eq}$ approaches 1 in the IG limit, we must calculate the $\lim_{\tilde{\rho}^{eq}\to 0} P^{eq}$ which, recalling eq. (2.9), is given by:

$$\lim_{\tilde{\rho}^{eq}\to 0} P^{eq} = \lim_{\tilde{\rho}^{eq}\to 0} -\frac{kT}{v^*}\left[ln(1-\tilde{\rho}^{eq}) - \tilde{\rho}^{eq}\left(\frac{l}{r} - v_H^{eq}\right) - \frac{z}{2} ln\left(1 - \tilde{\rho}^{eq} + \frac{q}{r}\tilde{\rho}^{eq}\right) + \frac{z}{2} ln\Gamma_{00}^{eq}\right] \tag{2.17a}$$

Observing that $\frac{l}{r}$ and $\frac{q}{r}$ are fixed, once the composition has been assigned~~,~~ and that *z* is a universal constant of the lattice model, the contributions associated respectively with the terms $\frac{z}{2} ln\left(1 - \tilde{\rho}^{eq} + \frac{q}{r}\tilde{\rho}^{eq}\right)$, $\frac{l\tilde{\rho}^{eq}}{r}$ and $ln(1-\tilde{\rho}^{eq})$, appearing in the square brackets of the EoS, are trivially equal to zero. Therefore, by the linearity property of limit calculation, we obtain:

$$\lim_{\tilde{\rho}^{eq}\to 0} P^{eq} = \lim_{\tilde{\rho}^{eq}\to 0} -\frac{kT}{v^*}\left[\tilde{\rho}^{eq} v_H^{eq} + \frac{z}{2} ln\Gamma_{00}^{eq}\right] \tag{2.17b}$$

The value of v_H^{eq} can be determined from the simultaneous solution of the equations expressing the minimization conditions for HB contacts, at the fixed T, V and $\underline{N}$, but it is, in the framework of physical constraints of the model, intrinsically a non-negative and superiorly bounded term, so that the product $\tilde{\rho}^{eq} v_H^{eq}$ is equal to zero in the calculated limit. It means that, as physically reasonable, the contribution of hydrogen bond (HB) contacts is not present in the expression of EoS in the limit of $V \to +\infty$.
By the linearity of limit calculation, it can be demonstrated that (see eq. (A.24) in section A.3 of the Appendices):

$$\lim_{\tilde{\rho}^{eq}\to 0} P^{eq} = \lim_{\tilde{\rho}^{eq}\to 0} -\frac{kT}{v^*}\left[\frac{z}{2} ln\Gamma_{00}^{eq}\right] = 0 \qquad (2.17c)$$

This result is physically consistent for a uniform system at equilibrium, at fixed *T* and composition, as $V \to +\infty$.

The procedure for the assessment of the consistency of NRHB model requires, in addition, the calculation of the values of the *internal* state variables in the limit of IG state. Details on this calculation are reported in Section A.3 of the Appendices. Regarding the lattice fluid contact variables, a relevant outcome of this calculation is that the number of lattice fluid contacts in the limit of IG state fulfils the following condition:

$$\lim_{N_0^{eq}\to+\infty} N_{0i}^{eq} = \lim_{N_0^{eq}\to+\infty} N_{0i}^{0,eq}\Gamma_{0i}^{eq} = zN_i q_i \qquad \text{for each } i = 1, \dots, t \qquad (2.18)$$

Equation (2.18), in the IG limit, provides values of non-random lattice fluid contacts (which represent a sub-set of *internal* state variables of the model) that are physically consistent. In fact, since $zN_i q_i$ represents the total number of external contacts of species *i* in the lattice fluid, as expected, equation (2.18) indicates that each molecule at equilibrium is surrounded only by empty sites (see Section A.3 of the Appendices).

Moreover, the equilibrium expression obtained from the set of minimization conditions for HB contacts predicts that, in the IG limit, each $N_{\alpha\beta}^{HB}$ is equal to zero, as physically expected (see Section A.3 of the Appendices).

Coming back to the assessment of the thermodynamic fundamental condition $\bar{Z}^{eq} = 1$ in the IG limit, we can write:

$$\lim_{\tilde{\rho}^{eq}\to 0} \bar{Z}^{eq} = \lim_{\tilde{\rho}^{eq}\to 0} \frac{P^{eq}\, v}{k\,T} = \lim_{\tilde{\rho}^{eq}\to 0} \frac{P^{eq}}{k\,T}\left(r\tilde{v}^{eq}v^* + \frac{1}{N}\sum_{\alpha}^{m}\sum_{\beta}^{n} N_{\alpha\beta}^{HB,eq}\, V_{\alpha\beta}^{0}\right) = \lim_{\tilde{\rho}^{eq}\to 0} \frac{P^{eq}}{k\,T\,\tilde{\rho}^{eq}} rv^* + \lim_{\tilde{\rho}^{eq}\to 0} \frac{P^{eq}}{k\,T\,N}\sum_{\alpha}^{m}\sum_{\beta}^{n} N_{\alpha\beta}^{HB,eq}\, V_{\alpha\beta}^{0} = \lim_{\tilde{\rho}^{eq}\to 0} \frac{P^{eq}}{k\,T\,\tilde{\rho}^{eq}} rv^* \qquad (2.19a)$$

In the last equality, we have observed that, according to equation (2.17c) and since $N_{\alpha\beta}^{HB,eq}$ and $V_{\alpha\beta}^{0}$ are superiorly bounded terms, $\lim_{\tilde{\rho}^{eq}\to 0} \frac{P^{eq}}{k\,T\,N}\sum_{\alpha}^{m}\sum_{\beta}^{n} N_{\alpha\beta}^{HB,eq}\, V_{\alpha\beta}^{0} = 0$.

Substituting the expression (2.17a) in (2.19a) we obtain:

$$\lim_{\tilde{\rho}^{eq}\to 0} \bar{Z}^{eq} = -\lim_{\tilde{\rho}^{eq}\to 0} \frac{r}{\tilde{\rho}^{eq}} \left[ln(1-\tilde{\rho}^{eq}) - \tilde{\rho}^{eq}\left(\frac{l}{r} - \nu_H^{eq}\right) - \frac{z}{2} ln\left(1 - \tilde{\rho}^{eq} + \frac{q}{r}\tilde{\rho}^{eq}\right) + \frac{z}{2} ln\Gamma_{00}^{eq}\right] = \lim_{\tilde{\rho}^{eq}\to 0} - \frac{r}{\tilde{\rho}^{eq}} \left[ln(1-\tilde{\rho}^{eq}) - \tilde{\rho}^{eq}\left(\sum_{i=1}^{t} \Phi_i \frac{l_i}{r_i} - \nu_H^{eq}\right) - \frac{z}{2} ln\left(1 - \tilde{\rho}^{eq} + \frac{q}{r}\tilde{\rho}^{eq}\right) + \frac{z}{2} ln\Gamma_{00}^{eq}\right] = r + l + \frac{z}{2}(q-r) - \lim_{\tilde{\rho}^{eq}\to 0} \frac{r}{\tilde{\rho}^{eq}}\left[\tilde{\rho}^{eq}\nu_H^{eq} + \frac{z}{2} ln\Gamma_{00}^{eq}\right] \tag{2.19b}$$

From (2.19b), by observing that $l = \frac{z}{2}(r-q) - (r-1)$, we finally obtain:

$$\lim_{\tilde{\rho}^{eq}\to 0} \bar{Z}^{eq} = r + l + \frac{z}{2}(q-r) = r + \frac{z}{2}(r-q) - (r-1) + \frac{z}{2}(q-r) = 1 \tag{2.20}$$

Equation (2.20) provides the proof that the equilibrium NRHB EoS for a multicomponent fluid mixture is thermodynamically consistent as the ideal gas state is approached. Notably, such consistency, expressed by the condition that $\lim_{\tilde{\rho}^{eq}\to 0} \bar{Z}^{eq} = 1$, is fulfilled also by the SL model.

However, as discussed in detail by Neau and Thomson [12-15], as $V \rightarrow +\infty$ at fixed T and $\underline{N}$, the expression provided by the SL model for the chemical potential of each generic species i in a multicomponent fluid mixture is not consistent with the behavior of a mixture of ideal gases, in contrast with the NRHB model that instead fulfills this requirement. This issue is the subject of the following section.

2.3 Thermodynamic consistency of the NRHB chemical potentials of a multicomponent mixture at equilibrium in the ideal gas limit

The molecular chemical potential of a generic component i in a mixture of ideal gases in the ensemble $(P, T, \underline{N})$ is provided by the fundamental thermodynamic equation [10]:

$$\mu_i^{(IG)}(P, T, \underline{N}) - \mu_i^{0(IG)}(P, T) = kT\, ln(x_i) \tag{2.21a}$$

where x_i represents the molar fraction of component i. Again, the superscript '0' indicates that the quantity is referred to the corresponding pure component i (at the same P and T in equation (2.21a) and at the same v and T in equation (2.21c), respectively) of the mixture and, as usual, superscript '(IG)' stands for ideal gas state. Equation (2.21a) holds for ideal gases, in which the invertibility between P and v is guaranteed by the IG EoS at fixed T and $\underline{N}$, for each v.

We can write for any multicomponent mixture of ideal gases:

$$\mu_i^{(IG)}\left(P(T,V(v,\underline{N}),\underline{N}),T,\underline{N}\right) = \mu_i^{(IG)}\left(v,T,\underline{N}\right) \tag{2.21b}$$

We can then recast (2.21a) as:

$$\mu_i^{(IG)}\left(v,T,\underline{N}\right) - \mu_i^{0(IG)}(v,T) = kT\, ln(x_i) \tag{2.21c}$$

Note that in (2.21c) the same value of v is present in both expressions of the chemical potentials since, for ideal gases, one has $P = \frac{RT}{v}$ for both the mixture and for any pure component.

To prove that the expressions provided by the NRHB model for the chemical potential of each of the components in a mixture are thermodynamically consistent, one should demonstrate that these expressions fulfil (2.21c) in the IG limit (i.e., when the mixture volume diverges at given T and $\underline{N}$) that is, one should verify the fulfilment of the following consistency condition:

$$\begin{aligned}&\lim_{v\to+\infty}\left[\mu_i^{eq}\left(v,T,\underline{N}\right) - \mu_i^{eq,0}(v,T)\right] = \\ &\lim_{v\to+\infty}\mu_i^{eq}\left(v,T,\underline{N}\right) - \lim_{v\to+\infty}\mu_i^{eq,0}(v,T) = kT\, ln(x_i)\end{aligned} \tag{2.22}$$

According to the NRHB model and the discussion of the section 2 regarding the equilibrium expression of chemical potential, the expression of $\mu_i^{eq}\left(v,T,\underline{N}\right)$ in the limit $v \to +\infty$ is given by:

$$\begin{aligned}&\lim_{v\to+\infty}\frac{\mu_i^{eq}}{kT} = \lim_{\tilde{\rho}^{eq}\to 0}\frac{\mu_i^{eq}}{kT} = \lim_{\tilde{\rho}^{eq}\to 0}\Bigg[ln\frac{\Phi_i}{\delta_i\, r_i} - r_i\frac{l}{r} + ln\,\tilde{\rho}^{eq} + r_i(\tilde{v}^{eq}-1)\, ln(1-\tilde{\rho}^{eq}) - \\ &\frac{z}{2}r_i\left(\tilde{v}^{eq} - 1 + \frac{q_i}{r_i}\right) ln\left(1 - \tilde{\rho}^{eq} + \frac{q}{r}\tilde{\rho}^{eq}\right) + \frac{z\, q_i}{2}\left[ln\, \Gamma_{ii}^{eq} + \frac{r_i}{q_i}(\tilde{v}^{eq}-1)\, ln\, \Gamma_{00}^{eq}\right] - \frac{q_i}{\tilde{T}_i} + \\ &r_i v_H^{eq} - \textstyle\sum_\alpha^m d_\alpha^i\, ln\left(\frac{v_d^\alpha}{v_{\alpha 0}^{eq}}\right) - \sum_\beta^n a_\beta^i\, ln\left(\frac{v_a^\beta}{v_{0\beta}^{eq}}\right) + r_i\frac{\tilde{P}^{eq}\,\tilde{v}^{eq}}{\tilde{T}}\Bigg]\end{aligned} \tag{2.23}$$

from which it can be also readily obtained, for the pure component, the expression of $\lim_{v\to+\infty}\mu_i^{eq,0}(v,T)$. By calculating the two limits in equation (2.22) (see Section A.4 of the

Appendices for details on the calculation procedure) for the case of NRHB model, one finally obtains:

$$\lim_{v\to+\infty} \mu_i^{eq}(v,T,\underline{N}) - \lim_{v\to+\infty} \mu_i^{0,eq}(v,T) =$$
$$kT \lim_{v\to+\infty} ln\left(\frac{x_i\, v^*}{\delta_i\, v}\right) - kT \lim_{v\to+\infty} ln\left(\frac{v^*}{\delta_i\, v}\right) = kT\, ln(x_i) \qquad (2.24)$$

thus, proving the consistency of the chemical potential expression. Actually, equation (2.24) follows from the two fundamental assumptions made in the NRHB model, i.e.: a) v^*, the segmental volume of the lattice, takes a constant 'universal' value for all fluids (9.75/N_A cm^3/molecular segment [16]) and b) the flexibility parameter of each species i, δ_i is a parameter assigned for any species i at a given T (and, in particular, it is independent of composition). Equations (2.20) and (2.22) provide the proof of NRHB consistency in a $(V,T,\underline{N})$ ensemble.

We recall here that also the SL model makes the same assumption for the flexibility parameter δ_i as the NRHB model (i.e., it is only dependent on temperature). However, since the SL model makes use of a concentration-dependent v^*, it is this last assumption that leads to an inconsistency in IG limit, as it is well-established in the literature. We have further investigated here this reported inconsistency using the same procedure for the SL model that we have applied above for the consistency assessment of the NRHB model in the IG limit. The details of this analysis are reported in Section A.5 of the Appendices for the case of the several different mixing rules used in the literature with the SL model, including the cases investigated by Neau [12]. We summarize here just the general conclusions we have obtained:

A) The compressibility factor, $\bar{Z}$, approaches 1 in the limit of ideal gas condition for any common mixing rule, in fact, the expression of EoS is not affected by mixing rules, which depend only on the composition.

B) The assumption of a constant 'universal' value of v^* for the pure components as well as for their mixtures represents a sufficient condition that allows to recover the consistency in the IG limit for any investigated version of the SL model.

C) Interestingly, it has been obtained that there is a particular composition-dependent mixing rule for v^*, never proposed before, which allows to recover the IG consistency for the general expression of SL model analysed by Neau. This mixing rule, however, is not physically sound. Therefore, in a strictly mathematical sense, a constant 'universal' value for v^* is not a necessary condition to guarantee the thermodynamics consistency of the SL model in the IG limit.

D) All the investigated versions of SL theory using the 'classical' mixing rules for v^* do not verify eq. (2.22), so that they do not recover the IG state behaviour in the limit of diverging volume at fixed V, T and $\underline{N}$.

Coming back to the NRHB model, as anticipated in the introduction section, the consistency in a $(P, T, \underline{N})$ ensemble trivially follows from the results obtained in this section for the $(V, T, \underline{N})$ ensemble, so that the assessment procedure of NRHB consistency is completed. In fact, one can recover from equation (2.22) the NRHB consistency of equilibrium chemical potentials in the $(P, T, \underline{N})$ ensemble. To this regard, starting from equation (2.22), by using NRHB EoS, we have:

$$kT\,ln(x_i) = \lim_{v\to+\infty}\left[\mu_i^{eq}(v,T,\underline{N}) - \mu_i^{eq,0}(v,T)\right] = \lim_{v\to+\infty}\left[\mu_i^{eq}\left(P^{eq}(T,V(v,\underline{N}),\underline{N}),T,\underline{N}\right) - \mu_i^{eq,0}\left(P^{eq,0}(T,V(v,\underline{N}),\underline{N}),T,\underline{N}\right)\right] = \lim_{P\to0}\left[\mu_i^{eq}(P,T,\underline{N}) - \mu_i^{eq,0}(P,T,\underline{N})\right] \tag{2.25}$$

having used equation (2.17c) and applying the theorem of limit of composite functions and the linearity of limit calculation. More in details, we can write:

$$\lim_{v\to+\infty}\left[\mu_i^{eq}\left(P^{eq}(T,V(v,\underline{N}),\underline{N}),T,\underline{N}\right)\right] = \lim_{P\to0}\mu_i^{eq}(P,T,\underline{N}) \tag{2.26a}$$

$$\lim_{v\to+\infty}\left[\mu_i^{eq,0}\left(P^{eq,0}(T,V(v,\underline{N}),\underline{N}),T,\underline{N}\right)\right] = \lim_{P\to0}\mu_i^{eq,0}(P,T,\underline{N}) \tag{2.26b}$$

In writing the equations (2.26a-b), we note that with classic abuse of notation, the external functions μ_i^{eq} and $\mu_i^{eq,0}$ represent here the corresponding expressions of the equilibrium chemical potentials in $(P, T, \underline{N})$ ensemble and that according to the theorem of limit of composite function, the variable P appears in the two limit calculations regarding the external functions.

We recall here that, as observed in Section A.2 of the Appendices, the NRHB equilibrium chemical potential in $(P, T, \underline{N})$ ensemble, corresponds to the NRHB equilibrium chemical potential in $(V, T, \underline{N})$ ensemble, provided that P=$P^{eq}(T, V(v, \underline{N}), \underline{N})$.

Finally, by linearity of limit calculation, the following relationship holds:

$$\lim_{v\to+\infty}\left[\mu_i^{eq}(v,T,\underline{N}) - \mu_i^{eq,0}(v,T)\right] = \lim_{P\to0}\left[\mu_i^{eq}(P,T,\underline{N}) - \mu_i^{eq,0}(P,T,\underline{N})\right] \tag{2.27}$$

The latter expression inserted in equation (2.25) provides that in $(P, T, \underline{N})$ ensemble, the following relationship holds:

$$\lim_{P\to 0}\left[\mu_i^{eq}\left(P,T,\underline{N}\right)-\mu_i^{eq,0}\left(P,T,\underline{N}\right)\right]=kT\,ln(x_i) \tag{2.28}$$

It is worth noting that, by repeating a similar procedure, starting from equations (2.15) and (2.20), it is trivial to prove that, for any multicomponent fluid phase the following relationship holds:

$$1=\lim_{v\to+\infty}\bar{Z}^{eq}\left(v,T,\underline{N}\right)=\lim_{v\to+\infty}\bar{Z}^{eq}\left(P^{eq}\left(T,V\left(v,\underline{N}\right),\underline{N}\right),T,\underline{N}\right)=\lim_{P\to 0}\bar{Z}^{eq}\left(P,T,\underline{N}\right) \tag{2.29}$$

where again, we recognize, that in (2.29) the expression of $\bar{Z}^{eq}$ for a $\left(P,T,\underline{N}\right)$ ensemble appears, as imposed by the theorem of limit of composite function.
In conclusion, equations (2.28) and (2.29) prove the consistency of NRHB model also in the $\left(P,T,\underline{N}\right)$ ensemble.

References

[1] A. Baldanza, V. Loianno, G. Mensitieri, C. Panayiotou, G. Scherillo, On the thermodynamic consistency of non-random hydrogen bonding lattice-fluid model for multicomponent mixtures, Fluid Phase Equilibria, 553 (2022) 113302.
[2] B. D. Coleman, M. E. Gurtin, Thermodynamics with Internal State Variables, J. Chem. Phys. (1967) 47, 597-613.
[3] G. Astarita, G. C. Sarti, Modern Thermodynamics in Chemical Engineering and Chemistry. I, Chem. and Industr., (1975) 57 (10), 680-688.
[4] G. Astarita, Thermodynamics: An Advanced Textbook for Chemical Engineers, Plenum Press, New York (1989).
[5] G. Astarita, An Introduction to Nonlinear Continuum Thermodynamics, SpA Editrice di Chimica, Milan (1975).
[6] Th. De Donder and P. Van Rysselberghe, Thermodynamic Theory of Affinity, Stanford University Press (1936).
[7] C. Panayiotou, M. Pantoula, E. Stefanis, I. Tsivintzelis, I. G. Economou, Nonrandom Hydrogen-Bonding Model of Fluids and Their Mixtures. 1. Pure Fluids, Ind. Eng. Chem. Res. (2004) 43, 6592-6606.
[8] C. Panayiotou, I. Tsivintzelis, I. G. Economou, Nonrandom Hydrogen-Bonding Model of Fluids and Their Mixtures. 2. Multicomponent Mixtures, Ind. Eng. Chem. Res. (2007) 46, 2628-2636.
[9] J. M. Prausnitz, R. N. Lichtenthaler, E. G. de Azevedo, Molecular Thermodynamics of fluid-phase equilibria, Prentice-Hall, Inc., Englewood Cliffs, New Jersey (1986).
[10] R. De Hoff, Thermodynamics in Materials Science, CRC Press, Taylor & Francis Group, Florida (2006).
[11] G. Mensitieri, G. Scherillo, C. Panayiotou, P. Musto, Towards a predictive thermodynamic description of sorption processes in polymers: The synergy between theoretical EoS models and vibrational spectroscopy, Materials Science & Engineering R (2020) 140, 100525.
[12] E. Neau, A consistent method for phase equilibrium calculation using the Sanchez–Lacombe lattice–fluid equation-of-state, Fluid Phase Equilibria (2002) 203, 133–140.
[13] K. von Konigslow, C.B. Park, R.B. Thompson, Phys. Rev. Appl. (2017) 8, 044009.
[14] K. von Konigslow, An Off-lattice Derivation and Thermodynamic Consistency Consideration for the Sanchez-Lacombe Equation of State, Ph.D. Thesis University of Waterloo, Waterloo, Ontario, Canada, 2017.
[15] K. von Konigslow, C.B. Park, R.B. Thompson, Soft Matter (2018) 14, 4603-4614.

[16] C. Panayiotou, J. H. Vera, Statistical Thermodynamics of r-Mer Fluids and Their Mixtures, *Polym. J.* (1982) 14, 681-694.

Chapter 3
PEI-CO_2 system

3.1 Materials

Amorphous Polyetherimide (PEI) films was purchased from Goodfellow Co. ($M_n = 1.2 \cdot 10^4$ Da, $M_w = 3.0 \cdot 10^4$ Da, $T_g = 210$ °C, thickness 50.0 μm). The films were dissolved in chloroform, 15% wt/wt concentration, to be solution cast on a tempered glass support. The cast film was sequentially dried 1 h at room temperature,1 h at 80°C and overnight at 120°C. Last, the film was removed from the glass substrate and immersion in distilled water at 80°C. The polymer density, $\rho_{2,ref}$, is measured by flotation in a $CaCl_2$ water solution at 25°C. The resulting density is 1.297 $g \cdot cm^{-3}$.

3.2 Methods

Stepwise sorption experiments have been conducted with a gravimetric apparatus based on a CAHN-D200 Microbalance by Thermo Electron Co. (Waltham, MA, USA). The balance has a resolution of 10^{-7} g and an uncertainty of $\pm 3 \cdot 10^{-7}$ g. It is placed within a leak proof chamber whose temperature is controlled with a Julabo CF41 thermal bath with an uncertainty of ±0.01°C. The whole apparatus is made leak proof with Swagelok fittings. A pumping station (P1 in Figure 3.1) combining a turbopump and a membrane backing pump (Pfeiffer HiCUBE 80, ultimate pressure 10^{-7} mbar, pumping speed 35 $l \cdot s^{-1}$) is used to dry the polymer specimen (S1 in figure 3.1) before each integral sorption step. A pressure transducer MKS Baratron 121 A (PI in Figure 3.1) from MKS Instruments of 100 Torr and 1000 Torr full scale (resolution 0.01% of full scale and an accuracy equal to ±0.5% of the reading) is used to record the pressure during the experiment. Further details about the apparatus can be found in the Appendix B.

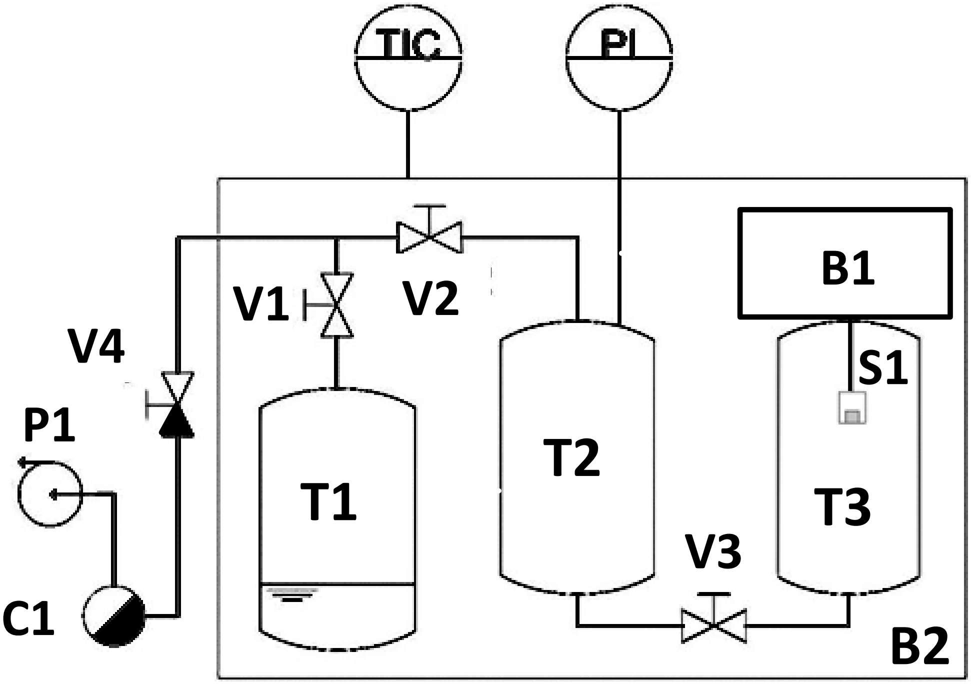

Figure 3.1: Cahn D-200 microbalance schematic representation.

3.3 Calculation of ΔH_i^{ISOS} with NETGP-NR model

For sorption (adsorption/absorption) of a pure gas 'i' in a solid matrix the isosteric heat of sorption is defined as follows [1]:

$$\Delta \underline{H}_i^{ISOST} = \underline{H}_i^g(T,P) - \overline{H}_i^a\left(T,P,\underline{n}\right) \tag{3.1}$$

where $\underline{H}_i^g(T,P)$ is the molar enthalpy of the pure gas phase and $\overline{H}_i^a(T,P)$ is the partial molar enthalpy of the sorbed (absorbed/adsorbed) gas, both evaluated at temperature T and pressure P. It can be demonstrated [1] that eq. (3.1) reduces to:

$$\Delta \underline{H}_i^{ISOST} = \underline{H}_i^g(T,P) - \underline{H}_i^{g,*}(T,P=1atm) - R\left(\frac{\partial lnP}{\partial 1/T}\right)_{q_i^a} \tag{3.2a}$$

where q_i^a represents the amount of sorbate in the adsorbed phase while and $\underline{H}_i^{g,*}(T,P=1atm)$ is the pure ideal gas molar enthalpy at T and P = 1 atm. Unless the pressure is high, the gas-phase excess enthalpy difference, i.e., $\underline{H}_i^g(T,P) - \underline{H}_i^{g,*}(T,P=1atm)$ can be neglected, so that equation (3.2a) can be approximated by [1]:

$$\Delta \underline{H}_i^{ISOST} = RT^2 \left(\frac{\partial lnP}{\partial T}\right)_{q_i^a} \tag{3.2b}$$

We remark here that eq. (3.2b) is based upon calculations performed only on the equilibrium external phase of the pure penetrant and has been obtained by imposing the equality of the chemical potentials of the penetrants in the external fluid phase and of the chemical potentials of the penetrants present within the polymer-penetrant phase. Then, equation (3.2b) can be used to gather the value of the isosteric heat of sorption from experimental sorption isotherms, without specifying any functional form for the chemical potentials [1] but only re-elaborating the experimental data.

Conversely, a theoretical estimate of the isosteric heat of sorption for a gas absorbed in a rubbery amorphous polymer can be obtained from equation (3.1) by calculating the value of $\underline{H}_i^g(T,P)$ and that of $\overline{H}_i^a(T,P,\underline{n})$ using the NRHB model. Predictions obtained from equation (3.1) can be compared to the value of isosteric heat obtained by applying equation (3.3) to re-elaborate the experimental sorption isotherms.

Equation (3.1) can be extended to the case of sorption in a glassy polymer in the framework of NETGP-NRHB model, under the *IE* hypothesis. In view of equations (1.66a) and (1.66b) reported in the Section 1.3.3, one can obtain the non-equilibrium enthalpy, *H*:

$$H = G + TS \tag{3.3}$$

By repeating the same procedure explained in Section 1.3.3, the equilibrium enthalpy, H^{eq}, is calculated by coupling the equation (3.2b) with equations (1.67b), (1.68b) and (1.69b). Consequently, in the case of pseudo-equilibrium between a pure penetrant phase and the binary polymer-penetrant glassy system, one can still utilize the definition (equation (3.1)) of the isosteric heat of sorption for the penetrant i, so that:

$$\Delta \underline{H}_i^{ISOST} = \underline{H}_{i,0}^{eq}(T,P) - \overline{H}_i^{IE}\left(T,\underline{n}\,,\rho_p\right) \tag{3.4}$$

where $\underline{H}_{i,0}^{eq}$ represents the corresponding equilibrium molar enthalpy of the pure penetrant phase at a given pressure *P* and temperature *T*. Its value is provided by the NRHB model, as applied to the pure component case. Regarding $\overline{H}_i^{IE}$, it can be calculated from:

$$\overline{H}_i^{IE} \equiv \left(\frac{\partial H^{IE}}{\partial n_i}\right)_{P,T,\rho_p,n_{j\neq i}} = \mu_i^{IE} + T\left(\frac{\partial S^{IE}}{\partial n_i}\right)_{T,\rho_p,n_{j\neq i}} \tag{3.5}$$

It is worth noting that $\overline{H}_i^{IE}$ does not depend on pressure since both μ_i^{IE} and S^{IE} are independent of *P*. In the framework of the proposed extension of the definition of isosteric enthalpy to *IE* conditions, in equation (3.5) the value of penetrant moles is dictated by phase pseudo-equilibrium condition at the given *P* and *T* and (fixed) number of moles of polymer. The value of μ_i^{IE} can be calculated based on NETGP-NRHB theory as shown in Section 1.3.3, while the value of $\left(\frac{\partial S^{IE}}{\partial n_i}\right)_{T,\rho_p,n_{j\neq i}}$ needs to be evaluated numerically based again on the NETGP-NRHB theory.

These equations can be easily specialized for the case of a binary system as is the case of PEI and CO_2 that we are considering in the present chapter. Equation (3.5) can be used to provide a theoretical prediction of the value of the isosteric heat of sorption for CO_2 in PEI that can be compared to the one gathered from experimental isotherms using equation (3.2b).

3.4 The estimation of the interaction energy by NETGP-NRHB model

We consider here the special case of a binary glassy polymer-penetrant mixture. The mean-field interaction energy per mole of penetrant in the limit of infinite dilution, $\underline{E}_{1p,0}$, (for the binary system under investigation, subscript '1' refers to the penetrant and subscript '*p*' refers to the polymer) can be estimated using the NETGP-NRHB model once the binary interaction parameters have been determined from fitting of experimental sorption isotherms. $\underline{E}_{1p,0}$ is defined as:

$$\underline{E}_{1p,0} = N_A \lim_{N_1 \to 0} E_{1p} = N_A E_{1p,0} = N_A \varepsilon_{1p} \lim_{N_1 \to 0} \frac{N_{1p}^{IE}}{N_1} = \underline{\varepsilon}_{12} \lim_{N_1 \to 0} \frac{N_{1p}^{IE}}{N_1} \qquad (3.6)$$

where N_A is the Avogadro's number, E_{1p} is the mean-field interaction energy per molecule of penetrant (it represents the total interaction energy between a molecule of species 1 and the surrounding species *p*), $E_{1p,0}$ is the value of E_{1p} in the limit of vanishing penetrant concentration (i.e., for $N_1 \to 0$), N_{1p}^{IE} represents the total number of LF contacts between the species 1 and the species *p* under the *IE* assumption, N_1 represents the total number of molecules of the penetrant, ε_{1p} represents the mean-field interaction per each LF contact between a segment of species 1 and a segment of species *p*. Finally, $\underline{\varepsilon}_{1\mathrm{p}}$ represents the mean-field interaction per mole of LF contact between a segment of species 1 and a segment of species p and it is calculated according to the mixing rules outlined in equation (1.43b) in Section 1.3.3:

$$\underline{\varepsilon}_{1\mathrm{p}} = \sqrt{\underline{\varepsilon}_{11}\, \underline{\varepsilon}_{pp}}\left(1 - k_{1p}\right) \tag{3.7a}$$

Once the value of k_{1p} linearly function of the temperature:

$$k_{1p} = k_{1p,0} + a_T\, T \tag{3.7b}$$

is known (e.g., by fitting with the NETGP-NRHB model the experimental sorption isotherms) one can gather the value of $\underline{\varepsilon}_{1\mathrm{p}}$ from equation (3.7a). To perform the calculation of $\underline{E}_{1p,0}$ according to equation (3.6), one further needs to estimate N_{1p}^{IE}/N_1. N_{1p}^{IE} is expressed as:

$$N_{1p}^{IE} = \Gamma_{1p}^{IE}\, N_{1p}^{0} \tag{3.8}$$

Where:

$$N_{1p}^{0} = z\, N_1 q_1 \cdot \frac{N_p q_p}{N_q} = z N_1 q_1 \Theta_p \tag{3.9}$$

N_{1p}^{0} represents the total number of LF contacts, between species 1 and species p, under the assumption of random distribution of contacts. In eq. (3.9) z represents the lattice coordination number, N_p represents the total number of molecules of the polymer, $q_i z$ represents the total number of external contacts for a molecule of species *i* (the parameter q_i accounts for the structure of the molecules of species *i* within the lattice, in terms of its subdivision in r_i segments), as already shown in Section 1.3.3. The factor zN_1q_1 represents the total number of external contacts of species 1 within the lattice. Finally, the factor $\frac{N_p q_p}{N_q}$ can be demonstrated to represent the ratio between the total number of contacts of species p and the total number of contacts within the lattice, which in turn provides, in the case of a random distribution of LF contacts, the probability that a contact involves the species p. It is recalled that:

$$zN_q = zqN + zN_0 \tag{3.10}$$

where N_0 represents the total number of empty cells. Moreover:

$$q = x_1 q_1 + x_p q_p \tag{3.11}$$

where x_{i} is the molar fraction of the species i. The voids are formally treated as an additional species characterized by $q_0 = 1$ since each molecule of the 'void' pseudo-species occupies only a cell within the lattice (i.e., $r_0 = 1$).
Regarding the term Θ_p in equation (3.9), the equations from (1.32) to (1.35) are recalled, where:

$$\mathrm{r} = x_1 r_1 + x_p r_p \tag{3.12}$$

We can now derive the final expression for N_{1P}^{IE}/N_1:

$$\frac{N_{1P}^{IE}}{N_1} = \frac{\Gamma_{1P}^{IE}\, N_{1p}^{0}}{N_1} = z N_1 q_1 \Theta_p \frac{\Gamma_{1P}^{IE}}{N_1} = z\, \Gamma_{1P}^{IE}\, q_1 \Theta_p \tag{3.13}$$

From which we finally obtain:

$$\underline{E}_{1p,0} = \underline{\varepsilon}_{1\mathrm{p}} \lim_{N_1 \to 0} \frac{\Gamma_{1P}^{IE}}{N_1}\, z N_1 q_1 \Theta_p = \underline{\varepsilon}_{1p} \lim_{x_1 \to 0} z\, \Gamma_{1P}^{IE}\, q_1 \Theta_p \tag{3.14}$$

The limit in equation (3.14) has been calculated numerically. We observe [2, 3] that the functional form of $\frac{N_{1P}^{IE}}{N_1}(N_1, T, \rho_p)$ can be put in terms of $\frac{N_{1P}^{IE}}{N_1}(x_1, T, \rho_p)$, as expected, since it is an intensive thermodynamic quantity. The calculation of $\underline{E}_{1p,0}$ can be then performed once $\Gamma_{1p}^{IE}(x_1, T, \rho_p)$ is known from the NETGP-NRHB model. Under the *IE* assumption the expressions of the set of the non-random factors Γ_{ij} (*i,j*=0,1,2 and *j*>*i*) are given by the equation (1.67b) at any fixed x_1, T and ρ_p [4, 5].

3.5 Modelling mutual diffusivity in a glassy polymer – penetrant binary system

In the limit of low penetrant concentrations in a rubbery polymer, a Fickian diffusive behavior [6, 7] is generally observed. As a consequence, in a sorption experiment of a penetrant in polymer slab (binary case) the following equation describes the sorption kinetics [6]:

$$\frac{M(t)-M_0}{M_\infty-M_0} = 1-\sum_{n=0}^{\infty}\frac{8}{(2n+1)^2\pi^2}\exp\left(-\frac{D_{12}(2n+1)^2\pi^2 t}{L^2}\right) \tag{3.15}$$

where M_0 is the initial mass of penetrant present within the polymer (uniform concentration), $M(t)$ is the penetrant mass present within the polymer at time *t,* M_∞ is the asymptotic value of penetrant mass present at infinite time, L represents the thickness of the sample slab and D_{12} is the so-called mutual diffusivity, assumed to be independent of penetrant concentration. The sorption experiment modelled by equation (3.15) is performed starting from an initial uniform concentration within the slab that is in equilibrium with the external fluid phase. At the start of the experiment, the pressure of the external fluid phase is stepwise increased to a higher value, thus determining the start of diffusion process of the penetrant within the polymer. The concentration of the penetrant thus reaches, at the end of the sorption process, a new uniform equilibrium concentration. A fingerprint of the Ideal Fickian behavior is the linear dependence of $\frac{M(t)}{M_\infty}\, vs\, \sqrt{t}$ up to $\frac{M(t)}{M_\infty} \cong 0.5$. For this reason, $\frac{M(t)}{M_\infty}$ is frequently reported as a function of $\sqrt{t}$.

In the case of glassy polymers, mutual diffusivity is dependent on concentration even at low concentrations [8]. However, one can still use equation (3.15) to interpret sorption kinetics provided that the change in concentration during the sorption run is not too high. In such a case, one can assume that the mutual diffusivity is rather constant during each sorption step. The value of D_{12} that one gathers from fitting of the sorption curve thus represents a mean value between the ones corresponding to the uniform initial and final values of penetrant concentration. This average value of diffusivity can be associated to the mean value of concentration (arithmetic average of the initial and final values of uniform concentration). In the present investigation step sorption experiments have been performed at different values of temperature, determining the dependence of mutual diffusivity as a function of penetrant concentration and temperature [6, 7, 9].

The mutual diffusivity coefficient, D_{12}, in a penetrant-rubbery polymer binary system can be expressed [10-12] in terms of the so-called *intra*-diffusion coefficient of the penetrant, D_1, that represents the intrinsic mobility of penetrant in a binary mixture in the case of a null value of the gradients of the chemical potentials of the two components:

$$D_{12} = D_{1p} = \frac{D_1 \cdot \rho_p \cdot \hat{V}_p \cdot \rho_1 \left(\frac{\partial \mu_1}{\partial \rho_1}\right)_{T,P,\rho_p}}{RT} \tag{3.16}$$

This equation holds true not only at small penetrant concentrations but also over a major portion of the concentration interval of the binary system [10]. In equation (3.16) $\hat{V}_p$ is the partial mass volume of the polymer in the mixture.

In the case of a glassy polymer, the “thermodynamic factor” present in equation (3.16), $\left(\frac{\partial \mu_1}{\partial \rho_1}\right)_{T,P,\rho_p}$, is calculated numerically on the basis of the NETGP-NRHB model. In the limit of low concentration of penetrant in a glassy polymer, $\hat{V}_p$ is approximately equal to $1/\rho_p$ (where ρ_p is the non-equilibrium polymer density) since the partial mass volume of the penetrant can be assumed to be equal to zero. Equation (3.16), where the mutual diffusivity coefficient depends upon a “thermodynamic factor” provided by the NETGP-NRHB theory, is referred to in the following as NETGP-NRHB-DM (where DM stands for “Diffusion Model”).

Inspired by the Cohen-Turnbull expression for the *self*-diffusion coefficient in the case of a one-component fluid [11] we have adopted for the *intra*-diffusion coefficient, D_1, of a penetrant in a binary glassy polymer-penetrant mixture a simple empirical law:

$$D_1 = D_{00} \cdot \exp\left(-\frac{E_d - \sigma_c \cdot c}{RT}\right) = D_{00} \cdot \exp\left(-\frac{E_d}{RT} \cdot (1 - \alpha \cdot c)\right) \tag{3.17}$$

with $\alpha = \sigma_c / E_d$

In equation (3.17) D_{00} and E_d represent, respectively, a constant pre-exponential factor and a constant activation energy term accounting for energetic barriers (related to the polymer-penetrant interactions and to the cohesive energy of polymer molecules) to be overcome to realize an effective diffusive jump, while σ_c represents a term accounting for the effect of penetrant concentration (c [mass of CO_2/ mass of polymer]) on the intrinsic penetrant mobility in the binary mixture. In principle, these three constant parameters only depend on the nature of the components of the binary mixture and their values can be retrieved from a non-linear fitting of the experimental D_{12} data, using equations (3.16) and (3.17).

3.6 Results

3.6.1 Sorption isotherms of CO_2 in PEI: Results and Modelling

In Figure 3.2 the experimental sorption isotherms of CO_2 in PEI are reported. The isotherms have been modelled using the NETGP-NRHB model. No hydrogen bonding or specific interactions are supposed to be present in this system, so that the HB part of the model has been disregarded. The model parameters for pure PEI and CO_2 have been retrieved from the literature [2, 13], and are reported in Table 3.1.

Table 3.1 NRHB Lattice fluid parameters of pure PEI and CO_2

	ε_h (Jmol^{-1})	ε_s (Jmol^{-1}K^{-1})	$v_{sp,0}$ (cm^{3}g^{-1})	s	Ref.
CO_2	3468.4	-4.5855	0.79641	0.909	[2]
PEI	6775.3	5.503	0.7228	0.743	[13]

As discussed in the Section 1.4, the phase pseudo-equilibrium calculations require the value of the out-of-equilibrium density of the polymer, ρ_p, within the glassy mixture. In view of low solubility displayed by CO_2 in the investigated pressure range, ρ_p and is assumed to be equal to the density of the dry polymer right after the starting desorption stage. The value of polymer density has been assumed to be a function only of the temperature [14-15].

Under the assumption that the coefficient of thermal expansion coefficient, α, is constant in the ranges of temperature and pressure investigated, $\rho_p(T)$ has been calculated according to the following expression:

$$\rho_p = \rho_{p,ref}\, e^{-\alpha\,(T-T_{ref})} \tag{3.18}$$

Using as a reference density, $\rho_{p,ref}$, the pure polymer density at $T_{ref} = 25°$

The determination of the mean-field interaction parameter, k_{1p}, as a function of temperature, according to equation (3.7), has been performed by fitting the sorption isotherms at several temperatures (0°C, 10°C, 18°C, 27°C, 35°C) with the NETGP-NRHB model, obtaining the values $k_{1p,0} = 0.301$ and $a_T = -0.00100\ K^{-1}$. As shown in Figure 3.2 the NETGP-NRHB model provides a good fitting of the experimental sorption isotherms of CO_2 in PEI.

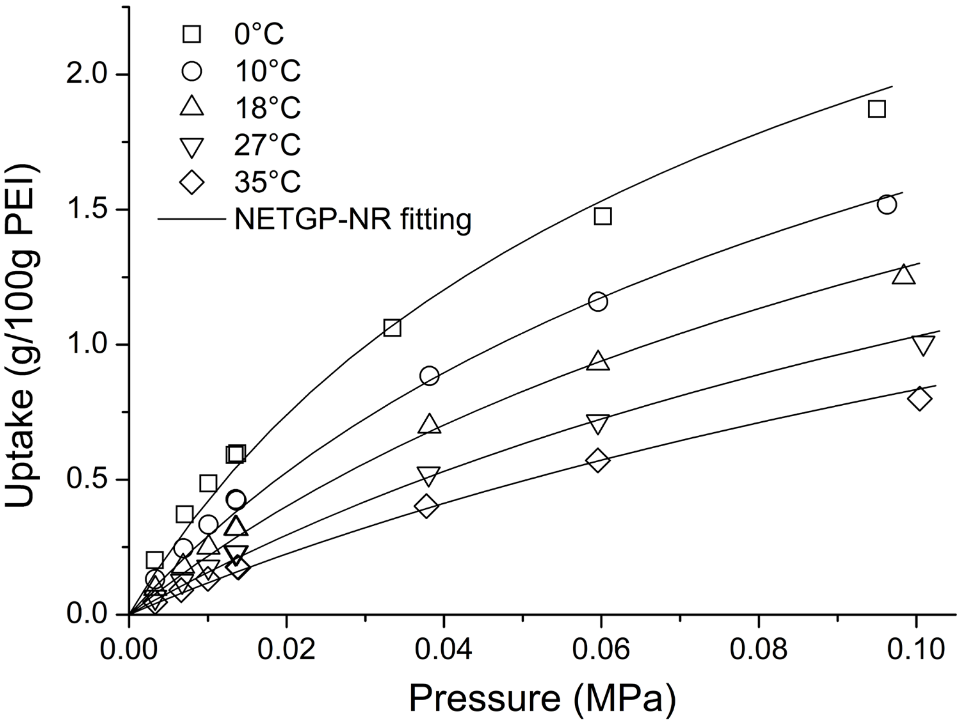

Figure 3.2: PEI-CO_2 pseudo-equilibrium sorption at different temperatures

The experimental data have been re-elaborated by means of equation (3.2b) to obtain and estimate of the value of $\Delta \underline{H}_i^{ISOST} = -31.1$ kJ/mol, which was obtained at T=18°C and at a value of CO_2 concentration equal to 0.4 [g of CO_2/100 g of PEI]. Based on the values of the binary interaction parameters determined by fitting experimental sorption isotherms with the NETGP-NRHB model, we were able to predict theoretically, in the same conditions as above, a value $\Delta H_1^{ISOS} = -28.3.$ kJ/mol by using the equation (3.4), that compares well with the value retrieved directly from the experimental data.

Moreover, still using the values of the binary interaction parameters determined by fitting procedures, we have used the NETGP-NRHB model to estimate a value of 18.6 kJ/mol for $\underline{E}_{1p,0}$ at 1K, that has been obtained by extrapolating at this value of temperature the values calculated in the 0 - 35°C temperature range. This value is quite close to the value of 20 kJ/mol determined for the interaction energy between one molecule of CO_2 and the polymer environment by Density Functional Theory (DFT) calculations. Actually, one would expect that these two quantities, in view of their definition, take a close value. This result points to the consistency between the thermodynamic and DFT approaches.

3.6.2 Sorption Kinetics of CO_2 in PEI: Results and modelling

Values of mutual diffusivity, D_{12}, at different concentration values of absorbed CO_2 and at several temperatures have been determined by fitting with equation (3.16) the sorption kinetics evaluated experimentally by imposing stepwise increase of the gas pressure values. An example of an experimental sorption kinetic curve for the 0 – 100 Torr pressure step at 0°C is reported in Figure 3.3, where $\frac{M(t)}{M_\infty}$ is plotted as a function of $\sqrt{t}$, along with the best fitting curve provided by equation (3.16), from which is evident the Fickian nature of the sorption mechanism.

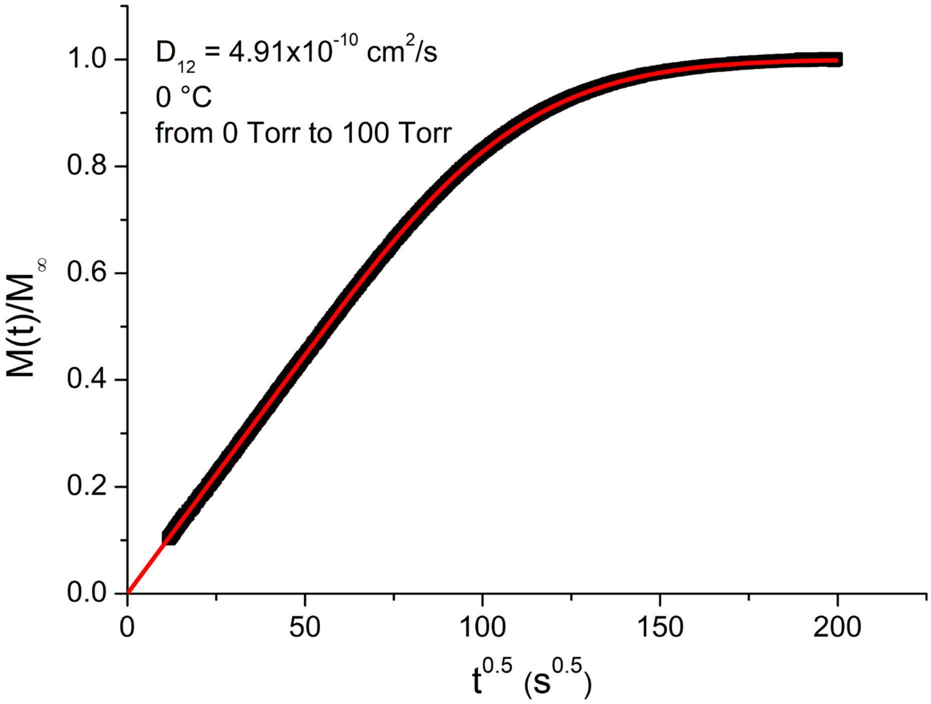

Figure 3.3: Sorption kinetics of CO_2 in PEI

By fitting all the sorption kinetics steps, the values of D_{12} have been determined and are reported in Figure 3.3 as a function of the average concentration during the sorption test at different temperatures. Best fitting curves were evaluated based on equations (3.16) and (3.17) are also reported. As evident, the NETGP-NRHB-DM provides an excellent interpretation of data. The values of best fitting parameters are reported in Table 3.2.

Table 3.2 CO_2 intra-diffusion parameters

E_d (kJ mol^{-1})	α [dimensionless]	D_{00} (cm^2 s^{-1})
39.29	2.82	0.011

The value of E_d and the corresponding concentration-dependent activation energy values $E_d(1-\alpha \cdot c)$ in the range of concentration investigated, are significantly higher than the mean-field interaction energy per mole of penetrant, $\underline{E}_{1p,0}$. It is recalled that E_d represents the activation energy in the limit of zero concentration and accounts for energetic barriers to diffusion related to the polymer-penetrant interactions and to the cohesive energy of polymer molecules. This is hence expected to be higher than $\underline{E}_{1p,0}$ that, instead, accounts only for penetrant-polymer interaction.

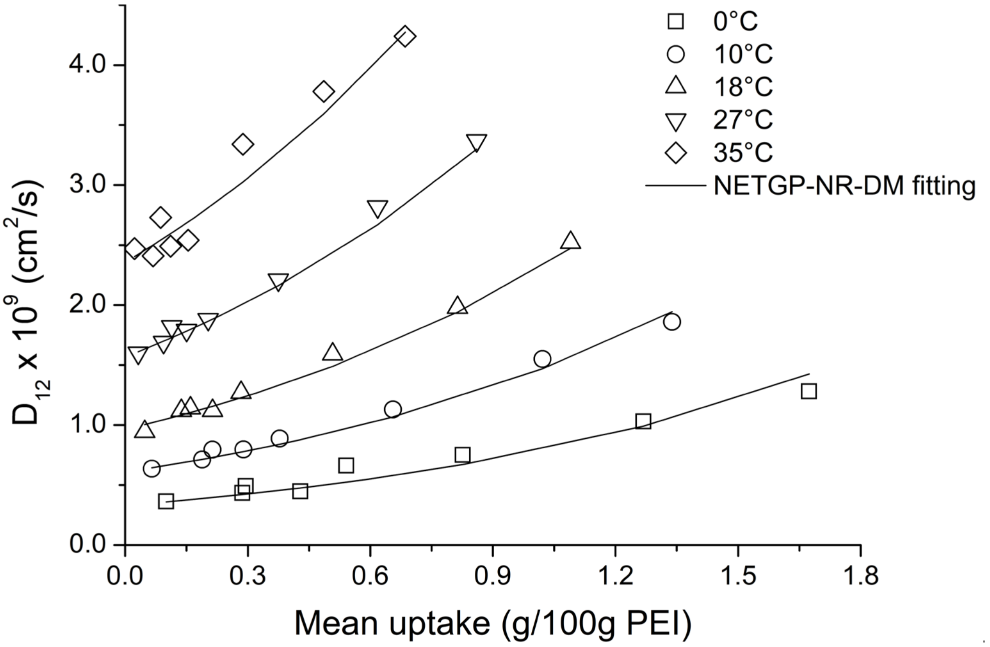

Figure 3.4: Mutual diffusion of CO_2 in PEI as function of average concentration

References

[1] S. Buoles, S.I. Sandler, R. Xiong, 'Isosteric heats of gas and liquid adsorption', Langmuir (2013) 29, 10416-10422.

[2] C. Panayiotou, M. Pantoula, E. Stefanis, I. Tsivintzelis, I. G. Economou, Nonrandom Hydrogen-Bonding Model of Fluids and Their Mixtures. 1. Pure Fluids, Ind. Eng. Chem. Res. (2004) 43, 6592-6606.

[3] C. Panayiotou, I. Tsivintzelis, I. G. Economou, Nonrandom Hydrogen-Bonding Model of Fluids and Their Mixtures. 2. Multicomponent Mixtures, Ind. Eng. Chem. Res. (2007) 46, 2628-2636.

[4] G. Mensitieri, G. Scherillo, C. Panayiotou, P. Musto, Towards a predictive thermodynamic description of sorption processes in polymers: The synergy between theoretical EoS models and vibrational spectroscopy, Materials Science & Engineering R (2020) 140, 100525.

[5] G. Scherillo, L. Sanguigno, L. Sansone, E. Di Maio, M. Galizia, G. Mensitieri, Thermodynamics of water sorption in poly(ε-caprolactone): A comparative analysis of lattice fluid models including hydrogen bond contributions, Fluid Phase Equilibria 313 (2012) 127– 139.

[6] J. Crank, The Mathematics of Diffusion, 2nd ed.; Clarendon Press: Oxford, UK (1975).

[7] J. Crank, G. S. Park, Diffusion in Polymers, 1st ed.; Academic Press: London, UK; New York, NY, USA (1968).

[8] J. S. Vrentas, J. L. Duda, Diffusion in polymer-solvent systems: I. Re-examination of the free-volume theory, J. Polym. Sci., Polym. Phys. Ed. 15 (1977) 403-416.

[9] D. Tammaro, L. Lombardi, G. Scherillo, E. Di Maio, N. Ahuja, G. Mensitieri, Modelling sorption thermodynamics and mass transport of n-hexane in a propylene-ethylene elastomer, Polymers 13 (2021) 1157-1173.

[10] J. S. Vrentas, J. L. Duda, Diffusion in polymer-solvent systems: II. A predictive theory for the dependence of the diffusion coefficient on temperature, concentration and molecular weight, J. Polym. Sci., Polym. Phys. Ed. 15 (1977) 417-439.

[11] J. L. Duda, J.M. Zielinski, Free-volume theory, in: P. Neogi (Ed.) Diffusion in Polymers, Marcel Dekker Inc., New York (1996) 143-172.

[12] E. Di Maio, S. Iannace, G. Mensitieri, Mass transport of low molecular weight compounds in polymer, in: Foaming with supercritical fluids, Elsevier, Amsterdam (2021) 179-230.

[13] G. Scherillo, M. Petretta, M. Galizia, P. La Manna, P. Musto and G. Mensitieri, Thermodynamics of water sorption in high performance glassy thermoplastic polymers, Frontiers in Chemistry 2, 25, (2014) 1-16.

[14] F. Doghieri, G.C. Sarti, Nonequilibrium Lattice Fluids: A Predictive Model for the Solubility in Glassy Polymers, Macromolecules 29 (1996) 7885.

[15] G.C. Sarti, F. Doghieri, Predictions of the solubility of gases in glassy polymers based on the NELF model, Chem. Eng. Sci. 19 (1998) 3435.

Chapter 4

Glass transition temperature as function of the penetrant concentration

4.1 PMMA-CO_2 system

The study of the polymer processing in presence of supercritical fluids and compressed gases is fundamental for many applications. For example, the polymer morphology may be tailored with modest changes in temperature and light gas pressure, like CO_2. Interesting observations have been made regarding the influence of a compressed fluid on the glass transition temperature of a polymer. Assink [1] showed that a low solubility fluid increases the T_g with increasing pressure, while a more soluble fluid can plasticize a polymer and decrease T_g increasing the pressure. In this section, we focus our attention to the depression of the glass transition temperature of PMMA-CO_2 system as a function of the sorption of the fluid by applying the Gibbs-Di Marzio criterion of the glass transition in the framework of NRHB model. The model reveals a phenomenon known as retrograde vitrification, where a polymer undergoes a liquid to glass transition with an increase in temperature. In the first part, we have obtained the NRHB PMMA pure parameters and calculated the flex energy by fitting PVT and T_g vs pressure data of pure PMMA, respectively. Next, retrograde vitrification and PE sorption data of glassy PMMA-CO_2 system have been fitted to obtain the binary interaction parameter as a linear function of the temperature according to an empirical law proposed in the previews chapters.

4.1.1 NRHB pure PMMA parameters

Considering the PMMA, the occurrence of self-HB interactions can be disregarded, based on their chemical structures. Therefore, only NRHB "mean field" LF model parameters for pure polymers need to be determined. The values of ε_h, ε_s and $v_{sp,0}$ have been gathered by a non-linear regression of equilibrium dilatometric data (PVT) using the expression of EoS provided by the NRHB theory, according to equations shown in Section 1.3.3, while s has been determined according to UNIFAC group contribution model [2-3]. The parameters for PMMA have been obtained by fitting PVT data available in the literature [4]. The NRHB EoS provides a good fitting of PVT data, as evident in Figures 4.1. The calculated values of the parameters are reported in Table 4.1.

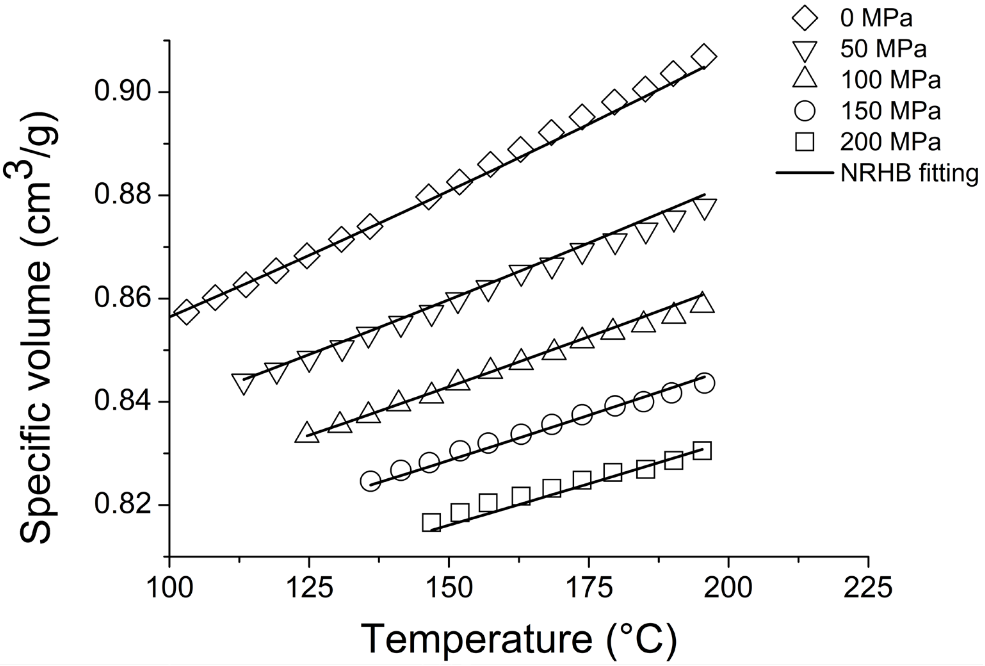

Figure 4.1: Fitting of PVT data for PMMA using NRHB EoS

In order to obtain the parameters Z and the flex energy, Δu_i, Tg vs pressure of pure PMMA are fitted according to the Gibbs-Di Marzio criterion (equation (1.93)). S^{eq} is the equilibrium entropy of the pure PMMA calculated by the equation (1.66b) properly adapted in the pure case. The flexibility parameter as function of the temperature is calculated according to the equations (1.28a) and (1.28b) by fitting the experimental data taken from [5] resulting $\Delta u_i =$ 3.011 kJ/mol, while Z has been imposed equal to 5, as already done by Condo et al. [6] for the same set of data. The prediction in correspondence of the fitting outcomes is shown in Figure 4.2.

Table 4.1 PMMA NRHB Lattice fluid parameters.

	ε_h (Jmol^{-1})	ε_s (Jmol^{-1}K^{-1})	$v_{sp,0}$ (cm^{3}g^{-1})	s	$\rho_{p,0}^{un}$ (g/cm^3)	Ref.
CO_2	3468.4	-4.5855	0.79641	0.909	-	[7]
PMMA	6398.5	4.8071	0.79954	0.843*	1.172	This work, data from [4] and [8]

*This "surface-to-volume" ratio, *s,* has been estimated by using the widely used UNIFAC group contribution model [2-3] with data taken from [9-14].

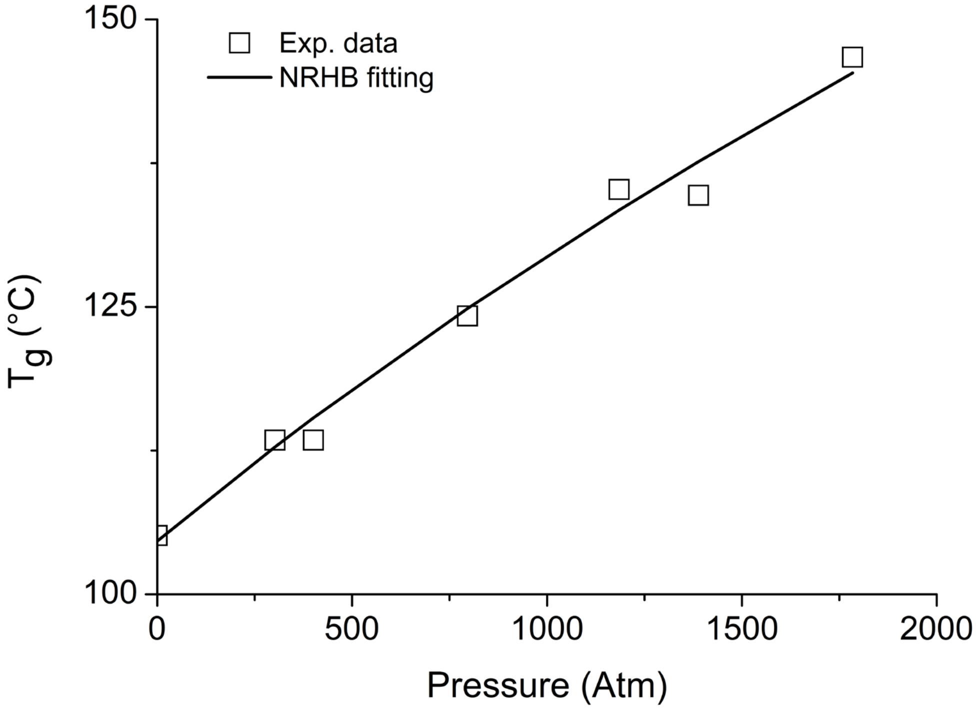

Figure 4.2: Fitting of T_g vs pressure of pure PMMA by NRHB Lattice

4.1.2 PMMA-CO_2 solubility and retrograde vitrification

The mean-field interaction parameter k_{ij} for the couple PMMA-CO_2 has been determined by simultaneously fitting (using NETGP-NRHB model) PE sorption data at 35°C and glass transition temperatures as function of CO_2 pressure (by NRHB model); experimental data were taken from the literature [6-8]. Being available data sets at different temperatures for the case of glass transition, the k_{ij} parameter has been assumed, in this case, to be temperature dependent according to the empiric linear relationship. Moreover, when dealing with sorption of a pure gas phase at high pressure the density of a glassy polymer in a binary mixture with an absorbed gas is assumed to depend on pressure of the penetrant, P. In fact, the out-of-equilibrium density, $\rho_{p,0}$, of a glassy polymer forming an amorphous binary mixture with a low molecular weight penetrant, at a fixed temperature, can be related to the out-of-equilibrium density of the unpenetrated polymer, $\rho_{p,0}^{un}$ according to the following empiric equation [8, 15-17]:

$$\rho_{p,0} = \rho_{p,0}^{un} \cdot (1 - k_{sw}P) \tag{4.1}$$

The term in the parenthesis accounts for the "elastic" effect of the external fluid phase on the non-equilibrium mixture volume (in PE conditions), which is in principle a non-linear combination of a mechanical pressure effect and of penetrants induced swelling of the polymeric matrix. k_{sw} is defined as the swelling factor associated to the polymer-penetrant couple.

The best-fitting values of the three parameters, $k_{ij,0}$, a_T and k_{sw} are obtained by a simultaneous fitting of the two sets of experimental data (taken from [18-19]) (see Figure 4.3) and their values are reported in Table 4.2.

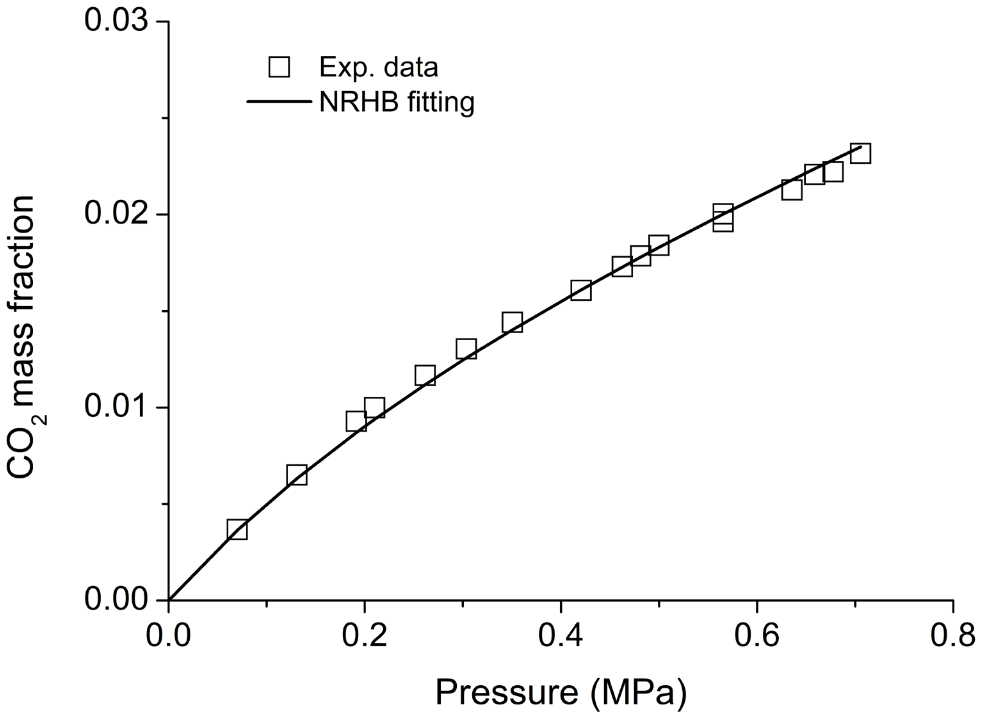

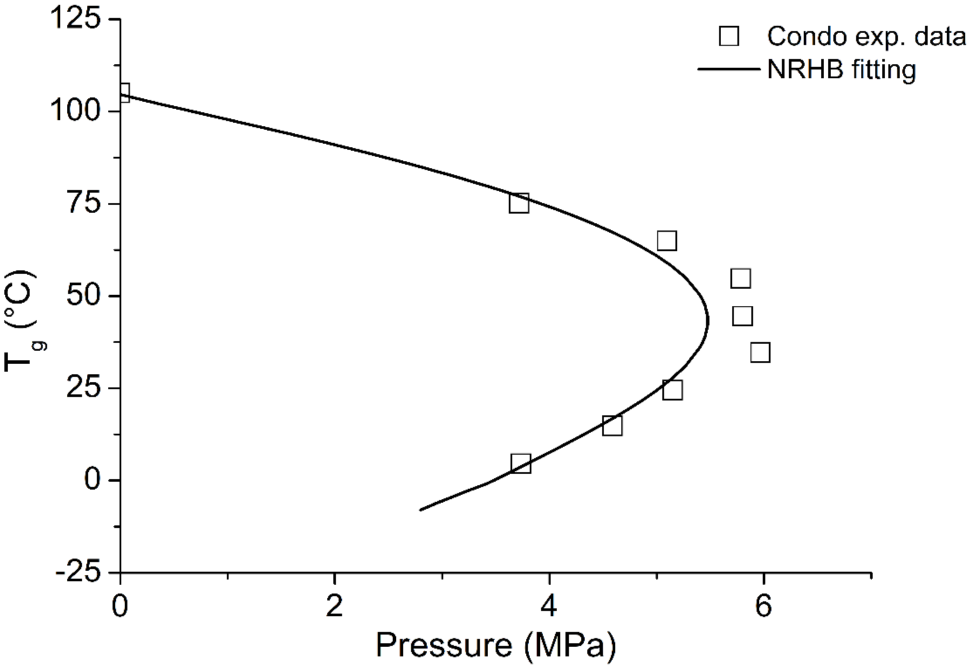

Figure 4.3: Fitting of PE sorption data of CO_2 in glassy PMMA (up) and fitting of PMMA T_g as function of the CO_2 pressure (down).

Table 4.2 PMMA-CO_2 fitting parameters

$k_{ij,0}$	a_T (K^{-1})	k_{sw} (MPa^{-1})
0.0686	$4.18\cdot 10^{-5}$	0.0191

With only three fitting parameters we have been able to fit simultaneously two phenomena, furthermore, the importance of the obtained results will arise in the next chapter, since the parameters in Table 4.1 and 4.2 will be used to predict the solubility of CO_2-C_2H_4 mixtures in glassy PMMA. This is an excellent outcome which confirms the goodness of the NETGP-NRHB model capability.

4.2 Nylon-H_2O system

Nylons are characterized by their good thermal stability, flexibility, and mechanical properties, in fact, they are widely used in flexible food packaging due to their moisture sensitivity, however the physical and transport properties of nylons change substantially as a function of the moisture content. In general, the modulus and yield stress decrease with increasing moisture content, while increases are seen in the elongation and energy to break.

The barrier to organic vapors and oxygen is generally good when the films are dry but weakens when exposed to high relative humidity (RH) environments. Such moisture-dependent transport characteristics may be suitable in fresh produce packaging, where it is desirable to limit water vapor and carbon dioxide build up within the package. Recently, studies have been carried out on the plasticization of these hydrophilic barrier layers by the sorbed water, which results in an increase in polymer chain segmental mobility. In addition, the shape of the sorption isotherms may vary with the amorphous content and thermal history of the polymer. Due to the moisture sensitivity of the polyamide, we believe that a study of water-vapor sorption in the polyamide to better understand the RH-dependent is necessary. The present study was undertaken to characterize the water vapor sorption in nylon 6,6 films as a function of RH by NRHB model. It is worth noting that the use of NRHB theory is necessary to better describe this system, since it presents strong specific interactions like hydrogen bonding which cannot be taken into account in the equilibrium Sanchez-Lacombe framework.

4.2.1 NRHB pure Nylon parameters

In the case of Nylon 6,6, both proton donor and proton acceptor groups are present on its repeating unit (see Figure 4.4), so that self (polymer-polymer) HB do occur. In fact, Nylon 6,6 repeating unit displays two NH groups with one proton acceptor and one proton donor site per group and two carbonyl groups with 2 proton acceptor sites per group, so that NH-NH and NH-CO hydrogen bonding (HB) self-interactions have been considered in the model. Hereafter, the subscripts 11 and 12 refer to NH-NH and NH-CO interactions, respectively.

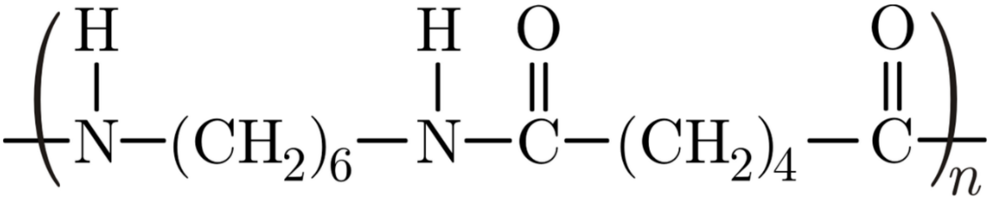

$$-\!\!\left(\overset{\displaystyle H}{\overset{|}{N}}-(CH_2)_6-\overset{\displaystyle H}{\overset{|}{N}}-\overset{\displaystyle O}{\overset{\|}{C}}-(CH_2)_4-\overset{\displaystyle O}{\overset{\|}{C}}\right)_{\!n}\!\!-$$

Figure 4.4: Nylon-6,6 repeating unit

As discussed in Section 1.3.3, each type of HB interaction involves two additional parameters, given by the associated molar energy and molar entropy of formation ($V_{\alpha\beta}^{0}$ is assumed null for this application). To minimize the number of fitting parameters, the values of energies of formation, E_{11}^{0} and E_{12}^{0},, and entropies of formation, S_{11}^{0} and S_{12}^{0}, have been assumed to take the corresponding average values for NH-NH and NH-CO interactions available in the literature [20] as determined from low molecular weight systems. This approach, rooted on the "local feature" of HB interactions, has been originally proposed in the framework of the NRHB model. In particular, the energies of formation $E_{11}^0 = -8500$ J/mol and $E_{12}^0 = -9176$ J/mol, while the entropies of formation $S_{11}^0 = -10.25$ J/(mol K) and $S_{12}^0 = -6.94$ J/(mol K).

Once the HB self-interaction parameters of the polymer have been determined, the remaining NRHB LF parameters of pure Nylon have been retrieved by a nonlinear fitting of equilibrium PVT data taken from the literature [21]. In Figure 4.5 are reported the equilibrium PVT data along with the best fitting curves provided by the NRHB model.

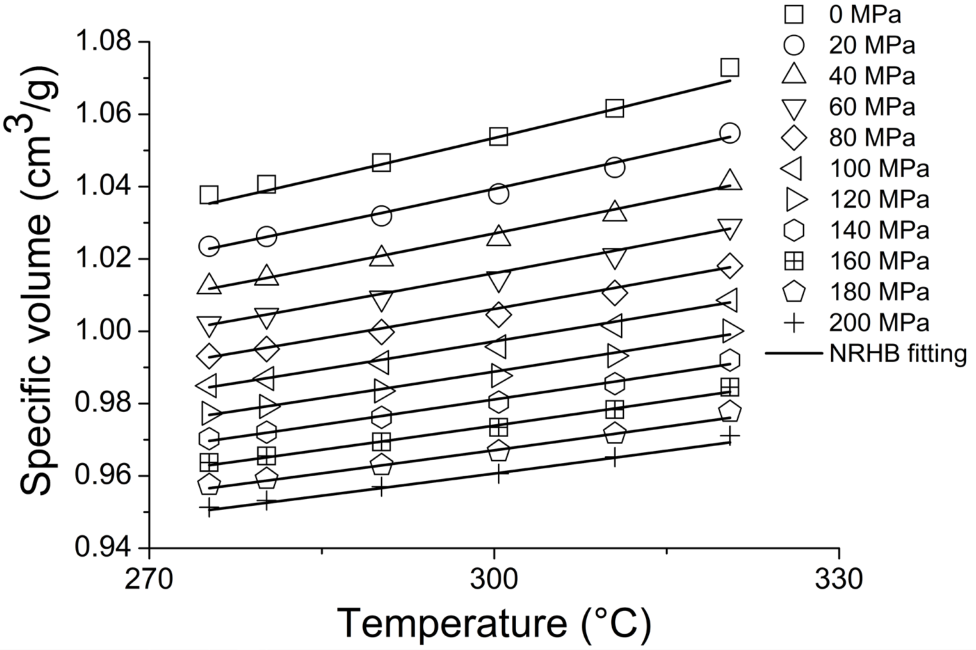

Figure 4.5: Fitting of PVT data for Nylon using NRHB EoS

Lattice fluid parameters resulting from the PVT data fitting are reported in the Table 4.3. About the flexibility parameter, the flex energy, Δu_i, has been calculated by the Gibbs-Di Marzio criterion applied to the equilibrium NRHB entropy in corresponding of the T_g of Nylon (equal to 44°C) at atmospheric pressure measured by Zoller et al. [21]. The resulting flex energy is $\Delta u_i = 0.838$ kJ/mol, while Z has been imposed equal to 4, as already done for other polymers [6].

Table 4.3 Pure Nylon and water NRHB Lattice fluid parameters.

	ε_h (Jmol^{-1})	ε_s (Jmol^{-1}K^{-1})	$v_{sp,0}$ (cm^{3}g^{-1})	s	Ref.
Nylon	7690.7	0.1161	0.8923	0.783	This work, s from [7]
H_2O	5336.5	6.50570	0.97034	0.861	[22]

4.2.2 Nylon-H_2O solubility and Tg as function of the relative humidity

As for PMMA-CO_2 system, simultaneous solubility and glass transition temperature as function of the sorbed penetrant of experimental data for nylon-water system (taken from [23]) have been fitted by equilibrium NRHB model. In the case under analysis, other specific interactions have been considered in the formulation of NRHB model equations used to fit the experimental equilibrium sorption isotherm. In particular, self-water interaction and cross H_2O-NH and H_2O-CO interactions are assumed to occur between water molecules (2 proton acceptors and 2 proton donors per molecule of water) and the repeating units of Nylon. Hereafter, the subscripts 13 (or equivalently 31), 32 and 33 refer to NH-H_2O (or equivalently H_2O-NH), H_2O-CO and H_2O-H_2O interactions, respectively. The new interactions involve two additional fitting parameters for each kind of interaction, i.e., the related molar energy and molar entropy of formation, however in order to minimize the number of fitting parameters, the values of energy and entropy of formation E_{33} and S_{33} have been taken from the ref. [20] and are equal to E_{33}=-16100 J/mol and S_{33}=-14.7 J/(mol K). However, the cross E_{13}, S_{13}, E_{32} and S_{32} are fitting parameters and their values, with in addition the values of $k_{ij,0}$ and a_T, are reported in the Table 4.4, while the fitting curves are shown in Figure 4.6.

Table 4.4 Cross hydrogen bonding and mean-field interaction fitting parameters of Nylon-H_2O system

E_{13} (J mol^{-1})	S_{13} (J mol^{-1}K^{-1})	E_{32} (J mol^{-1})	S_{32} (J mol^{-1}K^{-1})	$k_{ij,0}$	a_T (K^{-1})
-10019	-4.69	-11736	-2.31	-0.643	0.00213

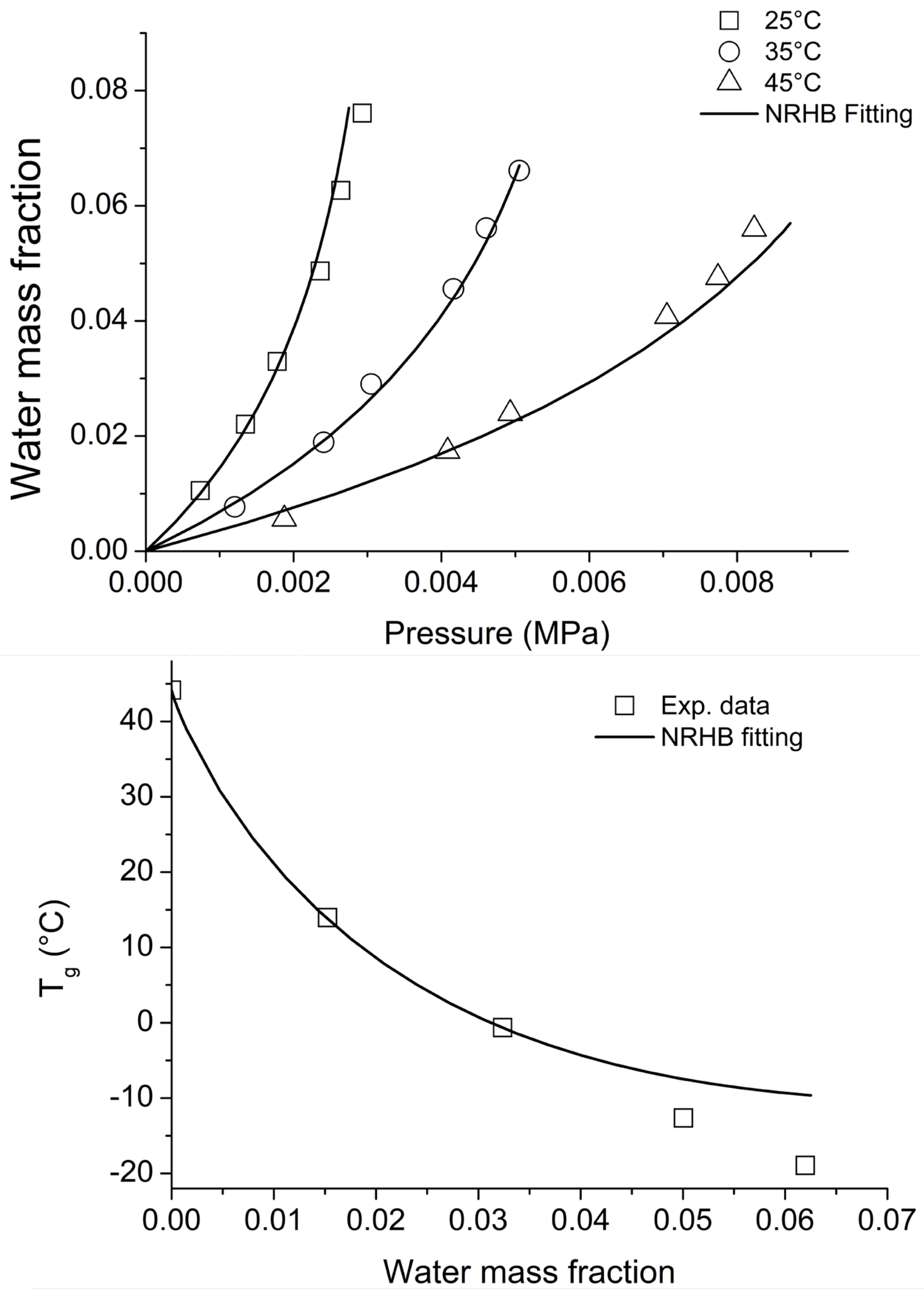

Figure 4.6: Fitting of equilibrium sorption data of water in rubbery nylon 6,6 (up) and fitting of nylon 6,6 T_g as function of the water mass fraction (down).

A good agreement of the experimental data has been obtained. It is worth noting that despite the numerous fitting parameters systems containing water can be hardly modelled with other lattice fluid models, such as Sanchez-Lacombe theory and its extension to non-equilibrium glassy polymers. Moreover, the energy and the entropy of hydrogen bonding formation are measurable quantity, e.g., by spectroscopic measurements.

References

[1] R. A. Assink, J. Polym. Sci.: Polym. Phys. Ed., 12 (1974) 2281.

[2] A. Fredenslund, R.L. Jones, J.M. Prausnitz, AIChE J. (1975) 21, 1086.

[3] A. Fredenslund, M.J. Sorensen, In: Models for Thermodynamic and Phase Equilibria Calculations; Sandler S., Ed.; Marcel Dekker: New York (1994).

[4] M. Schmidt, F. H. J. Maurer, Isotropic Pressure-Densified Atactic poly(methyl methacrylate) Glasses: Free-Volume Properties from Equation-of-State Data and Positron Annihilation Lifetime Spectroscopy, Macromolecules 33 (2000) 3879-3891.

[5] O. Olabisi, R. Simha, Pressure-Volume-Temperature Studies of Amorphous and Crystallizable Polymers. I. Experimental, Macromolecules 8 (1975) 206-210.

[6] P. D. Condo, I. C. Sanchez, C. G. Panayiotou, K. P. Johnston, Glass Transition Behavior Including Retrograde Vitrification of Polymers with Compressed Fluid Diluents, Macromolecules, 25 (1992) 6119-6127.

[7] C. Panayiotou, M. Pantoula, E. Stefanis, I. Tsivintzelis, I. G. Economou, Nonrandom Hydrogen-Bonding Model of Fluids and Their Mixtures. 1. Pure Fluids, Ind. Eng. Chem. Res. (2004) 43, 6592-6606.

[8] M. Minelli, S. Campagnoli, M. G. De Angelis, F. Doghieri, G. C. Sarti, Predictive Model for the Solubility of Fluid Mixtures in Glassy Polymers, Macromolecules 44 (2011) 4852–4862.

[9] S. Skjold-Joergensen, B. Kolbe, J. Gmehling, P. Rasmussen, Vapor-Liquid Equilibria by UNIFAC Group Contribution. Revision and Extension, Ind.Eng.Chem. Process Des.Dev. 18 (1979) 714-722.

[10] J. Gmehling, P. Rasmussen, A. Fredenslund, Vapor-Liquid Equilibria by UNIFAC Group Contribution. Revision and Extension. 2, Ind.Eng.Chem. Process Des.Dev., 21 (1982) 118-127.

[11] E. A. Macedo, U. Weidlich, J. Gmehling, P. Rasmussen, Vapor-Liquid Equilibria by UNIFAC Group-Contribution. Revision and Extension. 3, Ind.Eng.Chem. Process Des.Dev. 22 (1983) 676-678.

[12] D. Tiegs, J. Gmehling, P. Rasmussen, A. Fredenslund, Vapor-Liquid Equilibria by UNIFAC Group Contribution. 4. Revision and Extension, Ind.Eng.Chem.Res., 26 (1987) 159-161.

[13] H.K. Hansen, P. Rasmussen, A. Fredenslund, Schiller M., Gmehling J., Vapor-Liquid Equilibria by UNIFAC Group-Contribution. 5. Revision and Extension, Ind.Eng.Chem.Res. 30 (1991) 2352-2355.

[14] R. Wittig, J. Lohmann, J. Gmehling, Vapor-Liquid Equilibria by UNIFAC Group Contribution. 6. Revision and Extension, Ind.Eng.Chem.Res. 42 (2003) 183-188.

[15] M. Minelli, G.C. Sarti, Thermodynamic modeling of gas transport in glassy polymeric membranes, Membranes 7 (2017) 46.

[16] M. Minelli, G.C. Sarti, Permeability and solubility of carbon dioxide in different glassy polymer systems with and without plasticization, J. Membr. Sci. 444 (2013) 429-439.

[17] M. Minelli, Modeling CO_2 solubility and transport in poly(ethylene terephthalate) above and below the glass transition, J. Membr. Sci. 451 (2014) 305-311.

[18] E. S. Sanders, W. J. Koros, H. B. Hopfenberg, V. T. Stannett, Pure and mixed gas sorption of carbon dioxide and ethylene in poly(methyl methacrylate), J. Membr. Sci. 18 (1984) 53-74.

[19] P. D. Condo, I. C. Sanchez, C. G. Panayiotou, K. P. Johnston, In situ measurement of the glass transition temperature of polymers with compressed fluid diluents, 32 (1994) 523-533.

[20] I. Tsivintzelis, I. G. Economou, G. M. Kontogeorgis, Modeling the Solid–Liquid Equilibrium in Pharmaceutical-Solvent Mixtures: Systems with Complex Hydrogen-Bonding Behavior, American Institute of Chemical Engineers, 55 (2009) 756-770.

[21] P. Zoller, D. J. Walsh, Standard Pressure Volume Temperature Data for Polymers, Technomic Publishing: Lancaster, PA, USA (1995).

[22] I. Tsivintzelis, G. M. Kontogeorgis, Modeling the vapor–liquid equilibria of polymer–solvent mixtures: Systems with complex hydrogen bonding behavior, Fluid Phase Equilibria, 280 (2009) 100-109.

[23] L. T. Lim, I. J. Britt, M. A. Tung, Sorption and transport of water vapor in Nylon 6,6 film, Journal of Applied Polymer Science, 71 (1999) 197–206

Chapter 5

Prediction of Solubility and Permeability of mixtures of light gases in glassy polymers

Once the thermodynamic consistency of the NRHB model has been assessed, the subsequent step is to apply the model and its extension to the out-of-equilibrium thermodynamics, NETGP-NRHB model, to predict the solubility and the permeability of glassy polymer-penetrants mixtures of interest for technological applications, which include the use of glassy polymeric membranes in gas separation processes. For this purpose, CO_2/CH_4 and CO_2/C_2H_4 mixtures in glassy polymer are widely studied in literature [1-5], for their extensive use in Petrochemical Industry applications.

Despite its capability of describing the thermodynamics of complex multicomponent systems and its discussed thermodynamic consistency, the NETGP-NRHB has not yet been applied to investigate sorption thermodynamics of binary penetrant mixtures within a glassy polymer, which is of primary interest in gas separation processes. Moreover, the NETGP-NRHB theory, has not yet been applied to calculate the thermodynamic driving force for penetrant diffusion within a polymer-penetrant glassy mixture in the modelling of transient diffusion and steady-state permeation of penetrant mixtures through a glassy polymeric membrane.

To the aim of assessing the suitability of the NETGP-NRHB approach to deal with multicomponent systems, in the first part of this chapter, the model has been applied to predict the solubility of binary gaseous mixtures, CO_2/CH_4 and CO_2/C_2H_4 in glassy poly(2,6-dimethyl-1,4-phenylene oxide) (PPO) and polymethylmethacrylate (PMMA) membranes, respectively. Then, NETGP-NRHB in the framework of the diffusion model (NETGP-NRHB-DM) has been used to fit permeation data of pure CO_2 or CH_4 through various glassy polymeric membranes based on bisphenol-A polymers (polyarylate (PAr), polyethersulfone (PSf) and polyhydroxyether (PH); repeating units shown in figures 5.1a, 5.1b and 5.1c, respectively) using the NETGP-NRHB model to calculate both the solubility and the thermodynamic factor appearing in the constitutive equation of mass flux for each penetrant shown in the Section 1.5. Finally, it will be shown, based on the knowledge of transport data for each binary gas-polymer system, predictions of the permeability of binary mixtures in glassy polymers (ternary systems) are obtained that compare very well with experimental data available in literature.

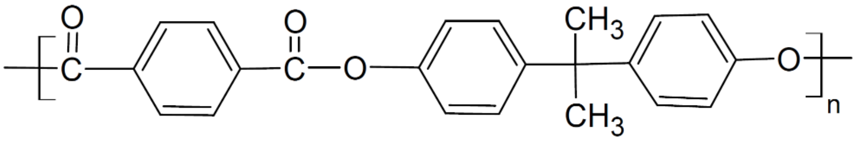

Figure 5.1a: Polyarylate (PAr) repeating unit

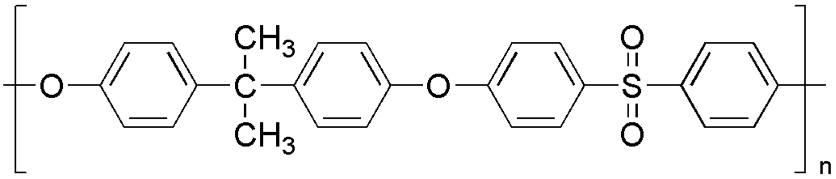

Figure 5.1b: Polyethersulfone (PSf) repeating unit

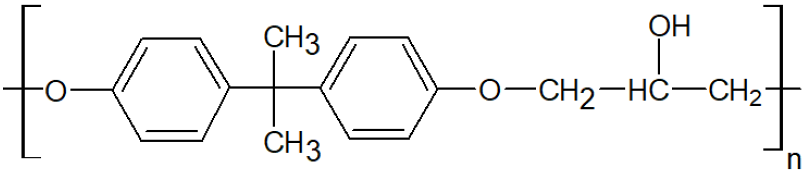

Figure 5.1c: Polyhydroxyether (PH) repeating unit

5.1 Pure polymer parameters

Considering first the polymers, as for the case of PMMA, in PPO, PAr and PSf the occurrence of self-HB interactions can be disregarded, based on their chemical structures. Therefore, only NRHB "mean field" LF model parameters for pure polymers need to be determined.

Once again, the values of ε_h, ε_s and $v_{sp,0}$ have been gathered by a non-linear regression of equilibrium dilatometric data (PVT) [6-7], while s has been determined according to UNIFAC group contribution model [8-9]. Following this procedure, in a previous contribution [10], we have determined the NRHB parameters of PPO, that are reported in Table 5.1, while the parameters of the PMMA are already reported in the Chapter 4. The NRHB EoS provides an excellent fitting of PVT data for all these polymers, as evident in Figures 5.2a and 5.2b. The calculated values of the parameters are reported in Table 5.1.

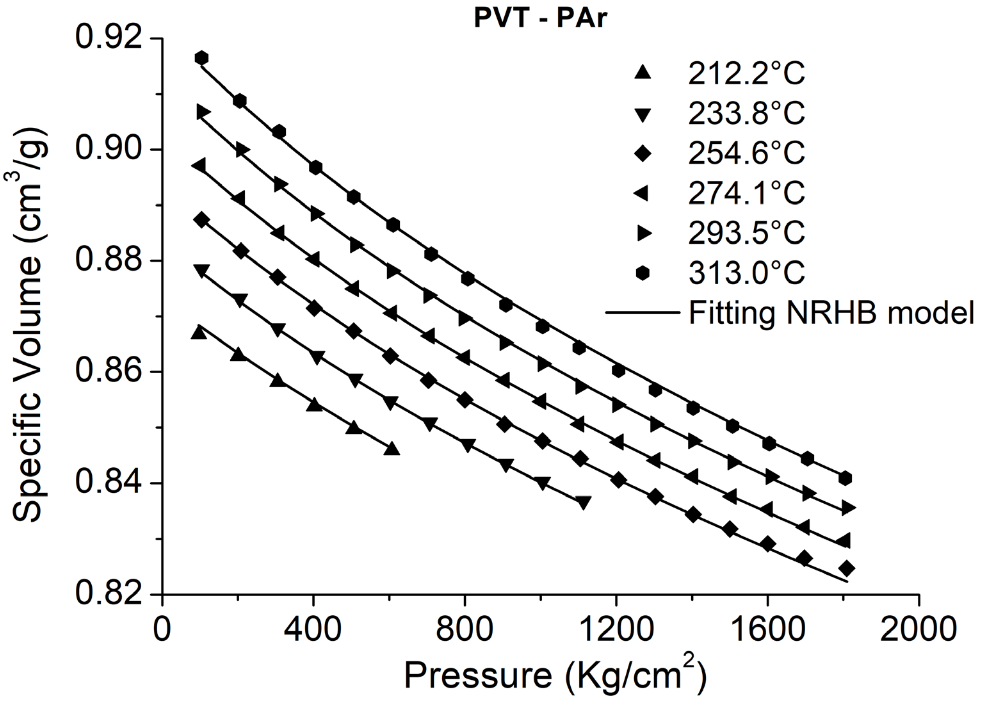

Figure 5.2a: Fitting of PVT data for PAr using NRHB EoS

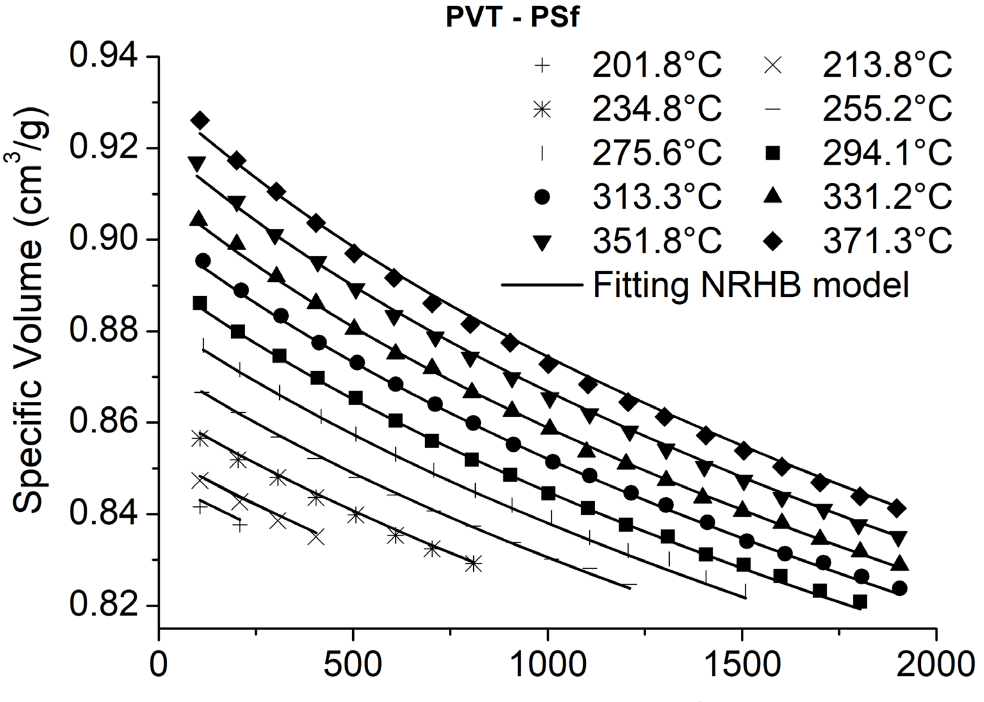

Figure 5.2b: Fitting of PVT data for PSf using NRHB EoS

Table 5.1 Pure components NRHB Lattice fluid parameters.

	ε_h (Jmol^{-1})	ε_s (Jmol^{-1}K^{-1})	$v_{sp,0}$ (cm^{3}g^{-1})	s	Ref.
CH_4	1956.2	-0.9181	2.12519	0.961	[11]
C_2H_4	2834.4	-0.7282	1.54153	0.944	[11]
PPO	5320	3.440	0.862	0.748	[10]
PAr	6272.3	4.5812	0.77032	0.713*	This work, data from [12]
PSf	6602.7	3.5470	0.75806	0.693*	This work, data from [12]

*This “surface-to-volume” ratio, s, has been estimated by using the widely used UNIFAC group contribution model [8] with data taken from [13-18].

In the case of PH, both proton donor and proton acceptor groups are present on its repeating unit, so that self (polymer-polymer) HB do occur. In fact, PH repeating unit displays one hydroxyl group and two ether-oxygen atoms, so that OH-OH and OH-O hydrogen bonding (HB) self-interactions have been considered in the model. Hereafter, the subscripts 11 and 12 refer to OH-OH and OH-O interactions, respectively. As discussed in Section 1.3.3 and shown in Section 4.2.2 for the Nylon, $V_{\alpha\beta}^0$ is assumed null, while the values of energies of formation, E_{11}^0 and E_{12}^0,, and entropies of formation, S_{11}^0 and S_{12}^0, have been assumed to take the corresponding average values for OH-OH and OH-O interactions available in the literature as determined from low molecular weight systems (see Table 5.2a).

As always, the remaining NRHB LF parameters of pure PH have been retrieved by a nonlinear fitting of equilibrium PVT data taken from the literature [11]. In Figure 5.3, the equilibrium PVT data are reported along with the best fitting curves provided by the NRHB model.

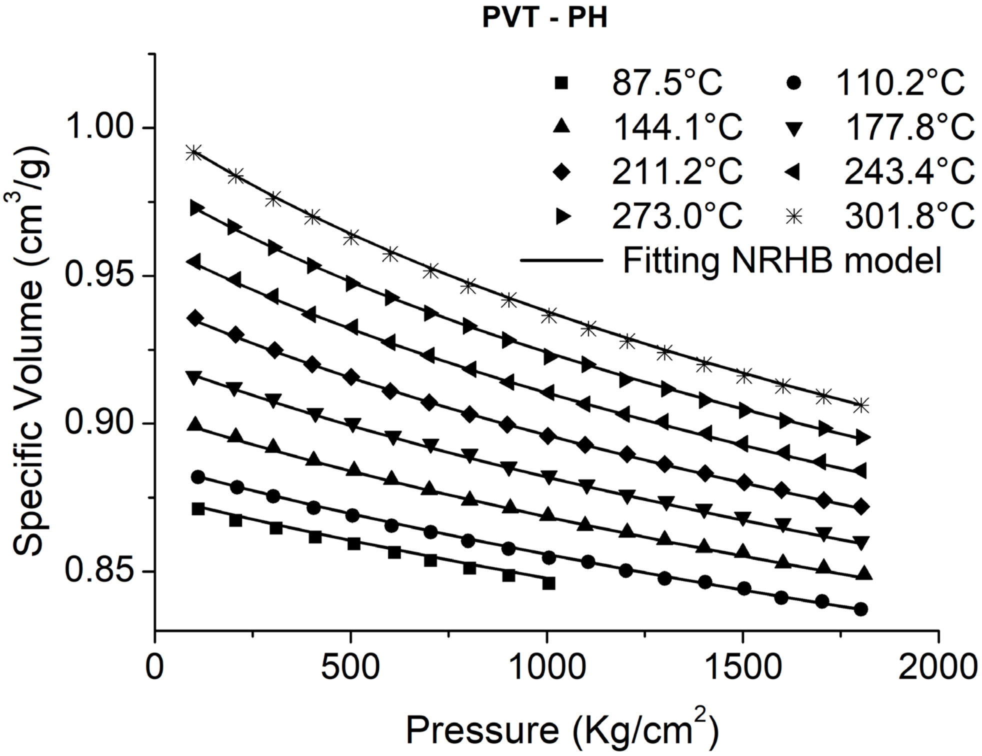

Figure 5.3: Fitting of PVT PH

A very good interpretation of dilatometric data is provided by the NRHB EoS and the calculated best fitting values are reported in Table 5.2b.

Table 5.2a Self specific interaction parameters for PH

E_{11} (J mol^{-1})	**S_{11} (J mol^{-1}K^{-1})**	**E_{12} (J mol^{-1})**	**S_{12} (J mol^{-1}K^{-1})**
-22500	-27.5	-19000	-24

Table 5.2b Lattice fluid parameters of PH

ε_h **(J mol^{-1})**	ε_s **(J mol^{-1}K^{-1})**	$v_{sp,0}$ **(cm^{3}g^{-1})**	**s**
6732.4	2.1049	0.82794	0.7592*

*"Surface-to-volume" ratio, *s,* has been estimated by using the widely used UNIFAC group contribution model [8] with data taken from [13-18].

As for the pure CO_2 of the Chapter 4, for the other penetrants in this study no-self HB interactions are expected, so that only their NRHB lattice fluid parameters need to be determined. Their values were taken from literature [11] and the values are again reported in Table 5.1.

Finally, the density of the out-of-equilibrium neat (unpenetrated) glassy polymers at 35°C, $\rho_{p,0}^{un}$, at 35°C were taken from the literature and are reported in Table 5.3.

Table 5.3 Unpenetrated glassy polymer density at 308K.

	$\rho_{p,0}^{un}$ (g/cm^3)	Ref.
PPO	1.067	[19]
Par	1.210	[20]
PSf	1.235	[20]
PH	1.175	[20]

5.2 NRHB binary interaction parameters

Modelling of sorption thermodynamics and transport of multicomponent gas mixtures based on NRHB and NETGP-NRHB approaches adopted in the present contribution requires the knowledge of binary (gas-gas and gas-polymer) "mean field" interaction parameters, that have been indicated as k_{ij}. As already explained, the k_{ij} involving a penetrant i and an amorphous glassy polymer j can be obtained by fitting PE solubility data of binary polymer-penetrant system. The k_{ij} involving a couple of penetrants can be instead obtained by fitting with the NRHB model equations a set of their binary LV equilibrium data.

Regarding the arguments about the $\rho_{p,0}$, to deal with the case of a mixture of an amorphous glassy polymer with a binary gas mixture, one can simply extend equation (4.2) according to the following equation [19]:

$$\rho_{p,0} = \rho_{p,0}^{un} \cdot \left(1 - k_{sw,1}P_1 - k_{sw,2}P_2\right) \tag{5.1}$$

that assumes that the effect of the penetrants is simply additive. In equation (5.1) P_i represents the partial pressure of penetrant i in the gaseous mixture. Hence, to model the sorption of multicomponent gas mixtures in a glassy polymer one only needs the corresponding binary swelling factors, $k_{sw,i}$, used to describe the binary cases, that can be retrieved by fitting the corresponding PE binary solubilities.

Finally, in the case that cross-specific interactions could be established between the penetrant molecule and the polymer backbone, one should also know the values of the parameters (energy and entropy of formation) for each of these possible interactions. As discussed in Section 1.3.3, to minimize the number of model parameters, predictions from equations

(1.51) and (1.52) or (1.53) and (1.54) have been used in the case that cross-specific interactions occur.

5.2.1 CO_2 – CH_4 mean field binary interaction parameter

The mean-field interaction parameter k_{ij} of the couple CO_2 – CH_4 has been estimated by a non-linear regression of L-V equilibrium data at -3°C taken from [21], using the NRHB model equations. As discussed above, the NRHB model has been implemented considering only mean-field interactions, so that k_{ij} is the only fitting parameter once the lattice fluid parameters of the pure component have been determined. In Figure 5.4, it is reported a comparison between the experimental data with the NRHB fitting lines. The quality of fitting is satisfactory and the best fitting value of k_{ij}, is reported in Table 5.4a.

Table 5.4a Binary fitting parameters, k_{ij} and k_{sw} for the systems PPO-CH_4-CO_2, PAr-CH_4-CO_2, PSf-CH_4-CO_2, PH-CH_4-CO_2.

	$k_{ij,CH4}$	$k_{sw,CH4}$ (MPa^{-1})	$k_{ij,CO2}$	$k_{sw,CO2}$ (MPa^{-1})
CO_2	0.0406	-	-	-
PPO	-0.278	0.00336	-0.0871	0.0147
PAr	-0.0833	-0.000232	-0.00870	0.0113
PSf	-0.0937	0.00108	0.0130	0.0105
PH	-0.196	-4.553×10^{-6}	-0.118	0.00587

Table 5.4b Binary fitting parameters of *kij* as function of the temperature for C_2H_4- CO_2 system

	$k_{ij,0}$	a_T (K^{-1})
CO_2-C_2H_4	0.151	-0.000419

Table 5.4c Binary fitting parameters, k_{ij} and k_{sw}, for PMMA-C_2H_4 system

	k_{ij}	k_{sw} (MPa^{-1})
PMMA-C_2H_4	-0.00319	0.00768

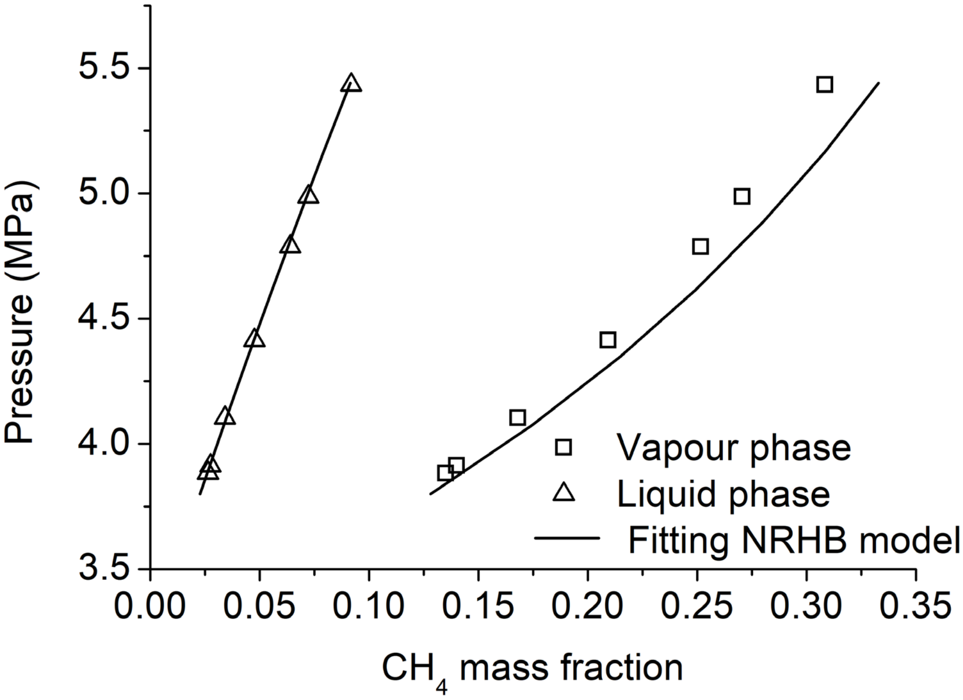

Figure 5.4: Fitting of VLE of CO_2 – CH_4 mixture at -3°C

This parameter is here assumed to be independent of temperature and the value determined from the described best fitting procedure will be used in the analyses performed in the present investigation at 35°C. The assumption of a temperature independent k_{ij} is often a good approximation in interpreting equilibrium data for several binary gaseous systems [5, 22-23]. Conversely, when lattice fluid models are applied to condensed phases a temperature dependence would be expected based upon the temperature dependence of mean-field potentials.

5.2.2 CO_2 – C_2H_4 mean field binary interaction parameter

The mean-field interaction parameter k_{ij} for the couple CO_2 –C_2H_4 has been determined by simultaneously fitting using NRHB model equations of L-V equilibrium data at respectively -10°C, 0°C and 10°C reported by Bae, et al. [24]. Being available data sets at different temperatures, the k_{ij} parameter has been assumed to be temperature dependent according to the equation (). The simultaneous fitting of L-V equilibrium experimental data at three different temperatures (see Figure 5.5) provides a satisfactory result. The best-fitting values of the two parameters, $k_{ij,0}$ and a_T are reported in Table 5.4b.

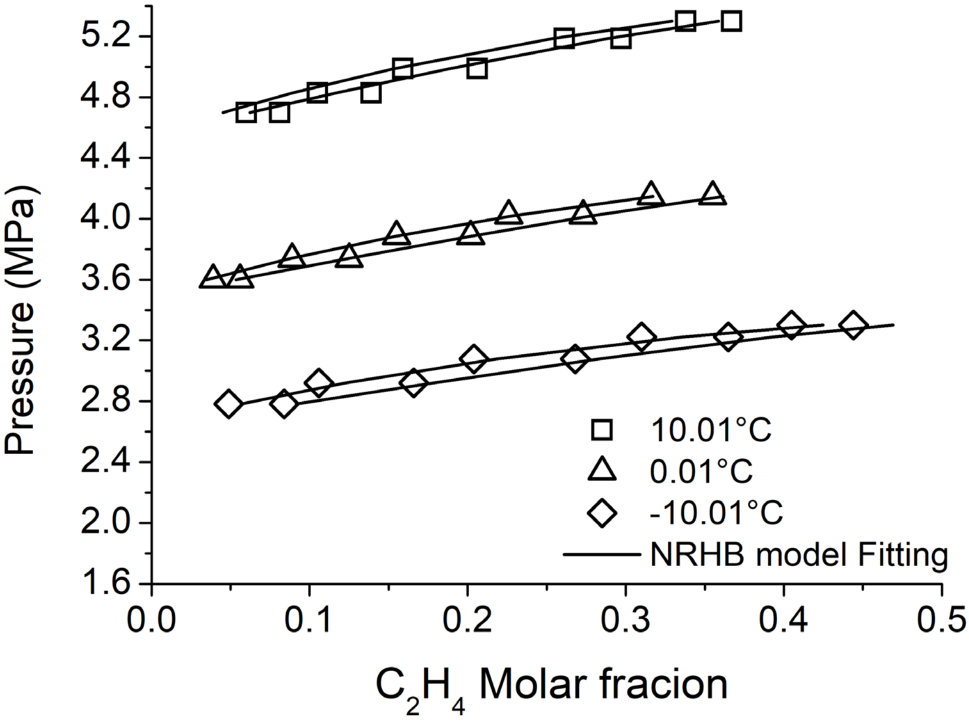

Figure 5.5: Fitting of VLE of CO_2 – C_2H_4 mixture

5.2.3 PPO-CO_2, PAr-CO_2, PSf-CO_2, PPO-CH_4, PAr-CH_4 and PSf-CH_4 binary mean field interaction and swelling parameters

The estimation of k_{ij} and k_{sw} for the couples PPO-CO_2, PAr-CO_2 and PSf-CO_2 have been performed by fitting the experimental sorption isotherms available in literature at 35°C for CO_2 in PPO (from ref [1]), PAr (from ref [2]) and PSf (from ref [3]). In Figures 5.6a, 5.6b and 5.6c are reported the very good results of fitting performed using the NETGP-NRHB theory. The estimated values of both mean-field interaction parameters, k_{ij}, and of the swelling parameters, k_{sw}, are reported in Table 5.4a. In all cases $k_{sw}>0$ indicating that the swelling effect associated to CO_2 sorption prevails on the mechanical action of pressure that would instead promote an increase of polymer density. For comparative purposes, in the same figures are also reported the best fitting curves obtained assuming no volume dilation (i.e., fixing $k_{sw}=0$) which indeed provides a less satisfactory interpretation of data. Similar results and conclusions were also obtained by De Angelis et al. [19] using the NELF approach for the same set of sorption data.

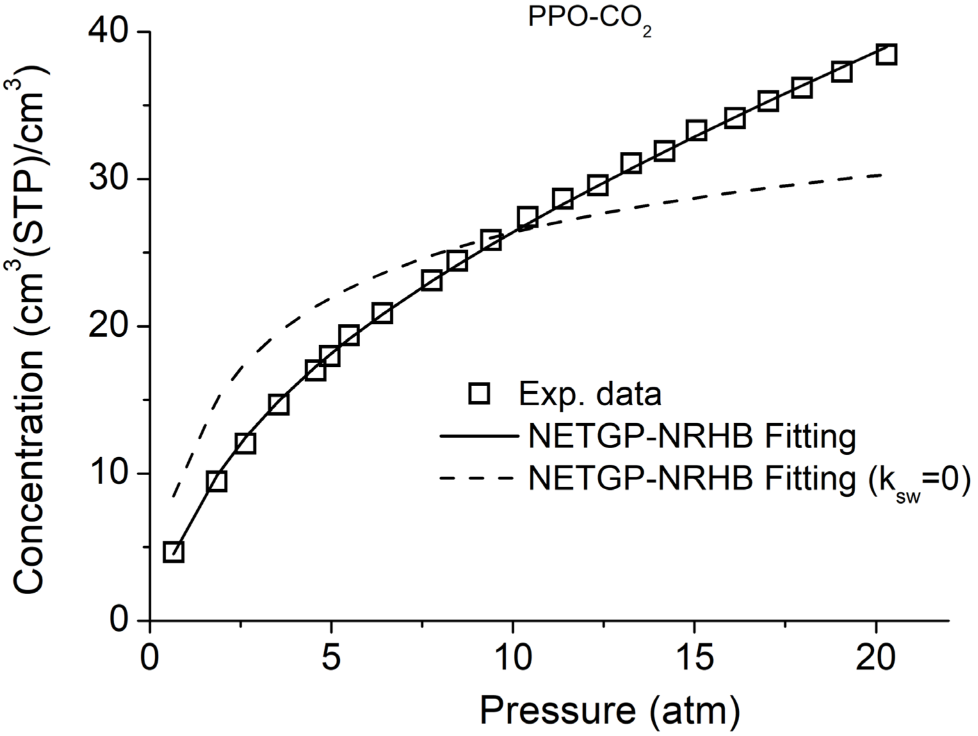

Figure 5.6a: Fitting of PPO – CO_2 solubility data at 35°C.

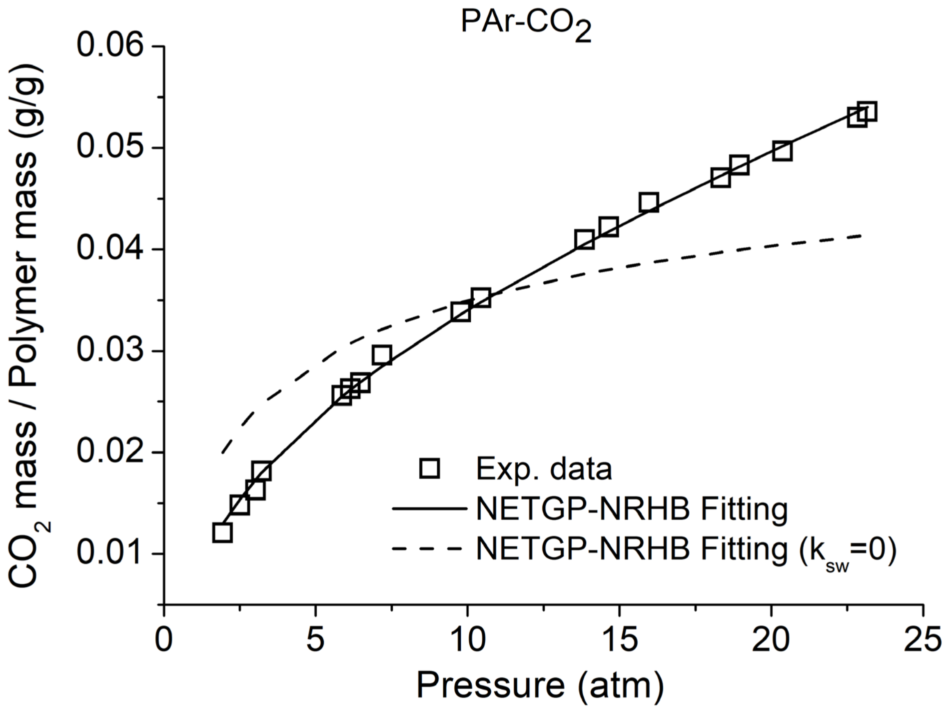

Figure 5.6b: Fitting of PAr – CO_2 solubility data at 35°C.

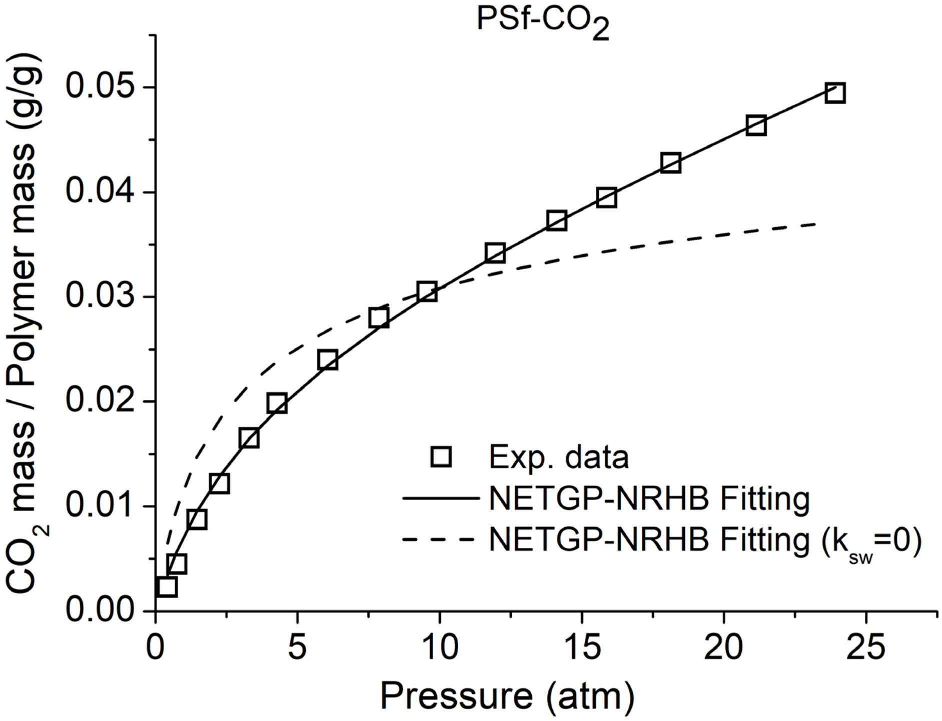

Figure 5.6c: Fitting of PSf – CO_2 solubility data at 35°C.

An analogous procedure has been followed to estimate k_{ij} and k_{sw} for the couples PPO-CH_4, PAr-CH_4 and PSf-CH_4 at 35°C (data taken, respectively, from refs. [1-3]). The results of fitting performed with the NETGP-NRHB model along with the experimental sorption isotherms are reported in Figure 5.7a, 5.7b and 5.7c and the best fitting values of both parameters are again reported in Table 5.4a.

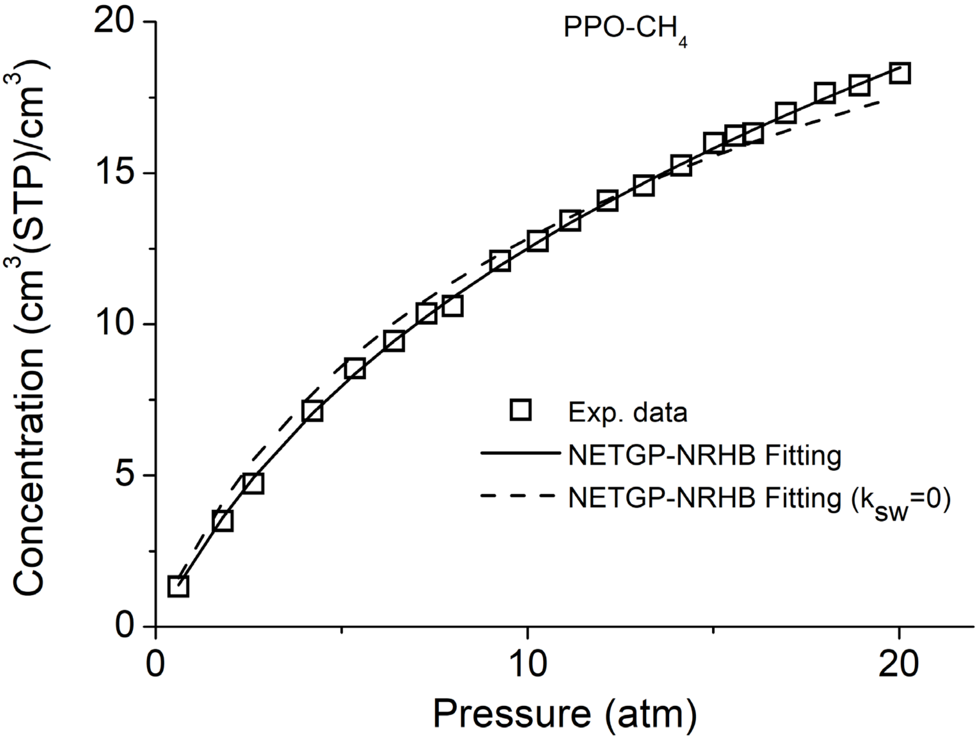

Figure 5.7a: Fitting of PPO – CH_4 solubility data at 35°C.

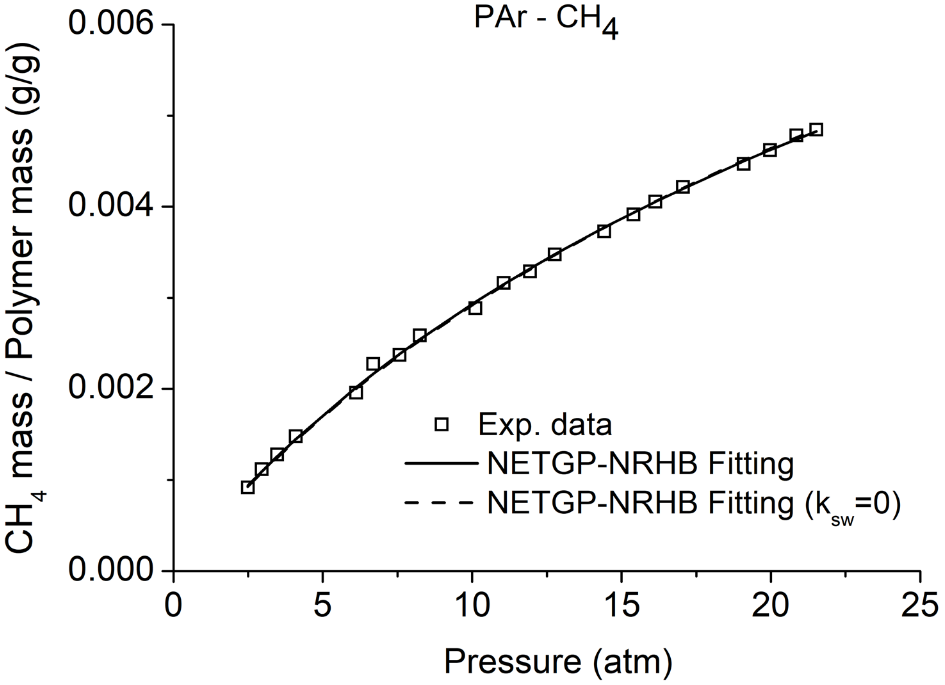

Figure 5.7b: Fitting of PAr – CH_4 solubility data at 35°C.

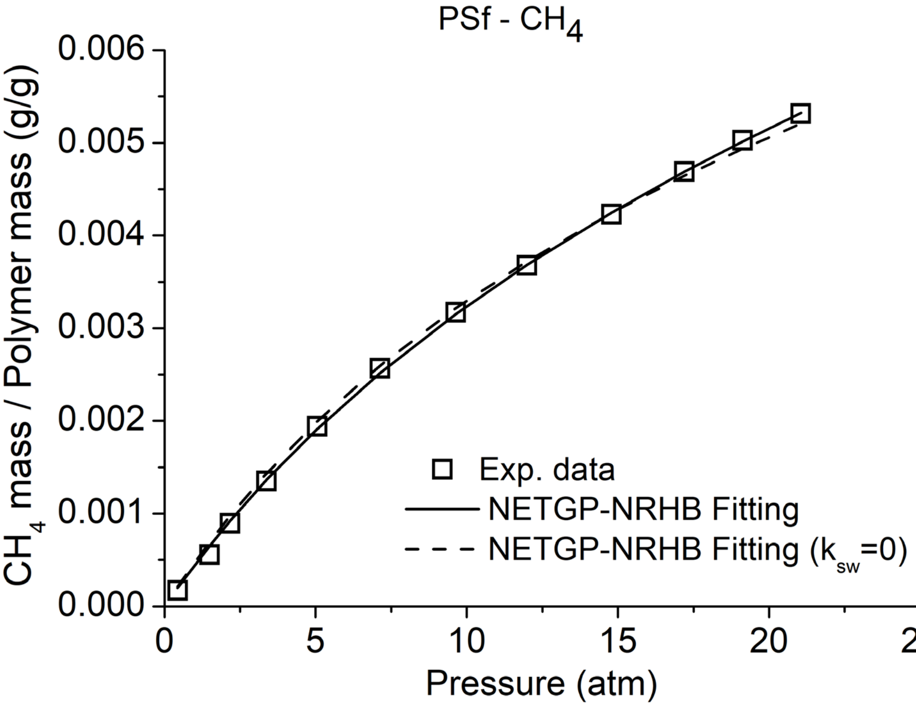

Figure 5.7c: Fitting of PSf – CH_4 solubility data at 35°C.

Notably, in these cases the values estimated for k_{sw} are positive but smaller than in the case of CO_2 (see the cases of PPO and PSf) or even negative (see the case of PAr), which is consistent with the slight swelling effect of CH_4, in view of its limited solubility, that is even overcome, in the case of PAr, by the mechanical effect of the pressure on the polymer matrix. Coherently, the nonlinear regression assuming $k_{sw}=0$, provides a fair (in the case of PPO) or very good fitting (in the cases of PAr and PSf) of experimental data.

5.2.4 PMMA-C_2H_4 binary mean field interaction and swelling parameters

The values of k_{ij} and k_{sw} for the binary system PMMA-C_2H_4 have been obtained by fitting with the NETGP-NRHB model the corresponding experimental sorption isotherms at 35°C (data from ref [2]). As for the previous binary systems, excellent results of the fitting procedure have been obtained using both fitting parameters (the values of best fitting parameters are reported in Table 5.4c) while a worse fitting quality has been obtained assuming no volume dilation, i.e., fixing $k_{sw}=0$ (see Figures 5.8). Regarding the binary parameters of PMMA-CO_2 system, they are reported in Table 4.2 of the previous chapter.

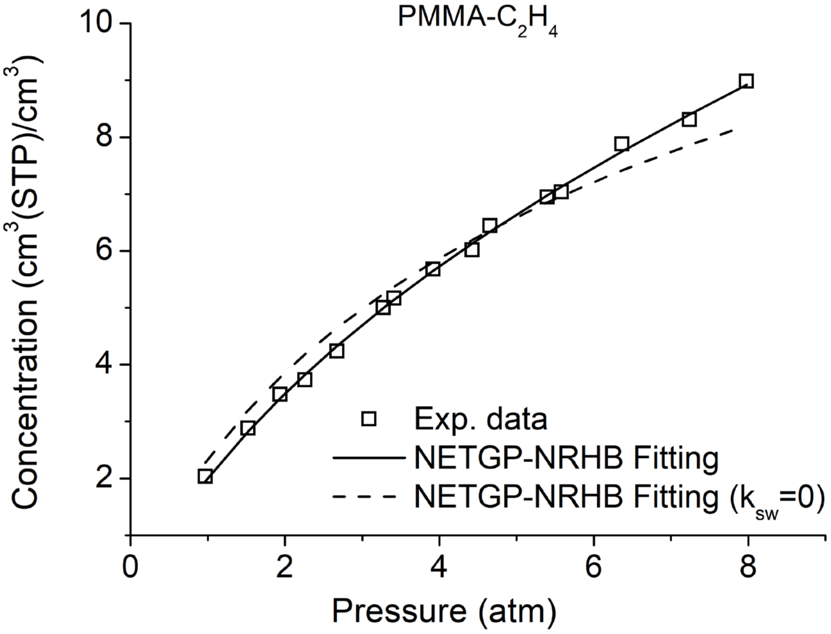

Figure 5.8: Fitting of PMMA – C_2H_4 solubility data at 35°C.

5.2.5 PH-CO_2 and PH-CH_4 binary mean field interaction and swelling parameters and PH-CO_2 cross-specific interaction parameters

In the case of the system PH– CO_2, cross OH-CO_2 specific interactions have been considered in the formulation of NETGP-NRHB model equations used to fit the experimental sorption isotherm. Cross interactions are assumed to occur between oxygen atoms of a carbon dioxide molecule (2 proton acceptor per molecule) and the hydrogen of the hydroxyl groups of PH (1 proton donor per polymer repeating unit). The subscript 13 refers to the OH-CO_2 interaction that involves two additional parameters, i.e., the related molar energy and molar entropy of formation. To minimize the number of fitting parameters, the values of energy and entropy of formation, E_{13} and S_{13}, have been estimated according to the combining rules proposed by Tsivintzelis, et al. [25-27] for the cross association between one self-associated and one non-associating group, which result in equations (1.53) and (1.54). The corresponding values are reported in Table 5.5.

Table 5.5 Cross specific interaction parameters of the system PH-CO_2

E_{13} (J mol^{-1})	S_{13} (J $mol^{-1}K^{-1}$)
-11250	-13.75

The estimated values of k_{ij} and k_{sw} for the two binary sub-systems PH – CO_2 and PH –CH_4, reported in Table 5.4a, have been obtained by a non-linear regression with the NETGP-NRHB model (where the cross-HB interaction parameters determined above have been used) of the experimental sorption isotherms at 35°C (data taken from ref [3]). An excellent quality of fitting has been obtained, as shown in Figures 5.9a and 5.9b. The model provides for the estimated values of the parameters for the PH – CO_2 system a positive value of k_{sw}, thus indicating the occurrence of a relatively small linear volume dilation of the mixture, induced by the penetrant. In the case of the PH – CH_4 system, the low solubility of methane results in a k_{sw} value close to zero.

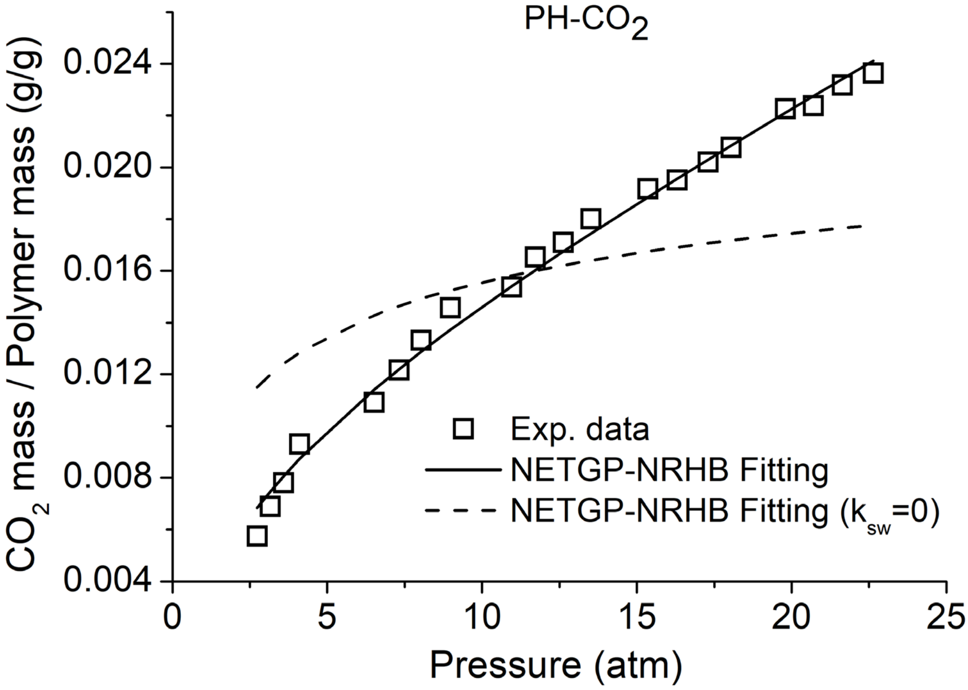

Figure 5.9a: Fitting of PH – CO_2 solubility data at 35°C.

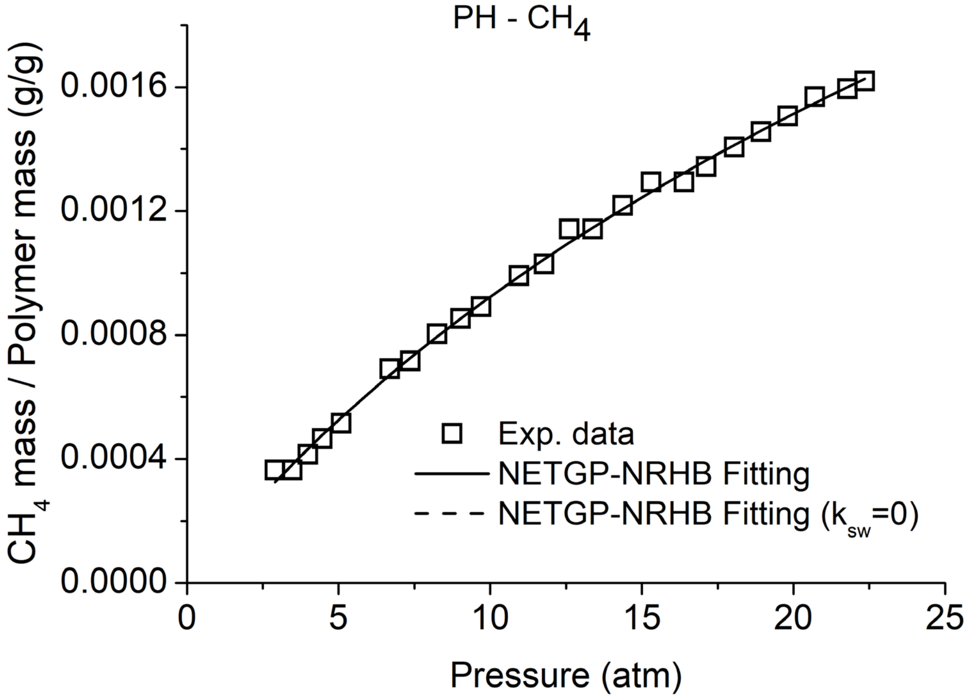

Figure 5.9b: Fitting of PH – CH_4 solubility data at 35°C.

5.3 Modelling the solubility of gas mixtures in glassy polymers using NETGP-NRHB

5.3.1 Solubility of CO_2-CH_4 mixture in PPO

Once all the binary k_{ij} and k_{sw} parameters have been determined, the NETGP-NRHB model has been used to predict the solubility of the CO_2-CH_4 mixture within PPO. The NETGP-NRHB predictions are in good agreement with the experimental data taken from [1, 19], as shown in Figure 5.10; for comparison purposes, NELF predictions obtained by De Angelis et al. [19] are also reported. As expected for systems not displaying strong specific interactions, the predictions of both models are quite close. A limited improvement in modelling capability is however observed with NETGP-NRHB model in the case of solubility of CO_2, which can be likely ascribed to the lattice-fluid statistics that accounts, differently from NELF, for the non-random nature of mean-field interactions and that does not suffer from the intrinsic thermodynamic inconsistency exhibited by NELF model in the case of multicomponent mixtures.

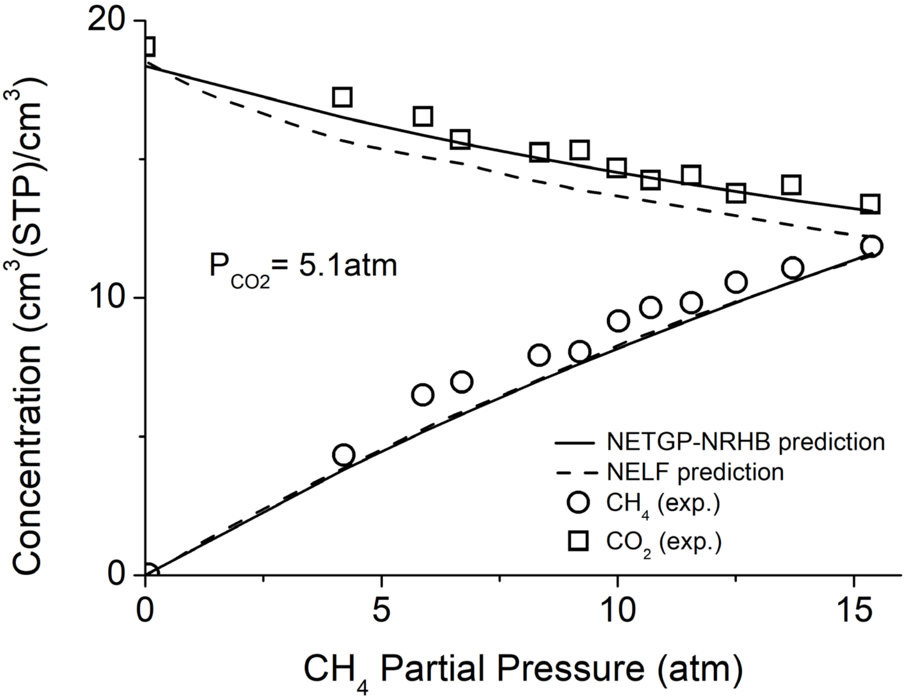

Figure 5.10: PPO – CO_2 – CH_4 prediction at 35°C and CO_2 partial pressure fixed at 5.1 atm.

5.3.2 Solubility of CO_2-C_2H_4 mixture in PMMA

NETGP-NRHB model has been used to predict the solubility of the CO_2 – C_2H_4 gas mixture within glassy PMMA at 35°C. As reported in Figure 5.11, also in this case model predictions are in good agreement with the experimental data taken from [2]. Predictions are slightly improved in comparison with those provided by NELF model [19]. It is worth noting that the k_{ij} for PMMA-CO_2 binary system is the one obtained in Section 4.1.2, consequently, this validates the goodness of the fitting parameters obtained from that simultaneous fitting procedure.

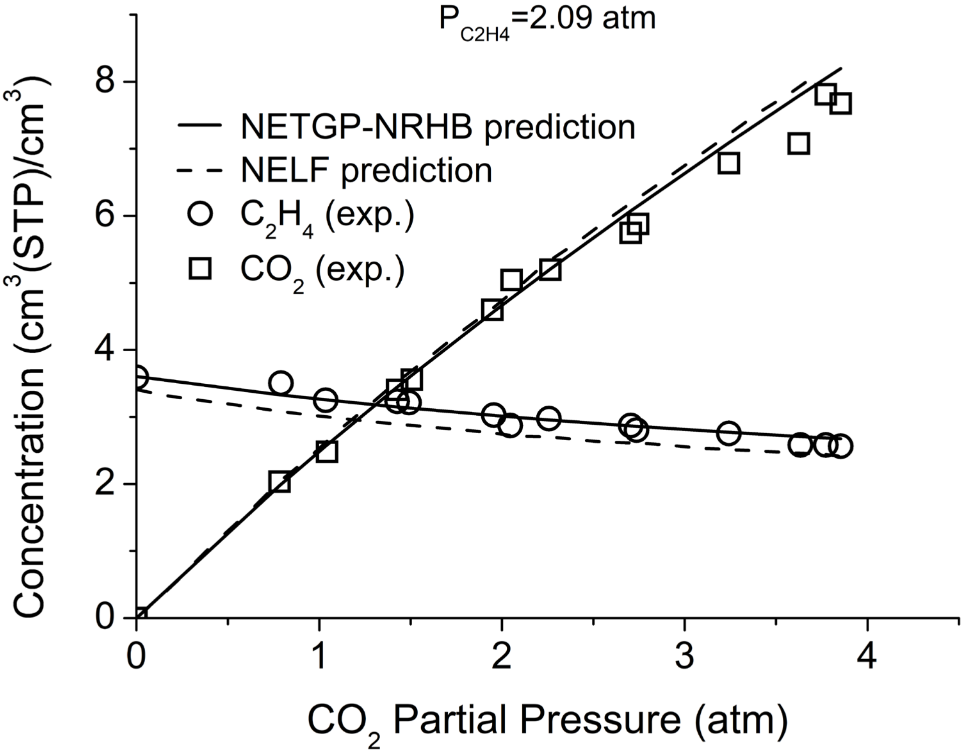

Figure 5.11: PMMA – CO_2 – C_2H_4 prediction at 35°C and C_2H_4 partial pressure fixed at 2.09 atm.

5.4 Modelling the permeability of gas mixtures in glassy polymers using the NETGP-NRHB-DM

Prediction of the permeability of binary gaseous mixtures in glassy polymers has been performed by using the NETGP-NRHB-DM that is based on the NRHB-NETGP model for non-equilibrium thermodynamics and on mass transport linear constitutive equations, originally proposed by Sarti et. al. [28-35], briefly summarized in Section 1.5.

In the NETGP-NRHB-DM for a multicomponent system are present both the set of parameters associated to the NETGP-NRHB model for the chemical potentials and the additional "mobility" parameters associated to the NETGP-NRHB-DM. In the case of permeation of binary gas mixtures in glassy polymers considered in the present context, reasonable simplifying assumptions can be applied in view of the low concentration of both penetrants within the polymer-penetrant mixture, as discussed in the Section 1.5. In fact, following the procedure of Sarti et. al. [20, 32], the problem can be restated only in terms of the diffusive fluxes of the two penetrants, so that just four "mobility parameters" are required, namely two mobility parameters for each penetrant *i*, i.e., L_{i0} and the "concentration factor" β_i, whose values have been assumed to be the same as those of the two corresponding polymer-penetrant binary sub-systems.

In what follows, each couple of L_{i0} and β_i has been retrieved by a non-linear regression of experimental binary permeability data available in literature for the associated binary sub-systems. Using this information, the NETGP-NRHB-DM has been used to predict the permeability of each ternary system, validating these results against experimental data taken from the literature.

5.4.1 Permeability of CO_2 – CH_4 mixture in PAr

Values of L_0 and β for the PAr – CO_2 and the PAr – CH_4 binary systems have been determined by a non-linear fitting of permeability data at 35°C at several gas pressures [3]. Best fitting curves obtained using the NETGP-NRHB-DM are reported in Figures 5.12a and 5.12b along with the experimental permeability data for the two binary systems, evidencing a quite satisfactory fitting. All the experimental data are reported in Barrer which is defined as: $1\ \mathrm{Barrer} = 3.35\ 10^{-16}\ \frac{\mathrm{mol\ m}}{\mathrm{m^2\ s\ Pa}}$. The values of best-fitting parameters are reported in Table 5.4. To this regard, it is worth noting that the overall effect of the penetrant concentration on its mass flux is lumped in a non-linear fashion way in the product of the penetrant mobility factor (L_{ii}), its thermodynamic factor $(\alpha_{i,j})$ and the dictated (by mass balance equation) corresponding concentration profile, so that the concentration factor, β_i, is not necessary expected to be higher for a penetrant with high solubility in a given polymer. Indeed, the higher solubility concentration of CO_2 could result in a lower concentration factor in the exponential law, as observed for the first two systems in the Table 5.4.

Using the mass transport parameters determined for the binary systems, the NETGP-NRHB-DM has been used to predict the permeability of the CO_2-CH_4 binary mixture in glassy PAr at 35°C. The calculations have been performed at 35°C for a 50:50 by mol gaseous mixture at several pressures. In Figure 5.13 model predictions are compared with experimental data taken from literature [3]. For the sake of comparison, in the same figure the diffusion model applied to the NELF framework (NELF-DM) predictions are also reported [20]. It is evident, that, for the system considered, both models exhibit a satisfactory predictive capability. The results of the two models are quite similar, as expected for a system which does not display any strong specific interaction.

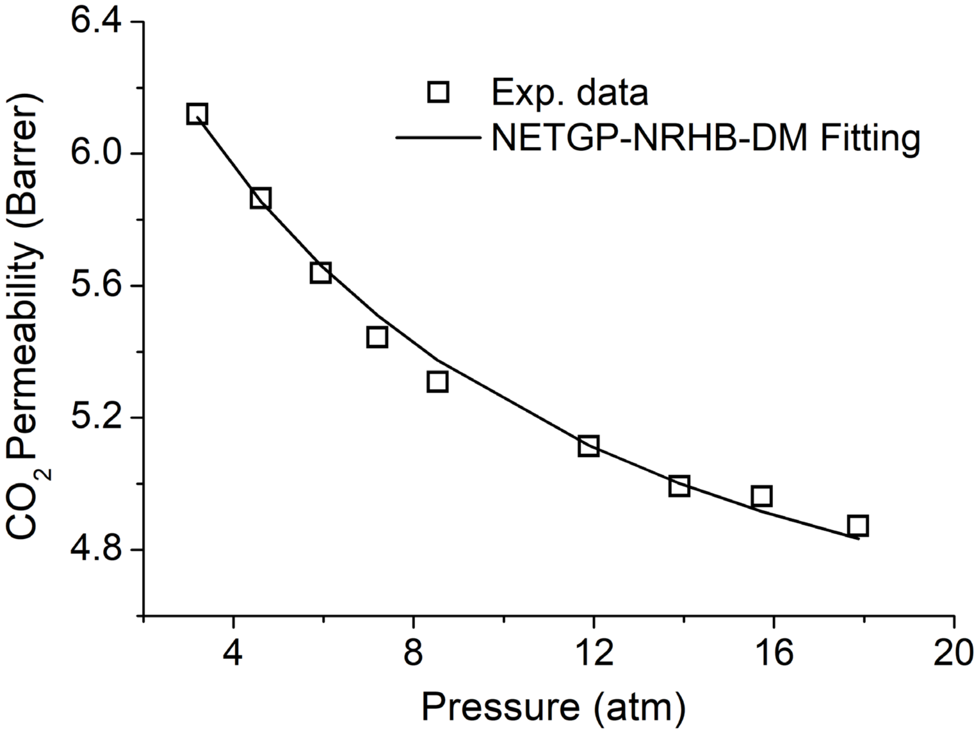

Figure 5.12a: Fitting of PAr – CO_2 permeability at 35°C.

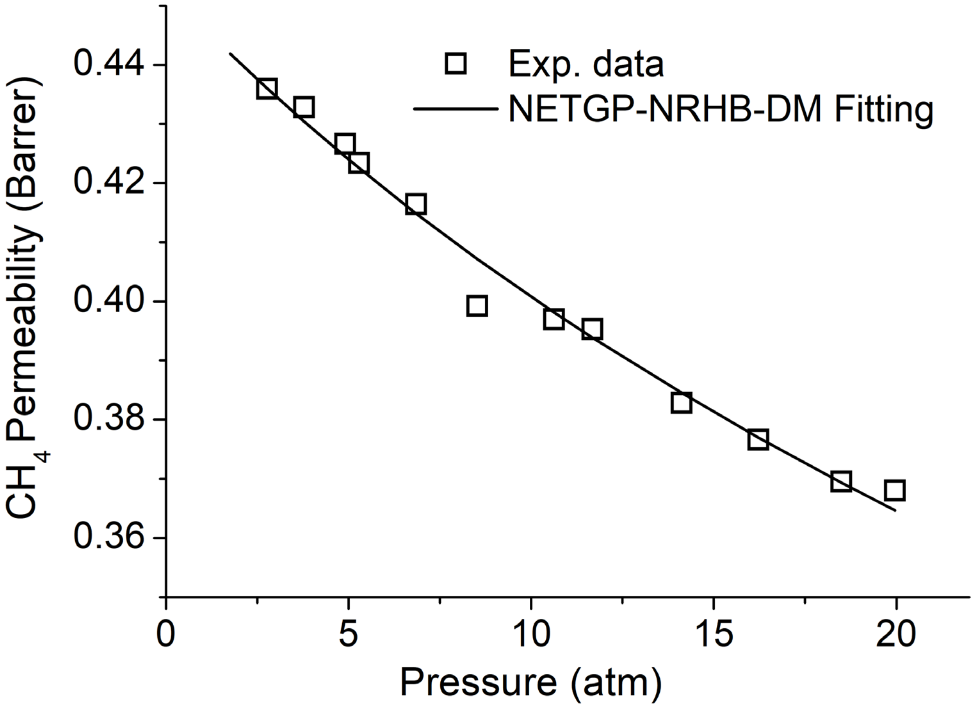

Figure 5.12b: Fitting of PAr – CH_4 permeability at 35°C.

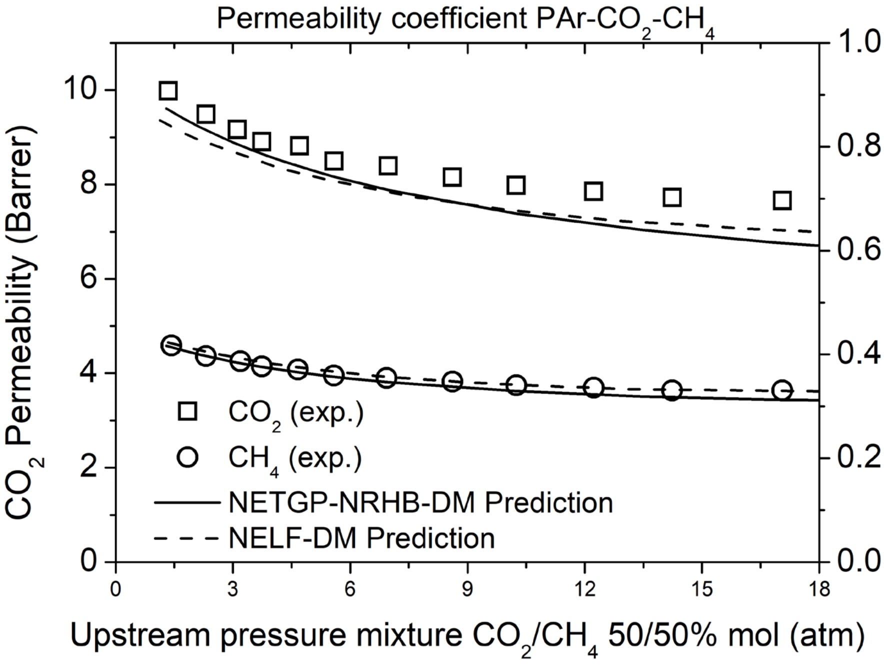

Figure 5.13: Prediction of PAr – CO_2 – CH_4 permeability at 35°C.

5.4.2 *Permeability of CO_2 – CH_4 mixture in PSf*

The same procedure as for PAr has been followed to deal with permeability of the CO_2 – CH_4 mixture in glassy PSf. First, the values of L_0 and β for the binary systems PSf - CO_2 and PSf - CH_4 have been retrieved by fitting binary permeability data at 35°C [3] with the NETGP-NRHB-DM. The results are reported in Figures 5.14a and 5.14b, showing a satisfactory fitting capability of the model. The values of the mobility parameters are reported in Table 5.6

Table 5.6 Permeability fitting parameters

Binary system	$L_0 \times 10^9$ ($cm^2\,s^{-1}$)	β
PAr – CO_2	12	23
PAr – CH_4	4.8	46
PSf – CO_2	9.1	23
PSf – CH_4	2.2	48
PH – CO_2	1.5	52
PH – CH_4	0.81	0

Then, the NETGP-NRHB-DM model has been used to predict permeability of the binary gaseous mixture CO_2-CH_4 in glassy PSf 35°C, for the case of a 50:50 by mol mixtures at several pressures. In Figure 5.15, model predictions are compared with experimental data available in literature [3] and with predictions provided by the NELF-DM [20]. Predictions obtained using the NETGP-NRHB-DM are in good agreement with experimental data and exhibit a detectable improvement if compared to NELF-DM predictions.

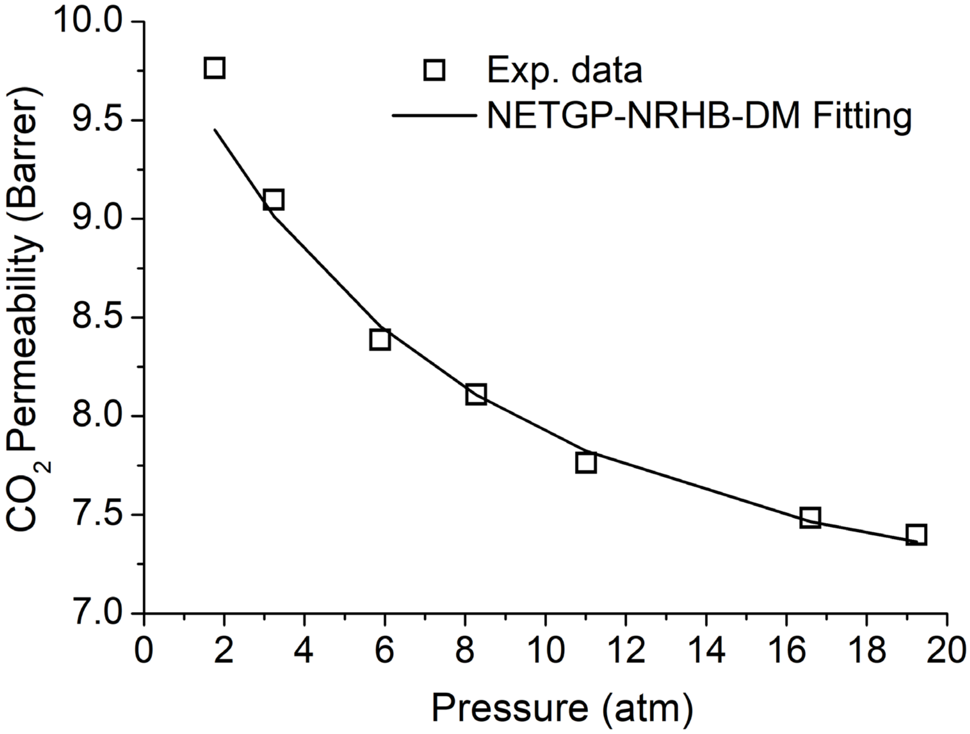

Figure 5.14a: Fitting of PSf – CO_2 permeability at 35°C.

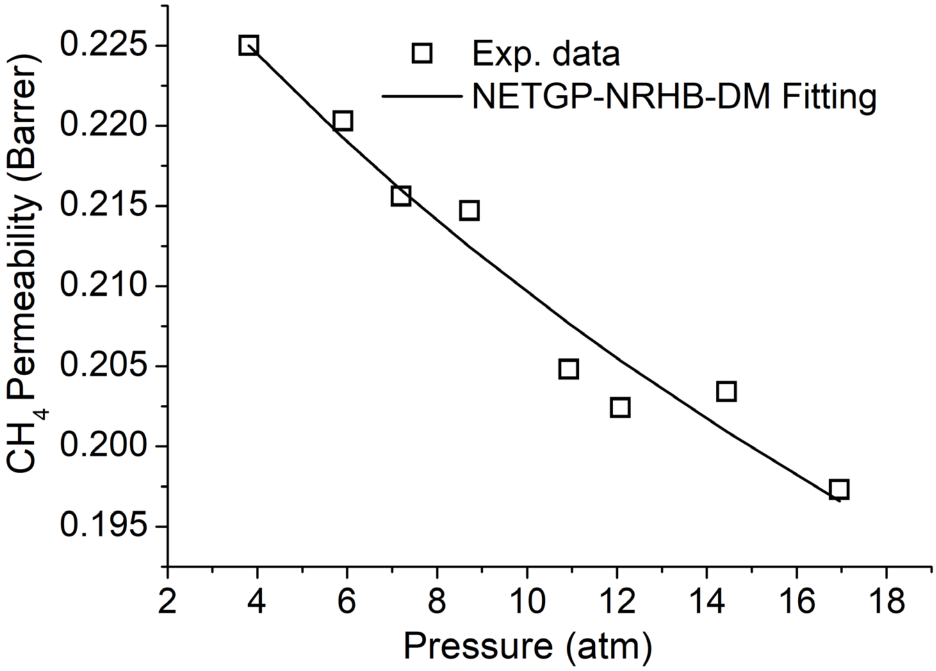

Figure 5.14b: Fitting of PSf – CH_4 permeability at 35°C.

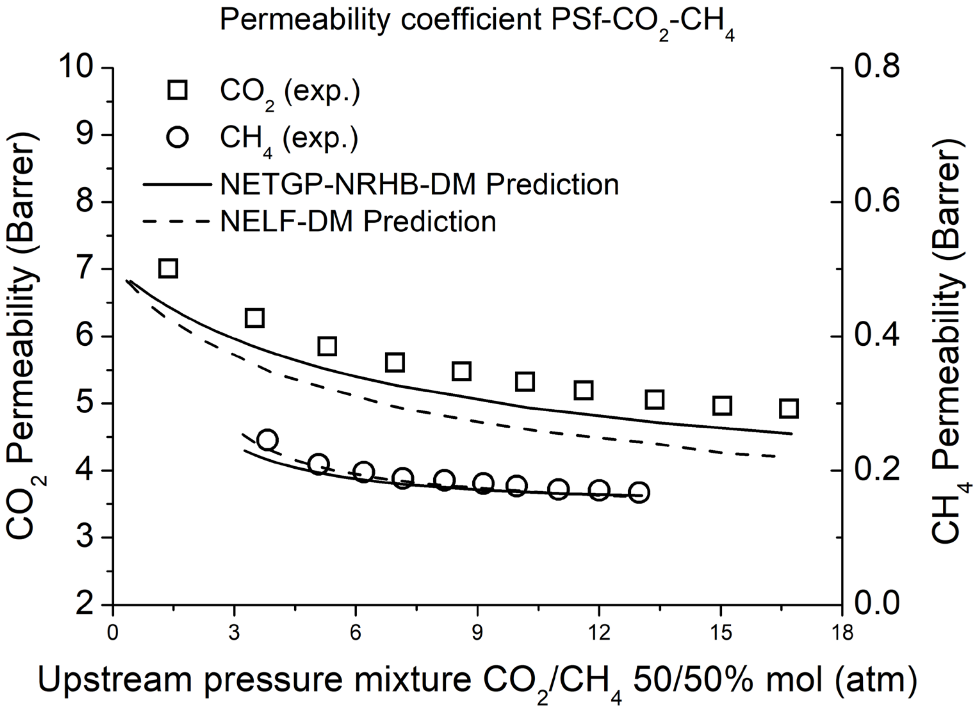

Figure 5.15: Prediction of PSf – CO_2 – CH_4 permeability at 35°C.

5.4.3 Permeability of CO_2 – CH_4 mixture in PH

Also, in this case the values of the two “mobility factors parameters”, L_0 and β, for the binary systems PH-CO_2 and PH-CH_4 have been retrieved by fitting experimental permeability data at 35°C (data taken from [3]) with the NETGP-NRHB-DM (see Figures 5.16a and 5.16b). The estimated values of these parameters are reported in Table 5.6.

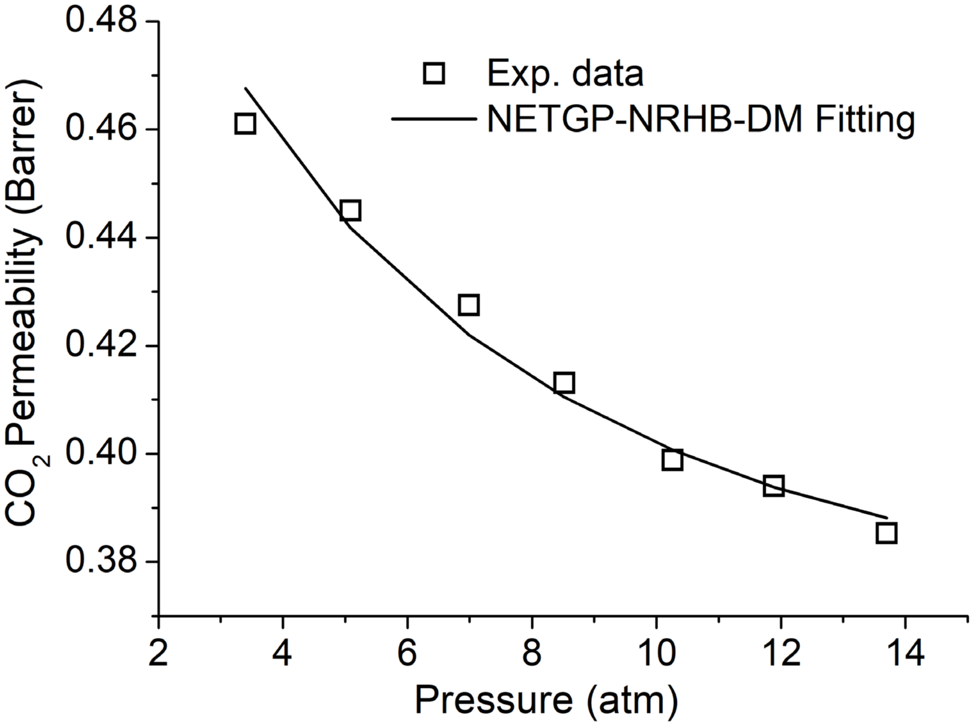

Figure 5.16a: Fitting of PH – CO_2 permeability at 35°C.

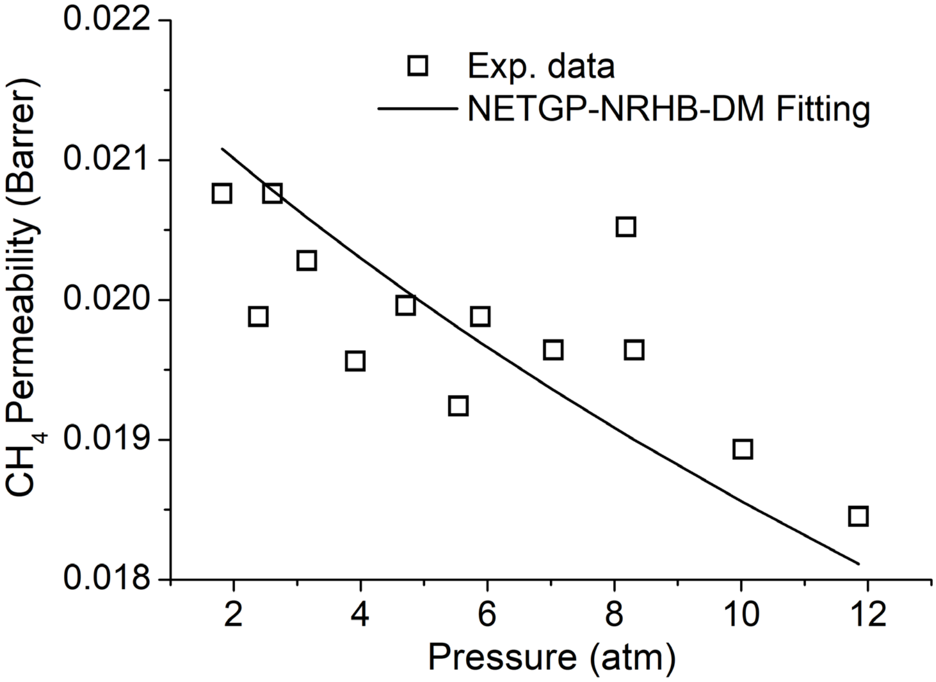

Figure 5.16b: Fitting of PH – CH_4 permeability at 35°C.

Notably, in the case of the PH – CH_4 system, the experimental data taken from [3] have a very weak dependence on pressure (which also results in scattered data) so that the parameter β has been fixed equal to 0 and only L_0 has been determined by the non-linear regression of the data.

The NETGP-NRHB-DM has been then used to predict the permeability of CO_2 and CH_4 in the case of PH- CO_2 -CH_4 ternary system. All the calculations have been carried out at 35°C for a fixed equimolar composition of the gaseous phase at several total pressures. The NETGP-NRHB-DM predictions have been validated against experimental data available in the literature [3] and the results of this comparison are reported in Figure 5.17. The NETGP-NRHB-DM provides good predictions, with some improvement as compared to the NELF-DM predictions calculated by Toni et. al. [20].

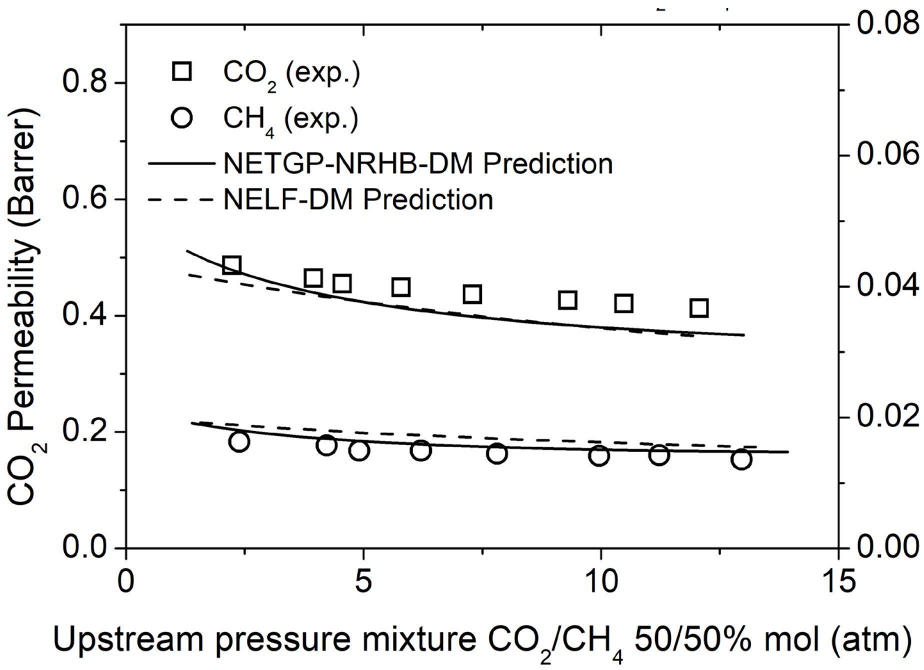

Figure 5.17: Prediction of PH – CO_2 – CH_4 permeability at 35°C.

References

[1] B. J. Story, W. J. Koros, Sorption of C0$_2$/CH$_4$ Mixtures in Poly(phenylene Oxide) and a Carboxylated Derivative, J. Appl. Polym. Sci. 42 (1991) 2613-2626.

[2] E. S. Sanders, W. J. Koros, H. B. Hopfenberg, V. T. Stannett, Pure and mixed gas sorption of carbon dioxide and ethylene in poly(methyl methacrylate), J. Membr. Sci. 18 (1984) 53-74.

[3] T. A. Barbari, W. J. Koros and D. R. Paul, Gas Transport in Polymers Based on Bisphenol-A, Journal of Polymer Science: P&B: Polymer Physics 26 (1988) 709-727.

[4] M.G. De Angelis, F. Doghieri, G.C. Sarti, B.D. Freeman, Modeling gas sorption in amorphous Teflon through the nonequilibrium thermodynamics for glassy polymers (NET-GP) approach, Desalination 193 (2006) 82-89.

[5] F. Doghieri, G.C. Sarti, Nonequilibrium Lattice Fluids: A Predictive Model for the Solubility in Glassy Polymers, Macromolecules 29, 24 (1996) 7885-7896.

[6] P. Zoller, A Study of the Pressure-Volume-Temperature Relationships of Four Related Amorphous Polymers: Polycarbonate, Polyarylate, Phenoxy, and Polysulfone, Journal of Polymer Science: Polymer Physics Edition 20 (1982) 1453-1464.

[7] R. P. Danner, M. S. High, Handbook of Polymer Solution Thermodynamics, A. I. Ch. E, New York, USA 1992.

[8] A. Fredenslund, M. J. Sorensen, Group Contribution Estimation Methods. In Models for Thermodynamic and Phase Equilibria Calculations; Sandler, S., Ed.; Marcel Dekker Inc.: New York, 1994.

[9] A. Fredenslund, R.L. Jones, J.M. Prausnitz, Group-contribution estimation of activity coefficients in nonideal liquid mixtures, AIChE J. 21 (1975) 1086-1099.

[10] P. Musto, V. Loianno, G. Scherillo, P. La Manna, M. Galizia, G. Guerra and G. Mensitieri, Benzene-Induced Crystallization of PPO: A Combined Thermodynamic and Vibrational Spectroscopy Study, Ind. Eng. Chem. Res. 59 (2020) 5402−5411.

[11] P. Zoller, A Study of the Pressure-Volume-Temperature Relationships of Four Related Amorphous Polymers: Polycarbonate, Polyarylate, Phenoxy, and Polysulfone, Journal of Polymer Science: Polymer Physics Edition 20 (1982) 1453-1464.

[12] I. Tsivintzelis, T. Spyriouni, I. G. Economou, Modeling of fluid phase equilibria with two thermodynamic theories: Non-random hydrogen bonding (NRHB) and statistical associating fluid theory (SAFT), Fluid Phase Equilibria 253 (2007) 19–28.

[13] S. Skjold-Joergensen, B. Kolbe, J. Gmehling, P. Rasmussen, "Vapor-Liquid Equilibria by UNIFAC Group Contribution. Revision and Extension", Ind.Eng.Chem. Process Des.Dev. 18 (1979) 714-722.

[14] J. Gmehling, P. Rasmussen, A. Fredenslund, "Vapor-Liquid Equilibria by UNIFAC Group Contribution. Revision and Extension. 2", Ind.Eng.Chem. Process Des.Dev., 21 (1982) 118-127.

[15] E. A. Macedo, U. Weidlich, J. Gmehling, P. Rasmussen, "Vapor-Liquid Equilibria by UNIFAC Group-Contribution. Revision and Extension. 3", Ind.Eng.Chem. Process Des.Dev. 22 (1983) 676-678.

[16] D. Tiegs, J. Gmehling, P. Rasmussen, A. Fredenslund, "Vapor-Liquid Equilibria by UNIFAC Group Contribution. 4. Revision and Extension", Ind.Eng.Chem.Res., 26 (1987) 159-161.

[17] H.K. Hansen, P. Rasmussen, A. Fredenslund, Schiller M., Gmehling J., "Vapor-Liquid Equilibria by UNIFAC Group-Contribution. 5. Revision and Extension", Ind.Eng.Chem.Res. 30 (1991) 2352-2355.

[18] R. Wittig, J. Lohmann, J. Gmehling, "Vapor-Liquid Equilibria by UNIFAC Group Contribution. 6. Revision and Extension", Ind.Eng.Chem.Res. 42 (2003) 183-188.

[19] M. Minelli, S. Campagnoli, M. G. De Angelis, F. Doghieri, and G. C. Sarti, Predictive Model for the Solubility of Fluid Mixtures in Glassy Polymers, Macromolecules 44 (2011) 4852–4862.

[20] E. Toni, M. Minelli, G. C. Sarti, A predictive model for the permeability of gas mixtures in glassy polymers, Fluid Phase Equilibria 455 (2018) 54-62.

[21] L. A. Webster and A. J. Kidnay, Vapor-Liquid Equilibria for the Methane-Propane-Carbon Dioxide Systems at 230 K and 270 K, J. Chem. Eng. Data 46 (2001) 759-764.

[22] G. Scherillo, M. Galizia, P. Musto and G. Mensitieri, Water Sorption Thermodynamics in Glassy and Rubbery Polymers: Modeling the Interactional Issues Emerging from FTIR Spectroscopy, Ind. Eng. Chem. Res. 52 (2013) 8674−8691.

[23] P. Musto, V. Loianno, G. Scherillo, P. La Manna, M. Galizia, G. Guerra and G. Mensitieri, Benzene-Induced Crystallization of PPO: A Combined Thermodynamic and Vibrational Spectroscopy Study, Ind. Eng. Chem. Res. 59 (2020) 5402−5411.

[24] H. K. Bae, K. Nagahama and M. Hirata, Isothermal Vapor-Liquid Equilibria for the Ethylene-Carbon Dioxide System at High Pressure, Journal of Chemical and Engineering Data 27 (1982) 25-27.

[25] G. Mensitieri, G. Scherillo, C. Panayiotou, P. Musto, Towards a predictive thermodynamic description of sorption processes in polymers: The synergy between theoretical EoS models and vibrational spectroscopy, Materials Science & Engineering R 140 (2020) 100525.

[26] I. Tsivintzelis, I. G. Economou, G. M. Kontogeorgis, Modeling the Phase Behavior in Mixtures of Pharmaceuticals with Liquid or Supercritical Solvents, J. Phys. Chem. B 113 (2009) 6446–6458.

[27] C. Tsioptsias, I. Tsivintzelis and C. Panayiotou, Equation-of-state modeling of mixtures with ionic liquids, Phys. Chem. Chem. Phys. 12 (2010) 4843–4851.

[28] M. Minelli, G.C. Sarti, Permeability and diffusivity of CO2 in glassy polymers with and without plasticization, J. Membr. Sci., 435 (2013), pp. 176-185.

[29] M. Minelli, G.C. Sarti, Thermodynamic model for the permeability of light gases in glassy polymers, AIChE J. 61 (2015) 2776-2788.

[30] M. Minelli, G.C. Sarti, Thermodynamic basis for vapor permeability in Ethyl Cellulose, J. Membr. Sci. 473 (2015) 137-145.

[31] M. Minelli, G.C. Sarti, Thermodynamic modeling of gas transport in glassy polymeric membranes, Membranes 7 (2017) 46.

[32] M. Minelli, G.C. Sarti, Permeability and solubility of carbon dioxide in different glassy polymer systems with and without plasticization, J. Membr. Sci. 444 (2013) 429-439.

[33] M. Minelli, Modeling CO2 solubility and transport in poly(ethylene terephthalate) above and below the glass transition, J. Membr. Sci. 451 (2014) 305-311.

[34] M. Minelli, G.C. Sarti, Gas permeability in glassy polymers: a thermodynamic approach, Fluid Phase Equilib. 424 (2016) 44-51.

[35] M. Minelli, G.C. Sarti, Elementary prediction of gas permeability in glassy polymers, J. Membr. Sci. 521 (2017) 73-83.

Chapter 6

Hyphenated technique based on pressure-decay and in situ FT-IR vibrational spectroscopy

Concerning the experimental part of the research, a new hyphenated technique based on concurrent pressure-decay and in situ FT-IR vibrational spectroscopy measurements has been implemented to study sorption and diffusion of a low molecular weight compound in a polymeric membrane. This new experimental technique has been the object a paper published during the PhD program [1]. This chapter follows the same study published in [1] and finally it extends the study to the thermodynamic sorption and kinetics of gas mixtures in polymeric membranes. For this part of the research an enormous contribution has been given by Dr. Loianno Valerio, which deserves a special mention and an acknowledgement for his fundamental work.

In order to validate this custom-made experimental apparatus CO_2 sorption in PDMS has been selected, since literature is plenty of experimental data for this system for its application in gas separation by polymeric membrane. Stepwise sorption measurements have been performed at 35°C by increasing progressively the gas pressure in the test cell from 0 to 9 bar approximately. Once the binary measurements have been validated, the experimental system is applied in the study of CH_4/CO_2 mixtures in PDMS at different temperatures.

6.1 Experimental apparatus and calibration

The apparatus used to perform the hyphenated technique is represented schematically in Figure 6.1, it consists of two chambers of known volume, the penetrant reservoir (V_1) and the measuring cell where the polymer sample is placed (V_2), separated by a shut-off valve. The valve is positioned at the top of the sample chamber in order to minimize the filling time during expansion. A pressure sensor Baratron 121A from MKS instruments is directly connected to reservoir chamber (PI in Figure 6.1). The sample cell, made of stainless steel, is jacketed to allow thermal control by circulating thermostatic water (accuracy of temperature control ±0.01°C). The cell is equipped with two coaxial windows made of ZnSe (thickness 4 mm) aligned with the IR beam.

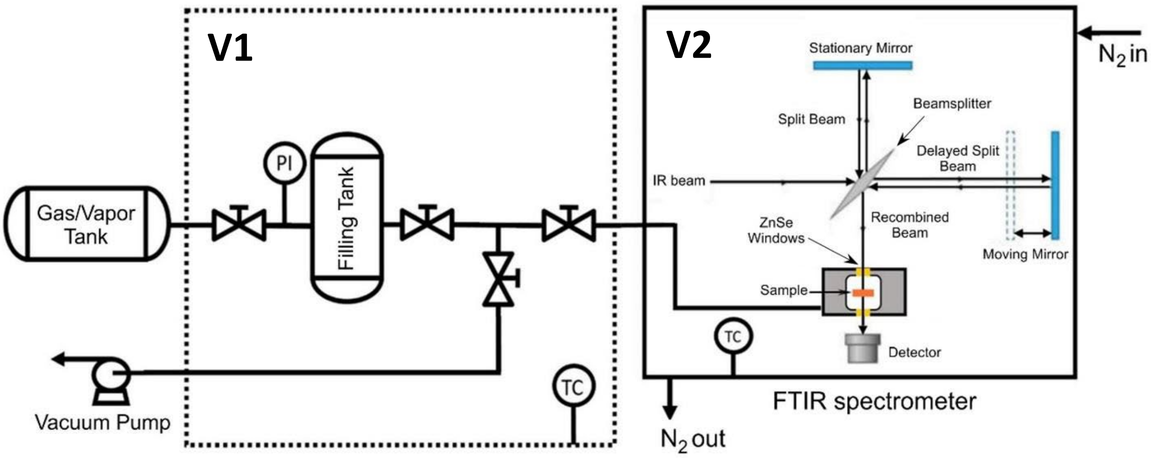

Figure 6.1: Schematic representation of the hyphenated apparatus

The volumes of the different sections of the apparatus have been evaluated by performing two gaseous carbon dioxide expansions with and without a known volume of stainless-steel spheres placed in the reservoir section. The NIST database of thermophysical properties has been used to determine the compressibility factors for the gas at the chosen thermodynamic conditions. The calibration measurements have been performed at room temperature (26.0 ± 0.1 °C), and so:

V_1=142.08 ± 0.03 cm^3
V_2=63.94 ± 0.04 cm^3

Since V_2 includes the volume of the shut off valve (V_v), in order to exclude this part which doesn't account as volume occupied by the penetrant during the measurement, an independent measure of the volume of the jacked section (V_j) has been carried out by weighting this part of the system filled with distilled water. The results are:

V_j=46.75 ± 0.06 cm^3
V_r=V_2-V_j=17.19 ± 0.1 cm^3

An accurate knowledge of these volumes is necessary to use the pressure decay technique: indeed, sorption experiments are conducted at 35.0 ± 0.1°C by controlling the temperature in the sample cell (V_j), the temperature of the remaining parts of the apparatus are at room temperature (26.0 ± 0.1 °C).

6.2 Experimental method

6.2.1 PDMS-CO_2 binary mixture

A typical pressure decay experiment starts by filling the part of the apparatus of volume V_1 (gas reservoir) with gas (carbon dioxide) reaching a prescribed pressure. The remaining part of the apparatus, that includes the measuring cell, has a volume V_2-V_p, where V_p is the volume of the polymer sample. At the starting, this volume is either kept under vacuum, if one starts from a fully desorbed sample, or is at the pressure of the previous sorption step. To start the test, the connecting valve is fully opened, allowing the expansion of the gas from a volume V_1 to a volume V_1+V_2-V_p. Pressure decay due to absorption of CO_2 within the polymer, is monitored as a function of time, until a constant equilibrium value is attained. Based on the values of the initial pressure in the regions of volume V_1 and in that of volume V_2-V_p and of the final pressure in the total volume of the apparatus V_1+V_2-V_p, one can perform a molar balance. By comparing the starting number of moles of gas initially present in the gaseous phase with those finally present, one can determine the amount of gas absorbed within the polymer at equilibrium and, in turn, its equilibrium concentration. The measurement error has been estimated by taking into account the error in the volume calculation during calibration, in the temperature value, in the pressure value and in the density value of the specimen. The propagation of these errors on the concentration has been estimated to be equal to about 5% of each concentration value. As expected, the trend is linear in the pressure range investigated and the absolute values are in excellent agreement with the data reported in the literature [2-5].

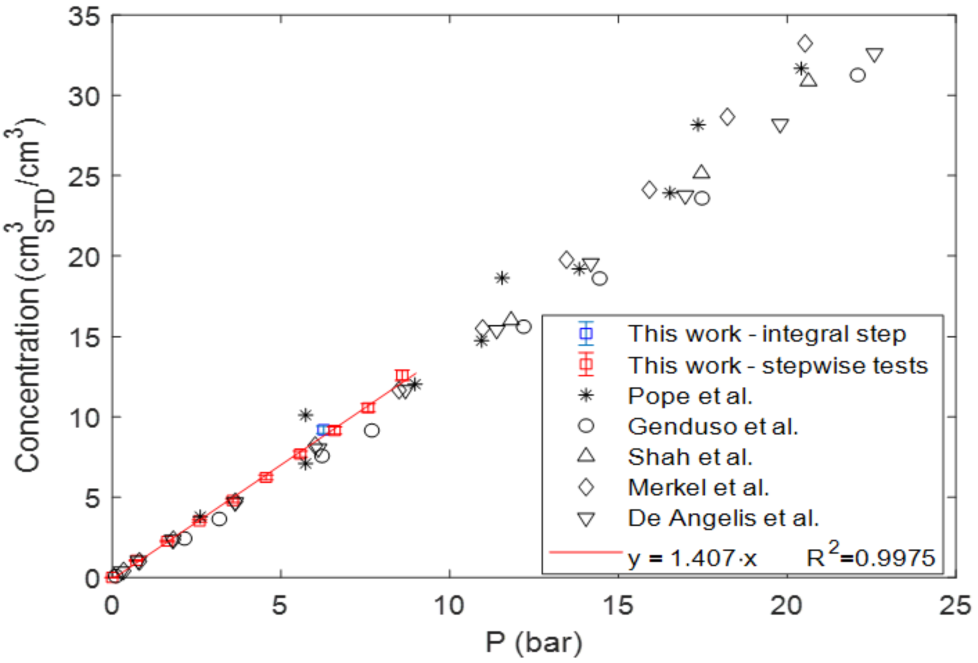

Figure 6.2: Comparison of our sorption data calculated by pressure-decay with the others present in literature measured with the same technique.

As anticipated, the determination of gas amount absorbed within the polymer at equilibrium, can be also performed by using Infrared spectroscopy. In FTIR applications, the absorbance, A, is calculated by the well-known Lamber-Beer law:

$$A = \frac{-N_A\,\sigma_{EXT}\,C_T\,L}{ln10} = \varepsilon C_T L \qquad (6.1)$$

where σ_{EXT} the extinction molecular cross-section, N_A is the Avogadro's number, L is the optical length-path and C_T is the total concentration of analyte. The descripted hyphenated technique allows the straightforward estimation of this quantity by comparing peak absorbance at equilibrium with gas concentration within the polymer measured by the pressure decay technique at equilibrium, in the same conditions. In order to correlate barometric and spectroscopy measurements an analysis of the CO_2/PDMS at different pressure up to 9 bar and temperature of 35°C has been carried out.

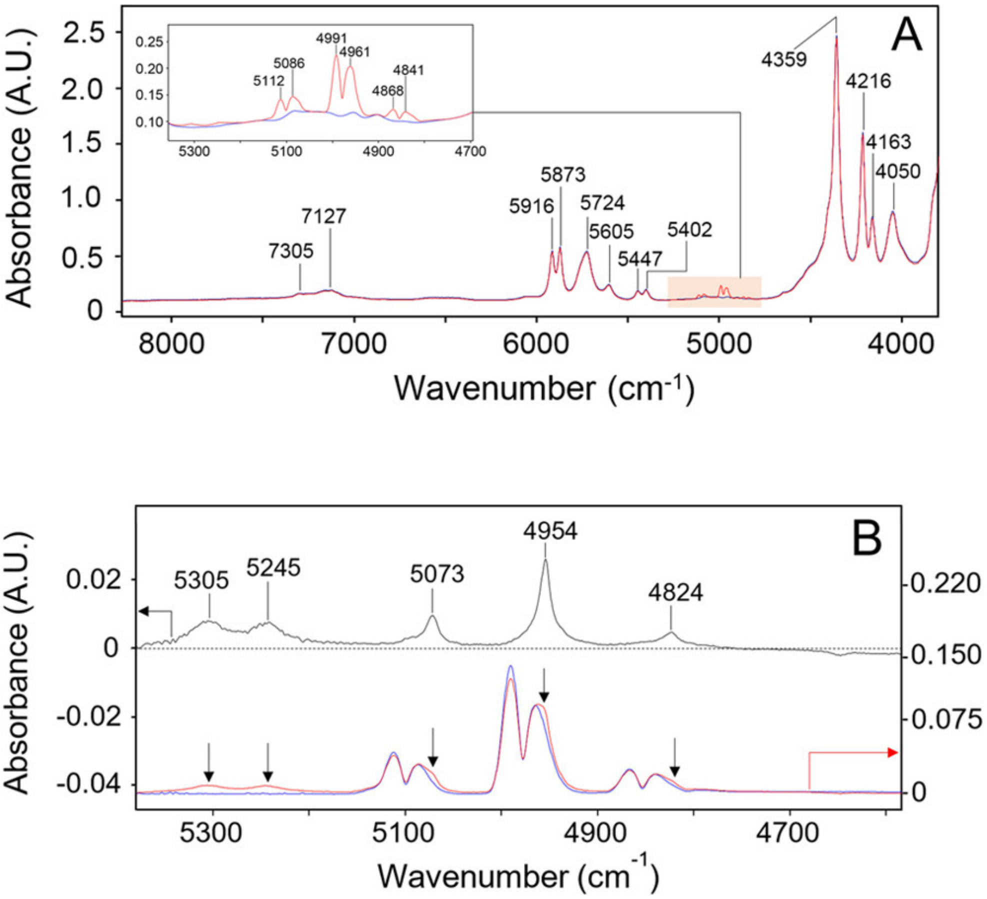

Figure 6.3: Blue trace: FT-NIR spectrum of PDMS under vacuum; red trace: FT-NIR spectrum of PDMS equilibrated at a CO_2 pressure of 9 bar. The inset highlights the analytical range (5320−4700 cm^{-1}) (A). Red trace: difference between the spectrum at CO_2 pressure=9 bar and the spectrum under vacuum (k=1); blue trace: gas-phase spectrum of CO_2 at 9 bar; black trace: difference spectrum (red trace − k blue trace) (B).

The MIR region of the spectrum does not provide any information about the absorbed penetrant. Indeed, the fundamental signal corresponding to the asymmetric stretching of carbon dioxide (2335cm^{-1}) is saturated. However, as shown in Figure 6.3, in the NIR region four overtones distinctly appear between 4800 and 5200cm^{-1}: the features of the spectrum of carbon dioxide in the gas phase are clearly recognizable. By applying the difference spectroscopy procedure, we have been easily isolated the signal of absorbed CO_2. First the dry PDMS spectrum is subtracted from the spectrum of the mixture; then the background spectrum is subtracted as well. Since the specimen reduces the optical path length of the gas phase in the test cell it is necessary to correct the background spectrum ($A_{bkg}(\nu)$) at the operating thermodynamic conditions with a factor proportional to the length change, i.e.:

$$A_p^{bkg}(\nu, P, T) = A^{bkg}(\nu, P, T) \cdot \frac{l-L}{l} \tag{6.2}$$

where A_p^{bkg} and A^{bkg} are the absorbance spectra of carbon dioxide in the gas phase with and without the specimen (subscript p) in the test cell, respectively, ν is the wavenumber, P the pressure and T the temperature at which the experiment is conducted. This procedure brings to light a sharp CO_2 peak centered at 4955 cm^{-1} for each investigated pressure (Figure 6.4).

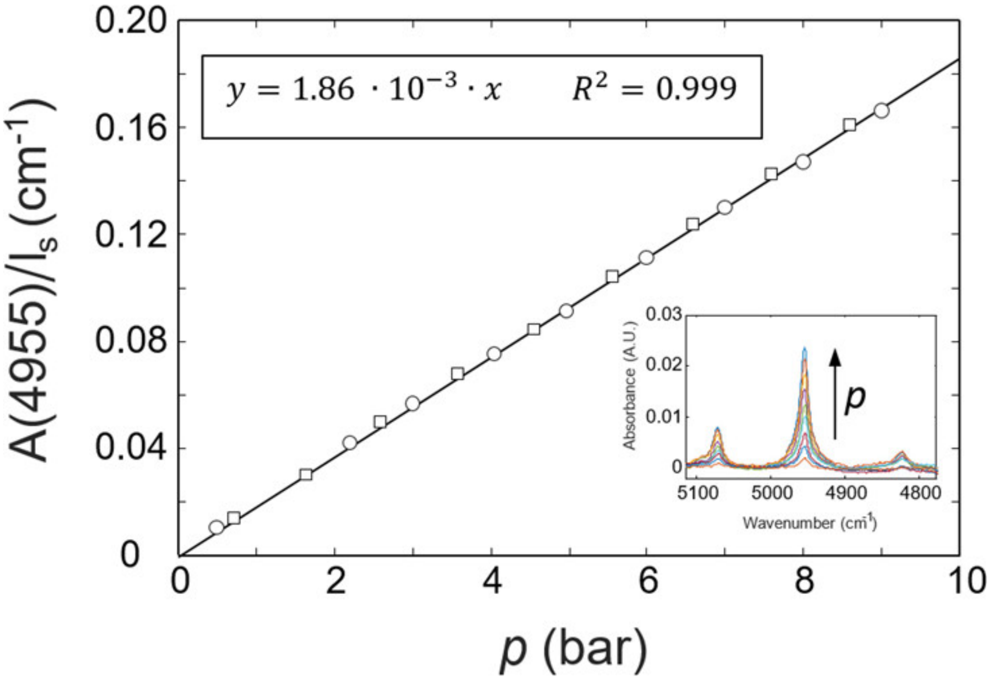

Figure 6.4: Sorption isotherm as measured by FT-NIR spectroscopy from the absorbance of the CO_2 band at 4955 cm^{-1}. circle, open: sample thickness=1.50 mm; square, open: sample thickness = 1.48 mm.

Moreover, the set of peak height intensity of specimen for each pressure is correlated with the solubility data reported in Figure 6.5.

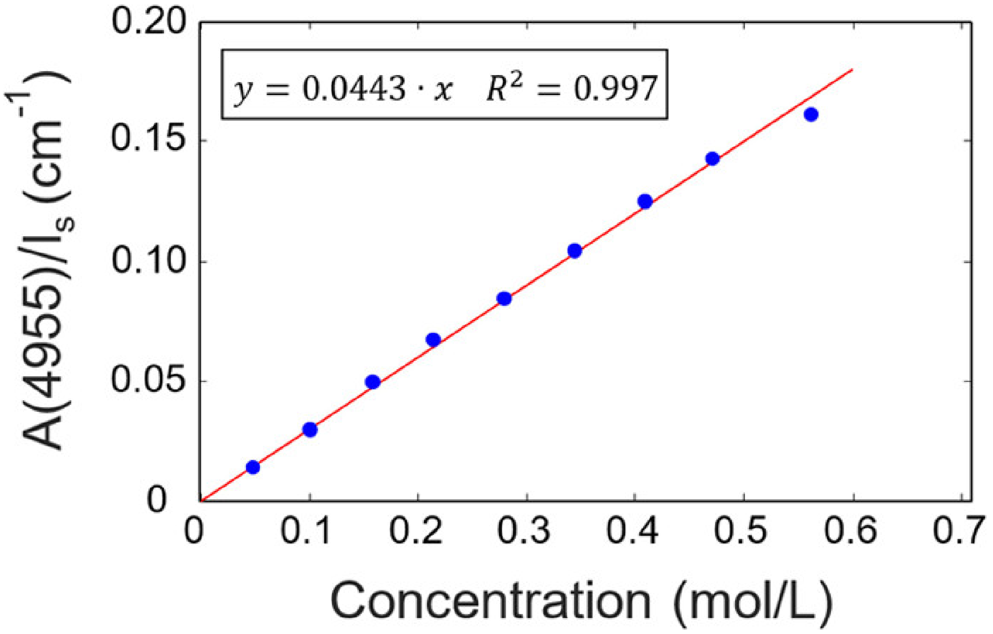

Figure 6.5: Correlation between the concentration of sorbed CO_2 measured by pressure decay and the absorbance of the CO_2 band at 4955 cm^{-1}.

A linear trend of this correlation confirms the validity of the classic Lambert-Beer law: the absorptivity of the overtone centered at 4955 cm^{-1} (ε_{4955}) is equal to 295.2 cm^2/mol with an $R^2=0.997$. Regarding the spectroscopic kinetics, an integral sorption step up to 5.976 bar is reported. The pressure reduction during the experiment is negligible because of the low weight of the sample and can be assumed constant. The behavior is Fickian and the kinetics is well described by the classic diffusion process in a slab of thickness L, as already shown in Section 3.5 and here reported:

$$\frac{M(t)}{M_\infty} = 1 - \sum_{n=0}^{\infty} \frac{8}{(2n+1)^2\,\pi^2} \exp\left[-\frac{D(2n+1)^2\,\pi^2\,t}{L^2}\right] \tag{6.3}$$

In which $\frac{M(t)}{M_\infty}$ can be calculated with the spectroscopy Absorbance by:

$$\frac{M(t)}{M_\infty} = \frac{A(t)\,L_\infty}{A_\infty\,L(t)} = \frac{A(t)}{A_\infty}\,\alpha \tag{6.4}$$

At the pressure involved, the swelling is neglectable, so it is assumed $\alpha = 1$.

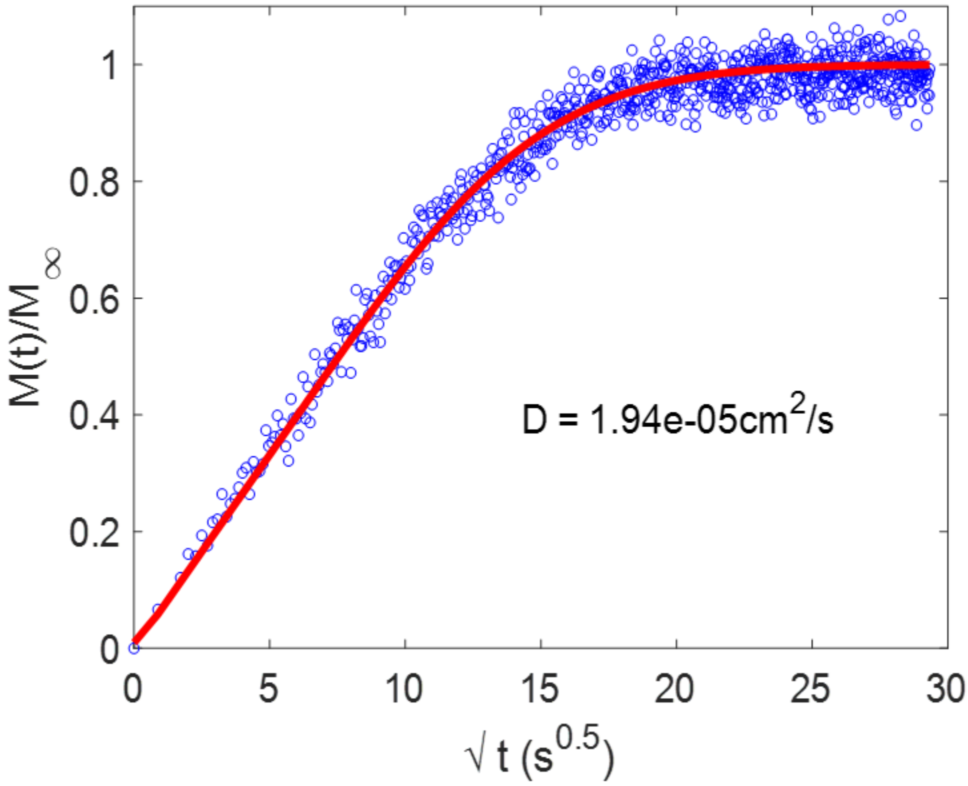

Figure 6.6: Sorption kinetics evaluated spectroscopically from the peak absorbance at 4955 cm^{-1}. Integral sorption test at p(CO_2)=0−5.976 bar. The blue symbols are the FT-NIR data; the continuous line represents the best fitting provided by the equation (6.3).

By the equations (6.3) and (6.4), the diffusivity coefficient of CO_2 in PDMS at 35°C is calculated and it is equal to $1.94 \cdot 10^{-5}$ cm^2 s^{-1}, this value is consistent with the results from Merkel et al. who calculated the diffusivity from independent permeability and solubility measurements finding a diffusivity coefficient of $1.8 \cdot 10^{-5}$ cm^2 s^{-1} [2].

6.2.1 PDMS-CH_4 binary mixture

Once the experimental procedure has been validated for PDMS-CO_2 mixture, in order to extend the experimental procedure to the equilibrium and sorption kinetics of CO_2/CH_4 mixtures in PDMS, the analogous study, already done for the CO_2, has been done for the CH_4. In Figure 6.7, three regions of the IR spectrum of pure gaseous methane are reported as a function of pressure at 27°C.

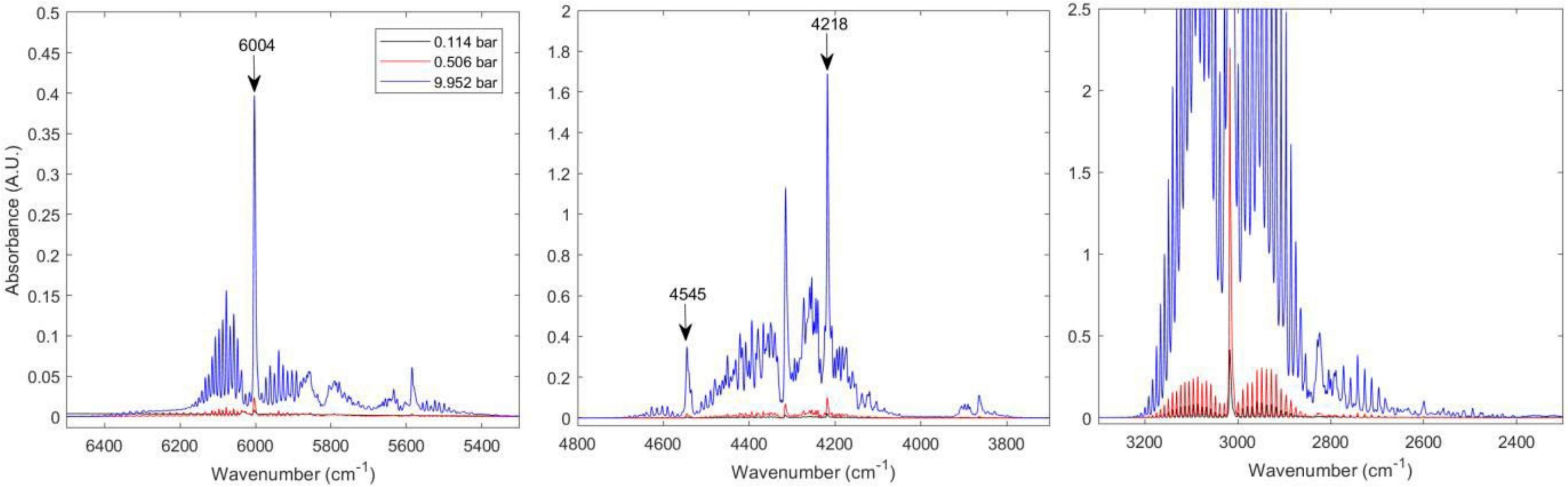

Figure 6.7: CH_4 IR spectra obtained with a spectrum resolution of 2 cm^{-1} and sapphire flat coplanar windows at 27°C.

The fundamental vibration centered at 3000 cm^{-1} saturates at 0.5 bar approximately and has not been considered for analytical purposes, while the black arrows identify the peaks that have been used for quantitative evaluations. The associated IR calibration curves are reported in Figure 6.8 and show a negligible dependence on the temperature in the 27 – 35 °C range.

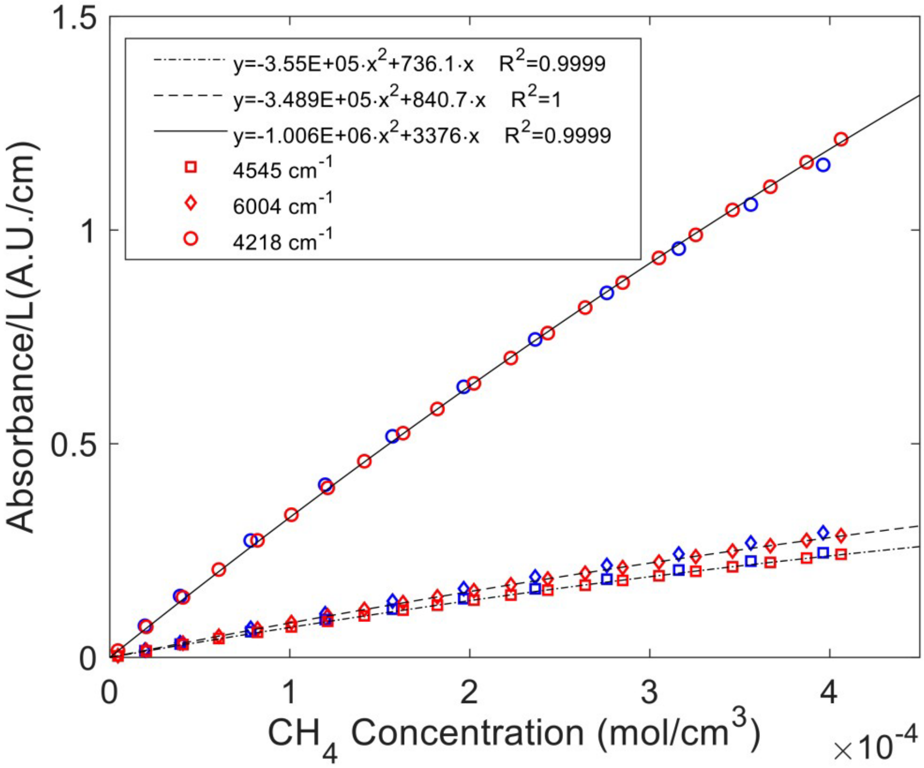

Figure 6.8: CH_4 IR calibration curves. Blue data: 35°C ZnSe windows. Red data: 27°C Sapphire windows. Spectrum resolution in 2 cm^{-1}. Baseline correction has been performed in the following frequency ranges: [3565, 4821] cm^{-1} for the signal at 4218 cm^{-1}, [5300, 6500] cm^{-1} for the signal at 6004 cm^{-1} and [4526, 4564] cm^{-1} for the signal at 4545 cm^{-1}.

The whole set of calibration curves was best fitted with a second order polynomial function whose intercept is imposed to be zero. The observed deviation from linearity is associated with a pressure broadening effect and with the detector response. The pressure and the IR spectrum were measured simultaneously and, following the approach adopted in Figures 6.5, the gas IR peaks were correlated with the gas density. Once the calibration curves for the IR signals have been obtained, in turn the IR signals can be used during a sorption experiment to retrieve the molar concentration in the gaseous phase, even in the case of gas mixtures. A key aspect of vibrational spectroscopy is the great number of signals available for the investigation of the gas concentration, each of them can be used as an independent measurement. Therefore, to increase the sensitivity of the concentration calibration curve, the outputs (absorbance or integrated absorbance value) of multiple signals may be added to each other at fixed thermodynamic conditions.

6.2.2 CH_4/CO_2 gas mixtures in PDMS

Finally, the extension of the technique to sorption of multiple penetrants from a gas mixture has been investigated by means of FTIR Spectroscopy analysing the spectra of the penetrant species both in the gas and the polymer phases with the same approach used for the investigation of sorption of pure substances. It is assumed that the molar absorptivity associated to the analytical peaks does not depend on the presence of other components. This hypothesis holds true for the system under investigation. We have preliminary used the described experimental methodology to investigate sorption of CO_2/CH_4 gas mixture in PDMS. For the current configuration (in terms of void volumes of the apparatus) and for the intrinsic characteristic of the system at hand, the analysis could be performed only on the signals associated to carbon dioxide, while the CH_4 signals can be used as a check of the results. To this aim, the IR gas calibration curves and the molar absorptivity of pure CO_2 absorbed in PDMS, as determined from the investigation of pure CO_2, were used. Gas mixtures of carbon dioxide and methane at certain compositions were prepared using mass flow controllers. Sorption tests α were conducted performing integral experiments up to 3.5 bar of total pressure and sorption tests β were conducted with integral steps up to a total pressure of approximately 5 bar. The IR signal of absorbed CO_2 at 4955 cm^{-1} returns the concentration of the probe in the polymer at equilibrium with an absorptivity already known from the Section 6.2.1. About the second penetrant, it was not possible to measure accurately methane concentration for both tests α and β. Work is in progress to upgrade the instrumental apparatus for the concentration determination of low sorbing components and to resolve accurately the IR spectrum of methane absorbed in PDMS. So that, the measurements have been carried out by measuring the evolution of the partial pressure of the CO_2 in the gaseous phase and of the concentration of penetrant in the polymer by the FT-IR, while the total external pressure is monitored by the pressure transducer. Since the initial concentration of two gases is known by the mass flow controller, the sorbed quantity of methane can be easily calculate by difference of concentration of methane between the initial and the final concentration in gas phase. In Figure 6.9, the solubilities of carbon dioxide from gaseous mixtures of different composition are compared (CO_2/CH_4 molar ratios respectively equal to 48/52 and 25/75). The analysis of the results puts in evidence how the solubility of carbon dioxide at a certain partial pressure, when in mixture with methane, is very close to the solubility of pure gaseous carbon dioxide at a pressure numerically equal to the partial pressure of CO_2 in the mixture, as also found by Genduso et al. [4].

Some deviation was observed from the data reported by Genduso et al. likely due to differences in the structure of the polymer and in the experimental techniques [4]. With respect to the classic approach based on gas chromatography, sorption thermodynamics and mass transport are investigated *in situ*. It may also be extended to systems of *n* low MW compounds one of which is homonuclear and, consequently, non-detectable with FTIR Spectroscopy. In this case, a thermodynamic model is required to identify its gas concentration. The spectroscopic uncertainty of the mole fraction composition is ±0.001. Finally, one can conclude that FTIR Spectroscopy in transmission mode is a versatile solution to the study of transport properties of low MW compounds – polymer systems.

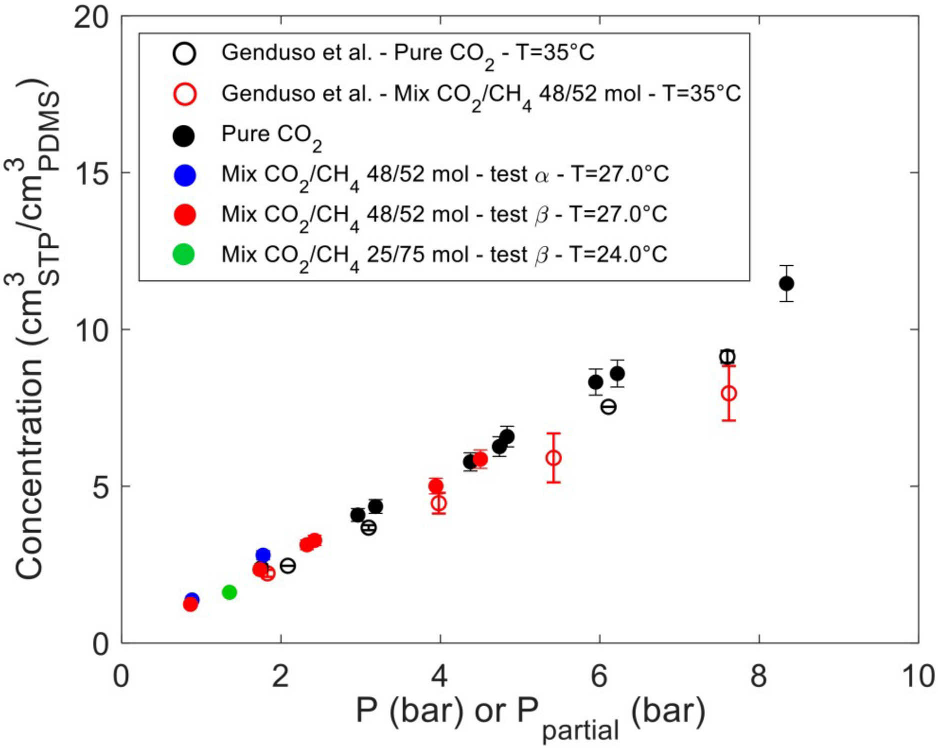

Figure 6.9: Experimental data of pure CO_2 and of CO_2/CH_4 mixtures in PDMS compared with data available in literature, data are reported in terms of partial pressure of CO_2 in the case of mixture and of total pressure in case of sorption of pure CO_2.

References

[1] V. Loianno, A. Baldanza, G. Scherillo, R. Jamaledin, P. Musto, G. Mensitieri, A Hyphenated Approach Combining Pressure-Decay and In Situ FT-NIR Spectroscopy to Monitor Penetrant Sorption and Concurrent Swelling in Polymers, Industrial & Engineering Chemistry Research, 60 (2021) 5494-5503.

[2] T. C. Merkel, V. I. Bondar, K. Nagai, B. D. Freeman, I. Pinnau, Gas sorption, diffusion and permeation in poly(dimethylsiloxane), J. Polym. Sci., Part B: Polym. Phys., 38 (2000) 415−434.

[3] V. M. Shah, B. J. Hardy, S. A. Stern, Solubility of carbon dioxide, methane, and propane in silicone polymers: effect of polymer side chains, J. Polym. Sci. Part B: Polym. Phys., 24 (1986) 2033−2047.

[4] G. Genduso, E. Litwiller, X. Ma, S. Zampini, I. Pinnau, Mixed gas sorption in polymers via a new barometric test system: Sorption and diffusion of CO2-CH4 mixtures in polydimethylsiloxane (PDMS), J. Membr. Sci., 577 (2019) 195−204.

[5] D. S. Pope, W. J. Koros, G. K. Fleming, Measurement of thickness dilation in polymer films, J. Polym. Sci., Part B: Polym. Phys, 27 (1989) 1173−1177.

Conclusions

During this PhD program the thermodynamic consistency of the NRHB model has been demonstrated as ideal state approaches. Soon after, an explicit expression of the NETGP-NRHB multicomponent chemical potential is found for the first time in order to describe the behavior of thermodynamic sorption of multicomponent mixtures involving glassy polymers also in presence of specific interactions, e.g., hydrogen bonding. To test the model capability of NRHB theory and its extension to the NETGP framework, relevant thermal quantities, i.e., the isosteric heat of sorption and the polymer-penetrant interaction energy of PEI/CO_2 system. The predicted value of isosteric heat of sorption and the value of the intermolecular interaction energy are compared with the outcomes evaluated form experimental data and with the results of DFT calculations, respectively. The study shows a good agreement between the predicted results and the values obtained with independent evaluations. In addition, the NETGP-NRHB and the equilibrium NRHB models are used to fit simultaneously solubility and the glass transition temperature as function of the penetrant gas data available in literature of PMMA/CO_2 and Nylon 6,6/H_2O systems (this latter displaying specific interactions like hydrogen bonding), respectively. In particular, Gibbs-Di Marzio criterion is applied in the NRHB framework to study the glass transition at different penetrant concentration exhibiting a phenomenon known as retrograde vitrification, confirmed by the aforementioned experimental data. The description of the mass transport (diffusion or the permeation phenomena) is completed starting from an approach based on Free Volume theories and applied to NETGP-NRHB. The predictions of solubility of ternary PPO/CO_2/CH_4 and PMMA/CO_2/C_2H_4 glassy mixtures show an excellent agreement with the experimental literature data and an improvement with respect to the wide used NELF, likely due to the non-random nature of mean-field interactions that NETGP-NRHB is able to take into account and to the intrinsic thermodynamic inconsistency exhibited by NELF model in the case of multicomponent mixtures. The permeability predictions of binary CO_2/CH_4 mixtures in glassy PAr, PSf and PH (the latter displaying specific interactions) by NETGP-NRHB-DM show a good agreement with the literature experimental data and slight improvement of the NEFL-DM prediction. Finally, the theoretical research has been accompanied by an experimental approach devoted to develop a new hyphenated technique based on concurrent pressure-decay and in situ FT-NIR vibrational spectroscopy measurements to study sorption of a low molecular weight compound in a polymeric membrane. The pressure-decay method is used to provide a quantitative information on the concentration of the penetrant within the polymer, then, this information is combined with one gathered from FT-IR analysis. As a test case, thermodynamic and kinetic sorption at 35°C of CO_2 in PDMS at pressure values up to 9 bar and to 5.976 bar, respectively, are investigated. The results are in trend with the literature data used to validate the technique.

Finally, a preliminary approach has been used to extend the technique to the case of CO_2/CH_4 mixtures sorption within PDMS at different temperature obtaining good results in line with the few data available in literature.

Appendices

Appendix A

The Appendix A is dedicated to study in deep the mathematical procedure and the details of the calculation shown in Chapter 2. Moreover, in Section A.5, the procedure developed in Chapter 2 is applied to the different versions of SL model investigated by Neau and, afterwards, we also examinate a further version of SL model, the one adopted by Sarti et al. in order to develop the NELF theory, which is widely implemented in literature to describe the solubility of a penetrant in a glassy polymer.

A.1 Revisiting NRHB in the framework of a $\left(\boldsymbol{V},\boldsymbol{T},\underline{\boldsymbol{N}}\right)$ constitutive class.

If the only work of deformation is related to the change in volume, the power of the contact forces acting on the system is given by $-P\dot{V}$, where P is the mechanical uniform pressure in the system and the dot superscript represents the material time derivative, i.e., the time derivative following the body represented by the closed system under consideration. With substitution of the energy balance into the second law, the following inequality is obtained:

$$-P\dot{V} - \dot{A} - S\dot{T} \geq 0 \tag{A.1}$$

where A (the Helmholtz energy of the system) is a function of the state which is represented by the set of state variables $\left(V,T,\underline{N},\underline{N}_{ij},\underline{N}_{\alpha\beta}^{HB}\right)$. For the material time derivatives in equation (A.1) one obtains:

$$\left(\frac{\partial A}{\partial V} + P\right)\dot{V} + \left(\frac{\partial A}{\partial T} + S\right)\dot{T} + \sum_{i=0}^{t}\sum_{j>i}^{t}\sum_{\alpha}^{m}\sum_{\beta}^{n}\left(\frac{\partial A}{\partial N_{ij}}\dot{N}_{ij} + \frac{\partial A}{\partial N_{\alpha\beta}^{HB}}\dot{N}_{\alpha\beta}^{HB}\right) \leq \tag{A.2a}$$

Hereafter, *n* represents the number of types of protons donors groups and *m* the number of types of proton acceptor groups. The summation in (A.2a) can be rewritten as a scalar product between a M-dimensional couple of vectors, where M represents the total number of internal state variables. In the following, the vector of internal state variables $\underline{N}_{ij}$ will be denoted by the symbol $\underline{x}_A$, while the vector of internal state variables $\underline{N}_{\alpha\beta}^{HB}$ will be denoted by the symbol $\underline{x}_B$. The whole set of internal state variables will be collectively referred to by the symbol $\underline{x}$:

$$\left(\frac{\partial A}{\partial V}+P\right)\dot{V}+\left(\frac{\partial A}{\partial T}+S\right)\dot{T}+\underline{\theta}_A\cdot\underline{\dot{x}}_A+\underline{\theta}_B\cdot\underline{\dot{x}}_B\leq 0 \qquad \text{(A.2b)}$$

in which $\underline{\theta}_A$ and $\underline{\theta}_B$ are quantities named 'affinity' vectors whose components are the partial derivatives of the Helmholtz energy function with respect to the homologous components of $\underline{x}_A$ and $\underline{x}_B$. In this case they represent, respectively, the two vectors whose components are the derivatives $\frac{\partial A}{\partial N_{ij}}$ and $\frac{\partial \mathrm{A}}{\partial N_{\alpha\beta}^{HB}}$. Moreover, $\underline{\dot{x}}_A$ and $\underline{\dot{x}}_B$, that represent the two vectors of material derivatives $\dot{N}_{ij}$ and $\dot{N}_{\alpha\beta}^{HB}$, are assumed (according to the postulates of thermodynamics with *internal* state variables) functions of the state of the system (i.e. of the set of state variables $(V,T,\underline{N},\underline{N}_{ij},\underline{N}_{\alpha\beta}^{HB})$). In the framework of the thermodynamics with *internal* state variables, for a closed system (i.e., a system that, in the absence of chemical reactions, is characterized by a constant number of molecules of each component, (i.e. $\underline{N}(t)=const=\underline{N}$), eq. (A.2b) holds true at any instant of time, t, for any conceivable transformation, i.e., for the case at hand, for any conceivable set of values that, at time t, V, T, $\dot{V}$, $\dot{T}$ and $\underline{x}$ may take. Note that, being V and T independent external variables, the conceivable value of $\dot{V}$ and $\dot{T}$ at given t span over $\mathbb{R}$. In particular, the second law inequality holds true for all transformations that share, at time t, the same values for the external state variables V and T, for the material time derivative, $\dot{T}$, as well as for the set of internal state variables $\underline{x}$. Consequently, the second, third and fourth terms take, at time t, well identified numerical values that are the same for all considered transformations, since the state variables, as well as the functions of state appearing in these terms and the material derivative $\dot{T}$, have the same fixed values. It then follows that the inequality (A.2b) must be fulfilled for any conceivable value that the material time derivative $\dot{V}$ may take, independently of its sign or magnitude, and so, the only possibility left, is that the coefficient of $\dot{V}$ is zero, thus resulting in the following equation:

$$\frac{\partial A}{\partial V}=-P \qquad \text{(A.3)}$$

that establishes a relationship between the two mappings *A(·)* and *P(·)*, so that the form of *P(·)* is determined once the form of *A(·)* has been assigned. In other words, the Helmholtz energy for such a constitutive class is a potential for pressure.

Based on these considerations, the expression of second law inequality reduces to:

$$\left(\frac{\partial A}{\partial T}+S\right)\dot{T}+\underline{\theta}_A\cdot\underline{\dot{x}}_A+\underline{\theta}_B\cdot\underline{\dot{x}}_B\leq 0 \qquad \text{(A.2c)}$$

One can proceed now considering that the inequality (A.2c) must hold, at any instant of time, t, for any conceivable transformation, i.e., for the case at hand, for any conceivable set of values that V, T, $\dot{T}$ and $\underline{x}$ may take. In particular, the II law inequality must hold, at any t, for all the transformations that share the same values for the external state variables V, T as well as for the set of internal state variables, $\underline{x}$. Consequently, the second and third terms of inequality (A.2c) take well identified numerical values that are the same for all considered transformations since the state variables, as well as the functions of state appearing in these terms, have the same fixed values. It then follows that the inequality (A.2c) must be fulfilled for any conceivable value that the material time derivative $\dot{T}$ may take, independently of its sign or magnitude, and so, the only possibility left, is that the coefficient of $\dot{T}$ is zero, thus resulting in the following equation:

$$\frac{\partial A}{\partial T} = -S \tag{A.4}$$

which establishes another relationship between the two mappings *A(·)* and *S(·)*, so that the form of *S(·)* is determined once the form of *A(·)* has been assigned. In other words, the Helmholtz energy for such a constitutive class, is a potential for entropy. It is worth noting that equations (A.3) and (A.4), that hold for any admissible value of set $(V, T, \underline{N}, \underline{x})$, are therefore also satisfied at any equilibrium state for the corresponding $(V, T, \underline{N}, \underline{x})$. This reflects a well-established result of the equilibrium thermodynamics literature.

Based on these considerations, the expression of II law inequality finally reduces to:

$$\underline{\theta}_A \cdot \underline{x}_A + \underline{\theta}_B \cdot \underline{x}_B = \underline{\theta} \cdot \underline{x} \leq 0 \tag{A.2d}$$

which cannot be simplified further.

In the following, the equilibrium values of all functions are identified by the superscript "*eq*". Since, at equilibrium, $\underline{\dot{x}}^{eq} = 0$, we identify the equilibrium value of $\underline{x}$, $\underline{x}^{eq}$, as the solution of the following equation:

$$\underline{\dot{x}}\left(V, T, \underline{N}, \underline{x}^{eq}\right) = 0 \tag{A.5}$$

The solution of (A.5) can be expressed as:

$$\underline{x}^{eq} = k\left(V, T, \underline{N}\right) \tag{A.6}$$

where *k* is a function only of the set of variables $(V, T, \underline{N})$ that defines the state of the system at equilibrium. Consequently, at any equilibrium state identified by the values of external state variables V, T and $\underline{N}$, the scalar product $\underline{\theta} \cdot \underline{\dot{x}}$ is zero and, in view of equation (A.2d), at such equilibrium state, this product takes its maximum value for the selected values of V, T and $\underline{N}$ and, consequently:

$$\left[\left(\frac{\partial(\underline{\theta}\cdot\underline{\dot{x}})}{\partial x_i}\right)_{V,T,\underline{N},x_{j\neq i}}\right]^{eq} = \left[\underline{\theta}\cdot\left(\frac{\partial\underline{\dot{x}}}{\partial x_i}\right)_{V,T,\underline{N},x_{j\neq i}} + \underline{\dot{x}}\cdot\left(\frac{\partial\underline{\theta}}{\partial x_i}\right)_{V,T,\underline{N},x_{j\neq i}}\right]^{eq} =$$

0 for each i (A.7)

Since, at equilibrium, $\underline{\dot{x}}\left(V, T, \underline{N}, \underline{x}^{eq}(V, T, \underline{N})\right) = 0$, (A.7) becomes:

$$\left[\underline{\theta}\cdot\left(\frac{\partial\underline{\dot{x}}}{\partial x_i}\right)_{V,T,\underline{N},x_{j\neq i}}\right]^{eq} = 0 \quad \text{for each } i \qquad \text{(A.8a)}$$

In line with the classic hypothesis of mathematically ‘smooth’ behaviour of thermodynamic functions, it is assumed that, in the neighbour of equilibrium state, for the assigned values of *external* variables of state V, T and $\underline{N}$, the rate of change of the internal state variables, $\underline{\dot{x}}$, is an invertible function of $\underline{x}$. Indeed, this reflects that in the neighbour of equilibrium state $\underline{\dot{x}}=\underline{0}$ holds only at equilibrium. This assumption implies that (actually, the smoothness hypothesis assures that this is also a sufficient condition for the local invertibility):

$$\left\{\det\left|\left(\frac{\partial\underline{\dot{x}}}{\partial\underline{x}}\right)_{V,T,\underline{N}}\right|\right\}^{eq} = \left\{\det\left|\left(\frac{\partial\dot{x}_i}{\partial x_j}\right)_{V,T,\underline{N},x_{k\neq j}}\right|\right\}^{eq} \neq 0 \qquad \text{(A.9)}$$

where $i = 1, \dots \mathrm{M}$; $j = 1, \dots, \mathrm{M}$ represent the row and column index respectively of the square matrix $\frac{\partial\underline{\dot{x}}}{\partial\underline{x}}$ and M represents the total number of internal state variables.

Noting that equation (A.8a) can be expressed in matrixial form as:

$$\left[\left|\left(\frac{\partial\dot{x}_i}{\partial x_j}\right)_{V,T,\underline{N},x_{k\neq j}}\right|^{eq}\right]^{tr} \cdot \underline{\theta}^{eq} = \underline{0} \qquad \text{(A.8b)}$$

where superscript *tr* stands for the matrix transposition operator and $\underline{\theta}^{eq}$ is interpreted as a column vector. Since the determinant is invariant to the transposition operator, therefore the smoothness assumption assures that:

$$\underline{\theta}^{eq} = \underline{0} \tag{A.10}$$

represents the only solution for $\underline{\theta}^{eq}$ given by (A.8a).

Equation (A.10), once expressed in terms of $\underline{N}_{ij}$ and $\underline{N}^{HB}_{\alpha\beta}$, provides the corresponding equilibrium minimization conditions:

$$\left[\left(\frac{\partial A}{\partial N_{ij}}\right)_{V,T,\underline{N},N_{rs\neq ij},\underline{N}^{HB}_{\alpha\beta}}\right]^{eq} = 0 \quad \text{for each } i = 0, 1, \dots, t \text{ and } j > i \tag{A.11}$$

$$\left[\left(\frac{\partial A}{\partial N^{HB}_{\alpha\beta}}\right)_{V,T,\underline{N},\underline{N}_{ij},N^{HB}_{\gamma\delta\neq\alpha\beta}}\right]^{eq} = 0 \quad \text{for each } \alpha = 1, 2, \dots, n \text{ and } \beta = 1,2, \dots, m \tag{A.12}$$

A.2 Details of calculation of the NRHB model expressions.

In this section we report some details of the calculations regarding the explicit expressions of equations (2.9), from (2.12) to (2.14), (2.16) and (2.17) of the main text. In particular this section shows that the minimization conditions and the non-equilibrium expression of the chemical potentials of species *i*, in $(V, T, \underline{N})$ ensemble take the same form of the corresponding equations in $(P, T, \underline{N})$ ensemble provide that *P* is given by equation (2.8).

The Helmholtz energy reported in eq. (2.4), actually, is expressed in terms of the constitutive class $(V, T, \underline{N}, T, \underline{N}_{ij}, \underline{N}^{HB}_{\alpha\beta})$ as dictated by the corresponding partition function in $(V, T, \underline{N})$ ensemble. Operatively, it can be re-expressed as $A(v, T, \underline{N}, \underline{N}_{ij}, \underline{N}^{HB}_{\alpha\beta}) = A(V(v, \underline{N}), T, \underline{N}, \underline{N}_{ij}, \underline{N}^{HB}_{\alpha\beta})$ (here, for the sake of simplicity, the same symbol *A* is used for the composite function as well as for its external function). Then, the two sets of minimization conditions in the ensemble $(V, T, \underline{N})$, equations (2.1) and (2.2), can be equivalently re-expressed in terms of the constitutive class$(v, T, \underline{N}, \underline{N}_{ij}, \underline{N}^{HB}_{\alpha\beta})$. In fact, by chain rules:

$$\left(\frac{\partial A}{\partial N_{ij}}\right)_{v,T,\underline{N},N_{rs\neq ij},\underline{N}_{\alpha\beta}^{HB}} = \left(\frac{\partial A}{\partial N_{ij}}\right)_{V,T,\underline{N},N_{rs\neq ij},\underline{N}_{\alpha\beta}^{HB}} = 0 \quad \text{for any } i = 0,1,\dots,t \text{ and } j > i \quad \text{(A.13a)}$$

$$\left(\frac{\partial A}{\partial N_{\alpha\beta}^{HB}}\right)_{v,T,\underline{N},\underline{N}_{ij},N_{\gamma\delta\neq\alpha\beta}^{HB}} = \left(\frac{\partial A}{\partial N_{\alpha\beta}^{HB}}\right)_{V,T,\underline{N},\underline{N}_{ij},N_{\gamma\delta\neq\alpha\beta}^{HB}} = 0 \quad \text{for any } a = 1,2,\dots,m \text{ and for any } \beta = 1,2,\dots,n \quad \text{(A.13b)}$$

where according to (2.5a), $v = \frac{V}{N}$.

A further operative step consists in writing $A\left(v\left(\tilde{v},\underline{N},N_{\alpha\beta}^{HB}\right),T,\underline{N},\underline{N}_{ij},\underline{N}_{\alpha\beta}^{HB}\right) = A\left(\tilde{v},T,\underline{N},\underline{N}_{ij},\underline{N}_{\alpha\beta}^{HB}\right)$. In this way, finally, by chain rules of derivatives, one can express the minimization conditions in terms of the original expressions derived by Panayiotou:

$$\left(\frac{\partial A}{\partial N_{ij}}\right)_{\tilde{v},T,\underline{N},N_{rs\neq ij},N_{\alpha\beta}^{HB}} = \left(\frac{\partial A}{\partial N_{ij}}\right)_{v,T,\underline{N},N_{rs\neq ij},N_{\alpha\beta}^{HB}} = 0 \quad \text{for any } i,j = 0,1,\dots,t \text{ and } j > i \quad \text{(A.13c)}$$

Eq. (A.13c) allows to calculate the minimization conditions for $\underline{N}_{ij}$ contacts in the constitutive class $\left(v,T,\underline{N},\underline{N}_{ij},\underline{N}_{\alpha\beta}^{HB}\right)$, through the derivative of its first member. In fact, the latter can be, in turn, straightforwardly calculated properly deriving equation (2.4), without the necessity of introducing all the equations (2.5) in (2.4) itself.

Analogously, for the minimization conditions for $\underline{N}_{\alpha\beta}^{HB}$:

$$\begin{aligned} 0 &= \left(\frac{\partial A}{\partial N_{\alpha\beta}^{HB}}\right)_{v,T,\underline{N},\underline{N}_{ij},N_{\gamma\delta\neq\alpha\beta}^{HB}} = \left(\frac{\partial A}{\partial N_{\alpha\beta}^{HB}}\right)_{\tilde{v},T,\underline{N},\underline{N}_{ij},N_{\gamma\delta\neq\alpha\beta}^{HB}} - \\ &\left(\frac{\partial A}{\partial v}\right)_{T,\underline{N},\underline{N}_{ij},\underline{N}_{\alpha\beta}^{HB}} \left(\frac{\partial v}{\partial N_{\alpha\beta}^{HB}}\right)_{\tilde{v},\underline{N},N_{\gamma\delta\neq\alpha\beta}^{HB}} = \left(\frac{\partial A}{\partial N_{\alpha\beta}^{HB}}\right)_{\tilde{v},T,\underline{N},\underline{N}_{ij},N_{\gamma\delta\neq\alpha\beta}^{HB}} - \\ &\left(\frac{\partial A}{\partial V}\right)_{T,\underline{N},\underline{N}_{ij},\underline{N}_{\alpha\beta}^{HB}} \left(\frac{\partial V}{\partial v}\right)_{\underline{N}} \left(\frac{\partial v}{\partial N_{\alpha\beta}^{HB}}\right)_{\tilde{v},\underline{N},N_{\gamma\delta\neq\alpha\beta}^{HB}} = \left(\frac{\partial A}{\partial N_{\alpha\beta}^{HB}}\right)_{\tilde{v},T,\underline{N},\underline{N}_{ij},N_{\gamma\delta\neq\alpha\beta}^{HB}} + \\ &PN\left(\frac{\partial v}{\partial N_{\alpha\beta}^{HB}}\right)_{\tilde{v},\underline{N},N_{\gamma\delta\neq\alpha\beta}^{HB}} \end{aligned}$$

for any $a = 1,2,\dots,m$ and for any $\beta = 1,2,\dots,n$ (A.13d)

By using equations (2.8) and (2.9), equation (A.13d) allows to calculate the minimization conditions for $\underline{N}_{\alpha\beta}^{HB}$ contacts in the constitutive class $\left(v,T,\underline{N},\underline{N}_{ij},\underline{N}_{\alpha\beta}^{HB}\right)$ through the two derivatives of its last member, which, in turn, can be directly calculated by properly deriving equations (2.4) and (2.5), respectively.

The minimization conditions can be compared to the minimization conditions originally proposed by Panayiotou et. al working in the ensemble $(P,T,\underline{N})$. To this aim, preliminarily, we observe that the non-equilibrium expression of *G* in the $(P,T,\underline{N})$ ensemble is given by definition as:

$$G = A + PV \tag{A.14}$$

Regarding the non-equilibrium expression of *A*, we recall that in the NRHB statistics, in the $(P,T,\underline{N})$ ensemble, it does not depend on P, i.e. it can be expressed as $A = A(V,T,\underline{N},\underline{N}_{ij},\underline{N}_{\alpha\beta}^{HB})$ and therefore the same constitutive function provides the non-equilibrium Helmholtz energy A in the $(V,T,\underline{N})$ ensemble (i.e. in the constitutive class $(V,T,\underline{N},\underline{N}_{ij},\underline{N}_{\alpha\beta}^{HB})$); consistently a unique symbol A has been therefore used in this contribution in both the ensembles. Since the same expression of $A(V,T,\underline{N},\underline{N}_{ij},\underline{N}_{\alpha\beta}^{HB})$ holds in both the ensembles, one can write eq. (A.14) in the $(P,T,\underline{N})$ ensemble, fixing the P in such ensemble (i.e. in the constitutive class $(P,V,T,\underline{N},\underline{N}_{ij},\underline{N}_{\alpha\beta}^{HB})$) equal to the value given in the ensemble $(V,T,\underline{N})$ by equation (2.8). Finally, using in (A.14) the expression of *A* in the ensemble $(V,T,\underline{N})$, the corresponding *G* in the $(P,T,\underline{N})$ ensemble is trivially obtained. Therefore, coming back to the equation (A.13c), since V is independent from the $\underline{N}_{ij}$ contacts, the following equality holds:

$$0 = \left(\frac{\partial A}{\partial N_{ij}}\right)_{\tilde{v},T,\underline{N},N_{rs\neq ij},\underline{N}_{\alpha\beta}^{HB}} = \left(\frac{\partial G}{\partial N_{ij}}\right)_{P,\tilde{v},T,\underline{N},N_{rs\neq ij},\underline{N}_{\alpha\beta}^{HB}} = 0 \tag{A.15a}$$

for any $i,j = 0,1,\dots,t$ and $j > i$

The second equality in (A.15a) follows from the previous discussion concerning the use of equation (A.14) so that it is intended that *P* is given by (2.8). Indeed, the minimization conditions, expressed by the third equality in (A.15a), represent formally the minimization conditions towards the LF contacts, imposed by Panayiotou et. al. working directly in the ensemble $(P,T,\underline{N})$, and they are explicitly given by:

$$\frac{{\Gamma_{ij}}^2}{\Gamma_{ii}\,\Gamma_{jj}} = exp\left(-\frac{\Delta\varepsilon_{ij}}{kT}\right) \quad \text{for each } i,j = 0,1,\dots,t \text{ and } j > i \tag{A.15b}$$

(see eq. (2.6). Analogously, coming back to the eq. (A.13d), the following equation holds:

$$0 = \left(\frac{\partial A}{\partial N_{\alpha\beta}^{HB}}\right)_{\tilde{v},T,\underline{N},\underline{N}_{ij},N_{\gamma\delta\neq\alpha\beta}^{HB}} + PN\left(\frac{\partial v}{\partial N_{\alpha\beta}^{HB}}\right)_{\tilde{v},\underline{N},N_{\gamma\delta\neq\alpha\beta}^{HB}} = \left(\frac{\partial A}{\partial N_{\alpha\beta}^{HB}}\right)_{\tilde{v},T,\underline{N},\underline{N}_{ij},N_{\gamma\delta\neq\alpha\beta}^{HB}} + P\left(\frac{\partial V}{\partial N_{\alpha\beta}^{HB}}\right)_{\tilde{v},\underline{N},N_{\gamma\delta\neq\alpha\beta}^{HB}} = \left(\frac{\partial G}{\partial N_{\alpha\beta}^{HB}}\right)_{P,\tilde{v},T,\underline{N},\underline{N}_{ij},N_{\gamma\delta\neq\alpha\beta}^{HB}} \qquad \text{(A.16)}$$

In the second equality (2.5a) has been used. On the bases of the previous discussion regarding the use of (A.14) in the last member of (A.16) G represents the non-equilibrium Gibbs energy in the $(P,T,\underline{N})$ at the P given by (2.8). After some algebra, starting from (2.4) and (2.5), one obtains:

$$\left(\frac{\partial A}{\partial N_{\alpha\beta}^{HB}}\right)_{\tilde{v},T,\underline{N},\underline{N}_{ij},N_{\gamma\delta\neq\alpha\beta}^{HB}} + PN\left(\frac{\partial v}{\partial N_{\alpha\beta}^{HB}}\right)_{\tilde{v},\underline{N},N_{\gamma\delta\neq\alpha\beta}^{HB}} = ln\left(\frac{\tilde{v}\,\nu_{\alpha\beta}}{\nu_{\alpha 0}\,\nu_{0\beta}}\right) + \frac{A_{\alpha\beta}^{0}}{kT} + \frac{PV_{\alpha\beta}^{0}}{kT} = 0 \quad \text{for any } a = 1,2,\dots,m \text{ and for any } \beta = 1,2,\dots,n \qquad \text{(A.17)}$$

As expected, (A.17) takes the same form of the corresponding minimization expressions obtained by Panayiotou et. al working directly in the ensemble $(P,T,\underline{N})$, provided that P is given by eq. (2.8) (see equations (2.7) and (2.13)).

Regarding the operative expression of the non-equilibrium chemical potential in the ensemble $(V,T,\underline{N})$, we can write again $A\left(\tilde{v}\left(V,\underline{N},N_{\alpha\beta}^{HB}\right),T,\underline{N},\underline{N}_{ij},\underline{N}_{\alpha\beta}^{HB}\right) = A\left(V,T,\underline{N},\underline{N}_{ij},\underline{N}_{\alpha\beta}^{HB}\right)$) so that by derivative chain rules we have:

$$\frac{\mu_i}{kT} \overset{\text{def}}{=} \frac{1}{kT}\left(\frac{\partial A}{\partial N_i}\right)_{V,T,N_{j\neq i},\underline{N}_{ij},\underline{N}_{\alpha\beta}^{HB}} = \frac{1}{kT}\left(\frac{\partial A}{\partial N_i}\right)_{\tilde{v},T,N_{j\neq i},\underline{N}_{ij},\underline{N}_{\alpha\beta}^{HB}} + \frac{1}{kT}\left(\frac{\partial A}{\partial \tilde{v}}\right)_{T,\underline{N},\underline{N}_{ij},\underline{N}_{\alpha\beta}^{HB}}\left(\frac{\partial \tilde{v}}{\partial N_i}\right)_{V,T,N_{j\neq i},\underline{N}_{ij},\underline{N}_{\alpha\beta}^{HB}} \qquad \text{(A.18)}$$

After some algebra, starting again from equations (2.4) and (2.5):

$$\frac{\mu_i}{kT} = ln\frac{\phi_i}{\delta_i\,r_i} - r_i\frac{l}{r} + ln\,\tilde{\rho} + r_i(\tilde{v}-1)\,ln(1-\tilde{\rho}) - \frac{z}{2}r_i\left(\tilde{v}-1+\frac{q_i}{r_i}\right)ln\left(1-\tilde{\rho}+\frac{q}{r}\tilde{\rho}\right) + \frac{z\,q_i}{2}\left[ln\,\Gamma_{ii} + \frac{r_i}{q_i}(\tilde{v}-1)\,ln\,\Gamma_{00}\right] - \frac{q_i}{\tilde{T}_i} + r_i\nu_H - \textstyle\sum_{\alpha}^{m} d_{\alpha}^{i}\,ln\left(\frac{\nu_d^{\alpha}}{\nu_{\alpha 0}}\right) - \textstyle\sum_{\beta}^{n} a_{\beta}^{i}\,ln\left(\frac{\nu_a^{\beta}}{\nu_{0\beta}}\right) - \left[ln(1-\tilde{\rho}) - \tilde{\rho}\left(\frac{l}{r}-\nu_H\right) - \frac{z}{2}ln\left(1-\tilde{\rho}+\frac{q}{r}\tilde{\rho}\right) + \frac{z}{2}ln\Gamma_{00}\right]r_i\tilde{v} = ln\frac{\phi_i}{\delta_i\,r_i} - r_i\frac{l}{r} + ln\,\tilde{\rho} + r_i(\tilde{v}-$$

$$1)\, ln(1-\tilde{\rho}) - \frac{z}{2} r_i \left(\tilde{v} - 1 + \frac{q_i}{r_i}\right) ln\left(1 - \tilde{\rho} + \frac{q}{r}\tilde{\rho}\right) + \frac{z\, q_i}{2}\left[ln\, \Gamma_{ii} + \frac{r_i}{q_i}(\tilde{v}-1)\, ln\, \Gamma_{00}\right] - \frac{q_i}{\tilde{T}_i} + r_i \nu_H - \sum_{\alpha}^{m} d_{\alpha}^{i}\, ln\left(\frac{\nu_d^{\alpha}}{\nu_{\alpha 0}}\right) - \sum_{\beta}^{n} a_{\beta}^{i}\, ln\left(\frac{\nu_a^{\beta}}{\nu_{0\beta}}\right) + \mathrm{r_i} \frac{\tilde{\mathrm{P}}\,\tilde{\mathrm{v}}}{\tilde{\mathrm{T}}} \qquad \text{(A.19)}$$

Eq. (A.19) corresponds to the expression of non-equilibrium chemical potential developed by Panayiotou et. al working directly in the ensemble $(P, T, \underline{N})$ (last member of (A.19)), provided that P is given by (2.8).

A.3 Calculation of the values of the internal state variables in the limit of IG state.

In order to calculate the limit of $ln\Gamma_{00}^{eq}$, as $\tilde{\rho}^{eq} \to 0$, or equivalently as $N_0^{eq} \to +\infty$, it is useful to investigate the functional form approached, as $N_0^{eq} \to +\infty$, by the system of the balance equations of contacts coupled with the corresponding minimization condition. To this aim, we recast the contacts balance equation (1.12) in terms of Γ_{ij} for each $i, j = 0,1, \dots, t$, where N_{ij}^{0} represents number of i-component and j-component lattice fluid pairs, including empty sites, in the random case at the same $(V, T, \underline{N})$. By performing the limit of the contacts balance equation as $N_0^{eq} \to +\infty$, we obtain:

$$\lim_{N_0^{eq} \to +\infty} \left(\Theta_i^{eq} \Gamma_{ii}^{eq} + \sum_{j \neq i}^{t} \Theta_j^{eq} \Gamma_{ij}^{eq}\right) = \lim_{N_0^{eq} \to +\infty} (1) = 1 \quad \text{for each } i = 0, \dots, t \qquad \text{(A.20)}$$

Now we focus on the limit on first member above, firstly for the case *i*=0, i.e.:

$$\lim_{N_0^{eq} \to +\infty} \left(\Theta_0^{eq} \Gamma_{00}^{eq} + \sum_{j \neq}^{t} \Theta_j^{eq} \Gamma_{ij}^{eq}\right) = 1 \qquad \text{(A.21)}$$

Substituting the expression of the Θ_i coefficients, (A.21) reads:

$$\lim_{N_0^{eq} \to +\infty} \left(\frac{N_0^{eq}}{N_0^{eq} + qN} \Gamma_{00}^{eq} + \sum_{j \neq 0}^{t} \frac{N_{0j}^{eq}}{z\, N_0^{eq}}\right) = 1 \qquad \text{(A.22)}$$

In fact, the general expression holds:

$$\Theta_j \Gamma_{j0} = \Theta_j \frac{N_{0j}}{N_{0j}^{0}} = \Theta_j \frac{N_{0j}}{z\, N_0\, \Theta_j} = \frac{N_{0j}}{z\, N_0} \qquad \text{(A.23)}$$

Once the composition is fixed, any N_{0j}^{eq} is a positive bounded term, limited by the total number of contacts of the fixed number of molecules of species j, i.e. $N_{0j} \leq zN_jq_j$, so that we finally have:

$$\lim_{N_0^{eq}\to+\infty} \Gamma_{00}^{eq} = 1 \tag{A.24}$$

In the same way, for the case $i\neq0$:

$$\lim_{N_0^{eq}\to+\infty} \left(\frac{q_iN_i}{N_0^{eq}+qN}\Gamma_{ii}^{eq} + \sum\nolimits_{j\neq0,i}^{t}\frac{q_jN_j}{N_0^{eq}+qN}\Gamma_{ij}^{eq} + \frac{N_0^{eq}}{N_0^{eq}+qN}\Gamma_{i0}^{eq}\right) = 1 \text{ for each } i = 1,2,\dots,t \tag{A.25}$$

Each *t+1* term of eq. (A.25) is defined positive and so cannot → +∞ since the limit of summation is equal to 1, moreover it is worth noting that the limit value of each term, as $N_0^{eq} \to +\infty$, can be at most 1, as imposed by eq. (A.25). This means that, formally, we have:

$$\lim_{N_0^{eq}\to+\infty} \frac{q_iN_i}{N_0^{eq}+qN}\Gamma_{ii}^{eq} = \lim_{N_0^{eq}\to+\infty} \frac{\Gamma_{ii}^{eq}}{N_0^{eq}} = a \ \ with\ 0 \leq a \leq 1 \tag{A.26}$$

$$\lim_{N_0^{eq}\to+\infty} \frac{q_jN_j}{N_0^{eq}+qN}\Gamma_{ij}^{eq} = \lim_{N_0^{eq}\to+\infty} \frac{\Gamma_{ij}^{eq}}{N_0^{eq}} = b \ \ with\ 0 \leq b \leq 1 \tag{A.27}$$

$$\lim_{N_0^{eq}\to+\infty} \frac{N_0^{eq}}{N_0^{eq}+qN}\Gamma_{i0}^{eq} = \lim_{N_0^{eq}\to+\infty} \Gamma_{i0}^{eq} = c \ \ with\ 0 \leq c \leq 1 \tag{A.28}$$

By definition, it turns out $\Gamma_{i0}^{eq} \in O(1), \Gamma_{ij}^{eq} \in O\left(N_0^{eq}\right)$ and $\Gamma_{ii}^{eq} \in O\left(N_0^{eq}\right)$ as $N_0^{eq} \to +\infty$. However, eq. (A.24) must be coupled with the IG limit of the set of minimization conditions expressed by equation (2.6), thus resulting in the following expression:

$$\lim_{N_0^{eq}\to+\infty} \frac{{\Gamma_{i0}^{eq}}^2}{\Gamma_{ii}^{eq}\,\Gamma_{00}^{eq}} = \lim_{N_0^{eq}\to+\infty} exp\left(-\frac{\varepsilon_i}{kT}\right) \Leftrightarrow \lim_{N_0^{eq}\to+\infty} \frac{{\Gamma_{i0}^{eq}}^2}{\Gamma_{ii}^{eq}} = exp\left(-\frac{\varepsilon_i}{kT}\right)$$

for each $i = 1, \dots, t$ (A.29)

$$\lim_{N_0^{eq}\to+\infty} \frac{{\Gamma_{ij}^{eq}}^2}{\Gamma_{ii}^{eq}\,\Gamma_{jj}^{eq}} = \lim_{N_0^{eq}\to+\infty} exp\left(-\frac{\Delta\varepsilon_{ij}}{kT}\right) \Leftrightarrow \lim_{N_0^{eq}\to+\infty} \frac{{\Gamma_{ij}^{eq}}^2}{\Gamma_{ii}^{eq}\,\Gamma_{jj}^{eq}} = exp\left(-\frac{\Delta\varepsilon_{ij}}{kT}\right)$$

for each $i, j = 1, \dots, \mathrm{t}$ and $j > i$ (A.30)

ε_i and $\Delta\varepsilon_{ij}$ are constants for a given system and T is fixed, so $exp\left(-\frac{\varepsilon_i}{kT}\right)$ and $exp\left(-\frac{\Delta\varepsilon_{ij}}{kT}\right)$ are strictly positive constants. This implies that, to comply to the constraint imposed by eq. (A.29) coupled with eq. (A.28), we obtain $\Gamma_{\text{ii}} \in O(1)$. Eq. (A.29) then becomes:

$$\lim_{N_0^{eq}\to+\infty} \frac{\Gamma_{i0}^{eq^2}}{\Gamma_{ii}^{eq}} = \frac{\lim\limits_{N_0^{eq}\to+\infty} \Gamma_{i0}^{eq^2}}{\lim\limits_{N_0^{eq}\to+\infty} \Gamma_{ii}^{eq}} = \frac{c^2}{\lim\limits_{N_0^{eq}\to+\infty} \Gamma_{ii}^{eq}} = exp\left(-\frac{\varepsilon_i}{kT}\right) \Leftrightarrow \lim_{N_0^{eq}\to+\infty} \Gamma_{ii}^{eq} = \frac{c^2}{exp\left(-\frac{\varepsilon_i}{kT}\right)} \quad \text{(A.31)}$$

Based on eq. (A.28) *c* is a bounded quantity while $exp\left(-\frac{\varepsilon_i}{kT}\right) > 0$, so:

$$\lim_{N_0^{eq}\to+\infty} \Gamma_{ii}^{eq} = \frac{c^2}{exp\left(-\frac{\varepsilon_i}{kT}\right)} = a_1 \quad with\, a_1 \geq 0 \qquad \text{(A.32)}$$

By definition, this leads to $\Gamma_{ii}^{eq} \in O(1)$ as $N_0^{eq} \to +\infty$. Trivially, the aforementioned $\Gamma_{ii}^{eq} \in O\left(N_0^{eq}\right)$ as $N_0^{eq} \to +\infty$ dictated by contacts balance is consistent with the stronger constraint $\Gamma_{ii}^{eq} \in O(1)$ imposed by minimization conditions. In the same way, also considering eq. (SI.32), from eq. (A.30) one infers that $\Gamma_{\text{ij}} \in O(1)$ as $N_0^{eq} \to +\infty$, which is consistent with $\Gamma_{ij}^{eq} \in O\left(N_0^{eq}\right)$, as dictated by the contacts balance equation.
Coming back to equation (A.25), based on the last results, by linearity of the limit calculations, it turns out that:

$$\lim_{N_0^{eq}\to+\infty} \left(\frac{q_i N_i}{N_0^{eq}+qN}\Gamma_{ii}^{eq} + \sum_{j\neq 0,i}^{t} \frac{q_j N_j}{N_0^{eq}+qN}\Gamma_{ij}^{eq} + \frac{N_0^{eq}}{N_0^{eq}+qN}\Gamma_{i0}^{eq}\right) = 1 \Rightarrow \lim_{N_0^{eq}\to+\infty} \Gamma_{i0}^{eq} = 1 \quad \text{for any } i \neq 0 \qquad \text{(A.33)}$$

Combining with (A.24), we conclude that:

$$\lim_{N_0^{eq}\to+\infty} \Gamma_{i0}^{eq} \overset{\text{def}}{=} \lim_{N_0^{eq}\to+\infty} \Gamma_{0i}^{eq} = 1 \qquad \text{for each } i = 0, \dots, t \qquad \text{(A.34)}$$

To simplify the notation, from now on we will indicate $\lim\limits_{N_0^{eq}\to+\infty} \Gamma_{ij}^{eq} = \Gamma_{ij,\infty}^{eq}$ for each *i*, *j*=0,1,..,*t*. Finally, we can determine the value of the entire set of $\Gamma_{ij,\infty}^{eq}$. Indeed, from equations (A.34) and (2.6):

$$\lim_{N_0^{eq}\to+\infty} \frac{\Gamma_{i0}^{eq^2}}{\Gamma_{ii}^{eq}\Gamma_{00}^{eq}} = exp\left(-\frac{\varepsilon_{ii}}{kT}\right) \Rightarrow \Gamma_{ii,\infty}^{eq} = exp\left(\frac{\varepsilon_{ii}}{kT}\right) \text{ for each } i = 1, \dots, t \qquad \text{(A.35)}$$

$$\lim_{N_0^{eq}\to+\infty} \frac{{\Gamma_{ij}^{eq}}^2}{\Gamma_{ii}^{eq}\,\Gamma_{jj}^{eq}} = exp\left(-\frac{\Delta\varepsilon_{ij}}{kT}\right) \Rightarrow \Gamma_{ij,\infty}^{eq} = exp\left(-\frac{\Delta\varepsilon_{ij}-\varepsilon_{ii}-\varepsilon_{jj}}{kT}\right) = exp\left(\frac{\varepsilon_{ij}}{kT}\right) \tag{A.36}$$

for each $i,j = 1,\dots,t$ and $j > i$

Having determined the values of the limit of each $\Gamma_{ij,\infty}^{eq}$ term, we can analyse the values of the limit of each corresponding value of each $N_{ij,\infty}^{eq}$ term. To calculate these terms, according to their definition, we need to determine the model for the contacts in the randomness hypothesis:

$$\lim_{N_0^{eq}\to+\infty} N_{00}^{0,eq} = \lim_{N_0^{eq}\to+\infty} \frac{z}{2} N_0^{eq} \frac{N_0^{eq}}{N_0^{eq}+qN} = +\infty \tag{A.37}$$

$$\lim_{N_0^{eq}\to+\infty} N_{0i}^{0,eq} = \lim_{N_0^{eq}\to+\infty} zN_iq_i \frac{N_0^{eq}}{N_0^{eq}+qN} = zN_iq_i \qquad \text{for each } i,j = 1,\dots,t \tag{A.38}$$

$$\lim_{N_0^{eq}\to+\infty} N_{ii}^{0,eq} = \lim_{N_0^{eq}\to+\infty} \frac{z}{2} N_iq_i \frac{q_iN_i}{N_0^{eq}+qN} = 0 \qquad \text{for each } i = 1,\dots,t \tag{A.39}$$

$$\lim_{N_0^{eq}\to+\infty} N_{ij}^{0,eq} = \lim_{N_0^{eq}\to+\infty} zN_iq_i \frac{q_jN_j}{N_0^{eq}+qN} = 0 \qquad \text{for each } i,j = 1,\dots,t \quad j > i \tag{A.40}$$

Combining eqs. (A.37-A.40) with the results obtained from equations (A.34-A.36) regarding $\Gamma_{ij,\infty}^{eq}$, it follows that:

$$\lim_{N_0^{eq}\to+\infty} N_{00}^{eq} = \lim_{N_0^{eq}\to+\infty} N_{00}^{0,eq}\Gamma_{00}^{eq} = +\infty \tag{A.41}$$

$$\lim_{N_0^{eq}\to+\infty} N_{0i}^{eq} = \lim_{N_0^{eq}\to+\infty} N_{0i}^{0,eq}\Gamma_{0i}^{eq} = zN_iq_i \qquad \text{for each } i = 1,\dots,t \tag{A.42}$$

$$\lim_{N_0^{eq}\to+\infty} N_{ii}^{eq} = \lim_{N_0^{eq}\to+\infty} N_{ii}^{0,eq}\Gamma_{ii}^{eq} = 0 \qquad \text{for each } i = 1,\dots,t \tag{A.43}$$

$$\lim_{N_0^{eq}\to+\infty} N_{ij}^{eq} = \lim_{N_0^{eq}\to+\infty} N_{ij}^{0,eq}\Gamma_{ij}^{eq} = 0 \qquad \text{for each } i,j = 1,\dots,t \quad j > i \tag{A.44}$$

In other words, as the ideal gas state is approached, focusing on the molecular species (i.e., not considering the empty site species), the number of LF external self-contacts between the *i* species and the number of cross LF contacts between species *i* and *j* (with $i \neq j$) is null. Eqs. (A.43) and (A.44) are results expected in view of $V \to +\infty$, that are physically consistent with the condition of equilibrium ideal gas mixture, in which the molecules of each species are assumed to be isolated. Moreover each N_{i0} ($i = 1,2,\dots,t$), in the limit of $V \to +\infty$, approaches zq_iN_i; since zq_i represents the total external contacts per molecule *i*, it means, as expected, that the LF external contacts of each species *i* are only with empty cells.

In the following, we detail the calculation of limits required for the first three terms on the last member of eq. (2.19b):

$$\lim_{\tilde{\rho}^{eq}\to 0} -\frac{r}{\tilde{\rho}^{eq}} ln(1-\tilde{\rho}^{eq}) = r \tag{A.45}$$

as obtained by applying the L’ Hopital theorem and by considering that r is fixed by the assigned composition.

$$\lim_{\tilde{\rho}^{eq}\to 0} r \sum_{i=1}^{t} \Phi_i \frac{l_i}{r_i} = l \tag{A.46}$$

where each term is only dependent upon the fixed composition.

$$\lim_{\tilde{\rho}^{eq}\to 0} r \frac{z}{2} \frac{ln\left(1-\tilde{\rho}^{eq}+\frac{q}{r}\tilde{\rho}^{eq}\right)}{\tilde{\rho}^{eq}} = \frac{z}{2}(q-r) \tag{A.47}$$

as obtained by applying the L’Hopital theorem and considering that $\frac{q}{r}$ is fixed by the composition.

Therefore, to calculate the value of limit in equation (2.19b), we must investigate the limit of the expression reported in square brackets. The first term of this expression reads:

$$\lim_{\tilde{\rho}^{eq}\to 0} r\, \nu_H^{eq} = r \lim_{\tilde{\rho}^{eq}\to 0} \sum_{\alpha}^{m} \sum_{\beta}^{n} \nu_{\alpha\beta}^{eq} =$$
$$r \lim_{\tilde{\rho}^{eq}\to 0} \tilde{\rho}^{eq} \sum_{\alpha}^{m} \sum_{\beta}^{n} \nu_{\alpha 0}^{eq} \nu_{0\beta}^{eq}\, exp\left(-\frac{A_{\alpha\beta}^{0}+P^{eq}V_{\alpha\beta}^{0}}{kT}\right) = 0 \tag{A.48}$$

In the second equality we have imposed the minimization condition for each kind of HB contact (eq. (2.13)).

Eq. (A.48) holds true since, from the physics of the model, $\nu_{\alpha 0}^{eq}, \nu_{0\beta}^{eq}$, are bounded terms, $V_{\alpha\beta}^{0}$ and $A_{\alpha\beta}^{0}$ do not depend on $\tilde{\rho}^{eq}$ and $P^{eq} \to 0$ according to equation (2.16c).

Since any $\nu_{\alpha\beta}^{eq}$ is intrinsically a non-negative quantity, the (A.48) imposes that each $\lim_{\tilde{\rho}^{eq}\to 0} \nu_{\alpha\beta}^{eq} = 0$. This is physically consistent with the ideal gas mixture condition, in which the molecules are assumed to be isolated so that specific interactions are not allowed in the framework of HB statistics adopted.

The limit calculation for the second term in the brackets, omitting r and z factors, and recalling $\Theta_j^{eq} = \theta_r \theta_i$ and $\theta_r = \frac{qN}{N_0+qN}$, reads:

$$\lim_{\tilde{\rho}^{eq}\to 0}\frac{ln\Gamma_{00}^{eq}}{\tilde{\rho}^{eq}} = \lim_{N_0^{eq}\to+\infty}\frac{ln\left(\frac{1}{\Theta_0^{eq}}-\frac{1}{\Theta_0^{eq}}\sum_{j\neq 0}^{t}\Theta_j^{eq}\Gamma_{0j}^{eq}\right)}{\frac{r\,N}{N_0^{eq}+rN}} = \lim_{N_0^{eq}\to+\infty}\frac{ln\left(\frac{N_0^{eq}+qN}{N_0^{eq}}-\frac{N_0^{eq}+qN}{N_0^{eq}}\,\theta_r^{eq}\sum_{j\neq 0}^{t}\theta_j\Gamma_{0j}^{eq}\right)}{\frac{rN}{N_0^{eq}+rN}} =$$

$$\lim_{N_0^{eq}\to+\infty}\frac{ln\left(\frac{N_0^{eq}+qN}{N_0^{eq}}-\frac{qN}{N_0^{eq}}\sum_{j\neq 0}^{t}\theta_j\Gamma_{0j}^{eq}\right)}{\frac{rN}{N_0^{eq}+rN}} =$$

$$\lim_{N_0^{eq}\to+\infty}\frac{ln\left[1+\frac{qN}{N_0^{eq}}\left(1-\sum_{j\neq 0}^{t}\theta_j\Gamma_{0j}^{eq}\right)\right]}{\frac{rN}{N_0^{eq}+rN}} =$$

$$\lim_{N_0^{eq}\to+\infty}\frac{ln\left[1+\frac{qN}{N_0^{eq}}\left(1-\sum_{j\neq 0}^{t}\theta_j\Gamma_{0j}^{eq}\right)\right]}{\frac{qN}{N_0^{eq}}\left(1-\sum_{j\neq 0}^{t}\theta_j\Gamma_{0j}^{eq}\right)}\,\frac{\frac{qN}{N_0^{eq}}\left(1-\sum_{j\neq 0}^{t}\theta_j\Gamma_{0j}^{eq}\right)}{\frac{rN}{N_0^{eq}+rN}} =$$

$$1\cdot\lim_{N_0^{eq}\to+\infty}\frac{N_0^{eq}+rN}{N_0^{eq}}\,\frac{q}{r}\left(1-\sum_{j\neq 0}^{t}\theta_j\Gamma_{0j}^{eq}\right) \qquad \text{(A.49)}$$

Since as seen each Γ_{0j}^{eq} has a limit equal to 1 and the θ_j are fixed by the assigned composition, the following relationship holds:

$$\lim_{N_0^{eq}\to+\infty}\frac{N_0^{eq}+rN}{N_0^{eq}}\,\frac{q}{r}\left(1-\sum_{j\neq 0}^{t}\theta_j\Gamma_{0j}^{eq}\right) = \frac{q}{r}\left(1-\sum_{j\neq 0}^{t}\theta_j\right) = 0 \qquad \text{(A.50)}$$

In particular, regarding the last identity in (A.50), we observe that the definition of θ_j (see Appendix), implies that $\sum_{j\neq 0}^{t}\theta_j = 1$. In obtaining (A.49) the following identity has also been used:

$$\lim_{N_0^{eq}\to+\infty}\frac{ln\left[1+\frac{qN}{N_0^{eq}}\left(1-\sum_{j\neq 0}^{t}\theta_j\Gamma_{0j}^{eq}\right)\right]}{\frac{qN}{N_0^{eq}}\left(1-\sum_{j\neq 0}^{t}\theta_j\Gamma_{0j}^{eq}\right)} = \lim_{y\to 0}\frac{\ln(1+y)}{y} = 1 \qquad \text{(A.51)}$$

In this calculation the theorem of limit of composite function with $y(N_0^{eq}) = \frac{qN}{N_0^{eq}}\left(1-\sum_{j\neq 0}^{t}\theta_j\Gamma_{0j}^{eq}\right)$ internal function has been applied. Performing the limit of the internal function as $N_0^{eq}\to+\infty$, according to (A.50) we obtain $\lim_{N_0^{eq}\to+\infty} y = 0$.

A.4 Calculation details of the IG limit value of the chemical potential expressions provided by the NRHB model

In eq. (4.3) the expression $\mu_i^{eq}(v, T, \underline{N})$ can be operatively obtained by coupling equations (1.12), (2.5), (2.6), (2.13) and (2.14).
So, by linearity of limits calculation, we have, applying de l'Hopital theorem:

$$\lim_{\tilde{\rho}^{eq}\to 0} r_i(\tilde{v}^{eq} - 1)\, ln(1 - \tilde{\rho}^{eq}) = -r_i \tag{A.52}$$

from equations (2.16c) and (2.20):

$$\lim_{\tilde{\rho}^{eq}\to 0} r_i \frac{\tilde{P}^{eq}\,\tilde{v}^{eq}}{\tilde{T}} = \lim_{\tilde{\rho}^{eq}\to 0} \left[r_i \frac{\tilde{P}^{eq}}{\tilde{T}} \frac{v}{rv^*} - r_i \frac{\tilde{P}^{eq}}{\tilde{T}} \frac{1}{rNv^*} \textstyle\sum_\alpha^m \sum_\beta^n N_{\alpha\beta}^{HB,eq}\, V_{\alpha\beta}^0 \right] = \lim_{\tilde{\rho}^{eq}\to 0} \frac{r_i}{r} \frac{P^{eq} v}{kT} - 0 = \lim_{\tilde{\rho}^{eq}\to 0} \frac{r_i}{r}\, \bar{Z}^{eq} = \frac{r_i}{r} \tag{A.53}$$

$$\lim_{\tilde{\rho}^{eq}\to 0} \left(ln \frac{\phi_i}{\delta_i\, r_i} - r_i \frac{l}{r} \right) = \lim_{\tilde{\rho}^{eq}\to 0} \left(ln \frac{x_i}{\delta_i r} - r_i \frac{l}{r} \right) = ln \frac{x_i}{\delta_i r} - r_i \frac{l}{r} \tag{A.54}$$

since each term is only dependent upon the fixed composition. Applying de l'Hopital theorem we obtain:

$$\lim_{\tilde{\rho}^{eq}\to 0} -\frac{z}{2} r_i \left(\tilde{v}^{eq} - 1 + \frac{q_i}{r_i} \right) ln \left(1 - \tilde{\rho}^{eq} + \frac{q}{r} \tilde{\rho}^{eq} \right) = -\frac{z}{2} r_i \lim_{\tilde{\rho}^{eq}\to 0} \frac{1}{\tilde{\rho}^{eq}} ln \left(1 - \tilde{\rho}^{eq} + \frac{q}{r} \tilde{\rho}^{eq} \right) = -\frac{z}{2} r_i \left(\frac{q}{r} - 1 \right) \tag{A.55}$$

From eq. (A.35):

$$\lim_{\tilde{\rho}^{eq}\to 0} \frac{z\, q_i}{2} ln\, \Gamma_{ii}^{eq} = \frac{z\, q_i}{2} ln\, \Gamma_{ii,\infty}^{eq} = \frac{z\, q_i}{2} \left(\frac{\varepsilon_{ii}}{kT} \right) \tag{A.56}$$

$$\lim_{\tilde{\rho}^{eq}\to 0} \frac{z\, r_i}{2} (\tilde{v}^{eq} - 1)\, ln\, \Gamma_{00}^{eq} = \frac{z\, r_i}{2} \lim_{\tilde{\rho}^{eq}\to 0} \frac{1}{\tilde{\rho}^{eq}} ln\, \Gamma_{00}^{eq} = 0 \tag{A.57}$$

The first equality in eq. (A.57) follows from eq. (A.24) and linearity of limit calculation, and the second equality in eq. (A.57) follows from eqs. (A.49-A.50).

$$\lim_{\tilde{\rho}^{eq}\to 0} -\frac{q_i}{\tilde{T}_i} = -\frac{q_i}{\tilde{T}_i} \tag{A.58}$$

since this term is fixed by assigned T and composition. From the results implied by eq. (A.48) we have:

$$\lim_{\tilde{\rho}^{eq}\to 0} r_i v_H^{eq} = r_i \lim_{\tilde{\rho}^{eq}\to 0} v_H^{eq} = 0 \qquad \text{(A.59)}$$

$$\lim_{\tilde{\rho}^{eq}\to 0} ln\left(\frac{v_d^{\alpha}}{v_{\alpha 0}^{eq}}\right) = \lim_{\tilde{\rho}^{eq}\to 0} ln\left(\frac{v_d^{\alpha}}{v_d^{\alpha}-\sum_{\beta}^{n} v_{\alpha\beta}^{eq}}\right) = \lim_{\tilde{\rho}^{eq}\to 0} ln\left(\frac{v_d^{\alpha}}{v_d^{\alpha}-\tilde{\rho}^{eq}\sum_{\beta}^{n} v_{\alpha 0}^{eq} v_{0\beta}^{eq}\, exp\left(-\frac{A_{\alpha\beta}^{0}+P^{eq}V_{\alpha\beta}^{0}}{kT}\right)}\right) = 0$$

for each α (A.60)

The result above has been obtained by recalling the same procedure concerning eq. (A.48). Since eq. (A.60) holds for each α and since each d_{α}^{i} is a fixed value for the species *i*:

$$\lim_{\tilde{\rho}^{eq}\to 0} \sum_{\alpha}^{m} d_{\alpha}^{i}\, ln\left(\frac{v_d^{\alpha}}{v_{\alpha 0}^{eq}}\right) = 0 \qquad \text{(A.61)}$$

The same procedure is here applied to show that:

$$\lim_{\tilde{\rho}^{eq}\to 0} ln\left(\frac{v_a^{\beta}}{v_{0\beta}^{eq}}\right) = 0 \quad \text{for each } \beta \qquad \text{(A.62)}$$

So that:

$$\lim_{\tilde{\rho}^{eq}\to 0} \sum_{\beta}^{n} a_{\beta}^{i}\, ln\left(\frac{v_a^{\beta}}{v_{0\beta}^{eq}}\right) = 0 \qquad \text{(A.63)}$$

since each a_{β}^{i} is fixed for the specie *i*. Finally, we can obtain the limiting value of the last terms:

$$\lim_{v\to+\infty} ln\,\tilde{\rho}^{eq} = -\lim_{v\to+\infty} ln\left(\frac{v}{rv^*}-\frac{1}{v^*}\sum_{\alpha}^{m}\sum_{\beta}^{n} v_{\alpha\beta}^{HB,eq}\, V_{\alpha\beta}^{0}\right) = -\lim_{v\to+\infty} ln\left(\frac{v}{rv^*}-g\left(\tilde{\rho}^{eq}(v)\right)\right) = -\lim_{v\to+\infty} ln\left(\frac{v}{rv^*}\right) \qquad \text{(A.64)}$$

by accounting for eq. (A.48) and considering the limit of composite function g.
Finally, substituting the equations from (A.52) to (A.64) into (2.23) and assembling the limits of the logarithmic terms in equations (A.54) and (A.63), we obtain:

$$\lim_{v\to+\infty} \mu_i^{eq} = kT\left[-r_i - r_i\frac{l}{r}-\frac{z}{2}r_i\left(\frac{q}{r}-1\right)+\frac{z\,q_i}{2}\left(\frac{\varepsilon_{ii}}{kT}\right)+\frac{r_i}{r}-\frac{q_i}{\tilde{T}_i}+\lim_{v\to+\infty} ln\left(\frac{x_i\,v^*}{\delta_i\,v}\right)\right] \qquad \text{(A.65)}$$

Recalling the definition of *l* and considering that:

$$\frac{q_i}{\tilde{T}_i} = \frac{\varepsilon_i^* q_i}{k\,T} = \frac{z\,q_i}{2}\frac{\varepsilon_{ii}}{kT} \tag{A.66}$$

(A.65) can be rewritten as:

$$\lim_{v \to +\infty} \mu_i^{eq} = kT \lim_{v \to +\infty} ln\left(\frac{x_i\,v^*}{\delta_i\,v}\right) = -\infty \tag{A.67}$$

The result provided by eq. (A.67) is expected since, on the basis of the entropic contribution, as $V \to +\infty$, the molar concentration of each species *i* approaches zero at fixed T and $\underline{N}$. As a matter of fact, we can repeat the same calculation described above to obtain the limiting value of $\mu_i^{0,eq}(v,\, T)$ as $v \to +\infty$. In this case $x_i = 1$ and, consistently, each mixture parameter approaches, by its mixing rules, the corresponding value of pure component *i*. Therefore, we obtain:

$$\lim_{v \to +\infty} \mu_i^{0,eq}(v,T) = kT \lim_{v \to +\infty} ln\left(\frac{v^*}{\delta_i\,v}\right) \tag{A.68}$$

We recall here that δ_i is the composition independent flexibility parameter of component *i*. Finally, by linearity of limit calculation, we can subtract equation (A.68) from (A.67), obtaining:

$$\lim_{v \to +\infty} \mu_i^{eq}(v,T,\underline{N}) - \lim_{v \to +\infty} \mu_i^{0,eq}(v,T) = kT \lim_{v \to +\infty} ln\left(\frac{x_i\,v^*}{\delta_i\,v}\right) - kT \lim_{v \to +\infty} ln\left(\frac{v^*}{\delta_i\,v}\right) = kT\, ln(x_i) \tag{A.69}$$

(A.69) is a consequence of the NRHB model assumption that v^* is a universal constant and that δ_i is a parameter assigned for any specie *i* at a given *T* (and in particular it is independent of composition). Finally, we note that (A.69) verifies equation (2.22). Indeed, this result represents the aim of the present section.

A.5 Calculation details of the IG limit value of Compressibility factor and chemical potential expressions provided by the SL model

In this section we firstly apply the procedure, detailed in Section 2.2 and Section 2.3, to the different versions of SL model investigated by Neau. Afterwards, we also examinate a further version of SL model, the one adopted by Sarti et al. in order to develop the NELF theory, which is widely implemented in literature to describe the solubility of a penetrant in a glassy polymer.

All the investigated versions of SL model differ only in the mixing rules for the characteristic cell molecular volume of the mixture, v^*, and/or the characteristic molecular energy of the mixture, ε^*. In particular, each version displays the same expression of the EoS, i.e.:

$$\tilde{P} = -\tilde{T}\left[\ln(1-\tilde{\rho}) + \left(1-\frac{1}{r}\right)\tilde{\rho}\right] - \tilde{\rho}^2 \tag{A.70}$$

and only differs in the expression for the chemical potential in mixtures. In this section, all symbols adopted, if not explicitly indicated, have the same definition in, both, LF and NRHB models.

By applying the same procedure used to assess the consistency in the case of NRHB theory, one can show that each considered version of SL model trivially satisfies equations (A.71) and (A.72):

$$\lim_{\tilde{\rho}\to 0} \tilde{P} = 0 \tag{A.71}$$

$$\lim_{\tilde{\rho}\to 0} \bar{Z} = \lim_{\tilde{\rho}\to 0} \frac{\tilde{P}\tilde{v}}{\tilde{T}}\, r = \lim_{\tilde{\rho}\to 0} r\left[-\frac{1}{\tilde{\rho}} ln(1-\tilde{\rho}) - \left(1-\frac{1}{r}\right) - \frac{\tilde{\rho}}{\tilde{T}}\right] = 1 \tag{A.72}$$

so that the EoS recovers the consistency at IG limit.

Regarding the expression for the chemical potential in the multicomponent system, we firstly examine the different versions of SL considered by Neau. Repeating the procedure developed for NRHB, we need to express the chemical potential of component *i* as a function of $\left(v, T, \underline{N}\right)$. In particular, starting from the general expression for the chemical potential of component *i* in the mixture, reported by Neau, it is given by:

$$\frac{\mu_i(v,T,\underline{N})}{kT} = \left(\ln\frac{\phi_i}{\delta_i} + 1 - \frac{r_i}{r}\right) + \ln\tilde{\rho} + r_i\left[-\frac{\tilde{\rho}}{\tilde{T}} + \left(\frac{1}{\tilde{\rho}} - 1\right)\ln(1-\tilde{\rho}) + \frac{\tilde{P}\tilde{v}}{\tilde{T}}\right] + \bar{Z}\left[\frac{N}{v^*}\left(\frac{\partial v^*}{\partial N_i}\right)_{N_{j\neq i}}\right] - \frac{\tilde{\rho}}{\tilde{T}}\left[\frac{Nr}{\varepsilon^*}\left(\frac{\partial \varepsilon^*}{\partial N_i}\right)_{N_{j\neq i}}\right] = \left(\ln\frac{\phi_i}{\delta_i} + 1 - \frac{r_i}{r}\right) + \ln\frac{rv^*}{v} + r_i\left[-\frac{rv^*}{v\tilde{T}} + \left(\frac{v}{rv^*} - 1\right)\ln\left(1 - \frac{rv^*}{v}\right) + \frac{\bar{Z}}{r}\right] + \bar{Z}\left[\frac{N}{v^*}\left(\frac{\partial v^*}{\partial N_i}\right)_{N_{j\neq i}}\right] - \frac{rv^*}{v\tilde{T}}\left[\frac{Nr}{\varepsilon^*}\left(\frac{\partial \varepsilon^*}{\partial N_i}\right)_{N_{j\neq i}}\right] \tag{A.73}$$

Any different version of the model is obtained by properly expressing the two latter terms of the R.H.S. of equation (A.73), according to the adopted mixing rules of v^* and ε^*. According to the procedure at hand, the following limit must be calculated:

$$\lim_{v\to+\infty}\frac{\mu_i(v,T,\underline{N})}{kT} = \lim_{v\to+\infty}\left\{\left(\ln\frac{\phi_i}{\delta_i}+1-\frac{r_i}{r}\right)+\ln\frac{rv^*}{v}+r_i\left[-\frac{rv^*}{v\tilde{T}}+\left(\frac{v}{rv^*}-1\right)\ln\left(1-\frac{rv^*}{v}\right)+\frac{\bar{Z}}{r}\right]+\bar{Z}\left[\frac{N}{v^*}\left(\frac{\partial v^*}{\partial N_i}\right)_{N_{j\neq i}}\right]-\frac{rv^*}{v\tilde{T}}\left[\frac{Nr}{\varepsilon^*}\left(\frac{\partial \varepsilon^*}{\partial N_i}\right)_{N_{j\neq i}}\right]\right\} = \left[\frac{N}{v^*}\left(\frac{\partial v^*}{\partial N_i}\right)_{N_{j\neq i}}\right]+1-\frac{r_i}{r}-r_i+\frac{r_i}{r}+\lim_{v\to+\infty}\ln\frac{x_i\,r_i\,v^*}{\delta_i\,v} = \left[\frac{N}{v^*}\left(\frac{\partial v^*}{\partial N_i}\right)_{N_{j\neq i}}\right]+1-r_i+\lim_{v\to+\infty}\ln\frac{x_i\,r_i\,v^*}{\delta_i\,v} \tag{A.74}$$

In obtaining eq. (A.74), we have applied the same calculation procedure as for NRHB case (see equation (A.45)). It is important to note that the contribution to the chemical potential deriving from different mixing rules for ε^* vanishes in the IG limit condition, so that only the mixing rule of v^* plays a role in the assessment of the consistency.

Repeating the calculation, as required by the procedure, for the pure *i*-th component, the following expression is obtained:

$$\lim_{v\to+\infty}\frac{\mu_i^0(v,T)}{kT} = 1-r_i+\lim_{v\to+\infty} ln\frac{r_i\,v_i^*}{\delta_i\,v} \tag{A.75}$$

In equation (A.75), v_i^* represents the characteristic cell molecular volume of the pure component *i*. Finally, re-expressing the limit of the L.H.S of equation (A.69) for the case at hand, the following result is obtained:

$$\lim_{v\to+\infty}\left(\frac{\mu_i(v,T,\underline{N})}{kT}-\frac{\mu_i^0(v,T)}{kT}\right) = \left[\frac{N}{v^*}\left(\frac{\partial v^*}{\partial N_i}\right)_{N_{j\neq i}}\right]+ln\left[\frac{x_i\,v^*}{v_i^*}\right] = ln\,x_i+\frac{N}{v^*}\left(\frac{\partial v^*}{\partial N_i}\right)_{N_{j\neq i}}+ln\frac{v^*}{v_i^*} \tag{A.76}$$

The consistency requires that:

$$\frac{N}{v^*}\left(\frac{\partial v^*}{\partial N_i}\right)_{N_{j\neq i}} = -\,ln\frac{v^*}{v_i^*} \qquad \text{for each } i=1, 2, \dots, t \tag{A.77}$$

Eq. (A.77) represents a set of *t* partial differential equations, which must be satisfied for any possible mixture in the only unknown $v^*(N_1, N_2, \dots, N_t)$. Each physically admissible solution must converge to the value of v_i^* of each pure component *i,* when $N \to N_i$ (for each *i*=1, 2,…, *t)*. Actually, a universal constant value of v^* represents a trivial sufficient condition which assures (A.77) to be fulfilled. It is to be established if this is also a necessary condition. Actually, analysing equation (A.77), one obtains the following mathematically admissible solution for it:

$$v^*(N_1, N_2, \dots, N_t) = e^{\frac{\sum_1^t N_i \ln v_i^*}{N}} \tag{A.78}$$

In fact, it is easy to verify that (A.78) is a solution of (A.77):

$$\frac{N}{v^*}\left(\frac{\partial v^*}{\partial N_i}\right)_{N_{j\neq i}} = -\ln\frac{v^*}{v_i^*} \Leftrightarrow \frac{N}{e^{\frac{\sum_1^t N_i \ln v_i^*}{N}}} e^{\frac{\sum_1^t N_i \ln v_i^*}{N}} \frac{N \ln v_i^* - \sum_1^t N_i \ln v_i^*}{N^2} = -\ln\frac{e^{\frac{\sum_1^t N_i \ln v_i^*}{N}}}{v_i^*} \Leftrightarrow$$
$$\frac{N \ln v_i^* - \sum_1^t N_i \ln v_i^*}{N} = \ln v_i^* - \frac{\sum_1^t N_i \ln v_i^*}{N} \tag{A.79}$$

Equation (A.78) also satisfies, trivially, the limit condition:

$$\lim_{N\to N_i} v^*(N_1, N_2, \dots, N_t) = v_i^* \quad \text{for each } i=1,\ 2,\ \dots,\ t \tag{A.80}$$

It is worth noting that the expression of v^* given by equation (A.78) includes as a sub case the universal constant solution. In fact, assuming in (A.78) $v_1^* = v_2^* = \cdots = v_t^* = C$ results in $v^*(N_1, N_2, \dots, N_t) = C$, with C a constant independent of $\underline{N}$. (A.78) shows that the assumption that v^* takes a universal constant value does not represent a necessary condition to obtain the IG consistency of the described version of SL model.
However, one cannot take for granted that equation (A.78) represents the only possible form of v^* which provides the IG consistency. In fact, one cannot exclude a priori that the mixing rules investigated by Neau could be as well a physically admissible solution for $v^*(N_1, N_2, \dots, N_t)$. In the following we will show that these mixing rules do not represent a solution for eq. (A.77), thus confirming the results inferred by Neau following a different procedure. By substituting in (A.77) the first form of $v^*(N_1, N_2, \dots, N_t)$ considered by Neau:

$$v^* = \sum \phi_i v_i^* \tag{A.81a}$$

we obtain:

$$\frac{1}{rv^*}\left[r_i(v_i^* - v^*)\right] = -\ln\frac{v^*}{v_i^*} \Leftrightarrow \frac{1}{\sum x_i r_i v_i^*}\left[r_i\left(v_i^* - \sum\frac{x_i r_i v_i^*}{\sum x_i r_i}\right)\right] + \ln\frac{\sum\frac{x_i r_i v_i^*}{\sum x_i r_i}}{v_i^*} = 0 \tag{A.81b}$$

Considering the second form of $v^*(N_1, N_2, \dots, N_t)$ investigated by Neau:

$$v^* = \sum\sum \phi_i \phi_j v_{ij}^* \tag{A.82a}$$

(A.77) becomes:

$$\frac{1}{rv^*}\left[2r_i\left(\sum \phi_j v_{ij}^* - v^*\right)\right] = -\,ln\frac{v^*}{v_i^*} \quad \Leftrightarrow \quad \frac{1}{\sum\sum x_i r_i \frac{x_j r_j}{\sum x_i r_i} v_{ij}^*}\left[2r_i\left(\sum \frac{x_j r_j}{\sum x_i r_i} v_{ij}^* - \sum\sum \frac{x_i r_i}{\sum x_i r_i}\frac{x_j r_j}{\sum x_i r_i} v_{ij}^*\right)\right] + ln\frac{\sum\sum \frac{x_i r_i}{\sum x_i r_i}\frac{x_j r_j}{\sum x_i r_i} v_{ij}^*}{v_i^*} = 0 \tag{A.82b}$$

v_{ij}^* is a parameter unequivocally determined once each v_i^*, v_j^* and an interaction parameter (independent of the composition) are assigned. When the pure component parameters involved are assigned, it is evident that equations (A.81a) and (A.82a) do not satisfy equation (A.77) for any conceivable $\underline{N}$, so that the investigated versions of SL model do not recover the consistency of the chemical potential of the species *i* in IG limit.

In the following we focus on an additional version of SL model, proposed in the literature for the case of binary mixtures, which introduces a mixing rule for the characteristic pressure of the mixture instead of a mixing rule for the energy.

According to the described procedure, we start to write the following expression (in which, without losing in generality, 1 represents an arbitrary component):

$$\frac{\mu_1(v,T,\underline{N})}{kT} = ln\frac{\phi_1}{\delta_1} + \left(1 - \frac{r_1}{r_2}\right)\phi_2 + r_1^0\tilde{\rho}X_1\phi_2^2 + r_1^0\left\{-\frac{\tilde{\rho}}{\tilde{T}_1} + \frac{\tilde{P}_1\tilde{v}}{\tilde{T}_1} + \tilde{v}\left[(1-\tilde{\rho})\,ln(1-\tilde{\rho}) + \frac{\tilde{\rho}}{r_1^0}ln\,\tilde{\rho}\right]\right\} \tag{A.83}$$

Here and in the following, r_i^0 and r_i represent the number of cells occupied by component *i* in the pure state and in the mixture, respectively.

Again, the following limit calculation for the chemical potential of the species 1 in the mixture and in pure phase are required:

$$\lim_{v\to+\infty}\frac{\mu_1(v,T,\underline{N})}{kT} = \lim_{v\to+\infty}\left(ln\frac{\phi_1}{\delta_1} + \left(1-\frac{r_1}{r_2}\right)\phi_2 + r_1^0\frac{rv^*}{v}X_1\phi_2^2 + r_1^0\left\{-\frac{1}{\tilde{T}_1}\frac{rv^*}{v} + \frac{\tilde{P}_1}{\tilde{T}_1}\frac{v}{rv^*} + \frac{v}{rv^*}\left[\left(1-\frac{rv^*}{v}\right)ln\left(1-\frac{rv^*}{v}\right) + \frac{1}{r_1^0}\frac{rv^*}{v}ln\frac{rv^*}{v}\right]\right\}\right) = ln\frac{\phi_1}{\delta_1} + \left(1-\frac{r_1}{r_2}\right)\phi_2 + r_1^0\left\{\frac{v_1^*}{rv^*} - 1\right\} + \lim_{v\to+\infty} ln\frac{rv^*}{v} \tag{A.84}$$

$$\lim_{v\to+\infty}\frac{\mu_1^0(v,T)}{kT} = ln\frac{1}{\delta_1} + 1 - r_1^0 + \lim_{v\to+\infty} ln\frac{r_1^0 v_1^*}{v} \tag{A.85}$$

Finally, according to equations (A.84) and (A.85), equation (A.69) reads:

$$\lim_{v\to+\infty}\frac{\mu_1(v,T,\underline{N})}{kT}-\lim_{v\to+\infty}\frac{\mu_1^0(v,T)}{kT}=\left(1-\frac{r_1}{r_2}\right)\phi_2+r_1^0\frac{v_1^*}{rv^*}+ln\frac{x_1r_1v^*}{r_1^0v_1^*}-1=ln\,x_1+\left(1-\frac{r_1}{r_2}\right)\phi_2+r_1^0\frac{v_1^*}{rv^*}+ln\frac{r_1v^*}{r_1^0v_1^*}-1 \tag{A.86}$$

Since in this version of the SL model $r_i v^* = r_i^0 v_i^*$ and recalling the proper expression of ϕ_i, equation (A.86) becomes:

$$\lim_{v\to+\infty}\frac{\mu_1(v,T,\underline{N})}{kT}-\lim_{v\to+\infty}\frac{\mu_1^0(v,T)}{kT}=ln\,x_1+\left(1-\frac{r_1}{r_2}\right)\phi_2=ln\,x_1+\left(1-\frac{r_1^0v_1^*}{r_2^0v_2^*}\right)\frac{r_2^0x_2}{\frac{v_1^*}{v_2^*}r_1^0x_1+r_2^0x_2} \tag{A.87}$$

It is evident that for any couple of components for which $r_1^0v_1^* \neq r_2^0v_2^*$, the second term in the R.H.S. of equation (A.87) is not null in the full concentration range, which implies that also this version of SL model is not consistent in the IG limit.

Appendix B

CAHN-D200 electronic microbalance (B1 in figure B.1) has a sensitivity of 10^{-7} g and an accuracy of $\pm 3\cdot 10^{-7}$ g. The sample (S1 in Figure B.1) and the hanging wire were located in a glass water jacketed compartment (B2 in Figure B.1) kept at a controlled temperature. The sample compartment is connected, by service lines to a flask dead volume (T2 in Figure B.1) and to a liquid reservoir (T1 in Figure B.1) which provides the vapor in case of vapor sorption experiments. Moreover, a combined pumping station incorporating turbopump and membrane backing pump (Pfeiffer HiCUBE 80, ultimate pressure 10^{-7} mbar, pumping speed 35 l/s; P1 in Figure B.1) is also installed to the balance. Finally, a pressure transducer (an MKS Baratron 121 A, absolute capacitance gauge with a full range of 100 Torr, a sensitivity of 0.01 Torr and an accuracy equal to ±0.5% of the reading, PI in Figure B.1) and to an electronically controlled throttle valve (V4 in Figure B.1) are mounted on the apparatus. Pressure of the vapor within the equipment and in the sample compartment was controlled by a MKS 651C controller, that receives the pressure value from the MKS Baratron 121 A transducer and drives the throttle valve to obtain the desired set point value of pressure. Pressure is maintained at the desired value by a dynamical balance between the vapor outflow through the throttle valve (separating the equipment from the vacuum pump) and the vapor inflow from a solvent reservoir with a manually controlled needle valve (V1 in Figure B.1). The set point for the pressure controller is provided by a Labview code that supplies to the controller the desired value of pressure at each time, enabling i) isobaric tests at variable sample temperature and constant pressure, ii) isothermal tests at constant sample temperature and pressure changing at a controlled rate and iii) isoactivity tests performed by concurrent control of sample temperature and pressure as function of time. The Labview code has been also designed to acquire and record the balance reading, the throttle valve status, the pressure reading and the temperature value of the sample, with a maximum acquisition frequency of 20 points per second. The temperature of the sample compartment is controlled by a programmable liquid fluid temperature bath (Julabo CF41) with an accuracy of ± 0.01°C. Balance head, pressure transducer, solvent reservoir, dead volume flask and service lines are contained in a case where a constant temperature value of 35°C is assured by an air flow at controlled temperature (accuracy ± 0.1°C). During the desiccation stage preceding the tests, a high vacuum was attained by activating both the turbomolecular pump and the membrane backing pump. Conversely, during the tests, only the membrane backing pump is activated for pressure control purposes.

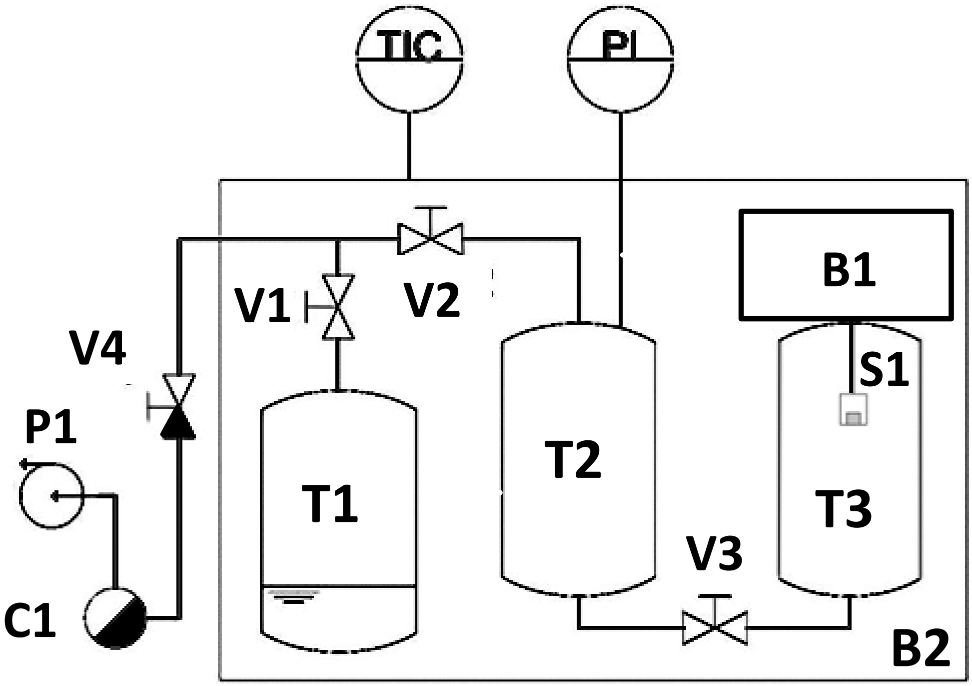

Figure B.1: Cahn D-200 microbalance schematic representation.